Matrix metalloproteinase-11 promotes mouse mammary gland tumor progression

Bing Tan

UNIVERSITÉ DE STRASBOURG

ÉCOLE DOCTORALE DES SCIENCES DE LA VIE ET DE LA SANTÉ

Thèse présentée par

Bing TAN

Pour obtenir le grade de

Docteur de l'Université de Strasbourg

Sciences du Vivant

Aspects Moléculaires et Cellulaires de la Biologie

La métalloprotéase matricielle-11 facilite la progression des tumeurs de la glande mammaire murine

Matrix metalloproteinase-11 promotes mouse mammary gland tumor progression

Soutenue publiquement le 13 septembre 2018

Devant le jury composé de:

Examinateur:	**Madame le Docteur Isabelle GRILLIER-VUISSOZ**
Rapporteurs Externe:	**Madame le Docteur Emmanuelle LIAUDET-COOPMAN**
	Monsieur le Docteur Stéphane DEDIEU
Rapporteur Interne:	**Monsieur le Docteur Olivier LEFEBVRE**
Directeur de Thèse:	**Madame le Docteur Catherine-Laure TOMASETTO**

Acknowledgements

The completion of my PhD thesis is attributed to many people's support.

First, I want to extend my heartfelt gratitude to my supervisor Dr. Catherine-Laure TOMASETTO, whose patient guidance, constant encouragement and valuable suggestions make me successfully complete this thesis. Her modest, open-minded personality and conscientious academic spirit will inspire me in future study. If without her help in daily life, I can't imagine what my four years in France would be like!

Second, I would give my greatest thanks to Dr. Nassim DALI-YOUCEF, he not only provided lots of guidance in my research, but also answered my questions extremely patient.

I would like to say many thanks to Dr. Fabien ALPY for his good suggestions and technical help in my research, especially how to analysis my data.

My thanks go to the laboratory members for their help, including Dr. Marie-Christine RIO, we spent and enjoyed a very pleasure time; my thanks go to the IGBMC animal facility, ICS histopathology service and CBI image center; and my thanks go to the friends and the people whose name are not mentioned but give me a lot of help during my study, etc.

Thanks for the jury members Docteur Emmanuelle LIAUDET-COOPMAN, Docteur Stéphane DEDIEU, Docteur Isabelle GRILLIER-VUISSOZ and Docteur Olivier LEFEBVRE.

I would give my special thanks to my parents, my brother, my girlfriend, and my uncle Jinxiang TAN for their support.

Last, acknowledgements give to La Ligue Contre Le Cancer and China Scholarship Council for provide me the scientific fundings.

THANK YOU ALL **MERCI À TOUTES/TOUS**

Table of Contents

List of Figures and Tables

List of Abbreviations

ADAMs	A Disintegrin and Metalloproteinases
AKT/PKB	Protein Kinase B
ARE	AU-rich Elements
aP2	Adipocyte Protein 2
BAT	Brown Adipose Tissue
BM	Basement Membrane
bFGF-2	Basic Fibroblast Growth Factor-2
b-MMP11	Bicistronic MMP-11
CAAs	Cancer-Associated Adipocytes
CAFs	Cancer-Associated Fibroblasts
CCL	Chemokine (C-C motif) Ligand
C/EBP	CCAAT/enhancer-binding-protein
CLS	“crown-like” Structures
COX-2	Cyclooxygenase-2
CTGF	Connective Tissue Growth Factor
CXCL	Chemokine (C-X-C motif) Ligand
DCIS	Ductal Carcinoma in Situ
DFS	Disease Free Survival
ECM	Extracellular Matrix
EGF	Epidermal Growth Factor
EGFR	Epidermal Growth Factor Receptor
EMT	Epithelial-Mesenchymal Transition
ER	Endoplasmic Reticulum
ERK	Extracellular-Related Kinase
ER-α	Estrogen Receptor-alpha
ETC	Electron Transport Chain
FASL	Fas Ligand
Fabp4	Fatty-acid-binding Protein 4
FASN	Fatty Acid Synthase
FFAs	Free Fatty Acids
FGF-2	Fibroblast Growth Factor-2

FGFR-1	Fibroblast Growth Factor Receptor-1
GAGs	Glycosaminoglycans
GFP	Green-fluorescent-protein
GPI	Glycosylphosphatidylinositol
gWAT	Gonadal White Adipose Tissue
HB-EGF	Heparin-Binding-EGF
Hb	Hemoglobin
HE	Hematoxylin Eosin
HGFR	Hepatocyte Growth Factor Receptor
HIF-1α	Hypoxia Inducible Factor-1 alpha
IDC	Invasive Ductal Carcinomas
IGF	Insulin-like Growth Factor
IGFBP	Insulin-like Growth Factor Binding Protein
IGF-1R	IGF-1 Receptor
IL-1	Interleukin-1
IL-2Rα	Interleukin-2 Receptor alpha
ITPP	Myo-inositol Trispyrophosphate
KGF	Keratinocyte Growth Factor
KO	Knockout
MAPK	Mitogen-Activated Protein Kinase
MCP	Monocyte Chemoattactant Protein
MECs	Mammary Epithelial Cells
MEFs	Mouse Embryonic Fibroblasts
MMPs	Matrix Metalloproteinases
MMP-11	Matrix Metalloproteinase-11
MMPIs	Matrix Metalloproteinase Inhibitors
MMTV-PyMT	Mouse Mammary Tumor Virus-Polyoma Virus Middle Tumor antigen
MMTV LTR	Mouse Mammary Tumor Virus LTR
MT-MMP	Membrane-type MMP
mWAT	Mammary Gland White Adipose Tissue
NK	Natural Killer
NF-κB	Nuclear Factor kappa-light-chain-enhancer of activated B cells
PARs	Protease Activated Receptors

PDGF	Platelet-derived Growth Factor
PGP	Proline-glycine-proline
PI3K	PhosphoInositide 3-Kinase/Phosphatidylinositol 3-Kinase
PPARγ	Peroxisome Proliferator-Activated Receptor gamma
PR	Progesterone Receptor
PSR	Picro-sirius Red
RANKL	Receptor Activator for Nuclear Factor κB Ligand
RARE	Retinoic-acid-responsive-element
RARβ	Retinoic Acid Receptor beta
RARγ	Retinoic Acid Receptor gamma
RASI	Rheumatoid Arthritis Synovial Inflammation
RECK	Reversion-inducing-cysteine-rich Protein with Kazal Motifs
RORγ	Retinoid-related Orphan Receptor gamma
ROS	Reactive Oxygen Species
RT-qPCR	Reverse Transcription-quantitative Polymerase Chain Reaction
ST-3	Stromelysin-3
TACE	TNFα Converting Enzyme
TEBs	Terminal End Buds
TGF-α	Transforming Growth Factor-alpha
TGF-β	Transforming Growth Factor-beta
Tg	Transgenic
TIMPs	Tissue Inhibitors of Metalloproteinases
TME	Tumor Microenvrioment
TNF-α	Tumor Necrosis Factor-alpha
TRE	Thyroid Hormone Responsive Element
UPR^{ER}	Unfolded Protein Response of ER
UPR^{mt}	Unfolded Protein Response of Mitochondrial
UPS	Ubiquitin Proteasome System
UTRs	Untranslated Regions
u-PAR	Urokinase Type Plasminogen Activator Receptors
VEGF	Vascular Endothelial Growth Factor
WT	Wildtype
3D	Three-dimensional

Summary

Breast cancer is the most common leading cause of cancer death in women patients (Polyak and Metzger Filho, 2012). Tumor cell microenvironment plays a crucial role in breast cancer development and progression (Hanahan and Coussens, 2012; Soysal et al., 2015; Martins and Schmitt, 2018). Several cell components exist in the periphery space of breast cancer including stem cells, immune cells, endothelial cells, epithelial cells, fibroblast cells, adipocytes (Quail and Joyce, 2013). Adipocytes, as predominant components of the breast stroma, can have an impact on cancer growth and metastasis not only by direct cell contact, but indirectly by paracrine action (Rio et al., 2015). Breast cancer cells are separated from the normal stroma by a specialized form of extracellular matrix called the basement membrane (BM). Matrix metalloproteinases (MMPs) are the main enzymes that can degrade the BM -a physical barrier for breast cancer- and favor cancer cells invasion into the adjacent normal tissues. This sequence of event is associated with disease progression and metastasis to distant organs. Matrix metalloproteinase-11(MMP-11), one of the MMPs family members, also called stromelysin-3, is a secreted protein by stromal cells of breast cancer and associated with poor outcome of these patients (Basset et al., 1990; Chenard et al., 1996). MMP-11 mediates a number of physiological and pathological processes in the microenvironment. Preclinical studies show that high level MMP-11 has a negative function during adipogenesis in the mouse (Andarawewa et al., 2005). Of interest, MMP-11 expression in breast cancer marks distinct cell populations from the tumor microenvironment (TME). In the tumor center, fibroblast cells are the prominent cellular components of the microenvironment. These cells called "Cancer-Associated Fibroblasts" (CAFs) express very high levels of MMP-11. In contrast, in the tumor periphery, adipocytes represent the principal cellular component of the microenvironment. These cells are called “Cancer-Associated Adipocytes” (CAAs). Unlike normal adipocytes in which MMP-11 is barely expressed, CAAs express high levels of MMP-11. These observations allowed to propose that MMP-11 expression by CAAs directly participate in breast tumor progression (Motrescu and Rio, 2008; Tan et al., 2011). However, how adipocyte-related MMP-11 acts at the interface of breast cancer cells and CAAs remains largely unknown. More studies about the role of adipose tissue-derived MMP-11 on breast cancer progression are urgently needed.

CHAPTER 1 Introduction and Review

1.1 MMPs family

Various types of proteinases are implicated in extracellular matrix (ECM) degradation, but the major enzymes are considered to be matrix metalloproteinases (MMPs), also called matrixins (Yadav et al., 2014; Galliera et al., 2015). MMPs are a family of highly conserved, structurally related zinc-dependent endopeptidases. They are major enzymes capable of extracellular matrix turnover through proteolytic degradation (Nagase and Visse, 2009; Pedersen et al., 2015). MMPs are important not only in normal, physiological and biological processes such as embryogenesis, normal tissue remodeling, tissue repair, wound healing and angiogenesis, but also in diseases such as arthritis, chronic tissue ulceration and cancer progression (Nagase and Visse, 2009; Vargová et al., 2012). At present, 28 MMP family members have been discovered among vertebrates, 23 of MMPs have been found in humans (Nagase and Visse, 2009; Chaudhary et al., 2010). The activities of most MMPs are very low or negligible in tissues under normal conditions, but their expression is transcriptionally controlled by growth factors, hormones, inflammatory cytokines, cell–cell and cell–matrix interaction. Moreover, precursor zymogens, endogenous inhibitors, and tissue inhibitors of metalloproteinases (TIMPs) are also regulating their activity (Nagase and Visse, 2009). Thus, besides the MMP expression level, the balance between pro and mature MMPs, inhibitors and TIMPs activity are critical for the ECM remodeling in tissues.

1.1.1 MMPs classification

On the basis of their chromosome localization, sequence similarity, protein domain organization and substrate preference, all MMPs family members from MMP-1 to MMP-28 are separated into 6 subgroups: collagenases, gelatinases, stromelysins, matrilysins, membrane type MMPs and other MMPs (Löffek et al., 2011). Several MMPs members have been found localized to the same cluster at chromosome 11q22 that contains MMP-1, -3, -7, -8, -10, -12, -13, -20 and -27, a region that shows amplification in several solid tumors (Curran and Murray, 1999; Yadav et al., 2014). Of note, MMP-4, -5 and -6 are missing in the list since they were shown to be identical

to other members. The canonical names of some MMPs members are according to their substrate specificities (Table 1.1).

Type	MMP members	Chromosomal location
Collagenases	MMP-1 (Collagenase-1)	11q22.2-22.3
	MMP-8 (Collagenase-2)	11q22.2-22.3
	MMP-13 (Collagenase-3)	11q22.2-22.3
	MMP-18 (Collagenase-4)	-
Gelatinases	MMP-2 (Gelatinase A)	16q13
	MMP-9 (Gelatinase B)	20q11.2-13.1
Stromelysins	MMP-3 (Stromelysin-1)	11q22.2-22.3
	MMP-10 (Stromelysin-2)	11q22.2-22.3
	MMP-11 (Stromelysin-3)	22q11.2
Matrilysins	MMP-7 (Matrilysin-1)	11q22.2-22.3
	MMP-26 (Matrilysin-2)	11q22.2
Membrane type MMPs	MMP-14 (MT-1 MMP)	14q12.2
	MMP-15 (MT-2 MMP)	16q12.2
	MMP-16 (MT-3 MMP)	8q21
	MMP-17 (MT-4 MMP)	12q24
	MMP-24 (MT-5 MMP)	20q11.2
	MMP-25 (MT-6 MMP)	16q13.3
Other MMPs	MMP-12 (Metalloelastase)	11q22.2-22.3
	MMP-19 (-)	12q14
	MMP-20 (Enamelysin)	11q22
	MMP-21 (XMMP (Xenopus))	-
	MMP-22 (CMMP (Chicken))	11q24
	MMP-23 (Cysteine array)	1q36.3
	MMP-27 (-)	11q24
	MMP-28 (epilysin)	17q11.2

Table 1.1 MMPs classification and their chromosomal location. (Adapted from (Yadav et al., 2014)).

1.1.1.1 Collagenases

Collagenase-1 (MMP-1), collagenase-2 (MMP-8), collagenase-3 (MMP-13) and collagenase-4 (MMP-18) (in Xenopus) are in one group. The key feature of these enzymes is their ability to cleave interstitial collagens I, II and III into characteristic 3/4 and 1/4 fragments from the N-terminus, but they can digest other ECM molecules and soluble proteins (Visse and Nagase, 2003). A recent study indicated that MMP-8 has a protective role in breast tumor growth and lung metastasis progression through decreasing miR-21 level via cleavage of decorin and a subsequent reduction of transforming growth factor β (TGF-β) signalling (Soria-Valles et al., 2014).

1.1.1.2 Gelatinases

Gelatinase-A (MMP-2) and Gelatinase-B (MMP-9) belongs to this group. They readily digest gelatin and denatured collagens, because of their three fibronectin type II domain repeats in the catalytic domain, which bind to gelatin, collagens, and laminin (Allan et al., 1995; Kumar et al., 2016). They also digest a number of ECM molecules including type I, IV, V and XI collagens, elastin, etc. (Hannocks et al., 2017). MMP-2, but not MMP-9, digests type II and III collagens (Patterson et al., 2001). Furthermore, three collagen binding residues were identified, which are essential for gelatinolysis and constitute promising targets for selective inhibition of MMP-2 (Mikhailova et al., 2012).

1.1.1.3 Stromelysins

Stromelysin-1 (MMP-3) and stromelysin-2 (MMP-10) are similar in structure and substrate specificities. They degrade many different ECM components, but they are not able to cleave native collagen. MMP-3 and MMP-10 digest a number of ECM molecules and participate in proMMP activation. For example, MMP-3 action on a partially processed proMMP-1 is critical for generation of active form of MMP-1 (Suzuki et al., 1990; Nagase et al., 1992). MMP-12 or metalloelastase is the most potent elastolytic enzyme of the family, it has been implicated in regulating the matrikines Val-Gly-Val-Ala-Pro-Gly (elastin peptide) and proline-glycine-proline (PGP) (Wells et al., 2015).

Stromelysin-3 (MMP-11) has a collenogenic activity against type VI collagen, however it is not known whether it is direct or indirect (Motrescu et al., 2008). The

MMP genes from this subgroup cluster on chromosome 11, except for the MMP-11 gene that is located on chromosome 22. MMP-11 is usually grouped with "other MMPs" because of its distinct sequence and substrate specificity. On the other hand, MMP-11 has very weak activity toward ECM molecules (Murphy et al., 1993), but cleaves insulin-like growth factor binding protein-1 (IGFBP-1) more readily (Mañes et al., 1997).

1.1.1.4 Matrilysins

Matrilysin-1 (MMP-7) and Matrilysin-2 (MMP-26), also called endometase, are in this group (Park et al., 2000; Uría and López-Otín, 2000). These MMPs lack the linker peptide and the hemopexin domain (Figure 1.1).

MMP-7 is synthesized by epithelial cells and is secreted apically. Besides ECM components, it processes cell surface molecules such as E-cadherin, pro-α-defensin, pro-tumor necrosis factor-alpha (TNF-α), and Fas-ligand (FASL). MMP-26 is expressed in normal cells like those of the endometrium and in some cancers (Pilka et al., 2005; Gutschalk et al., 2013; Khamis et al., 2016). MMP-26 is largely stored intracellularly and digests several ECM molecules (Marchenko et al., 2004), but does not cleave pro-MMP-2 (Zhao et al., 2003).

1.1.1.5 MT-MMPs

Six MT-MMPs exist in mammals, they include four type I transmembrane proteins (MMP-14, -15, -16 and -24) and two glycosylphosphatidylinositol (GPI) anchored proteins (MMP-17 and -25). They are all capable of activating proMMP-2, except MMP-17 (English et al., 2000). All these members have a furin recognition sequence RX[R/K]R at the C-terminus. They are activated intracellularly and are likely to be expressed on the cell surface as active enzymes (Turunen et al., 2017).

MMP-14 has a collagenolytic activity on collagens I, II, and III (Ohuchi et al., 1997). MMP-17 is a brain specific protein, and is predominantly expressed in the cerebellum (Luo, 2005). MMP-25 is exclusively found in peripheral blood leukocytes and in anaplastic astrocytomas and glioblastomas, with the exception of meningiomas (Sohail et al., 2008; Blumenthal et al., 2010).

1.1.1.6 Other MMPs

Seven MMPs (MMP-12, -19, -20, -21, -23, -27 and -28) are not classified in the above categories. MMP-12, -20 and -27 have similar structures and chromosome location. MMP-21, -23 and -28 have a furin recognition site before the catalytic domain and may be activated intracellularly and secreted as active form.

MMP-12 is expressed primarily in macrophages (Stawski et al., 2014). MMP-19 is found in activated also called rheumatoid arthritis synovial inflammation (RASI). Because it was found in the T-cell-derived activated lymphocytes from patients with rheumatoid arthritis (Kolb et al., 1997). Moreover, MMP-19 digests many ECM components including the basement membranes (Stracke et al., 2000). MMP-20 is primarily located in newly formed tooth enamel and digests amelogenin (Ryu et al., 1999). MMP-21 digests gelatin, it is found in Xenopus, mice and human (Marchenko et al., 2003), are expressed in various tissues and in squamous and basal cell carcinomas (Ahokas et al., 2003). MMP-23 is also named cysteine-array MMP. It is a unique member as it has a cysteine-rich domain instead of a hemopexin domain, and lacks the cysteine switch motif in the pro-domain (Figure 1.1). It is proposed to be a type II membrane protein harboring the transmembrane domain at the N-terminal. It also has a furin site in the pro-domain (Pei et al., 2000). MMP-27 modulates immune response and was found in both chicken and pig (Atikuzzaman et al., 2017). MMP-28 is expressed in many adult organs, including the heart (Illman et al., 2008). It was also detected in pulmonary emphysema (Manicone et al., 2017).

1.1.2 MMPs structures

MMP have common and distinct structural features (Figure 1.1). Typically, a minimal MMP is made of 3 domains. A “pre” domain, which addresses the protein in the secretory pathway; a “pro” domain necessary to maintain the protein inactive or latent form (zymogen); a “catalytic” domain responsible for the degradative activity. Additionally, a regulatory “hemopexin” subunit is thought to confer much of the substrate specificity to the MMPs. Except MMP-7 and MMP-26: they lack the linker peptide and the hemopexin domain, and also MMP-23 has a unique cysteine/proline-rich domain after the catalytic domain instead of hinge and hemopexin domain. Two gelatinases, MMP-2 and MMP-9 have three repeats of a collagen-binding fibronectin type II inserted in the catalytic domain. The “cysteine switch” motif PRCGXPD in the prodomain and the zinc binding motif HEXXHXXGXXH in the catalytic domain are

common structural signatures of MMPs, where three histidines in the zinc binding motif and the cysteine in the propetide coordinate with the catalytic zinc ion. This Cys-Zn2+ complex coordination makes proMMP zymogens inactive by preventing hydrophilic motif essential for catalysis from binding to the zinc atom. The catalytic domain also contains a conserved methionine, forming a "Met-turn" eight residues after the zinc binding motif, which forms a base to support the structure around the catalytic zinc (Bode et al., 1993). While the minimal domain structures of metalloproteinases have little homology among the families, the overall protein folding is similar (Gomis-Rüth, 2003). (Summarized in Figure 1.1).

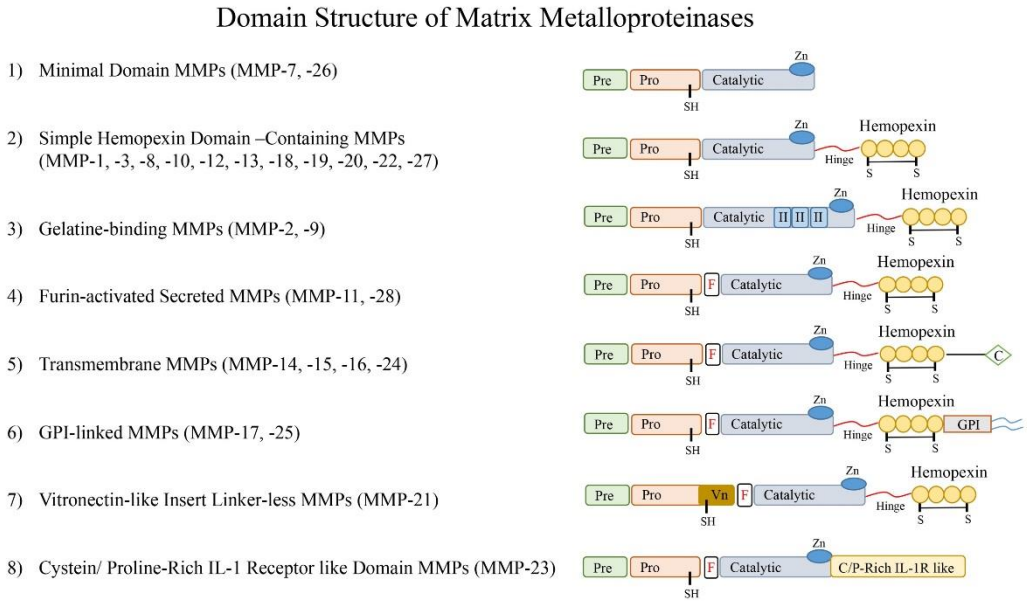

Figure 1.1 Domain structure of MMP family members.

1.1.3 MMPs substrates

MMPs were originally associated with remodeling and degradation of the ECM, but now MMPs are considered as multifunctional proteases. Here, I list the main substrates of MMPs and provide selected examples (Table 1.2). MMP-mediated breakdown of ECM barriers has been thought to be the primary effect to facilitate cell migration. However, different ECM components are susceptible to proteolysis by different MMPs and not all ECM components are cleaved by every MMP. Cleavage of ECM proteins also generate fragments with new function. Fibrillary collagens, such as collagen I, II and III are cleaved predominantly by MMP-1, -2, -8, -13 and -14 (Robichaud et al., 2011; Lauer et al., 2014). Collagen IV which locates in the basement

membrane is susceptible to proteolysis by gelatinases, stromelysins, matrilysins and some other MMPs, such as macrophage metalloelastase (Sand et al., 2013; Narimiya et al., 2017).

The non-ECM components, TGF-β, can be proteolytically activated by MMP-2 and MMP-9 in cancer (Yu and Stamenkovic, 2000; Santibanez et al., 2018). Data indicated that TGF-β could be released by MMP-14 from the cell surface complexes with αvβ3 integrin (Mu et al., 2002). Furthermore, the MMP-14-dependent release of active TGF-β leads to autocrine and paracrine effects on cell growth and matrix production. On the other hand, TGF- β is able to regulate MMPs expression in several ways (Santibanez et al., 2018). Some other non-ECM components are also MMP substrates, like cell-adhesion molecules CD44, αVβ/αβ1/αβ2 integrins and Ku protein. Cleave of these signal transduction molecules have subsequent effects on cell survival, migration and angiogenesis (Chetty et al., 2010; Bauvois, 2012).

MMPs are of outstanding importance in the site-specific cleavage of growth factors and cytokines. For example, MMP-2 converts monocyte chemoattractant protein (MCP)-3 into a receptor-blocking antagonist by removal of its four N-terminal residues (McQuibban, 2000). The cell surface growth factor precursors, like the epidermal growth factor (EGF) family, particularly heparin-binding-EGF (HB-EGF) precursor, is cleaved and activated by MMP-3 (Suzuki et al., 1997) and MMP-7 (Cheng et al., 2007). Growth factor receptors are also MMP substrates. MMP-2 cleaves fibroblast growth factor receptor-1 (FGFR-1) (Levi et al., 1996). While the hepatocyte growth factor receptor (HGFR) c-MET, and two members of the epidermal growth factor receptor (EGFR) family, HER2/ERBB2 and HER4/ERBB4, are the substrates of unknown MMPs (Vecchi et al., 1998; Codony-Servat et al., 1999; Nath et al., 2001). Importantly, chemokine processing by MMPs is selective: MMPs differ in processing of chemokines and chemokines differ in cleavage susceptibility (McQuibban et al., 2002; Cox et al., 2008).

Besides, MMPs may also cleave and activate their zymogens or their inhibitors. Activation of proMMPs involves detaching of the hemopexin domain, which can be accomplished extracellularly by other MMPs or other proteases. For example, proMMP-2 is not activated by general proteinases, instead its activation takes place on the cell surface by most MT-MMPs, but not MT4-MMP (Nagase, 1998). MMP-14-mediated activation of proMMP-2 requires TIMP-2 (Shen et al., 2010). ProMMP-2

forms a complex with TIMP-2 through their C-terminal domains, thus permitting the N-terminal inhibitory domain of TIMP-2 to bind to MMP-14 on the cell surface. The cell surface-bound proMMP-2 is then activated by an MMP-14 that is free of TIMP-2. Alternatively, MMP-14 inhibited by TIMP-2 can act as a "receptor" for proMMP-2. The MMP-14-TIMP-2-proMMP-2 complex is then presented to an adjacent free MMP-14 for activation (Itoh et al., 2001). Thus, the TIMP-2 environment may determine the MMP-14 choice between direct cleavage of its own substrates and activation of MMP-2 (Kudo et al., 2007). However, as a non-classic MMP family member, MMP-11 activation occurs intracellularly via the endopeptidase furin, which selectively cleaves paired base residues (Pei and Weiss, 1995). Moreover, MMP-11 cleaves IGFBP-1 in vitro (Mañes et al., 1997). And in vivo experiment suggests MMP-11 cleaves IGFBP-1 and releases free form of insulin-like growth factor-1 (IGF-1) in mice plasma (Dali-Youcef et al., 2016).

In summary, MMPs not only proteolyze classic ECM components with subsequent release of bioactive fragment and proteins, but also play an important role in non-ECM components, including chemokine processing and alteration of the activity status of other proteases.

MMP members	Substrates
MMP-1	Collagen (I,II,III,VII,VIII,X), Casein, Perlecan, Entactin, Laminin, Pro-MMP-1, -2, -9 &Serpins
MMP-8	Collagen (I, II, III, V, VII, VIII, X), Gelatin, Aggrecan, Fibronectin
MMP-13	Collagen (IIV, IX, X, XIV), Gelatin, Plasminogen, Aggrecan, Perlecan, Fibronectin
MMP-18	Type I Collagen
MMP-2	Gelatin, Collagen (IV-VI, X), Elastin, Fibronectin
MMP-9	Gelatin, Collagens (IV, V, VII, X, XIV), Elastin, Fibrillin & Osteonectin
MMP-3	Laminin, Aggregan, Gelatin, Fibronectin
MMP-10	Collagens (III-V), Gelatin, Casein, Aggregan, Elastin, MMP-1, -8
MMP-11	Collagen VI, IGFBP-1, PAI1
MMP-12	Elastin, Gelatin, Collagen I, IV, Fibronectin, Laminin, Vitronectin, Proteoglycan
MMP-7	Collagen (IV-X), Fibronectin, Laminin, Gelatin, Aggregan, Pro-MMP-9
MMP-26	Gelatin, Collagen IV, Pro-MMP-9
MMP-14	Collagen (I, II, III), Gelatin, Fibronectin, Laminin, Aggrecan, Tenascin
MMP-15	Fibronectin, Laminin, Aggrecan, Perlecan
MMP-16	Collagen III, Gelatin, Casein
MMP-17	Fibrinogen, TNF precursor
MMP-24	Proteoglycans
MMP-25	Collagen IV, Gelatin, Fibronectin, Fibrin
MMP-19	Collagen I
MMP-20	Amelogenin, Aggrecan
MMP-21	Gelatin
MMP-22	-
MMP-23	Gelatin
MMP-27	-
MMP-28	Casein

Table 1.2 The substrates of MMP family members. (Adapted from (Yadav et al., 2014)).

1.1.4 Regulation of MMPs

1.1.4.1 The expression of MMPs genes

Most MMPs are little expressed under quiescent conditions. Their transcription is individually and tightly regulated (Yan and Boyd, 2007; Kim et al., 2016b). No single growth factor, oncogene, chemokine, and cytokine has been identified to be exclusively responsible for the overexpression of MMPs in special tumors (Köhrmann et al., 2009; Schröpfer et al., 2010), although interleukin-1 (IL-1) and TNF-α are often implicated. Several signalling pathways are involved in the modulation of MMP promoter activities. MMPs promoter regions share several cis-elements. Consistent with that some MMPs are co-regulated by various inductive factors, like cytokines and growth factors, or with co-repressed by retinoids and glucocorticoids (Vincenti and Brinckerhoff, 2007).

The promoters of functionally related MMPs such as MMP-1/MMP-8 (collagenase) or MMP-2/MMP-9 (gelatinase) are clearly distinct, pointing to different ways of activation. MMP promoters can be categorized into three groups (Yan and Boyd, 2007). The first group contains an AP-1 binding site and a TATA box close to their transcription start site and is very often combined with an upstream PEA3-binding site, for the control of MMP transcription by several growth factors and cytokines, like TGF-β, TNF-α, platelet-derived growth factor (PDGF), vascular endothelial growth factor (VEGF), keratinocyte growth factor (KGF) and EGF (Yan and Boyd, 2007; Clark et al., 2008). The second group also contain a TATA box, but lack the AP-1 site. The regulation of these promoters is relatively simple and distinct from the first group. The last group of promoters does not have a TATA box (MMP-2, -14 and -28), and transcription from these promoters starts at multiple sites. Furthermore, in the third group MMPs expression is mainly determined by the transcription factors of ubiquitous Sp-1 family, which bind to a proximal GC box. These MMPs also have a modest sensitivity to induction by cytokines or growth factors (Chakraborti et al., 2003).

Epigenetic mechanism has effects on the control of MMPs transcription like chromatin remodeling with histone acetylation and/or DNA methylation. Hypomethylation of MMP promoters can lead to increase enzyme expression in cancer, as reported for MMP-3 in colon cancer cells (Yan and Boyd, 2007) or increased expression of MMP-3, MMP-9 and MMP-13 in chondrocytes (Roach et al., 2005). Epigenetic chromatin remodeling has been demonstrated for IL-1β induced MMP-1

and MMP-13 expression with changes in histone acetylation states and increased binding of the AP-1 proteins (Vincenti and Brinckerhoff, 2002). Furthermore, MMPs expression is susceptible to be regulated by DNA methylation, histone acetylation and microRNAs (Chernov and Strongin, 2011; Li and Li, 2013).

Post-transcriptional gene regulation can be driven by cytosolic mRNA stability, which is mediated via trans-acting RNA-binding proteins that interact with multiple AU-rich elements (ARE) mostly located in their 3' untranslated regions (UTRs). MMP-2, MMP-9 and MMP-13 expression has been shown to be regulated by mRNA stability. For instance, IL-1β increased MMP-9 gene expression in rat renal mesangial cells was enhanced by ATPγS via increasing binding of HuR to the AREs in the 3'-UTR of MMP-9 mRNA (Yan and Boyd, 2007; Clark et al., 2008).

1.1.4.2 The MMPs compartmentalization

In general, MMPs are extracellular proteins, but some data indicated that MMP-1 (Limb et al., 2005), MMP-2 (Kwan et al., 2004) and MMP-11 (Luo et al., 2002) are also found intracellularly. The localization of MMPs in the pericellular space have a strong impact on their activation and proteolytic efficiency (Ra and Parks, 2007). Secreted MMPs are often associated to the cell surface. Three examples for substrate recruitment include binding of MMP-7 to cholesterol sulfate (Yamamoto et al., 2014), MMP-9 binding to CD44 (Ugarte-Berzal et al., 2014), and binding of MMP-1 to α2β1 integrin (Stricker et al., 2001). MMP14 has been most studied by Philippe Chavrier laboratory (Poincloux et al., 2009; Castro-Castro et al., 2016). MMP-14 zymogen activation occurs constitutively in the trans-Golgi network by furin or other proprotein convertase mediated removal of the N-terminal prodomain upon trafficking from the endoplasmic reticulum (ER) to the cell surface (Yana and Weiss, 2000). It is localized to invadosomes which are actin-based structures for spatially coordinated matrix degradation to support invasion (Castro-Castro et al., 2016; Gucciardo et al., 2016). Localization of MMP-14 is not only on cell membrane but also can be sorted to soluble sheded form and extracellular vesicles (Hakulinen et al., 2008; Clancy et al., 2015).

1.1.4.3 The activation of pro-MMPs

Most MMPs are synthesized and secreted as zymogen forms (inactive state) (Löffek et al., 2011). The pro-domain has to be cleaved for activation. MMPs remain

inactive by an interaction between cysteine-sulphydryl of the propeptide domain and zinc ion bound to the catalytic domain (Sternlicht and Werb, 2001). The activation of MMP zymogen depends on the pro-domain which pulls out the cysteine residue and enables water to interact with the zinc ion in the active site (Ra and Parks, 2007) (Figure 1.2).

Furin is a transmembrane serine proteinase in the trans-Golgi network. It is responsible for sorting proteins from secretory pathway to the secretory granules and cell surface. Nine MMPs members, including all MT-MMPs, are activated by a furin protease (Ra and Parks, 2007). After the cleavage at the furin recognition site (R-x-R/K-R) in the amino acid sequence before the catalytic domain, active MMPs can be secreted in the pericellular space and start their catalytic action (Löffek et al., 2011).

Other MMPs are secreted as inactive pro-forms. In vitro experiment demonstrated that MMPs can be activated by plasmin, chymase, and other MMPs. However, this has not been firmly established in vivo. In fact, there is more than one participant involved in the process of MMP zymogens activation. A well-established model is pro-MMP-2 activation by the cooperation between TIMP-2 and MMP-14 to build up a complex with 1:1:1 stoichiometric ratio on the cell surface (Itoh et al., 2001).

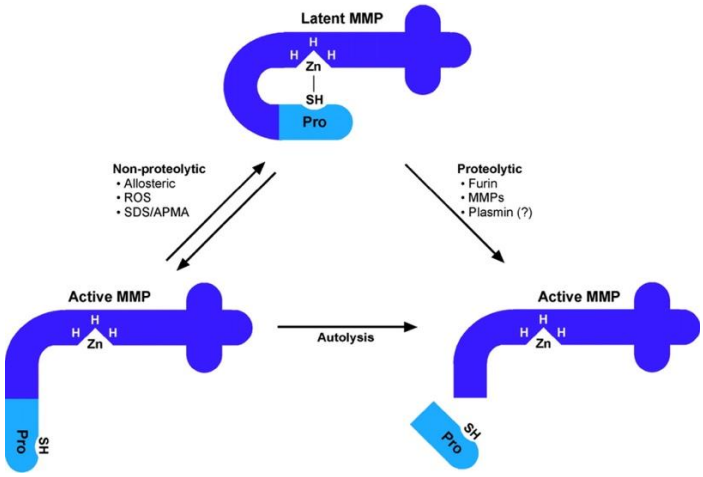

Figure 1.2 Mechanisms of MMPs activation. proMMPs is maintained by an electrostatic interaction between the free thiol of a conserved cysteine in the prodomain with the HIS-ligated zinc atom in the catalytic pocket. The prodomain covers the catalytic cleft thereby barring an interaction with a protein substrate. Proteolytic cleavage of the prodomain by furin/proteases removes the thiol constraint. The thiol-Zn interaction can also be disrupted by APMA or SDS. In tissues and cells, proMMPs can be anchored to other macromolecules, like proteoglycans and integrins, these interactions can lead to allosteric disruption of the thiol-Zn bond. Even though the prodomain may not be cleaved, the MMP can be active. However, the final activation of MMP involves prodomain cleavage, which following a conformational perturbation of the cysteine switch by autolysis. (Adapted from (Ra and Parks, 2007)).

Initiation by intrinsic allostery of MMP molecule is probably another activation mechanism of MMP zymogens. Evidence for this pathway is the pericellular activation of MMP-7 by tetraspanin CD151, which is over-expressed in osteoarthritic chondrocytes and most likely leads to increase cartilage destruction by excessive MMP-7 activation (Fujita et al., 2006).

1.1.4.4 The inhibition of MMPs

The two major inhibitors of MMPs in tissues are endogenous TIMPs and α-macroglobulin. The right balance between active enzymes and their inhibition is essential to avoid the uncontrolled ECM turnover, dysregulated cell proliferation and migration.

There are four members of TIMPs. Each TIMP molecule consists of around 190 amino acids composed of a larger N-terminal domain and a smaller C-terminal domain. The N-terminal domain can fully inhibit MMPs by chelating their catalytic zinc atom with a 1:1 molar ratio. The C-terminal domain can bind tightly to the hemopexin domain of latent MMPs. In general, all TIMP members are broad spectrum inhibitors. TIMPs can inhibit almost all active MMPs, but not with the same efficacy (Murphy, 2011; Arpino et al., 2015). For instance, TIMP-1 has low activity against MMP-14, -16, -19 and -24, but is more efficient for MMP-3 and MMP-7 than other TIMPs (Murphy and Nagase, 2008). The expression of TIMP-2 is constitutive. TIMP-2 and TIMP-3 have the ability to inhibit all MMPs. But the inhibitory profile of TIMP-3 further extends to members of "a disintegrin and metalloproteinases" (ADAMs). In addition, TIMP-3 is a unique member because it binds tightly to the ECM with its N- and C- domain to inhibit MMPs (Lee et al., 2007). In vivo experiments demonstrate loss of TIMP-3 in mice enhanced mammary gland epithelial cells apoptosis and is associated with pulmonary alveolar enlargement (Aiken and Khokha, 2010). By contrast knockout of TIMP-1 or TIMP-2 in mice does not show any unchallenged abnormalities.

The second is α-macroglobulin. It's a broad spectrum proteinase inhibitor which inhibits almost all endopeptidases by entrapping the whole enzyme, while these complexes are rapidly cleared by endocytosis (Rehman et al., 2013). (Summarized in Figure 1.3).

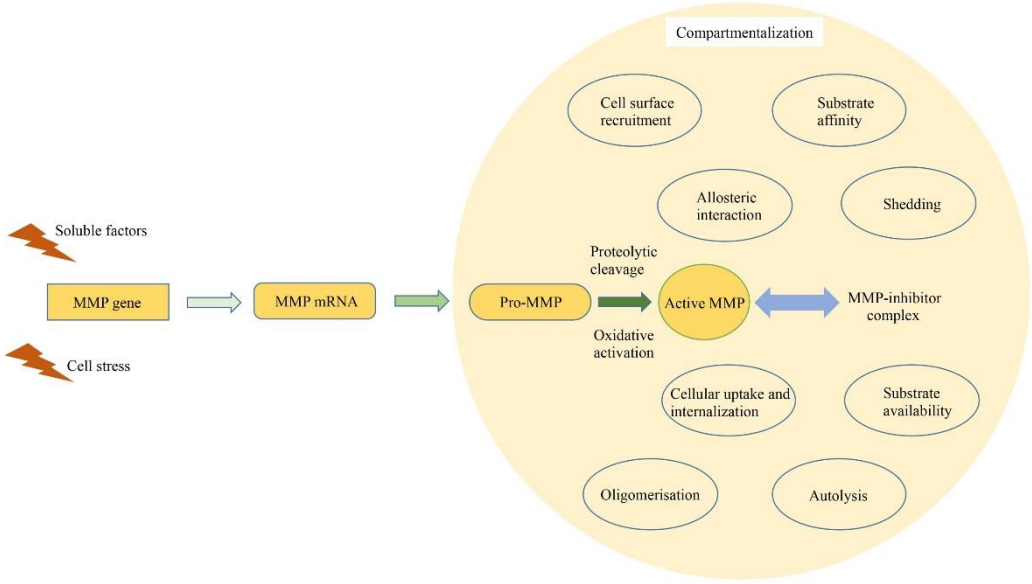

Figure 1.3 MMP activity is tightly regulated at four different levels. 1) gene expression, mainly by regulating transcription and mRNA stability; 2) compartmentalisation (as light yellow filled eclipse), which regulates efficiency of proteolysis through cell surface recruitment, substrate availability and protein interactions, but also influences 3) pro-enzyme activation and 4) inhibition of proteolysis. (Adapted from (Löffek et al., 2011)).

1.1.5 Biological functions of MMPs

Under the normal physiological conditions, MMPs genes are expressed at a low level. When ECM remodeling is required, the genes are induced. Increased expression of MMPs is detected in many circumstances like embryogenesis, wound repair, bone remodeling and cancer progression (Paiva and Granjeiro, 2014; Schlage and auf dem Keller, 2015).

1.1.5.1 MMPs and mouse mammary gland development

The development of the mammary gland begins at embryonic day 10.5, when the single-layered ectoderm enlarges to form the mammary lines. These lines of cells extend from the anterior limb bud to the posterior limb bud (Hens and Wysolmerski, 2005; Musumeci et al., 2015). At E11.5, lens-shaped placodes are observed, rising slightly above the surrounding ectoderm. The mammary placodes then become bulbs of epithelial cells that are distinct from the surrounding epidermis. These buds are elevated knob-like structures at E12-E13.5 but sink into the underlying dermis at around E13.5 (Watson and Khaled, 2008). Female mammary gland development continues at E15.5, with epithelial cell proliferation and elongation in the bud leading to the formation of a sprout that invades the fat pad precursor. The nipple is formed

from epidermal cells overlying the bud, and a lumen is formed in the sprout at E16.5 (Macias and Hinck, 2012). The sprout then branches into the fat pad, giving rise to the rudimentary ductal tree by E18.5 (Sakakura, 1987; Veltmaat et al., 2003) (Summarized in Figure1.4). After birth, the mammary gland distal ends swell into bulbous structures, which are composed of multiple layers of cuboidal epithelial cells, called terminal end buds (TEBs). The TEBs are then invading and branching into the fat pad until they reach the edge of the fat pad (Inman et al., 2015). During female pregnancy and lactation period, mammary gland is induced by progesterone and differentiated into a secretory, milk-producing alveoli, the adipocyte deposition also dedifferentiate into pre-adipocyte (Hennighausen and Robinson, 2001; Inman et al., 2015). After about three weeks breeding, the mammary gland is remodeled back to a state as which adult nulliparous house (Musumeci et al., 2015).

ECM components are a large part of the stroma and are also believed to play a critical role during mammary gland branching morphogenesis. Mammary gland TEB formation and duct invasion into the surrounding adipose-rich mesenchyme are dependent on the degradation of ECM which surrounds epithelial cells. Some MMPs are only present in epithelial cells (MMP-7), some MMPs are only present in stroma fibroblasts (MMP-2 and MMP-3), but MMP-14 is expressed both in epithelial and stromal cells (Rabot et al., 2007; Gomes et al., 2015). Almost all the ECM network can be degraded by the collective activity of MMPs. For example, laminin-5 cleavage by MMPs will generate bioactive fragments that induced breast epithelial cells to migrate (Koshikawa et al., 2000). Currently, mammary gland epithelial cell invasion is thought to depend on the membrane-anchored MMP-14 and MMP-15, remodeling the extracellular matrix triggers associated signalling cascades (Feinberg et al., 2016). MMP-14 showed a reciprocal signalling association with the heparanase levels in mammary gland branching morphogenesis (Gomes et al., 2015). Postnatal mammary gland development is also dependent on MMP-11 expression status. MMP-11 knockout mouse model has decreased periductal collagen content, impaired mammary gland branching, reduced ductal tree, alveolar structures and milk production (Tan et al., 2014). Ectopic expression of proteolytically active form of MMP-3 in the mouse mammary epithelium triggers supernumerary lateral branching. The hemopexin domain of MMP-3 is critical for invasion because of the interaction with the intracellular chaperone heat-shock protein 90 β (Correia et al., 2013). Of note, MMP-2

deficient mice have less TEB invasion, but more lateral branching during Mid-puberty. MMP-3 deficient mice have impaired secondary and tertiary lateral branching of ducts during puberty and pregnancy (Wiseman et al., 2003). TNF-induced secretion of MMP-9 was involved in branching morphogenesis and proliferation. MMP-9 neutral antibody blocked the TNF-stimulated function, inhibiting the invasion process of the fad pad that occurs during normal mammary gland development (Lee et al., 2000).

TIMP group members were reported to be involved in the dynamic process of mammary ductal morphogenesis. TIMP-1 mRNA was unique and limited to the stage at which epithelial proliferation was high. In contrast, mammary gland ductal expansion was notably attenuated in the vicinity of implanted recombinant TIMP-1-releasing pellets (Fata et al., 1999). Loss of TIMP-3 is followed by increased -MMP-7 expression and increased beta-catenin signalling in mouse embryonic fibroblasts (MEFs) and mammary epithelial cells (MECs). Furthermore, recombinant TIMP1, TIMP3 and TIMP4 inhibited ductal elongation, whereas TIMP2 promoted this process (Hojilla et al., 2007).

Steroid hormones are critical for normal mammary gland development. However, differences exist between human and mice regarding their actions (Timmermans-Sprang et al., 2017). In mouse, the initial proliferative response of the mammary epithelium to progesterone is mediated by the A isoform of progesterone receptor (PR), while the B isoform is needed for a proper lobular alveolar development during pregnancy (Kariagina et al., 2007). By contrast, in the normal human breast, both PRA and PRB are coexpressed in the same cells implying species-specific regulation of the isoforms (Mote et al., 2006). MMP-2 expression correlate with the levels of PR. The balance of expression levels of PR-A and PR-B isoforms is important for establishing a link between hormonal response, modulation of MMP activity and maintenance of basement membrane integrity (Simian et al., 2009).

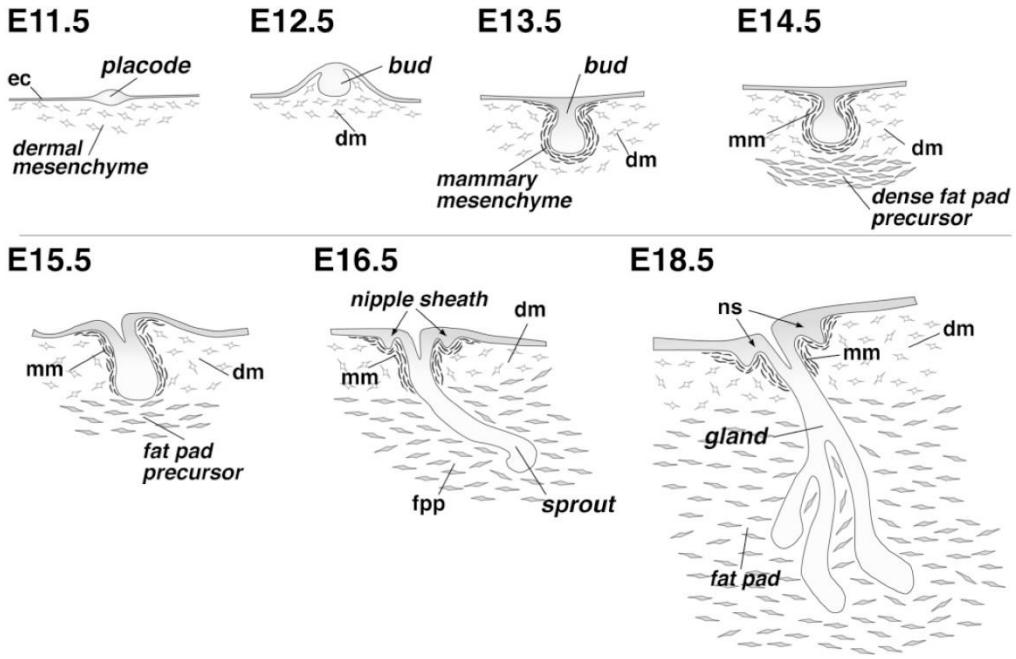

Figure 1.4 Schematic overview of mammogenesis in the mouse embryo. At E11.5 each mammary rudiment exists as a placode, a lentiform ectodermal thickening that is visible as a slight elevation above the surrounding ectoderm. At E12.5 each placode has transformed into a bulb of epithelial cells that is morphologically distinct from the surrounding ectoderm. Each bud with its contiguous mesenchyme is elevated above the ectoderm as a knob or dome. At E13.5 the buds have sunk into the underlying dermal mesenchyme. A few layers of mesenchymal cells directly adjacent to the bud condense and are referred to as the mammary mesenchyme. At E14.5 the deeper mesenchyme under the mammary bud differentiates into the dense fat pad precursor. At around E15.5 each bud elongates as a sprout, and the ectodermal cells of the epidermis ingress into this sprout, forming a ductular structure called the mammary sprout. The fat pad precursor becomes less dense and is also in contact with the distal part of the sprout. At E16.5 this sprout forms a lumen and opens up at the skin, where the nipple sheath forms by epidermal invagination. At E18.5, 1 day before birth, the sprout has developed into a small arborized gland invading the fat pad. Abbreviations: ec, ectoderm; dm, dermal mesenchyme; mm, mammary mesenchyme; fpp, fat pad precursor; ns, nipple sheath. (Adapted from (Veltmaat et al., 2003)).

1.1.5.2 MMPs trigger bone growth

The human and mouse bone growth and remodeling require metalloproteinase activity and extensive matrix remodeling (Paiva and Granjeiro, 2014, 2017). Several geneticly modified mice model were generated, namely for MMP-2, -9, -13, -14 and -16. Because of the cell specific expression of these proteins in mice, there are extreme variations in the mice phenotypes and involved molecular mechanisms (Aiken and Khokha, 2010).

Data reported that MMP-2 knockout mice displayed progressive loss of bone mineral density, articular cartilage destruction and abnormal long bone (Mosig et al., 2007). Moreover, these changes are associated with decrease in the number of osteoclast and osteoblast in vivo. Compare with wildtype mice, loss of MMP-2 in

murine osteoblasts upregulates bone sialoprotein and osteopontin expression in a circuit regulating bone homeostasis (Mosig and Martignetti, 2013).

MMP-9 knockout mice exhibit an impaired skeletal growth plate vascularization and ossification. But transplantation of wildtype bone marrow rescues vascularization and ossification, indicating that MMP-9 expressing cells is of bone marrow origin (Vu et al., 1998; Vandooren et al., 2013). Mutant mice models both deficient for MMP-9 and MMP-13 display severely impaired endochondral growth, prolonged chondrocyte survival time and decreased ECM remodeling (Stickens et al., 2004).

Membrane type MMPs also have crucial functions in skeletal defects, due to the fact that MMP-14 collagenolytic activity is essential for remodeling of skeletal and connective tissues. MMP-14 is the main protease responsible for development of secondary ossification centers (Ulici et al., 2009). MMP-16 is expressed in mesenchymal tissues of the skeleton, and MMP-16 knockout mice have reduced proliferation and migration ability of mesenchymal cells in the bone. Moreover, double deficiency for MMP-14 and MMP-16 leads to severe embryonic defects in palatogenesis and bone formation because of the loss of indispensable collagenolytic activities for ECM remodeling (Shi et al., 2008).

1.1.5.3 MMPs in wound healing and cell migration

Single MMP substrate may not be sufficient to explain the whole course of wound healing. Recent data indicated the expression of several MMPs in several cell types after injury, like immune cells, epithelial cells and mesenchymal cells. The spatial and temporal expression of MMPs and their inhibitors play essential roles in acute or chronic wound repair and regulate extracellular matrix degradation and deposition (Krishnaswamy et al., 2017). Thus defining the expression of MMPs is essential to understand the cell migration and wound healing.

MMP-1 cleaves specific components of the ECM, thereby providing new substrates that facilitate keratinocytes migration and invasion (Seo et al., 2015). After injury, invariably MMP-1 expression is induced in basal keratinocytes by the binding of α2β1 integrin to type I collagen. Based on the catalytic activity of MMP-1, basal keratinocytes are able to move on type I collagen. In vitro assays demonstrated the motility of human keratinocyte on type I collagen (Pilcher et al., 1997). MMP-1 is also able to digest fibrous scar tissue and improves injured muscle healing, further

enhancing muscle regeneration by improving myoblast migration (Wang et al., 2009). This illustrates that MMP-1 is promoting cell movement.

MMP-8 knockout mice have an altered inflammatory response and a significant delay of wound closure, with the delay of recruitment of immune cells at early time points (Gutiérrez-Fernández et al., 2007). Furthermore, TGF-β pathway alterations were involved in these changes. But bone marrow transplantation from wildtype mice rescued the delay of wound repair. Analysis of other MMPs indicated an increased expression of MMP-9 in MMP-8 null mice (Gutiérrez-Fernández et al., 2007). Another study indicate that the serum level of MMP-8 and MMP-9 may be used as early markers for remission after traumatic spinal cord injury (Moghaddam et al., 2017), suggesting that MMP-8 and MMP-9 might act together in the injury process.

Pro-angiogenic factors are important for the success of wound healing processes. The release of ECM bound TNF-α and VEGF factors can be induced by MMP-2 and MMP-9. Then it led to the proliferation and migration of endothelial cells to promote wound healing angiogenesis (Galis et al., 2002). MMP-2 knockout mice have altered wound repair processes in the injured mouse spinal cord because of leading to vascular instability and regression (Trivedi et al., 2016).

1.1.5.4 MMPs and vascular development

Degradation of the endothelial basement membrane is the first step of sprouting angiogenesis. Then cells migrate into the matrix and generate space to allow endothelial cells to form a proper lumen. MMP-9 has a crucial function in the angiogenic switch of human endothelial cells (Yang et al., 2015). MMP-9 knockout mice show angiogenic phenotype during development of long bones as mentioned above. Selective cleavage of VEGFR1 by MMP-14 may play an important role in VEGFA-induced angiogenesis (Han et al., 2016). MMP-14 null mice also display pathological vascular development defects (Oblander et al., 2005). These suggest that the vascular network complex can be damaged by MMPs dysfunction.

During angiogenesis, the processing of growth factors and cytokines by MMPs always contributes to new vessels formation and cell signalling transduction. Such as ECM-bound VEGF, which is in an inactive form in complex with connective tissue growth factor (CTGF), becomes active after cleavage by MMP-1, -3, -13 and -14 (van Hinsbergh and Koolwijk, 2008).

MMPs and TIMPs play a complex role in regulating angiogenesis. MMP-1, MMP-2 and MMP-9 facilitate vascularization, but all four TIMP members generally function to inhibit angiogenesis. Evidence showed that TIMP-1, TIMP-2 and TIMP-3 have anti-angiogenic activity both in vivo and in vitro by different molecular mechanisms (Baker et al., 1998; Fink and Boratyński, 2012). Moreover, the chemical synthetic general MMP inhibitors was sufficient to block angiogenesis in cancer, autoimmune and cardiovascular disease (Benjamin and Khalil, 2012; Liu and Khalil, 2017). These data indicate that the angiogenesis activity of MMPs could be inhibited by either TIMPs members or chemical MMPs inhibitors.

MMPs have two-side effect in the process of angiogenesis, both promoting and inhibiting angiogenesis processes. The function of MMPs on promoting angiogenesis hands on the following events : i) initiating the intracellular integrin signalling pathway; ii) releasing ECM-bound proangiogenic factors; iii) degrading ECM substrates in the periphery of angioblastic endothelial cells (Stetler-Stevenson, 1999). The following mechanisms are involved in the way MMPs inhibit angiogenesis: i) cleavage of the NC1 domain of collagen XVIII and generation of the angiogenesis inhibitor endostatin by cathepsin L (Ferreras et al., 2000); ii) shedding of angiogenesis-related cell surface bound urokinase type plasminogen activator receptors (u-PAR) and decreasing the outgrowth of capillary structures (Koolwijk et al., 2001); iii) cleavage of plasminogen and generation of angiostatin that inhibits the proliferation of microvascular endothelial cells (Cornelius et al., 1998).

1.1.5.5 MMPs and immune response

Tissue inflammation can lead to chronic inflammatory diseases. Recent researches provide results that MMPs modulate different aspects of inflammation (Butler and Overall, 2013).

Observation suggested that threefold reduction of IL-1β and TNFα and fourfold increase in vein wall monocytes in MMP-2 knockout mice following venous thrombosis (Deatrick et al., 2013). Selective ablation of MMP-2 in mice showed exacerbates experimental colitis (Garg et al., 2006). This indicates that MMP-2 involves in inflammatory response in different diseases.

MMP-3 plays an important role in the pathology of rheumatoid arthritis. Human serum active MMP-3 level is correlated with erythrocyte sedimentation rate and C-

reactive protein. Moreover, after patients receiving anti-TNF-α treatment, active MMP-3 level in the serum was significantly reduced (Sun et al., 2014), reflecting the anti-inflammatory effects of the treatment. Nitric oxide and pro-inflammatory mediator synthesis promoted by lipopolysaccharide was significantly down-regulated by MMP-3 in vitro (Takimoto et al., 2014), indicating that MMP-3 possesses anti-inflammatory functions.

MMP-7 was also detected in the lung airway epithelium. A study showed that MMP-7 is required for neutrophil recruitment and is responsible for the lung inflammatory response through the shedding of syndecan-1 (Chen et al., 2009). MMP-7 shedding of syndecan-1 accelerates cell migration and wound closure by controlling α2β1-integrin to assume a less active conformation, thereby amplifying cell adhesion to collagen.

Leukocyte derived MMP-9 is the main airway MMP which controls neutrophils egression. Allergen-challenged MMP-9 knockout mice display severe allergic lung phenotype, and less neutrophils and eosinophils accumulated in bronchi alveolar lavage. This can be explained by the contribution of MMP-9 to immune cell recruitment by providing a chemokine gradient of chemokine (C-C motif) ligand 7 (CCL7), CCL17 and etotaxin (Corry et al., 2004). Another study defined MMP-9 roles in mediating the inflammation profile by modifying macrophage polarization (Ma et al., 2015), explaining early mechanisms that stimulate ageing-induced diastolic dysfunction.

MMP-12 reduced macrophage migration and influx in cigarette smoke-induced emphysema by releasing TNF-α from macrophages, and only MMP-12 wildtype mice showed increased lung tumor TNF-α protein and the endothelial activation marker E-selectin (Churg et al., 2003). Biological assays carried out in vitro showed compound 4a is a promising hit compound since it displayed a nanomolar affinity for MMP-12 with a marked selectivity over MMP-1, -9, and -14 (Nuti et al., 2018). Thus MMP-12 selective inhibitors displayed a significant role in the treatment of lung inflammation.

1.1.5.6 MMPs associate with adipogenesis and body metabolism

Adipose tissue produces different MMPs, and MMPs are involved in adipogenesis. Many studies revealed the relationship between MMPs expression and insulin resistance or obesity.

MMP-2 deficient MEFs demonstrated markedly reduced differentiation into mature lipid-containing adipocytes, as showed by decreased expression of pro-adipogenic markers and 90% reduced intracellular lipid content (Bauters et al., 2015). But loss of MMP-9 in vitro has no obvious effect on the differentiation of 3T3-F442A pre-adipocytes into mature adipocytes (Bauters et al., 2014). In a model of rats fed on a sucrose-rich diet, expanded adiposity and insulin resistance are associated with decreases in MMP-2 and MMP-9 levels in epididymal adipose tissues (Miksztowicz et al., 2014). In human type 2 diabetic and healthy subjects, TIMP-1, TIMP-2, MMP-2 and MMP-9 plasma levels are increased in diabetic patients than those in healthy condition, which may reflect dysfunction of ECM metabolism (Derosa et al., 2007).

Decreased level of MMP-3 has been reported in the adipose tissue of transcription factor retinoid-related orphan receptor gamma (RORγ) knockout mice, and differentiation of adipocyte progenitor cells in vivo from RORγ knockout mice is boosted. RORγ knockout mice are protected from hyperglycemia and insulin resistance (Meissburger et al., 2011).

High protein level of MMP-13 was detected in adipose tissue. MMP-13 knockdown by siRNA in 3T3-L1 cells results in reduced adipocyte differentiation (Shih and Ajuwon, 2015).

In addition, TIMPs are also involved in the adipogenesis process. The increased plasma levels of of TIMP-1 and TIMP-2 were reported in human type 2 diabetes (Meissburger et al., 2011). TIMP-1 is a negative regulator of adipogenesis. Recombinant murine TIMP-1 inhibited subcutaneous primary pre-adipocytes differentiation. In vivo, recombinant TIMP-1 treated over nutrition mice displayed an impaired metabolic profile and enlarged adipocytes (Meissburger et al., 2011). This might contribute to detrimental metabolic consequences like insulin resistance, lipid accumulation and fatty acid overload. On the other hand, the absence of TIMP-3 in insulin receptor haploinsufficient mice results in vascular inflammation and type 2 diabetes (Federici et al., 2005).

1.1.5.7 MMPs functions from mutant mice

Analysis of genetic knockout mutants provide a good way to study the function of MMPs. But single mutants are always showing benign phenotypes, with all MMP-

knockout mice surviving at least the first three postnatal weeks (Table1.3), indicating adaptive development and enzymatic compensation.

So far 16 mutants have been analyzed. Most of them only show significant defects under pathological conditions, like inflammation, infection and wound healing (Table1.3). One exception is MMP-20, MMP-20 null mouse has a severe and profound tooth phenotype. Specifically, the null mouse does not process amelogenin properly, possesses an altered enamel matrix and rod pattern, has hypoplastic enamel that delaminates from the dentin, and has a deteriorating enamel organ morphology as development progresses (Caterina et al., 2002) .

MMP	Phenotype	Ref.
MMP-2	No overt phenotype, reduced body size	
	Reduced tumor progression and neovasculation	
	Decreased primary ductal invasion in the mammary gland	
	Defects in osteoblast and osteoclast growth, decreased joint erosion, bone mineralization	(Mosig et al., 2007)
MMP-3	No overt phenotype	(Mudgett et al., 1998)
	Impaired onset of T-cell proliferation, impaired contact dermatitis	(Wang et al., 1999)
	Defect in wound contraction	(Bullard et al., 1999)
	Altered secondary branching morphogenesis in the mammary gland	(Wiseman et al., 2003)
MMP-7	No overt phenotype	
	Impaired tracheal wound repair	(Dunsmore et al., 1998)
	Innate immunity defects	(Wilson et al., 1999)
	Defective prostate involution	(Powell et al., 1999)
MMP-8	More susceptible to develop skin cancer, impaired wound healing in skin	
	Altered inflammatory response in wounds, delay of neutrophil infiltration	
	Altered TGF-β signalling	(Gutiérrez-Fernández et al., 2007)
MMP-9	Impaired primary angiogenesis in bone growth plates	(Vu et al., 1998)
	Resistant to bullous pemphigoid	(Liu et al., 1998)
	Contact dermatitis: delayed resolution	(Wang et al., 1999)
	Impaired vascular remodeling	(Galis et al., 2002)
	Delayed healing of bone fractures	(Colnot et al., 2003)
MMP-10	No overt phenotype	
	Pathological induced phenotype: pulmonary inflammation and mortality	(Kassim et al., 2007)
MMP-11	No overt phenotype	
	Decreased chemical-induced mutagenesis	(Masson et al., 1998)
MMP-12	No overt phenotype	(Shipley et al., 1996)
	Impaired macrophage proteolysis	(Shipley et al., 1996)
	Resistant to cigarette smoke-induced emphysema	(Hautamaki et al., 1997)
MMP-13	No overt phenotype	
	Induction of MMP-8 expression in *MMP13*-/- wounds	(Hartenstein et al., 2006)

	Bone remodeling defects	(Stickens et al., 2004)
MMP-14	Premature death; skeletal defects and dwarfism	
	Normal at birth but defect in remodeling of the connective tissue, increased bone resorption and defective secondary ossification centers and die by 3–12 weeks	(Holmbeck et al., 1999)
	Angiogenesis defect and defects in submandibular gland and lung	(Oblander et al., 2005)
MMP-16	Growth retardation	(Shi et al., 2008)
MMP-17	No overt phenotype	(Rikimaru et al., 2007)
MMP-19	Decreased skin carcinogenesis and obesity	(Pendás et al., 2004)
MMP-20	Defects in tooth enamel	(Caterina et al., 2002)
MMP-24	Abnormal response to sciatic nerve injury	(Pendás et al., 2004)
MMP-28	No overt phenotype; elevated macrophage recruitment in lung	(Komori et al., 2004)
MMP-2, -9	Impaired tumor invasion and angiogenesis	(Masson et al., 2005)
MMP-2, -14	Die immediately after birth. Because of immature muscle fibers, abnormal vessels and respiratory failure	(Oh et al., 2004)
MMP-9, -13	Shortened bones	(Stickens et al., 2004)
MMP-14, -16	Die on day after birth due to cleft palate	(Shi et al., 2008)

Table 1.3 Phenotypes of MMPs knockout mice. (Adapted from (Löffek et al., 2011)).

1.1.6 MMPs and cancer

In the context of tumor microenvironment, numerous evidence support the notion that MMPs facilitate tumor cell metastasis through extracellular matrix remodeling and breakdown of physical barriers like the basement membrane (Kessenbrock et al., 2010; Yadav et al., 2014). But now some MMPs appear to have multiple biological roles during cancer progression, depending on tumor stage and tumor site on both primary and metastatic tumors (Giannandrea and Parks, 2014; Ren et al., 2015). MMPs expression in the tumor neighboring stroma is induced by cancer cells in a paracrine manner. Through the secretion of growth factors and interleukins, cancer cells stimulate neighboring fibroblasts to constitute a major source of MMPs, MMPs are therefore considered as a good target for therapeutic intervention by natural and synthetic inhibitors (Murphy, 2008). Many matrix metalloproteinase inhibitors (MMPIs) have been developed to control MMPs enzymatic activity in pre-clinical trials for tumor treatment (Alaseem et al., 2017; Winer et al., 2018).

1.1.6.1 MMPs in cancer cell proliferation

Uncontrolled cell growth is a common characteristic of cancer. It includes the notion that cancer cells are sensitive to growth promoting signals and/or insensitive to antigrowth signals. MMPs may potentially modulate the bioavailability of many important factors, and play pivotal roles in perturbing the balance between growth and antigrowth signals in the tumor cell microenvironment.

MMPs are involved in modulation of tumor cell growth by a variety of mechanisms. The extracellular domain of many membrane-associated proteins are released from cell membrane by proteolysis to yield soluble regulators. For instance, TNFα converting enzyme (TACE) has been identified as a responsible protease for the shedding of TNFα, and by deficiency of TACE uncovered larger role of TACE in the processing of other cell surface factors, like transforming growth factor-α (TGF-α), L-selectin adhesion molecule and TNF receptor (Peschon et al., 1998). ADAMs family members also play key functions. Members of the ADAM and MMP can release the cell-membrane-precursors of many growth factors, like IGFs and the EGFR ligands that promote proliferation. Several MMPs (MMP-1, -2, -3, -7, -9, -11 and -19) was reported to cleave IGF-binding proteins that regulate the function of the growth factors (Mañes et al., 1997; Nakamura et al., 2005). Cancer cells derived MMP-7 was reported

cleaved all six IGFBPs in the microenvironment surrounding the tumor, resulting in IGF-mediated IGF-1R phosphorylation, thereby favoring cancer cell growth and survival (Nakamura et al., 2005). It was also found that ADAM 12-S cleaves IGFBP-3 and IGFBP-5, but not IGFBP-1, -2, -4, or -6 (Loechel et al., 2000). EGFR is overexpressed in several types of solid tumors, and implicated in cancer cell progression as a mediator of cell proliferation (Gialeli et al., 2009; Cancer Genome Atlas Network, 2015). Shedding of membrane-anchored ligands of EGFR were observed under the action of ADAM-10 and ADAM-17 (Sahin et al., 2004; Urriola-Muñoz et al., 2018). After the shedding of E-cadherin by ADAM-10, β-catenin translocates to the cell nucleus and leads to cell proliferation (Maretzky et al., 2005).

TGF-β signalling pathway plays an important role in carcinogenesis. MMPs might inhibit cancer-cell growth through the activation of TGF-β in the tumor microenvironment (Derynck et al., 2001; Santibanez et al., 2018). As an important biomolecule in cancer that regulates cell behavior, the inactive pro-form of TGF-β is proteolytically activated by MMP-9, -2 and -14 in a similar way (Yu and Stamenkovic, 2000; Mu et al., 2002). Knockdown of TGF-β1 expression in the tumor cells negatively affected MMP-9 gene expression (Moore-Smith et al., 2017).

Markedly, MMPs can be recruited by glycosaminoglycans (GAGs) chains to release growth factors from cell surface and induce cancer cell proliferation. For instance, MMP-7 exerts high affinity for heparan sulfate chains. And the cell surface receptors of heparan sulfate chains, such as some variant isoforms of CD44, anchor the proteolytically active form of MMP-7, resulting in the cleavage of HB-EGF (Yu et al., 2002).

The researches mentioned above provide us a different insight on the proteolytic enhancement of tumor cell proliferation. Future work might focus on specific inhibition of these metalloproteinases to interfere with uncontrolled cell growth and proliferation in several tumors.

1.1.6.2 MMPs in cancer cell apoptosis

Apoptosis is a process of programmed cell death, including blebbing, cell shrinkage, nuclear fragmentation, chromatin condensation, chromosomal DNA fragmentation, and global mRNA decay (Monti et al., 1992). Elude regulation of

normal apoptosis permits cell survival in the presence of genetic instability, thus increases the tumor size and cell number (Hassan et al., 2014).

MMP-3, -7, -9 -11 and -14 regulate apoptosis. Nuclear localization of MMP-3 can induce apoptosis via its catalytic activity (Si-Tayeb et al., 2006). MMP-7 and ADAM10 exert anti-apoptotic signals on cancer cells by cleaving FASL. This proteolytic process inactivates Fas receptor activity and induces resistance to apoptosis signal and cancer cells chemoresistance or promotes apoptosis of the neighboring cells (Mitsiades et al., 2001; Kirkin et al., 2007). Moreover, MMP-7 inhibits apoptosis by cleaving pro-HB-EGF to generate mature HB-EGF, which promotes cell survival by stimulating the ERBB4 receptor tyrosine kinase (Yu et al., 2002). MMP-9 (Bergers et al., 2000) and MMP-11 (Boulay et al., 2001) not only reduce cancer cell apoptosis, but also increase apoptosis during development (Vu et al., 1998; Ishizuya-Oka et al., 2000). MMP-11 might act as a survival factor and inhibit cancer cell apoptosis by cleaving IGFBP-1 and releasing IGFs (Mañes et al., 1997; Baserga, 2000). Deficiency of MMP-11 increases spontaneous apoptosis in nude mice tumor xenografts by implantation of MCF-7 transfectants (Wu et al., 2001). In the presence of MMP-14-dependent proteolysis, it confers luminal-like breast cancer cells with the ability to circumvent apoptosis when embedded in a collagen gel and after orthotopic implantation in vivo (Maquoi et al., 2012).

MMPs or ADAMs are also involved in the apoptotic process by cleaving E-cadherin and PECAM-1 during apoptosis of epithelial or endothelial cells (Ilan et al., 2001; Steinhusen et al., 2001). Shedding of these adhesion molecules might actively interrupt extracellular signals and contribute to the typical rounding up of apoptotic cells. Moreover, proteolytic shedding of tumor-associated major histocompatibility proteins complex class-I related proteins by ADAM-17 may facilitate tumor immune escape under natural killer (NK) cell-mediated cytotoxicity toward cancer cells (Waldhauer et al., 2008).

1.1.6.3 MMPs in cancer angiogenesis

It is already known that different MMPs are expressed by a variety of tumors and each MMP can contribute to specific vascular events in the same tumor type (Littlepage et al., 2010). The main MMP members participating in tumor angiogenesis are MMP-

2, -9 and -14 (Deryugina and Quigley, 2015; Deok-Hoon Kong et al., 2017), while MMP-1 and MMP-7 are less involved.

VEGF is the most important mediator of blood vessel formation in tumor tissue and a main target for clinical therapy. Conveyed by inflammatory cells, MMP-9 triggers the angiogenic switch during carcinogenesis by making sequestered VEGF bioavailable for its receptor VEGFR-2 in pancreatic islet tumors (Bergers et al., 2000). The activation of MMP-9 is associated with angiogenesis via regulation of secretion of angiostatin and VEGF in prostate cancer cells (Gupta et al., 2013). Interestingly, VEGF prevents tumor cell migration along blood vessels, but it promotes perivascular tumor cell invade deep into the brain parenchyma (Du et al., 2008). Furthermore, VEGF bioavailability is regulated extracellularly by MMPs through intramolecular processing. The cleavage of matrix-bound isoforms of VEGF by MMP-3, -7, -9, or -16 results in modified VEGF molecules with altered bioavailability, which alters the vascular patterning of tumors (Lee et al., 2005).

MMP-9 is also regulating vasculogenesis (Deryugina and Quigley, 2015). Tumors angiogenesis and growth was prevented by transplanting into irradiated tissue in MMP-9-deficient mice, but it was restored by transplanting CD11b-positive myeloid cells from MMP-9-sufficient mice, indicating that MMP-9 is essential for tumor vasculogenesis (Ahn and Brown, 2008). The results suggest that MMP-9 could be an effective target for adjunct therapy to enhance the tumor radiotherapy.

Among MMP-9-expressing cell types, a special role is attributed to MMP-9 released by inflammatory neutrophilic granules. Neutrophil-derived pro-MMP-9 is more readily activated to drive tumor angiogenic response, because it is not complexed with TIMP-1 and the catalytic domain is activated (Ardi et al., 2007). Moreover, the hemopexin domain and active site together with the basic fibroblast growth factor-2 (bFGF-2) pathway are required for the neutrophil MMP-9-driven angiogenesis (Ardi et al., 2009). This shows that different source of MMPs may function in different ways and highlights the important functions of proteinase inhibitors on MMPs. In a mouse model of pancreatic cancer, depleting neutrophils significantly reduces angiogenic switching in dysplasia (Nozawa et al., 2006). These data point to an important role of neutrophils in the induction of tumor angiogenesis.

MMPs also regulate vascular permeability and stability. Particularly MMP-14 appears to mediate the vascular response to tumor progression though activation of

TGF-β signalling (Sounni et al., 2010). TGF-β signalling antagonists or metalloproteinase inhibitors potentially could improve patient care as they may increase the delivery of therapeutics or molecular contrast agents into premalignant tissue and tumors.

The degradation of extracellular molecules may generate bioactive fragments that inhibit angiogenetic processes. For example, angiostatin is a cleavage product with antiangiogenic function and angiostatin production by MMP-12 may explain the role for MMP-12 in suppressing the growth of lung metastases (Houghton et al., 2006). The active form of endostatin is generated from the cleavage of type XVIII collagen by MMP-3, -7, -9, -13, and -20 (Heljasvaara et al., 2005). In conclusion, the effects of MMPs on angiogenesis might be diverse, they can generate both angiogenesis promoting and inhibiting signal factors.

1.1.6.4 MMPs in cancer lymphangiogenesis

Lymphangiogenesis has crucial functions in tumor progression. It is directly linked with the formation of lymphatic metastases. The use of the broad-spectrum MMP inhibitory compound MMI270, showed that MMPs definitely have a general impact on lymphangiogenesis (Nakamura et al., 2004). But only a few papers directly link MMPs to the formation of lymphatic vessels.

MMP-2 modulating the VEGF bioavailability may also affect lymphangiogenesis and, in turn, promotes the lymph dissemination of metastases. For example, in a three-dimensional culture model for lymphangiogenesis by using mouse thoracic duct fragments embedded in a collagen gel, results proved that MMP-2 as an indispensable factor for lymphangiogenesis, as the lymphatic vasculature is impaired by targeted deletion of MMP-2 (Bruyère et al., 2008). Increased expression of MMP-1, -2 and -3 is linked with lymphatic invasion and lymph node metastases in human patients (Langenskiöld et al., 2005; Işlekel et al., 2007). Blockade of MMP-2 and -9 could inhibit corneal lymphangiogenesis by a selective MMP-2 and -9 inhibitor SB-3CT (Du et al., 2017). Data identified MMP-14 as an endogenous inhibitor of physiological lymphangiogenesis as mice lacking MMP-14 in either macrophages or lymphatic endothelial cells recapitulate corneal lymphangiogenic phenotypes, suggesting that the spontaneous lymphangiogenesis is both macrophages and lymphatic endothelial cells associated (Wong et al., 2016).

More researches are needed to clarify the biological functions of MMPs in the regulation of lymphangiogenesis.

1.1.6.5 MMPs in cancer epithelial to mesenchymal transition

The initial process of tumor cell invasion shares many characteristics with the epithelial-mesenchymal transition (EMT) program during tumor development, including loss of cell-cell adhesion and polarity, reduced intercellular interaction and increased cellular mobility, also reduced expression of epithelial markers such as E-cadherin, and increased expression of mesenchymal markers such as fibronectin and type I collagen (Kalluri and Weinberg, 2009; Polyak and Weinberg, 2009; Son and Moon, 2010). EMT has been associated with overexpression of several MMPs.

A noteworthy mechanism is brought up by showing that overexpression of MMP-3 is TGFβ induced eIF4E phosphorylation to promote the induction of EMT (Robichaud et al., 2015). The effects of MMP-3 are also associated with the expression of an alternative splice form of Rac1, which subsequently causes an increase in the generation of cellular reactive oxygen species (ROS) by mitochondria. The ROS stimulate the expression of the transcription factor Snail and EMT, and cause oxidative damage to DNA and genomic instability (Radisky et al., 2005). Recent evidence suggests that MMP-7 is not only a main pathogenic mediator in fibrotic lesion progression bot also a biomarker of renal fibrosis (Zhou et al., 2017). Pharmacological blockade of MMP-7 expression effectively attenuates renal fibrosis (Xiao et al., 2016). Another results indicate that MMP-28 induces cell invasion through a TGF-β dependent mechanism, which is also a powerful inducer of EMT (Illman et al., 2006). This suggests novel biological roles of TGF-β in the regulation of EMT and other epithelial cell functions in the induction of carcinogenesis (Heldin et al., 2009).

On the other hand, ADAM-10 is responsible for the shedding of E-cadherin, resulting in the disruption of communication between the cells, leading to disrupted cell adhesion and induction of EMT, followed by increased cell migration (Maretzky et al., 2005). Moreover, exosomes from Ras-transformed Madin-Darby canine kidney cells are reprogrammed with ADAM-10 or MMPs factors which may be capable of inducing EMT in recipient cells (Tauro et al., 2013).

1.1.6.6 MMPs in cancer migration

By regulating the dynamic cell-cell and cell-ECM interactions, the proteolytic activity of MMPs contribute to cancer cell migration. Evidence provided that αvβ3 and α2β1 integrins play an active role in regulation of MCF7 cell migration because they can serve as substrates for MMP-14 (Baciu et al., 2003). The cytoplasmic residue of MMP-14 is subjected to phosphorylation, and this post-translational modification regulates its activity. Ovarian cancer cells expressing MMP-14-Thr567 phosphomimetic mutants exhibit enhanced cell migration (Yang et al., 2017).

In gastric cancer patients, decreased endogenous MMP-14 level in gastric cancer suppressed cell migration and invasion via modulating EMT, MMP-2, -9, and -13 (Li et al., 2015). Hyaluronan was shown to promote head and neck squamous cell carcinoma migration and increased MMPs secretion, specifically the increased active form of MMP-2, through Rho kinase-mediated signalling (Torre et al., 2010). Perturbation of hyaluronan-CD44 mediated Rho and PI-3 kinase signalling pathways may be a novel therapy strategy.

Interestingly, the most important region for endothelial migration and invasion is the tumor cell invasive front, which adds on malignant behavior like invasion and metastasis. Membrane type MMP-14 is always exposed and activated at the cell surface in the vicinity of the invading endothelial sprouting (Jacob and Prekeris, 2015). But how proteolytic activity can help cells to move forward at the invasive front is a complex issue. The cellular protrusions with integrin-mediated matrix contacts enable the cell to pull itself forward, cell movement will be impeded by cell-matrix interactions fixed in the original position, or by collagen fibrils trapping thin cellular protrusions. In a model of tumor cell invasion through a three-dimensional (3D)-collagen matrix, a report showed that MMP-14 is present at both the leading and retracting edges of invading cells, but the collagenolytic activity was only present at the retracting edge (Figure 1.5). This allows the cell to generate pulling force between the cell body and leading edge. Cell movement in the front region was allowed by proteolytic activity, which is especially present in the area where collagen fibers interfered with cell movement (Wolf et al., 2007). The activity of MMP-14 must be blocked until the cell has moved from the protrusion to the adjacent zone. Several mechanisms contribute to this blocking step, which delays the activation process after cleavage by furin protease (Golubkov et al., 2007). One is temporary binding of inhibitors, like reversion-inducing-cysteine-rich protein with kazal motifs (RECK) and TIMP-2, another is the

delay of MMP-14 dimerization, which is needed for MMP-2 activation and cell migration (Itoh et al., 2006). Once MMP-14 is activated, both MMP-2 and MMP-14 can degrade various cell matrix proteins (Jacob and Prekeris, 2015).

The localization of MMPs to specialized cell surface protrusions, named invadopodia, is necessary for promoting migration and invasion. MMP-2, -9 and -14 were observed to localize to invadopodia, even by different mechanisms (Clark and Weaver, 2008; Jacob and Prekeris, 2015). It is known that MMP-2 and MMP-9 are enriched at the invadopodia, they are transported via specialized secretory vesicles directly from the trans-Golgi network to the invadopodia, Rab40b GTPase may play an important role in this process (Jacob et al., 2013). MMP-14 is recruited to invadopodia by means of its transmembrane and cytoplasmic domains (Nakahara et al., 1997). Endocytosis of MMP-14 is an important way of regulation of MMP-14 intracellular trafficking (Poincloux et al., 2009). Furthermore, polarity protein atypical PKCι controls endosome-to-plasma membrane traffic of MMP-14 in breast cancer cells (Rosse et al., 2014). These findings bring new insight for the design of potential therapeutic interventions.

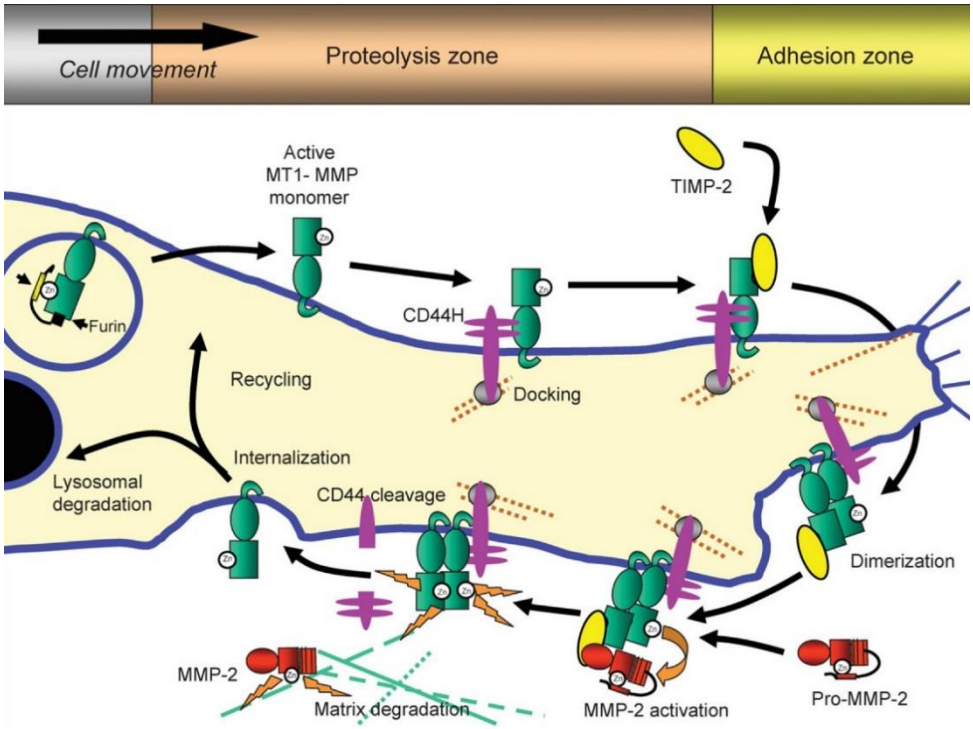

Figure 1.5 Schematic presentation of MMP-14 at the surface of the invading endothelial sprout. MMP-14 is activated and exposed at the cell surface in the vicinity of the invading sprout. It should be noted that the steps that are depicted at the upper part of the invading front of the cell, actually are concentrated at the leading front, as the endothelial sprout has no luminal-abluminal polarity. (Adapted from (van Hinsbergh and Koolwijk, 2008)).

1.1.6.7 MMPs in cancer invasion and metastasis

Dissemination of metastatic cancer cells and the outgrowth of secondary tumors at distant organs is the lethal outcome of majority of cancer patients. During invasion and metastasis, cancer cells must cross physical ECM barriers, paving the way through the peripheral space for invasion. The initiation of metastasis involves the destruction of the epithelial basement membrane and other matrix components, then cancer cells invade the surrounding tissue, leading to invasion into blood or lymphatic vessels from where cancer cells disseminate into distant organs, and establish new proliferating colonies (Kelley et al., 2014; Liotta, 2016; De Ieso and Yool, 2018). Publications suggest that metastatic tumor cells specifically localize to receptive sites, called premetastatic niches, in a complex interplay with hematopoietic progenitor cells and inflammatory cells (Peinado et al., 2017).

Experimental evidence for the role of MMPs in metastasis not only relies on in vitro invasion assays but also on in vivo xenograft model. An interesting mechanism of MMP-mediated signal transduction linked with increased metastasis is studied in the presence of MMP-1. The protease activated receptors (PARs) are a set of G protein-coupled receptors that have distinct functions in thrombosis, inflammation and tumor cell migration. An important role of MMP-1, which derived from tumor infiltrating mesenchymal cells, by cleaving of PAR-1, drives tumor cell migration and invasion (Boire et al., 2005; Malaquin et al., 2013). This result exemplify that MMP-1 in the stromal-tumor microenvironment can alter the behavior of malignant tumors through PAR1 and promote cell migration and invasion.

MMPs expressed at the interface between cancer and stromal cells play a pivotal function in osteolysis and dissemination into bone. In a rodent model of metastatic prostate cancer, a microarray analysis identified MMP-7 as being upregulated at the tumor-bone interface. It is expressed by osteoclasts triggers osteolysis and subsequent bone metastasis. MMP-7 was capable of processing receptor activator for nuclear factor κB ligand (RANKL) to a soluble form that promoted osteoclast activation. MMP-7-deficient mice documented reduced prostate tumor-induced osteolysis and RANKL processing (Lynch et al., 2005). In this context, cleavage by MMP-7 releases an active form of RANKL that promotes osteoclast activation without osteoblasts in the close proximity. A similar effect was then elucidated for MMP-1 and ADAMTS-1 by orchestrating a paracrine signalling cascade to modulate the bone microenvironment in favor of osteoclastogenesis and bone metastasis (Lu et al., 2009). Knocking down these

proteases in a highly bone-metastatic clone of the human breast cancer cell line MDA-MB-231 decreased the risk of bone metastasis (Lu et al., 2009). These findings support the idea that MMP-1 gene is one part of the multigenic program that mediates bone metastasis of breast cancer cells (Henckels and Prywes, 2013). Taken together, these proteinases could be promising therapeutic targets to prevent prostate or breast cancer metastasis to the skeleton system.

Coordinated targeting of MMP-2 and MMP-9 by microRNA or long non-coding RNA exerts anti-tumor effects in choroidal malignant melanoma (Wang et al., 2017). Moreover, in a immunohistochemistry analysis of human samples, expression of MMP-2 and MMP-9 proteins increased with the degree of extra-gastrointestinal stromal tumor risk (Wang et al., 2014).

By using high-resolution multimodal microscopy, studies have confirmed the importance of ECM remodeling by MMP-14 driven pericellular collagenolysis, which may facilitate individual and collective cell migration and invasion (Wolf et al., 2007; Lagoutte et al., 2016). Cross-talk between MMP-14 and CD44 results in phosphorylation of EGFR. Synthetic peptides mimicking the essential outermost strand motifs within the hemopexin domain of MMP-14 inhibit cancer cell metastasis and tumor growth (Zarrabi et al., 2011). Thus, MMP-14 serves as the major cell-associated proteinase necessary to confer normal or neoplastic cells with invasive activity.

Dysfunction of E-cadherin is shown associated with cancer progression (Carneiro et al., 2012, 2013). E-cadherin is cleaved by MMP-2, -3, -7, -9, and -14 (Grabowska and Day, 2012). For example, proteolytic cleavage of the cytosolic tail or extracellular domain of E-cadherin by MMP-9 generated soluble E-cad (sE-cad) fragment. Knockdown of MMP-9 by siRNA inhibited sE-cad production induced by EGF in SCC10A squamous carcinoma and further inhibited cancer cell migration and invasion (Zuo et al., 2011).

The MMP members are involved earlier in tumorigenesis, but also involved in the late events of the metastatic process, when cancer cells enter, survive and exit the blood vessels or lymph vessels (Hua et al., 2011). The plasma level of MMP-1 may serve as a useful noninvasive marker of detecting the advanced-stages of esophageal cancer (Chen et al., 2016). Expression of MMP-9 is also required for the latter phase of pancreatic cancer cells to liver metastasis (Lin et al., 2018). Therefore, MMPs activity is also involved in the final steps of malignant cell dissemination.

However, MMP activity might not be important for extravasation. For example, TIMP1-overexpressing cancer cells exit the vasculature equally as the control group, but after they leave the blood, there are smaller and fewer metastases due to diminished cancer-cell growth (Koop et al., 1994).

TIMP-1 has been thought to suppress tumor metastasis, but elevated TIMP-1 level also correlate with poor prognosis in cancer patients, suggesting its metastasis-stimulating role. For instance, in colorectal cancer patients, plasma TIMP-1 levels were correlated with liver and distant metastasis-associated disease relapse (Seubert et al., 2015). In mice, high levels of systemic TIMP-1 increased the liver susceptibility towards metastasis by triggering the formation of a premetastatic niche (Seubert et al., 2015). In H2009 lung adenocarcinoma cells, TIMP-1 overexpression enhances tumorigenicity and invasive behavior in brain metastasis (Rojiani et al., 2015). Although inhibition of MMP has been the primarily identified function of TIMP-1, MMP-independent interactions may also contribute to the growth of metastatic tumors.

1.1.6.8 MMPs in cancer immune surveillance

Inflammatory reaction and cancer cell development have complicated relations. The production of chemokines by immune cells are in many ways linked to tumor progression (Sarvaiya et al., 2013). The immune system is able to recognize and attack cancer cells, but cancer cells in the microenvironment have developed many ways to escape the immune surveillance. MMPs modulate the function of cytokines and chemokines resulting in the immune escape (Kessenbrock et al., 2010).

The inflammatory cells that infiltrate tumors include macrophages, neutrophils, NK cells and T lymphocytes. The proliferation of T lymphocytes is regulated by cytokine by means of the interleukin-2 receptor-α (IL-2Rα). In vitro studies showed MMP-9 can cleave IL-2Rα and thereby down-regulates the proliferation of cancer-encountered T lymphocytes (Sheu et al., 2001). The MMP-9-cleaved osteopontin fragment, OPN-32kDa, was responsible for myeloid-derived suppressor cells expansion, which may contribute to mice tumor evasion of the immune response (Shao et al., 2017). Additionally, NK cell cytotoxicity was significantly decreased in the oral squamous cell carcinoma cells which were pretreated with either MMP-2 or MMP-9 (Lee et al., 2008). MMP-11 generates a product by cleaving α1-proteinase-inhibitor, which suppress the sensitivity of tumor cells to NK cells (Kataoka et al., 1999).

Moreover, an increased number of macrophages and neutrophils infiltrates colon tumors in MMP-11 knockout mice compared with wildtype control (Boulay et al., 2001), demonstrating that MMP-11 inhibits a chemoattractant for these cells.

Numerous studies have shown that many members of the CCL/MCP family of chemokines are cleaved by MMPs into non-activating receptor antagonists with inflammation-dampening effects (McQuibban et al., 2002). For example, CCL8/MCP-2 is processed by MMP-1 and MMP-3. Indeed, the proteolytic cleavage of CCL8 can counteract the antitumor capacity of this chemokine in a melanoma model (Struyf et al., 2009). MMP-2 cleaves CCL7, and the cleaved fragment is inactivated and becomes an antagonist to the receptors that dampen inflammation (McQuibban et al., 2000). MMP-2 has also been shown to be responsible for the shedding of the MHC class I polypeptide-related sequence A, which is important for stimulating NK and T-cell anti-renal cell carcinoma immunity (Yang et al., 2014). These data indicate that proteolytic cleavage of a chemokine have strong effect in a clinically relevant setting of tumor development.

MMPs action on several chemokines results in decreased or increased migration and infiltration of leukocytes. The chemokine (C-X-C motif) ligand 8 (CXCL8) and its murine homologue are cleaved by MMP-9, leading to an increased their activity. But MMP-9 inactivates the CXCL7 precursor, CXCL1 and CXCL4 (Opdenakker et al., 2001). The bioactivity of CXCL11/I-TAC, a potent Th1 lymphocyte-attracting chemokine, is modulated by MMP-8, -9 and -12 (Cox et al., 2008). Although MMP-mediated N-terminal truncation of CXCL11 leads to inactivation of the chemokine and creates a potent receptor antagonist, further C-terminal cleavage abolishes the antagonist function and removes heparin-binding capacity of CXCL11, thereby solubilizing the chemokine from the ECM (Cox et al., 2008). These findings indicate that MMPs by regulating T cells may have pivotal effects on the adaptive antitumor immune response.

CXCR7, the chemokine receptor for CXCL11, is also expressed on many tumor cell types and can transmit growth- and survival-promoting signals. High affinity small molecule antagonist to CXCR7 impedes in animal tumor growth (Burns et al., 2006). Modulation of CXCL11 by MMPs might decrease the antitumor immune response and therefore have direct consequences on tumor survival (McQuibban et al., 2001). CXCL12 is cleaved and inactivated by several MMPs, like MMP-1, -3, -9, -13 and -14.

CXCR4 is a receptor for CXCL12 on leukocytes. Intriguingly, CXCR4 are highly expressed in human breast cancer cells, and neutralizing the interactions of CXCL12/CXCR4 by blocking antibodies greatly impairs metastasis of breast cancer cells to lungs and regional lymph nodes (Müller et al., 2001). Thus, cleavage of CXCL12 by MMPs might reduce tumor metastasis.

Although the immune system possibly delays tumor progression, chronic inflammation is also associated with cancer of the urinary bladder, liver, large intestine, gastric mucosa, ovary, prostate gland, breast and skin (Coussens and Werb, 2001). In animal models, macrophages, neutrophils and mast cells are contributors to the progression of cancer (Coussens and Werb, 2001). Numerous studies from genetic mutant mice show that MMPs play an important role in chronic as well as acute inflammation (Parks et al., 2004). One of the most conspicuous proinflammatory cytokines is TNF-α, which is expressed as a membrane-bound precursor (pro-TNF-α) on different kind of cells including macrophages and T cells. Proteolytic cleavage by ADAM-17 generate the soluble cytokinetic form of pro-TNF-α (Mohan et al., 2002). So ADAM-17 is also known as one of the major TACE. Furthermore, MMP-1, -2, -3, -9, -12, -14, -15, and -17 can be also the responsible converting mediators (Manicone and McGuire, 2008). These MMPs may be crucial TNF-α convertase in specific physiological or pathological conditions, as described for MMP-7 in the regulation of inflammation in a model of herniated disc resorption (Haro et al., 2000). Several tumors produce TNF-α, which promotes tumor growth in an nuclear factor kappa-light-chain-enhancer of activated B cells (NF-κB)-dependent manner (Luo et al., 2004), suggesting that the conversion of TNF-α by ADAM-17 and MMPs might be an important step in the tumor-promoting cascade. In addition, inflammatory cells synthesize several MMPs, including MMP-9, -12 and -14, that might promote tumor progression by secreting MMPs (Figure 1.6). Therefore, inflammatory cells can be coconspirators in carcinogenesis.

The proteolytic fragments of MMPs-processed ECM components may exert chemotactic properties. Macrophage elastase MMP-12 produces neutrophil-attracting peptides by degrading elastin (Houghton et al., 2006). Furthermore, breakdown of ECM during airway inflammation generates the neutrophil chemoattractant N-acetyl Pro-Gly-Pro (PGP), a tripeptide with chemotactic activity through activation of CXC chemokine receptors on neutrophilic granulocytes. Thus PGP might be a good

biomarker for neutrophilic inflammatory (Weathington et al., 2006). Mice deficient in MMP-8 in neutrophils are more susceptible to develop carcinogen-induced skin cancer (Balbín et al., 2003). MMP-8 is involved in the neutrophil recruitment to the sites of inflammation. There is a significant delay in wound closure and an altered inflammatory response in MMP-8 knockout mice, with a delay of neutrophil infiltration. These changes were accompanied by alterations in the TGF-β signalling pathway and a significant increase in the expression of MMP-9 (Gutiérrez-Fernández et al., 2007). The tendency to develop chronic inflammation in mice deficiency of MMP-8 might explain how loss-of-function mutations of MMP-8 contribute mechanistically to increased susceptibility of skin adenocarcinoma and melanoma progression in humans (Palavalli et al., 2009). But expression of MMP-8 in tumor cells might function as a metastasis suppressor through modulation of tumor cell adhesion and invasion behavior (Gutiérrez-Fernández et al., 2008). Thus, interference with the tumor-suppressing function of MMP-8 should be considered as one of the unwanted effects of broad-spectrum MMP inhibitors.

Therefore, MMPs orchestrate the recruitment of inflammatory cells as an essential component of tumor microenvironment-associated inflammation (Figure 1.6).

1.1.6.9 MMPs have nonproteolytic functions

Similar to a number of ADAMs, MMPs also show nonproteolytic capacities (Kessenbrock et al., 2015). The hemopexin domain of MMPs plays a crucial role in the nonproteolytic function. The first key evidence was established with the observation that TIMP-1 and TIMP-2 bind to several MMPs via their hemopexin domains. Indeed, activation of MMP-2 requires TIMP-2 that is bound to one molecule of MMP-14 via its catalytic domain and also is bound to pro-MMP-2 via its hemopexin domain (Itoh et al., 2001, 2008). A second molecule of MMP-14 then catalytically activates MMP-2.

Some MMP family members trigger cancer cell migration. But recent evidence suggests that they mediate chemotaxis even without their proteolytic domain. MMP-2 and MMP-9 precursor forms enhance cell migration. The hemopexin domain of MMP-9 is necessary for epithelial cell migration in a transwell assay independent of its proteolytic activity (Dufour et al., 2008). In this context, mitogen-activated protein kinase (MAPK) and phosphoinositide 3-kinase/phosphatidylinositol 3-kinase (PI3K)

pathways were found to be involved in this nonproteolytic function of MMP-9 (Dufour et al., 2008). Moreover, the cytoplasmic residue of MMP-14 regulates macrophages via its cytoplasmic-dependent non-proteolytic activity to boost cell migration, as genetic depletion of the cytoplasmic tail but not of the hemopexin or catalytic domain reduces the migration of macrophages during matrigel migration assay (Sakamoto and Seiki, 2009).

MMP members may interact with other extracellular components without inducing proteolytic cleavage. MMP-14 interacts with the C1q component of the complement system in a nonproteolytic, receptor-ligand manner, without inducing C1qr and C1qs proteinase activity, suggesting that this binding may inhibit activation of the complement proteinase cascade (Rozanov et al., 2004). More studies are yet required to elucidate the biological relevance of MMP-14-mediated inhibition of the complement system in tumorigenesis. MMPs also bind to members of the integrin family of cell surface receptors. A study showed that MMP-1 can stimulate dephosphorylation of AKT and neuronal death in cell culture through a non-proteolytic mechanism that involves changes in α2β1 integrin signalling (Conant et al., 2004). This study indicates that integrin binding, rather than proteinase activity, is relevant for MMP-1 transmitted cytotoxicity. In chronic lymphocytic leukemia, MMP-9 promotes B cell survival in a non-proteolytic manner via its hemopexin domain by docking to the surface receptors α4β1 and CD44v, which prevents B cell apoptosis (Redondo-Muñoz et al., 2010). The hemopexin domain of MMP-3 specifically binds and inactivates Wnt5b, further promotes hyperplastic mammary epithelial outgrowth in vivo in a nonproteolytic manner (Kessenbrock et al., 2013). This nonproteolytic functions of MMPs might be considered as one of the important aspects implicated in the failure of clinical trials using inhibitors of the MMPs catalytic domains.

In conclusion, these studies indicated that the complexity of the mode of MMPs action has expanded considerably from proteinases that simply degrade the ECM to various biological functions, even nonproteolytic capacities. MMPs have both cancer-promoting and cancer-inhibiting functions (Figure 1.6).

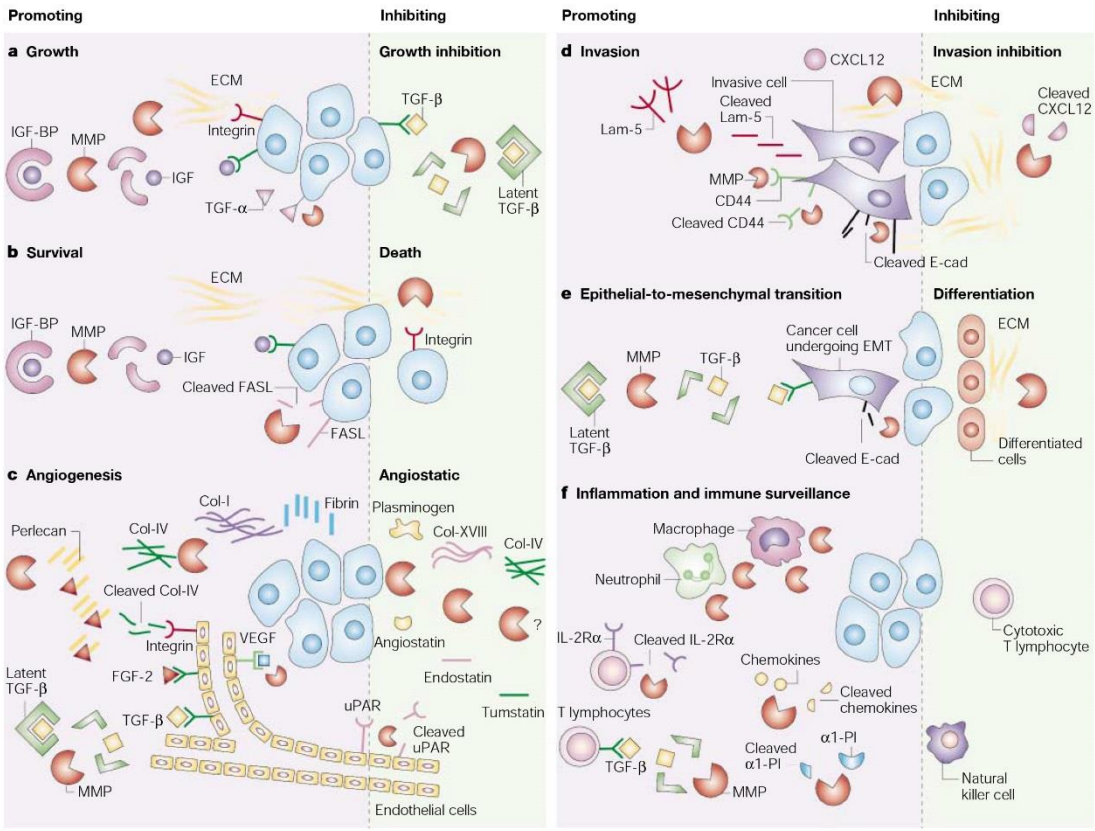

Figure 1.6 The MMPs have both cancer-promoting and cancer-inhibiting functions. And pathways with opposing effects on cancer progression are sometimes initiated by cleavage of the same substrate. a) MMPs promote growth of cancer cells by cleaving IGFBP, thereby liberating IGF; by shedding transmembrane precursors of growth factors including TGF-α; and by regulating the ECM, which promotes growth indirectly through interactions between ECM molecules and integrins. MMPs can inhibit cancer-cell growth by liberating TGF-β from the latent TGF-β complex. b) MMPs promote survival of cancer cells by liberating IGF and by cleavage of FAS ligand (FASL). MMPs also promote apoptosis, probably indirectly by changing the ECM composition, which influences integrin signalling. c) MMPs promote angiogenesis by increasing the bioavailability of the pro-angiogenic growth factors VEGF, fibroblast growth factor 2 (FGF-2), and TGF-β. These factors stimulate proliferation and migration of endothelial cells. FGF-2 is liberated by cleavage of the ECM protein perlecan. In addition, MMPs promote invasion of endothelial cells by cleaving structural components of the ECM, such as collagen types I (Col-I) and IV (Col-IV) and fibrin. Cleaved Col-IV acts pro-angiogenically by binding to αvβ3 integrin. MMPs act anti-angiogenically through cleavage of plasminogen and Col-XVIII, resulting in generation of the anti-angiogenic factors angiostatin and endostatin. MMPs might also participate in the generation of tumstatin, a fragment of Col-IV. Cleavage of urokinase-type plasminogen activator receptor (uPAR) on the cell surface of endothelial cells might inhibit angiogenesis. d) MMPs regulate invasion by degrading structural ECM components. Specifically, the MMPs promote invasion and migration by cleaving laminin 5 (Lam-5). MMPs also promote invasion by cleavage of the adhesion molecules CD44 and E- cadherin (E-cad). The released part of E-cad might then bind and inhibit the function of other uncleaved E-cad molecules. In addition, docking of MMP-9 to CD44 is required for cancer-cell invasion. MMPs might inhibit metastasis by cleavage of CXCL12. e) MMPs promote the EMT by cleaving the cell-adhesion molecule E-cad and by liberating TGF-β. MMPs also promote differentiation. For instance, tumors evolving in MMP-9-null mice are less differentiated than tumors evolving in wild-type mice. f) Reactive inflammatory cells provide some of the key MMPs involved in cancer progression, but MMPs also inhibit immune reactions against the cancer cells. MMPs cleave the interleukin-2 receptor-α (IL-2Rα) on T lymphocytes, thereby inhibiting the proliferation of the T lymphocytes; they liberate TGF-β, an important suppressor of T-cell reactions against cancer cells; they cleave α1-proteinase inhibitor (α1-PI), resulting in decreased cancer-cell sensitivity to natural killer cells; and they cleave various members of the CC and CXC chemokine families, with the result that these factors no longer attract leukocytes. (Adapted from (Egeblad and Werb, 2002)).

1.2 MMP-11

1.2.1 MMP-11 discovery

MMP-11 was originally discovered due to its high expression in a c-DNA library established from a human breast cancer biopsy (Basset et al., 1990). It was initially recognized as a member of the stromelysin subfamily according to its similarity with the other stromelysin members, so the gene product was also named stromelysin-3 (ST-3) (Basset et al., 1990). Unlike ST1 and ST2, ST3 has distinct mechanism of activation and proteolytic activity (Murphy et al., 1993; Pei and Weiss, 1995; Santavicca et al., 1996). MMP-11 appears to be a unique member exhibiting peculiar features and functions (Rio, 2002). Many studies confirmed the high overexpression of MMP-11 in cancer versus normal or benign breast samples (Chenard et al., 1996; Andarawewa et al., 2005).

1.2.2 MMP-11 genomic organization

MMP-11 is localized on human chromosome 22q11.2 and to the C band of mouse chromosome 10 showing a syngeneic conservation during evolution (Levy et al., 1992; Cole et al., 1998). The mouse and human MMP-11 gene were found to span 9.2 kb and 11.5 kb respectively, and contain eight exons and seven introns. The genomic organization of MMP-11 gene exons is well conserved compared with other MMP members, except for the last three exons corresponding to the hemopexin-like domain and to a long 3'UTR (Anglard et al., 1995). The first four exons match those of other classic MMPs while the remaining four exons are organized differently: 1) the hinge region in MMP-11 is an extension of exon five which encodes a portion of the catalytic domain; 2) the first Cys residue for the conserved disulfide bond in the hemopexin domain is not part of the exon encoding the hinge region as in other MMPs, but part of the first exon of the hemopexin-like domain; 3) a conserved intron located between the second and third exons of the hemopexin domains present in other MMPs is absent in MMP-11. These differences place MMP-11 outside of the main MMP cluster between the mammalian MMPs and the bacterial metalloproteinases (Murphy et al., 1991). The Xenopus MMP-11 gene also has a structure distinct from other MMPs, with its hemopexin domain encoded by four instead of six exons.

Analysis of the 5' region upstream of the TATA box shows several functional regulatory elements common to the human, mouse and/or Xenopus MMP-11 genes. A

proximal cis-acting retinoic-acid-responsive-element (RARE) of the DR1 type (direct repeat of the core motif PuGGTCA separated by 1 bp), and two distal RAREs of the DR2 type are present in the human and mouse MMP-11 genes. The Xenopus MMP-11 promoter is devoid of RARE element. The proximal DR1 is sufficient for MMP-11 promoter activity in vitro. This RARE may be responsible, at least partially, for the in vivo expression of MMP-11 since retinoic acid receptor beta and gamma (RARβ and RARγ)-deficient mice exhibit lower levels of MMP-11 (Guérin et al., 1997; Dupé et al., 1999). Additional distal elements have been reported (Luo et al., 1999; Ludwig et al., 2000). An AP1-like responsive element is responsible for the basal human MMP-11 promoter activity. This element is not present in the mouse promoter. One (human) and two (mouse) CCAAT/enhancer-binding-protein (C/EBP)-binding sites that efficiently bind the C/EBPβ transcription factor, are involved in the TPA-regulated induction of MMP-11 gene expression. The MMP-11 promoter also contains one (human and mouse) or two (Xenopus) GAGA factor binding sites. Moreover, a thyroid hormone responsive element (TRE), shared by human, mouse and Xenopus, is present in the distal region of the MMP-11 promoter. This TRE has been shown to be functional in frog, and MMP-11 is a direct immediate-early thyroid hormone (T3) responsive gene (Shi et al., 2007). In contrast to the other MMPs, no proximal AP1-binding site was identified in the MMP-11 promoter in all the species studied (Luo et al., 1999; Ludwig et al., 2000). Finally, in Xenopus, two transcription start sites (+1, -94) and a second TATA box (-87, -82) were reported, suggesting a possible second MMP-11 messenger RNA (Li et al., 1998). Similar organization leading to two types of messenger RNAs also exists in the human MMP-11 gene (Luo et al., 2002). Recently, it has been indicated that Sp1 is able to bind to the GC-boxes within the MMP-11 proximal promoter region and regulate MMP-11 expression. This regulation requires the formation of Sp1/Smad2 heterocomplexes, which are stimulated by an increase in the acetylation status of Smad. Besides, ERK1/2-MAPK, but not p38-MAPK or JNK, are also involved in the regulation of MMP-11 (Barrasa et al., 2012).

These results suggest that the MMP-11 gene evolved prior to most other MMP genes and uses distinct regulation pathways to achieve similar expression profiles and serve similar functions in mammals and amphibians.

1.2.3 MMP-11 protein structure

The MMP-11 gene encodes a pre-pro-protein from N-terminal end to C-terminal end, which containing a signal peptide, a pro-peptide, a furin recognition site, a catalytic domain and a hemopexin-like domain (Figure 1.7).

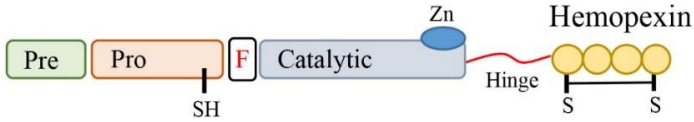

Figure 1.7 Scheme of MMP-11 protein structure. Pre: signal peptide; Pro: pro-domain; F: furin recognition site; SH: thiol group; Zn: zinc ion.

1.2.4 MMP-11 crystal structure

The catalytic domain of MMP-11 is made up of a 5 stranded β-sheet and 3 α-helices and displays the topology common to MMPs (Gall et al., 2001).The asymmetric unit contains six molecules related by a non-crystallographic imperfect 6-fold axis forming large solvent channels to which the active site is exposed. Each molecule is complexed with one molecule of the phosphinic inhibitor, two zinc atoms (one structural and one catalytic) and one calcium ion (Figure 1.8a). The active site is a large, negatively charged groove with the catalytic zinc atom lying on its surface, ligated by the side-chains of three histidine residues and the oxygen atoms of the inhibitor phosphinyl group (Figure 1.8b).

The topology of MMPs is remarkably well conserved, making the design of highly specific inhibitors difficult. The crystal structure clearly demonstrates that its S1' pocket looks like a tunnel running through the enzyme. This open channel is filled by the inhibitor P1' group which adopted a constrained conformation to fit this pocket, together with two water molecules interacting with the MMP-11 specific residue Gln215, which plays a pivotal role in determining the PI' selectivity as determined by site-directed mutagenesis (Holtz et al., 1999). These observations provide clues for the design of more specific inhibitors and show how MMP-11 can accommodate a phosphinic inhibitor mimicking a (D, L) peptide. The presence of a water molecule interacting with one oxygen atom of the inhibitor phosphinyl group and the proline residue of the Met-turn, suggests how the intermediate form during proteolysis may be stabilized. Furthermore, the hydrogen bond distance observed between the methyl of the phosphinic group and the carbonyl group of Ala182 mimics the interaction between this carbonyl group and the amide group of the cleaved peptidic bond. Thus, this characteristic of the MMP-11 protein structure allows to design synthetic inhibitors

exhibiting a longer chain in their P1' position leading to a higher specificity against MMP-11 than other MMPs, MMP-11 therefore represents an appropriate target for specific inhibitors in future cytostatic therapeutic approaches directed against the stromal compartment of human carcinoma (Rio, 2002).

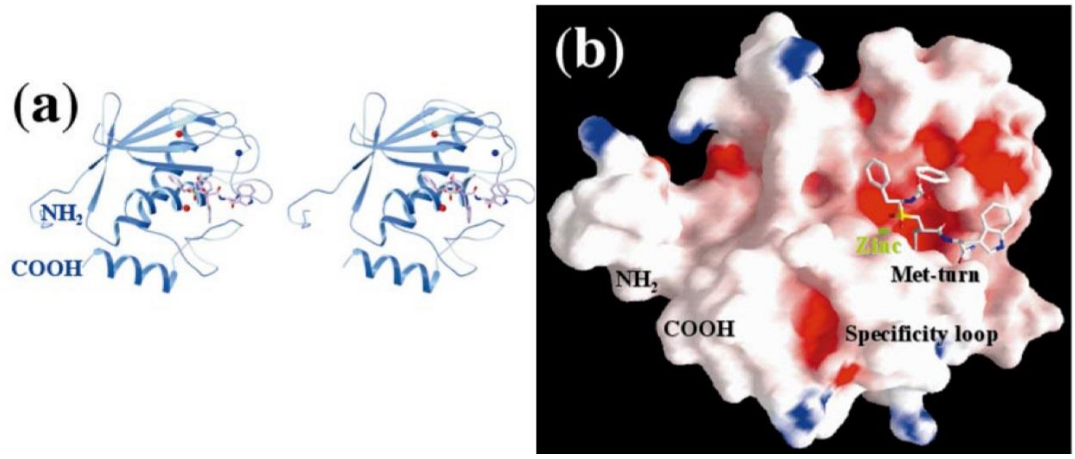

Figure 1.8 Crystal structure of the MMP-11 catalytic domain complexed with the phosphinic inhibitor. (a) Ribbon diagram showing the catalytic domain of ST3 (blue), the phosphinic inhibitor (pink), the two zinc atoms (red spheres) and the calcium atom (blue sphere). The Figure was created with Setor. (b) The molecular surface of the MMP-11 catalytic domain is coloured according to its potential (red: negatively charged residues; blue, positively charged residues). The catalytic zinc atom (green) lies on the surface of the active site. Adapted from (Gall et al., 2001).

1.2.5 MMP-11 secretion and activation

Unlike other MMPs, MMP-11 zymogen cannot be activated by organomercurials or detected by standard zymographic techniques in vitro. This unusual behavior has been attributed to structural characteristics peculiar to both its pro- and catalytic domains (Pei and Weiss, 1995; Santavicca et al., 1996). Moreover, several MMPs are normally synthesized and secreted as inactive zymogens, while MMP-11 is secreted as an active form.

The 54-56 kDa precursor form of MMP-11 is post-translationally modified in the cis- or media-Golgi into a 62-65 kDa pro-form. Thereafter, its processing into the 45-47 kDa mature form occurs in the trans-Golgi network, presumably following the glycosylation of serine/threonine residues in the pro-domain (Pei and Weiss, 1995; Santavicca et al., 1996). Subsequently, the 45-47 kDa mature species is generated intracellularly by furin, a trans-Golgi network-associated pro-protein convertase, which cleaves pro-MMP-11 at the C-terminal end of a unique RXRXKR motif, and is followed by secretion into the extracellular space. In the absence of MMPIs, the 45 kDa form is unstable and undergoes autocatalytic processing (Pei and Weiss, 1995).

Interestingly, MMP-14 which is produced by HT-1080 cancer cells cleaves MMP-11 catalytic domain at two sites, the PGG(P1)-I(P10)LA and V/IQH(P1)-L(P10)YG scissile bonds. Since MMP-14 is present at the invasive cancer cell membrane, whereas MMP-11 is secreted into the tumor microenvironment, this irreversible MMP-11 proteolytic inactivation by MMP-14 might represent a pivotal regulatory mechanism to control the inappropriate/excessive MMP-11 bioavailability (Buache et al., 2014).

1.2.6 MMP-11 mature and recombinant protein

The pro- and the mature forms of human MMP-11 are usually observed at about 56 and 47 kDa by western blot analysis (Santavicca et al., 1996). However, several other MMP-11 forms are also observed. A 28 kDa form was found after furin cleavage of recombinant human MMP-11 (Santavicca et al., 1996). Two forms of 28 and 35 kDa are also observed in human atherosclerotic plaques (Schönbeck et al., 1999). Furthermore, a 35 kDa MMP-11 lacking enzymatic activity is the most abundant protein in a malignant bronchial epithelial cells/normal pulmonary fibroblasts co-culture model (Mari et al., 1998). The diversity of the MMP-11 forms reveals the existence of possible various post-translational maturations of this protein.

Because of the impractical large-scale purification in vivo, recombinant MMP-11 has been produced in mammalian cell lines (Murphy et al., 1993; Pei et al., 1994; Santavicca et al., 1996), bacterial prokaryotes (Kannan et al., 1999), and baculovirus-infected insect cells (del Mar Barbacid et al., 1998). In the presence of the reversible hydroxamate MMPI BB94, a 45-47 kDa active species can be purified in large scale by a combination of dye-affinity, heparin-affinity and gel-filtration chromatographies (Pei et al., 1994). In the absence of BB94, a 27-28 kDa C-terminally truncated species has been obtained (Murphy et al., 1993). The bacteria- or baculovirus-based system is more efficient than mammalian expression system to produce recombinant MMP-11, and it was already utilized successfully in the laboratory.

1.2.7 MMP-11 substrates

MMP-11 is a very selective enzyme that does not cleave major components of the ECM. So far, only three main substrates have been identified, namely the insulin-like growth factor-binding protein-1 (IGFBP-1) (Mañes et al., 1997), the laminin receptor (Amano et al., 2005; Fiorentino et al., 2009) and the native α3 chain of collagen VI, but

not the α1 and α2 chains (Motrescu et al., 2008). Collagen VI is an adipocyte-related ECM component, but the precise site of cleavage remains to be determined. Furthermore, a 28 kDa C-terminally truncated form of MMP-11 exhibits weak matrix-degrading activity against laminin as well as collagen IV in mouse (Murphy et al., 1993), but not in human (Noël et al., 1995). Probably due to an unusual Ala 'substitution' of the Pro235 in human MMP-11, a residue conserved in all MMPs. IGFBP-1 is also cleaved by MMP-11 in human, the cleavage site is between His140-Val141 within in the mid-region of IGFBP-1. Since IGFBP-1 inhibits the function of IGF-I, cleavage of IGFBP-1 by MMP-11 releases active IGF-1 for cell survival and proliferation (Mañes et al., 1997). Given the fact that IGFs play a prominent role in the development of cancer, MMP-11 may contribute to tumorigenesis by releasing IGF-1 from IGFBP-1. This sharp specificity is possible because of its particular S1' pocket structure looking like a tunnel running through the enzyme (Gall et al., 2001).

By using synthetic substrates, recombinant MMP-11 cleaves the fluorogenic substrate Dns-Pro-Leu-Ala-Leu-Trp-Ala-Arg-NH2, where Xaa in the P1' position represents unusual amino acids containing either long arylalkyl or alkyl side chains (Mucha et al., 1998; Holtz et al., 1999). Purified human MMP-11 also cleaves serine proteinase inhibitor (serpin). Proteolysis occurred at Ala350-Met351 site within the reactive-site loop of the inhibitor, which results in a complete loss of anti-proteolytic activity (Pei et al., 1994).

1.2.8 MMP-11 is a paracrine factor

It is well documented that tumor microenvironment is crucial for cancer progression. In this context, MMP-11 represents a paracrine factor of bad prognosis in almost all human invasive carcinomas (Motrescu and Rio, 2008; Zhang et al., 2016; Gómez-Macías et al., 2018). The expression of MMP-11 is always considered as mesenchymal origin. It is restricted to a cell sub-population located at the vicinity of malignant epithelial cells, particularly when the integrity of the basement membrane, which separates epithelial and stromal compartments, is altered and permits cell-stroma interaction/crosstalk (Basset et al., 1990). Accordingly, diffusible bio-factors from adjacent epithelial cells can induce MMP-11 expression by mesenchymal cells.

Several cytokines, including IGF-II, EGF, PDGF and IL-6, are able to induce the selective expression of MMP-11 in cultured human endometrial fibroblasts (Singer et

al., 1999). Growth factors (bFGF and PDGF) and/or 12-O-tetradecanoylphorbol-13-acetate could induce MMP-11 expression in normal human pulmonary fibroblasts (Anderson et al., 1995). Malignant bronchial epithelial cells also stimulate normal pulmonary fibroblasts to express and secrete MMP-11 (Mari et al., 1998). MMP-11 can also be induced in osteoblasts by FGF2 (Delany and Canalis, 1998). Using breast epithelial cancer cell/stroma cell co-culture models, both soluble factors and cell/cell contact allow the expression of MMP-11 (Ahmad et al., 1997). In addition, adipocyte, as the most abundant component of mammary gland tissue, could express MMP-11 in condition of co-culture with murine and human cancer cells (Tan et al., 2011). Finally, MMP-11 mRNA and protein co-localized with endothelial cells, smooth muscle cells, and macrophages within the atherosclerotic lesions (Schönbeck et al., 1999).

These data in accordance with the expression of MMP-11 by adjacent stromal cells in invasive cancer cells (Andarawewa et al., 2005; Motrescu and Rio, 2008).

1.2.9 MMP-11 physiological functions

1.2.9.1 MMP-11 and embryonic development

MMP-11 is present in several tissues during development processes (Lefebvre et al., 1995). It is involved in amphibian development and metamorphosis (Patterton et al., 1995; Ishizuya-Oka et al., 1996), and also required for cell migration and apoptosis during tissue remodeling in Xenopus laevis (Damjanovski et al., 1999; Ishizuya-Oka et al., 2000). In addition, MMP-11 mRNA was observed in trophoblastic cells at the site of mouse embryonic implantation (7.5-8.5 days) and in a variety of developing embryonic tissues, which including limb, tail, snout, bone and spinal cord morphogenesis (Masson et al., 1998). In limb, tail and snout, MMP-11 expression was specifically detected in mesenchymal cells lining the basement membrane at the junction of primitive dermis and epidermis (Figure 1.9), and adjacent to epithelial cells undergoing proliferation and/or apoptosis. In bone, MMP-11 was expressed in invasive mesenchymal cells and in the spinal cord in neuroepithelial cells of the floor plate (Lefebvre et al., 1995). MMP-11 was also expressed in the progressively smaller zone of undifferentiated cells toward the outer margin of the decidua in the implantation site (Alexander et al., 1996).The skeletal muscle of the tongue in mouse also expresses MMP-11 (Chin and Werb, 1997). Moreover, during human placentation, extravillous trophoblasts invading the maternal decidua produce MMP-11. In floating villi, its

expression is restricted to the syncytiotrophoblasts that line intervillous vascular spaces (Maquoi et al., 1997).

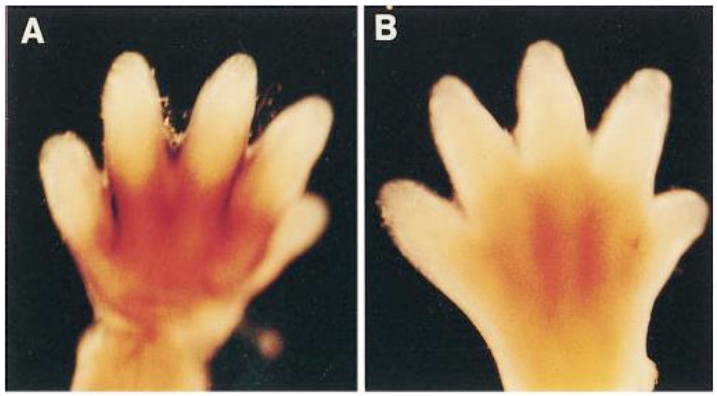

Figure 1.9 Whole mount RNA in situ hybridization of limb buds of MMP-11 wildtype and knockout mouse embryos (E14.5). MMP-11 mRNA was detected in the interdigital parts of the limb of wildtype (A) but not in that of MMP-11 knockout (B) mice. No morphological differences were observed between limb buds from A and B. (Adapted from (Masson et al., 1998)).

1.2.9.2 MMP-11 and mammary gland involution

MMP-11 participates in several tissue remodeling process, like uterus post-partum involution, endometrial menstrual breakdown and post-weaning mammary gland involution (Lefebvre et al., 1995; Tan et al., 2014).

Although the rudimental mammary ductal tree is formed prior to birth, the main mammary gland development occurs postnatally. First during puberty through ductal structure growth including TEB appearance, ductal elongation and branching, invasion and filling of the fat pad. Second during pregnancy through growth and differentiation of functional mature alveoli. Reciprocal interactions between the epithelium and the connective tissues dictate the terminal branching pattern of the ducts and contribute to mammary gland morphogenesis, although the details of these events are not fully understood (Naylor and Ormandy, 2002; Green and Lund, 2005; Khokha and Werb, 2011). It is well known that stromal cells, especially adipocyte, are potent mediators in the proper development and maintenance of mammary gland ductal morphogenesis (Couldrey et al., 2002; Landskroner-Eiger et al., 2010; Pavlovich et al., 2010). Data suggest that stromal MMP-11 is involved in mammary epithelium morphogenesis and growth in a paracrine manner. Mice deficient MMP-11 display impaired mammary ductal morphogenesis, although TEB and ductal epithelial architecture are not obviously altered (Figure 1.10a). Moreover, mammary alveolar morphogenesis and

differentiation are impaired in MMP-11 knockout mice at pregnancy and lactation (Figure 1.10b). But MMP-11 mutant epithelial transplants develop normally into wildtype cleared fat pad (Tan et al., 2014). Thus, local stromal MMP-11 is crucial for correct postnatal mammary gland development.

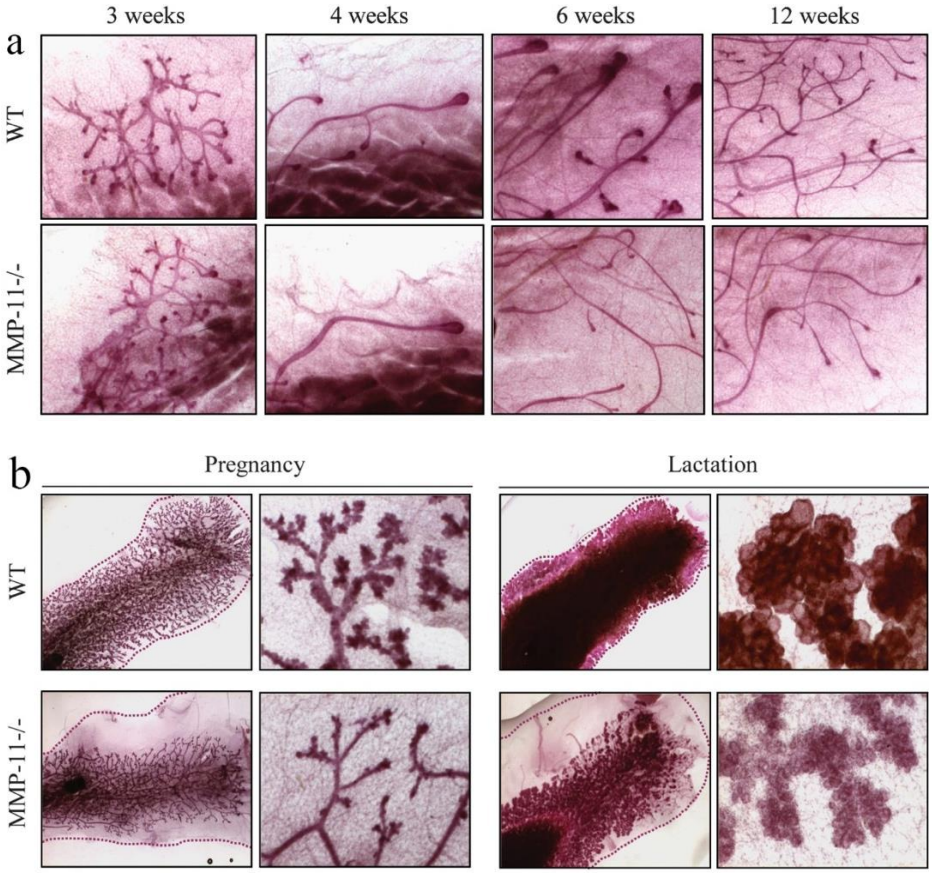

Figure 1.10 Mammary ductal postnatal morphogenesis is impaired in MMP-11 knockout mice. (a) Whole-mount carmine red staining of wildtype and knockout mammary glands at 3, 4, 6 and 12 weeks of age. Less number of TEBs and less developed ductal trees in mutant group. (b) Whole-mount carmine red staining of wildtype and knockout mammary gland at pregnancy and lactation. Alveolar morphogenesis and differentiation are impaired in mutant group. (Adapted from (Tan et al., 2014)).

1.2.9.3 MMP-11 and adipogenesis

The adipose tissue formation is a complex process requiring the preadipocyte lineage conversion into mature adipocytes (Capilla and Navarro, 2015; Ma et al., 2015a). This differentiation switch activates a series of gene expression, two adipogenic markers were remarkably increased, adipocyte protein (aP2), and peroxisome proliferator-activated receptor (PPAR) (Farmer, 2006). Adipose precursor cells are believed to be present throughout life. Preadipocyte differentiation is characterized by a change in morphology from the elongated fibroblast-like form to the round lipid-filled mature fat cells. Mature adipocytes which accumulated excess triglyceride are

generally considered incapable of division (Farmer, 2006). In stress conditions, mature adipocytes can discard lipid droplets and dedifferentiate into fibroblast-like cells, this is one possible way by which cells react to minimize damage (Shoshani and Zipori, 2011).

MMP-11 was reported to negatively regulate adipogenesis in an autocrine manner. In vitro, MEFs from MMP-11 mutant mice differentiate faster into adipocytes compared with wildtype control. Treatment of fully differentiated mutant MEFs with recombinant MMP-11 protein leads to lipid depletion and reversal of the adipocyte phenotype (Andarawewa et al., 2005; Motrescu et al., 2008) (Figure 1.11a). Moreover, in vivo studies revealed that MMP-11 knockout mice have significantly higher mean body weight than wildtype littermates both in normal fat diet (Andarawewa et al., 2005; Dali-Youcef et al., 2016) and in high fat diet condition (Lijnen et al., 2002) (Figure 1.11b). MMP-11 overexpressing mice display smaller adipocytes, but also have less body fat mass than wildtype control (Figure 1.11c) (Dali-Youcef et al., 2016). Overexpression of miR125b-5p reduced adipogenesis, microarray-analysis identified MMP-11 as a direct target of miR125b-5p by showing that upregulation of miR125b-5p significantly reduces MMP-11 luciferase activity (Rockstroh et al., 2016).

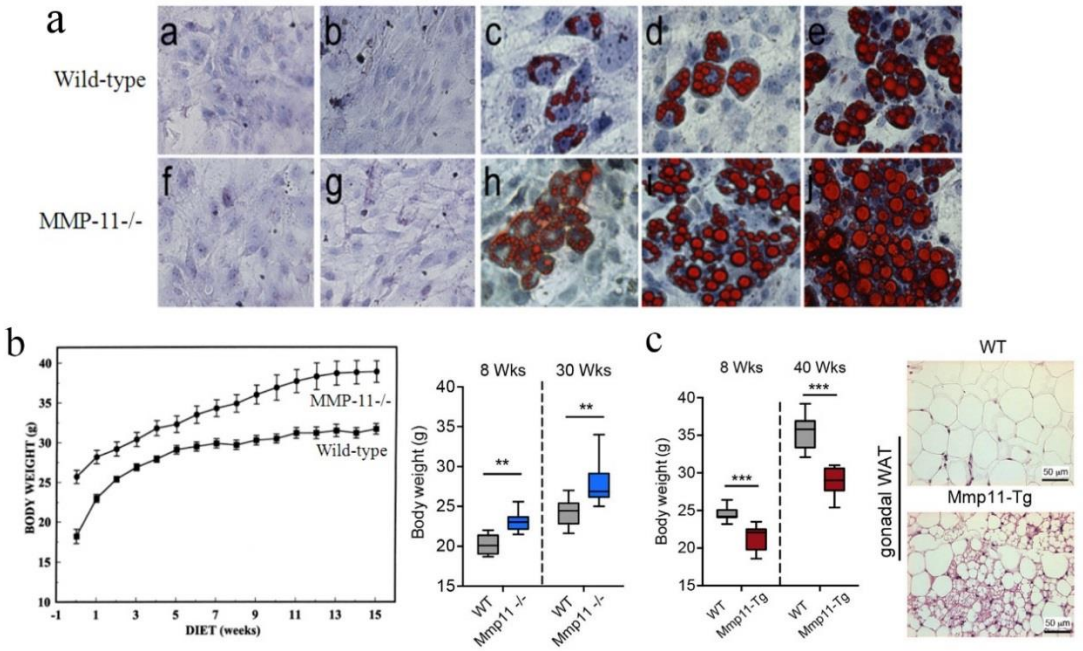

Figure 1.11 MMP-11 negatively regulates adipogenesis. (a) Oil Red O staining analysis of MEFs to adipocyte differentiation. Increased number and size of lipid droplets were observed in MMP-11 knockout MEFs compared to wildtype group at 2 (b, g), 4 (c, h), 6 (d, i), 8 (e, j) days of adipocyte differentiation (Adapted from (Andarawewa et al., 2005)). (b) The body weight of MMP-11 knockout mice significantly higher than wildtype littermates both under high fat diet (Adapted from (Lijnen et al., 2002)) and normal fat diet condition (Adapted from (Dali-Youcef et al., 2016)). (c) MMP-11 transgenic mice not only have less body weight but also display smaller size of adipocyte than wildtype group. (Adapted from (Dali-Youcef et al., 2016)).

Thus, MMP-11 acts as an anti-adipogenic regulator and controls fat mass homeostasis by limiting pre-adipocyte differentiation and/or promoting mature adipocyte dedifferentiation.

1.2.10 MMP-11 pathological functions

1.2.10.1 MMP-11 and cancer

Similar to some other MMPs, overexpression of MMP-11 is found in the specimens of solid tumor tissues as well as in sera of cancer patients, but almost absent in adjacent normal tissues. Apart from invasive primary tumors, MMP-11 was also expressed in lymph nodes and distant metastatic lesion, but rarely in other non-epithelial malignancies (Hsin et al., 2014; Eiro et al., 2017). Tumor stromal fibroblasts instead of tumor cells were initially considered as the origin of MMP-11 expression (Wolf et al., 1993). However, other studies uncovered that both epithelial tumor cells and stromal cells express MMP-11 (von Marschall et al., 1998; Barrasa et al., 2012). Tumor cells-to-stromal fibroblasts interaction was found to facilitate the expression and activation of MMP-11, promoting cancer cell invasion (Rio, 2013; Zhang et al., 2016). Some prognostic factors in breast cancer including central tumor fibrosis, p53, ER and HER2 expression are found to be correlated with MMP-11 expression (Min et al., 2013). These studies imply that MMP-11 is probably involved in certain signalling transduction pathways or unknown malignancy behavior, indicating a more complex role in cancer progression than its proteolysis function.

1.2.10.1.1 MMP-11 and breast cancer

MMP-11 was originally discovered from a human breast cancer biopsy (Basset et al., 1990). It is more frequent in primary tumors (50-100%) than in secondary tumors (30-70%) (Rouyer et al., 1994; Rio et al., 1996). Clinical trials showed that high levels of MMP-11 expression correlate with poor prognosis in breast cancer patients (Chenard et al., 1996; Min et al., 2013) (Figure 1.12). Moreover, MMP-11 is associated with tumor invasion, it is a gene expression signature that distinguishes invasive ductal carcinomas (IDC) from ductal carcinoma in situ (DCIS) (Hannemann et al., 2006). Both in vitro and in vivo techniques demonstrated that overexpression of MMP-11 in breast cancer cells leads to enhanced cell proliferative capacity and increased tumor volumes (Kasper et al., 2007). This observation was dependent upon the presence of IGF-1

signalling pathway, and MMP-11 induction in tumor fibroblasts leads to the stimulation of the IGF-1R pathway in carcinoma cells. More recently, circulating free MMP-11 and corresponding spontaneous antibodies were also detected in the serum of clinical breast cancer patients (Roscilli et al., 2014).

The breast cancer ECM adaptation involves a desmoplastic response, notably adipocytes disappear, and fibroblast-like cells accumulate. In this context, MMP-11, appears to be a paracrine key factor, which negatively regulates adipogenesis by limiting pre-adipocyte differentiation and/or reversing mature adipocyte differentiation, accumulate and/or maintain fibroblast-like cells at the tumor center and peritumoral space. Indeed, invasive breast cancer cells induce the expression of MMP-11 in neighboring cancer-associated-adipocytes (CAAs) and cancer-associated-fibroblasts (CAFs) (Andarawewa et al., 2005) (Figure 1.12). CAAs become smaller than those observed at a distance and tend to the phenotype of CAFs probably because of the dedifferentiation function of MMP-11 (Rio, 2011). In vitro data indicate that cancer-derived CAFs, especially those derived from MMP-11 positive stromal mononuclear inflammatory cell tumors, can promote breast tumor cell invasion and angiogenesis (Eiro et al., 2018). Thus, MMP-11 and CAAs participate in a highly complex vicious cycle orchestrated by the invasive cancer cells to support tumor progression (Motrescu and Rio, 2008).

Crossing MMTV-ras transgenic mice with MMP-11 deficient mice permitted to study the mammary gland cancer development on a MMP-11 wildtype or deficient background. Although the total number and size of primary tumors were lower and tumor-free survival was higher in MMP-11 deficient mice, a systematic search for lung metastases revealed an unexpected higher number of metastases in the absence of MMP-11 (Andarawewa et al., 2003). Moreover, MMP-11 deficient mice developed more metastases for a similar number and size of primary invasive tumors, indicating that cancer cells developing in MMP-11 deficient stroma have increased potential for hematogenous dissemination. This might result from the high number of blood vessels. Thus, MMP-11 function differs throughout cancer progression, it is a tumor enhancer for primary tumor, but a repressor for metastasis.

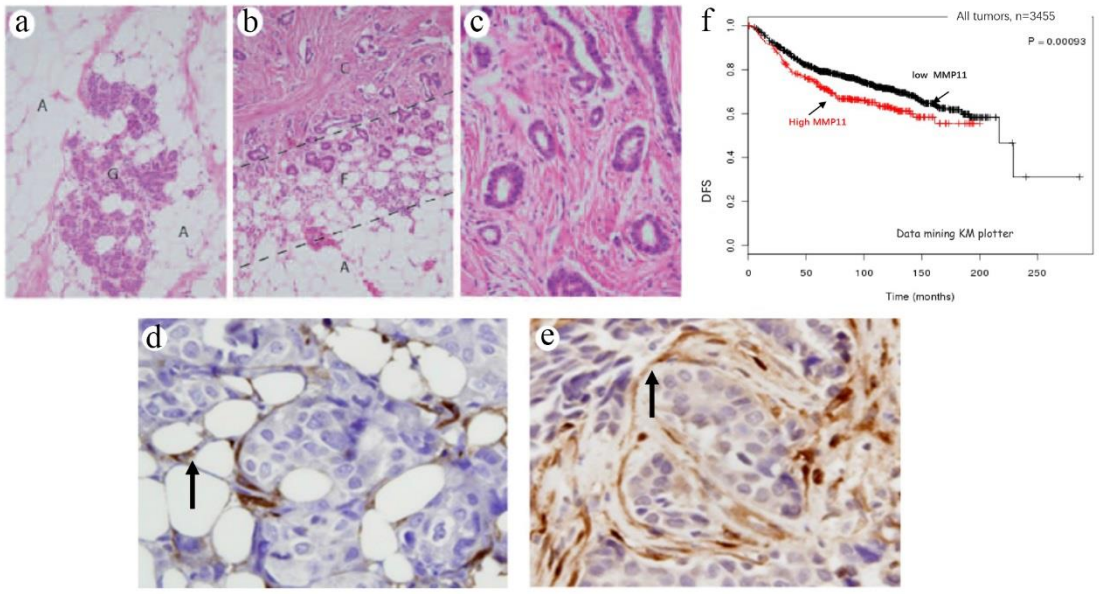

Figure 1.12 Histology examination of human normal breast tissue and invasive breast tumor. H&E staining compared with normal adipose tissue (a), the number and the size of adipocytes are remarkably reduced at the tumor invasive front (b). Whereas adipocytes completely disappeared instead of peritumoral fibroblasts in the tumor center (c). At the invasive front (d), MMP-11 immunostaining shows that CAAs express MMP-11 (brown staining, indicate by arrow). At the tumor center (e), numerous CAFs also express MMP-11. High level of MMP-11 expression correlated with lower disease free survival (DFS) in clinical breast cancer patients from KM plotter data base (f). A, adipose tissue; C, tumor center; F, tumor front; G, mammary gland. (Adapted from (Chenard et al., 1996; Andarawewa et al., 2005; Tan et al., 2011)).

1.2.10.1.2 MMP-11 and other cancers

Pancreatic cancer is a disease with extremely high mortality and poor prognosis, surgery probably is the only potential option to cure (Rossi et al., 2014). More than 80% of pancreatic cancer specimens reveal strong signals for MMP-11 located in the epithelial cancer cells and in peripheral stromal cells, yet MMP-11 has not been detected in normal pancreatic tissues (von Marschall et al., 1998; Bournet et al., 2012).

Gastric cancer cells express endogenous MMP-11 confirmed by IHC staining and western blot (Deng et al., 2005). Compared with normal tissues, MMP-11 expression was significantly higher in cancer specimens at both transcriptional and protein levels (Zhao et al., 2010). Consistent with the expression profile in tissues, the serum levels of MMP-11 were also higher in advanced gastric adenocarcinoma patients than in healthy controls (Yan et al., 2011).

Colorectal cancer is one of the most common malignant neoplasms, high serum levels of MMP-11 correlate with poor prognosis in colon cancer patients (Pang et al., 2016). Studies revealed that the expression of MMP-11 can be detected not only in stromal cells, but also in three different colon adenocarcinoma cell lines from epithelial

origin (Barrasa et al., 2012). The mRNA expression levels of MMP-11 in liver metastatic lesions were notably lower compared with matched primary colon cancer tissues (Asano et al., 2008). Nevertheless, a higher level of MMP-11 was detected in lymph node metastatic sites by immunohistochemistry (Skoglund et al., 2004). We speculate that MMP-11 may play different roles between primary cancer cells and multiple subgroups of metastatic lesions.

Furthermore, the role of MMP-11 in tumor progression has been shown to be a complicated process in mouse model. MMP-11 increased syngeneic colon tumors development and this function does not result from enhancing cell proliferation but from decreasing cell apoptosis and necrosis (Figure 1.13). These data indicated that host MMP-11 is a key regulator during cancer invasion, favoring malignant cell survival through an anti-apoptotic/resistance-to-anoikis function (Boulay et al., 2001; Wu et al., 2001; Takeuchi et al., 2011). Of interest, another study has shown that siRNA targeting MMP-11 in the gastric cancer cell line BGC823, resulted in decreased proliferation ability compared with mock transfectants and parental cells, without modification in the cell cycle or apoptotic ability (Deng et al., 2005). Moreover, this study showed that soft agar colony formation of MMP-11 deficient cells was dramatically inhibited, as well as tumorigenicity in nude mice (Figure 1.14).

However, besides the reduction of the number of primary tumors, MMP-11 deficient mice have an unexpected increased number of colon-to-lung metastases (Brasse et al., 2010). X-ray computed tomography showed that wildtype mice developing lung metastases occur earlier and grow faster, but lower numbers of lesions were observed compare with MMP-11 deficient mice. Thus, these data point out the complex function of MMP-11 in favoring lung metastases.

Similarly, overexpression of MMP-11 has also been identified in various types of human cancers, such as prostate cancer (Eiro et al., 2017), bladder cancer (Yonemori et al., 2016), renal cell carcinoma (Wu et al., 2014), urothelial carcinomas (Li et al., 2016), oral squamous cell carcinoma (Lin et al., 2015), gastric cancer (Kou et al., 2013), esophageal squamous cell carcinoma (Tang et al., 2013), and cervical cancer (Valdivia et al., 2011), etc.

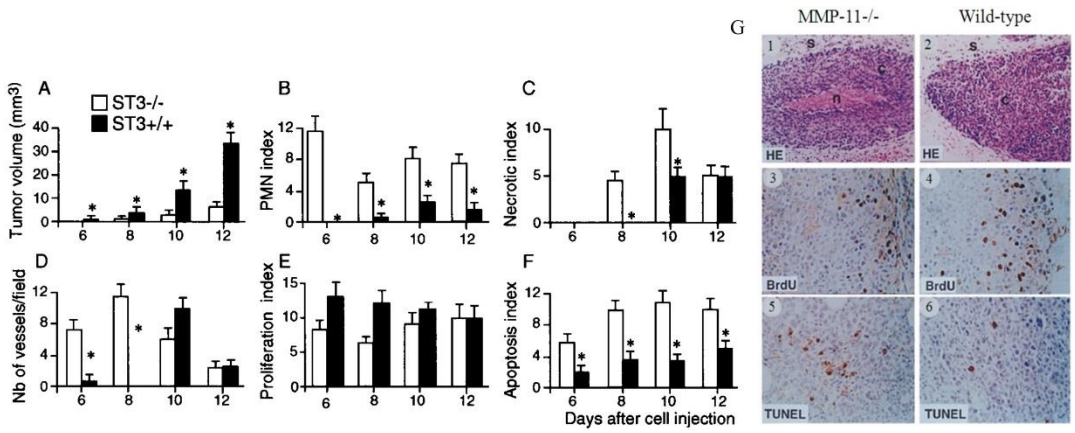

Figure 1.13 Quantitative analysis of histological (H&E) and immunohistological differences of C26 colon cancer syngeneic model micro-carcinomas in MMP-11 wildtype and knockout mice. Diagrams corresponding to the tumor volumes (A), PMN index (B), necrotic index (C), number of vessels (D), proliferation index (E), and apoptosis index (F) at 6, 8, 10, and 12 days after s.c. C26 cell injection. Histological features (G) of micro-carcinomas found in two groups. BrdU and TUNEL stained in brown indicated proliferating and apoptotic cells, respectively. MMP-11 deficiency led to increased cancer cell death through necrosis (1, 2) and apoptosis (5, 6), but did not modify cancer cell proliferation (3, 4). s, stroma; c, carcinoma; n, necrosis. Plotted from six individual tissue sections. Statistical differences $P < 0.01$. (Adapted from (Boulay et al., 2001)).

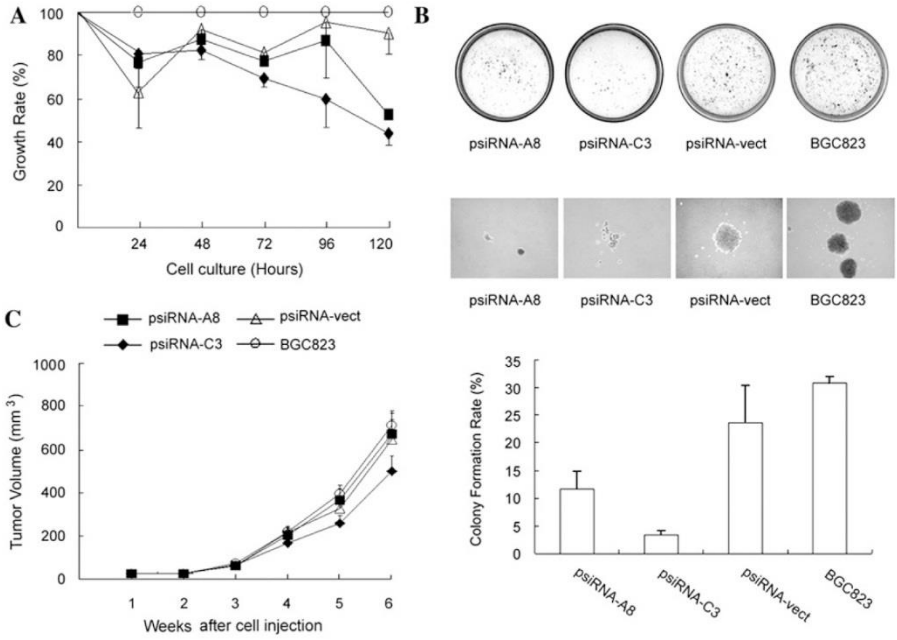

Figure 1.14 siRNA targeted to MMP-11 inhibited gastric cancer cell BGC823 proliferation in vitro and in vivo. (A) MTT assay of proliferative suppression of siRNA-treated cells. (B) Colony forming activities were inhibited of MMP-11 deficient cells in soft agar. (C) Tumor progression in nude mice was delayed in MMP-11 deficient group. (Adapted from (Deng et al., 2005)).

1.2.10.2 MMP-11 and other diseases

In human atherosclerotic plaques, MMP-11 mRNA and protein were observed in endothelial cells, smooth muscle cells, and macrophages (Schönbeck et al., 1999). The synthesis of MMP-11 appears to be induced by T cell-derived as well as recombinant CD40 ligand (CD40L, CD154), which acts on the CD40 receptor in recipient cells.

Interruption of the CD40-CD40L signalling pathway in low density lipoprotein receptor-deficient hyperlipidemic mice substantially decreased the MMP-11 expression within atherosclerotic plaques. In addition, MMP-11 cleaves and inactivates α1-PI, a serpin known to regulate cellular functions related to atherosclerosis (Schönbeck et al., 1999). Additionally, neointima formation was significantly enhanced in MMP-11 deficient mice compared with wildtype counterparts after electric injury of the femoral artery, suggesting that MMP-11 might suppress the formation of neointima (Lijnen et al., 1999).

MMP-11 might be a genetic factor associated with intervertebral disc degeneration, but it is not the only factor (Aras et al., 2016).

In the Korean population, single nucleotide polymorphisms of MMP-11 may be associated with Kawasaki disease (Ban et al., 2010), which is an acute, self-limited, and systemic vasculitis that leads causes of acquired heart disease in children (Sundel, 2015). Considering the limited studies, additional work of other populations should be conducted to confirm.

1.2.11 The summary of MMP-11 functions

Several biological roles of MMP-11 have been discovered, but numerous questions remain to be further addressed. In conclusion (Table 1.4): 1) MMP-11 is involved in tissues remodeling during embryonic and postnatal period; 2) MMP-11 expressed by CAAs/CAFs acts as a malignant epithelial cell enhancer at the cancer cell/stromal cell interface; 3) MMP-11 is a negative regulator of adipogenesis, it protects from diabesity and promotes metabolic switch; 4) MMP-11 exerts anti-apoptotic function in cancer progression; 5) during cancer progression, MMP-11 can exert a dual effect, depending on the invasive steps; 6) although the development of MMP inhibitors for cancer treatment is more challenging than originally thought, MMP-11 remains an interesting target for potential clinical therapeutics.

Time of MMP-11 expression	Cells/Tissues	Biological processes
Development	Invading trophoblasts	Embryonic implantation
	Syncytiotrophoblasts	Placentation
	Limb bud mesenchyme	Interdigitation
	Invading osteoblasts	Osteogenesis
	Neuroepithelial cells	Spinal cord morphogenesis
	Snout, tail mesenchyme	Epithelium growth
	Tongue	Not known
Metamorphosis	Tail	Larval tissue resorption
	Intestine	Morphogenesis
Adult tissues	Endometrium	Menstrual breakdown
	Uterus	Post-partum involution
	Ovary	Ovulation
	Mammary gland	Post-partum involution
	Adipose tissue	Adipogenesis
Non-malignant diseases	Atherosclerosis	Inflammation, repair
	Skin	Wound healing
	Arthritis	Inflammation
	Dermatofibroma	Benign tumor proliferation
Malignant tumors (Carcinomas)	Fibroblast-like cells, adipocytes	Tumor progression

Table 1.4 MMP-11 in physiopathological tissue remodeling processes. (Adapted from (Rio, 2013)).

1.3 Adipocytes are involved in mammary gland tumor progression

Obesity is characterized by adipose tissue dysfunction, leading to adipocyte hypertrophy, hypoxia, inflammation and induced angiogenesis, extracellular matrix remodeling and fibrosis as well as additional stress responses. Mounting evidence indicate that obesity is a well-established risk factor for certain malignancies as well as cancer-related mortality (Hefetz-Sela and Scherer, 2013).

Breast cancer cells are embedded in "cancer cell nests" that are surrounded by stromal cells. The stromal environment in the mammary gland is rather complex, including many different cells types such as adipocytes, fibroblasts, endothelial cells, and various cells of the immune system (Bussard et al., 2016). Adipocyte is the most common cell type in the mammary gland stroma and dysfunctional adipose tissue plays a pivotal role in obesity-related carcinogenesis. Several molecular mechanisms are linking dysfunctional adipocytes to breast cancer progression. These include: 1) adipose tissue remodeling; 2) alterations in adipokines profiles; 3) chronic inflammation; 4) sex hormones; 5) altered insulin signalling and IGF-I axis; and 6) lipid metabolites (Gallagher and LeRoith, 2011; Park et al., 2011; Bussard et al., 2016).

1.3.1 Cancer-associated adipocytes

Adipocytes surrounding tumors exhibit profound phenotypic changes that include both morphological and functional alterations. These phenotypically altered adipocytes mostly locate close to invasive breast cancer cells and are referred to as CAAs. Patient's mammary tumor contain few adipocytes, or often are totally devoid of adipocytes. The tumor invasive front exhibits a high ratio of adipocytes to fibroblasts, and include reduced size adipocytes. In contrast, in the tumor center, stromal environment displays an extremely high fibroblast-like cell to adipocyte ratio (Tan et al., 2011; Rio et al., 2015). These observations based on the histological examination of breast tumors support the notion that the direct interaction between breast cancer cells and adipocytes promote the phenotypic changes of CAAs, which lead to "adipocyte dedifferentiation" and ultimately to an accumulation of fibroblast-like cells (Tan et al., 2011; Bochet et al., 2013). These tumor surrounding fibroblast-like cells are known as CAFs. These fibroblasts play important roles in tumor initiation, progression, metastasis and resistance to cancer therapy, these effects have been well documented (Buchsbaum and

Oh, 2016). To date, the mechanisms which promote adipocytes-to-fibroblasts transition are still unknown.

CAAs which are located in the breast tumor invasive front are prompted to express MMP-11. In turn, MMP-11 was reported to act as a potent negative regulator of adipogenesis by reducing pre-adipocyte differentiation and reversing mature adipocyte differentiation (Andarawewa et al., 2005; Motrescu and Rio, 2008). It was also found that malignant breast epithelial cells secrete large quantities of IL-11 and TNF-α, which have an effect of anti-adipogenesis by inhibiting the differentiation of fibroblasts to mature adipocytes, primarily via selectively down-regulating the peroxisome proliferator-activated receptor-γ (PPARγ) and adipogenic transcription factors C/EBPα (Meng et al., 2001). Additionally, pro-inflammatory cytokines like IL-1β and IL-6 were also shown to be associated with a modified adipocytes phenotype, in terms of delipidation and decreased adipocyte markers (Dirat et al., 2011). Finally, deleterious CAAs modify the cancer cell phenotype/characteristics leading to a more aggressive behavior.

CAFs induce EMT of breast cancer cells through paracrine TGF-β signalling (Yu et al., 2014). Moreover, CAFs undergo the reverse Warburg effect and provide breast cancer cells with glycolytic metabolites. The interaction between cancer cells and CAFs helps malignant cells to manage the Warburg effect (Sazeides and Le, 2018).

Interestingly, the aspartic protease cathepsin D, as a marker of poor prognosis in human breast cancer, is overexpressed and secreted by malignant mammary epithelial cells (Vashishta et al., 2009; Nicotra et al., 2010). Cathepsin D is also up-regulated in adipose tissue from obese mouse and human beings. Silencing cathepsin D in 3T3-F442A murine preadipocytes leads to fibroblast-like cells after adipogenesis induction, and inhibits of the expression of aP2 and PPARγ adipocyte markers (Masson et al., 2011).

1.3.2 Adipokines

Adipocyte-derived factors (generally called as “adipokines”), include adiponectin, leptin, HGF, collagen VI, IL-6 and TNFα (Trujillo and Scherer, 2006). Altered circulating levels of some of these factors are seen in obesity and related metabolic disorders, but are also associated with increased breast cancer risk (Vona-Davis and Rose, 2007; Carter and Church, 2012; Gui et al., 2017). Soluble secretory products from

adipocytes impact on breast cancer cell proliferative, anti-apoptotic, migratory, invasive and pro-angiogenic behaviors both in vitro and in vivo (Iyengar et al., 2003, 2005; Landskroner-Eiger et al., 2009; Carter and Church, 2012). In hereditary breast cancer syndrome, adiponectin was confirmed to be associated with BMI, and the plasma level of leptin seems an independent and direct biomarker of a breast cancer risk (Sambiasi et al., 2017).

1.3.3 Inflammation

The pathological changes of chronic inflammation in the breast adipose tissue help to establish a microenvironment that favors mutagenesis, cancer cell proliferation and progression. Adipocyte hypertrophy, hypoxia and fibrosis are the most common stress factors for inducing inflammation. Inflamed white adipose tissue within the breast is associated with elevated levels of proinflammatory mediators, enhanced expression of aromatase, and increased estrogen receptor-α (ER-α)-dependent gene expression. In early-stage breast cancer, the adipose tissue inflammation in mammary gland occurs in overweight and obese patients (Vaysse et al., 2017). IL-6 is an important growth factor for ERα-positive breast cancer, and elevated serum IL-6 is associated with poor prognosis (Won et al., 2013). The aggregation of proinflammatory cytokine-secreting macrophages (M1 macrophages) around individual adipocytes that consequently undergo apoptosis and necrosis is a characteristic feature of adipose tissue inflammation (Lumeng et al., 2007). These syncytial "crown-like" structures (CLS) provide a histological marker of tissue inflammation (Cinti et al., 2005). Increased numbers of CLS in the stromal component of the mammary tissue of obese mice was associated with elevated TNF-α, IL-1β and cyclooxygenase-2 (COX-2) expression and increased NF-κB binding activity (Subbaramaiah et al., 2011). These similar abnormalities were also observed in the breast cancer tissue of both premenopausal and postmenopausal obese women (Morris et al., 2011).

1.3.4 Sex hormones

Epidemiological evidence supports the role of estrogens derived from adipose tissue in the pathogenesis of the breast cancer. Indeed, over-weight postmenopausal women exhibit a threefold increased risk for developing breast cancer compared with normal-weight postmenopausal women (Bulun et al., 2012). Estrogen, a product of the

aromatase enzyme in adipose tissue, has been considered as the hormone responsible for increasing breast cancer risk in obese postmenopausal women (Brown and Hankinson, 2015). Studies suggested that breast adipose tissue fibroblasts are crucial site for aromatase expression and estrogen production, and has linked them to the development of breast cancer (Bulun et al., 2012). Therefore, aromatase overexpression is linked to inhibition of adipogenic differentiation and a desmoplastic reaction. In fact, aromatase inhibitors that block aromatase activity and reduce the amount of local estrogen production are the most effective hormonal treatment of postmenopausal breast cancer (Bulun et al., 2012).

1.3.5 Insulin signalling and IGF-1 axis

Over expressed insulin, IGF-1 and IGF-1 receptor (IGF-1R) are present in obesity-associated breast cancer (Belardi et al., 2013). Binding of IGF-1R to its ligand leads to its dimerization, activation of tyrosine kinase and phosphorylation of key substrates which in turn activate various intracellular signalling pathways. Analysis of genetic polymorphism showed a significant correlation between the expression of specific insulin-related genes and increased risk of breast cancer in postmenopausal women exposed to estrogens (Slattery et al., 2007). Given that obese postmenopausal women have more estrogens, and that insulin and IGF-1 reduce weight, it is logical to conclude that the crosstalk between the IGF pathways and estrogen-mediated signalling may favor an increased risk of breast cancer in obese postmenopausal women (Macciò and Madeddu, 2011).

Despite the promising experimental results, the results from clinical trials is rather disappointing. Blocking for the IGF-1 system in breast cancer therapeutics may become an efficient strategy. Further studies will be needed to target the various components of the IGF-1/IGF-1R axis in several pathophysiological aspects of breast cancer (Christopoulos et al., 2018), including the cancer stemness and tumor microenvironment.

1.3.6 Lipid metabolism

Tumor microenvironment has a major role in determining the metabolic phenotype of breast tumor cells. The best characterized metabolic phenotype observed in tumor cells is the “Warburg effect”, which is a shift of ATP generation from

oxidative phosphorylation to glycolysis, even under normal oxygen concentrations. Moreover, in “the Reverse Warburg Effect”, stromal fibroblasts undergo aerobic glycolysis and provide adjacent cancer cells with ketones, pyruvate and/or lactate in a paracrine manner (Pavlides et al., 2009; Migneco et al., 2010; Bonuccelli et al., 2010; Whitaker-Menezes et al., 2011). In line with this concept, enhanced lipolysis in host tissues can potentially fuel breast tumor growth by releasing free fatty acids (FFAs) from host adipocytes to be recycled via β-oxidation in cancer cell mitochondria (Balaban et al., 2017; Wang et al., 2017, 2018).

Interestingly, breast tumor cells also display a lipogenic phenotype. Elevated levels of fatty acid synthase (FASN), a key lipogenic multi-enzyme complex catalyzing the terminal steps in the biogenesis of fatty acids, correlates with poor prognosis in breast cancer patients, while inhibiting FASN results in decreased cell proliferation, tumor growth inhibition and loss of cell viability (Menendez and Lupu, 2007).

1.4 Thesis project

A recent study from the laboratory showed that MMP-11 is a metabolic regulator acting at the level of the whole organism. Increased MMP-11 expression is associated with lean phenotype and protection from diet-induced obesity, consistently loss of MMP-11 expression is associated with weight gain and metabolic syndrome (Dali-Youcef et al., 2016). Moreover, MMP-11 induction is an early event in the adipose tissue dysfunction (Arcidiacono et al., 2017). However, the metabolic role of MMP-11 on tumor progression was not addressed.

To address the systemic role of MMP-11 on breast tumor progression, we used a mouse genetic model of mammary gland cancer formation and progression. Transgenic mouse models have been widely used to study breast cancer, and the PyMT mouse model is widely utilized (Herschkowitz et al., 2007). In this model, the oncoprotein, polyoma middle T (PyMT) antigen from mouse polyoma virus, is under the control of the mouse mammary tumor virus (MMTV) long terminal repeats (LTR) and is expressed by the mammary epithelial cells (Guy et al., 1992a; Lin et al., 2003). The primary tumors developed in this mouse model undergo distinct stages of cancer progression, notably hyperplasia, adenoma/ mammary intraepithelial neoplasia, early and late carcinoma and therefore evolution from pre-malignancy to malignancy (Lin et al., 2003). Because MMP-11 is expressed at early stage of tumor conversion from in situ to invasive carcinoma in all molecular subtypes, we reasoned that this model would be suitable to examine the role of MMP-11 in the full range of breast tumor development from hyperplasia to late carcinoma.

In the present research, we used a series of mouse models of MMP-11 gain-of-function (K14-MMP11 transgenic, GOF) and loss-of-function (MMP-11 knockout, LOF) to examine the role of MMP-11 on mammary tumor growth and metabolism. We crossed these mice with MMTV-PyMT genetic strain. Mammary hyperplasia can be detected in this model as early as 4 weeks of age, and most of these mice have developed carcinoma and pulmonary metastases at 14 weeks old. PyMT acts as a potent oncogene by direct interaction with a variety of signal transduction pathways (Src family, the ras and PI3 kinase pathways) and is found to be associated with increased c-myc levels (Rodriguez-Viciana et al., 2006; Fluck and Schaffhausen, 2009). A detailed histological analysis of PyMT tumors showed many similarities to the histology of human tumors (Fluck and Schaffhausen, 2009). Moreover, there was

altered expression of integrin-β1, the molecule that plays an important role in regulating cell proliferation, differentiation, and apoptosis of normal mammary epithelium (White et al., 2004). Overall, this model recapitulates many processes found in human breast cancer progression, females develop with high penetrance palpable mammary tumors which metastasize to the lung (Fluck and Schaffhausen, 2009).

To precisely address the role of MMP-11 released by adipocytes during the early step of tumor progression, we generated a new mouse model of MMP-11 overexpression in the adipose tissue.

Tumor resident adipocytes are essential for breast cancer development/ progression. Beside systemic effects, their tumor-promoting impact is dependent on local functions, notably via a complex adipocyte cancer cell paracrine loop (Rio et al., 2015). In the context of breast cancer progression, it is important to mention that MMP-11 expression marks distinct cell populations from the TME. In the tumor center, fibroblast cells are the prominent cellular components of the microenvironment. These CAFs express very high levels of MMP-11. In contrast, in the tumor periphery, CAAs represent the principal cellular component of the microenvironment. Unlike remote breast adipocytes in which MMP-11 is barely expressed, CAAs located in the tumor invasive front express high level of MMP-11, show lipid droplets leakage and tend to have an elongated fibroblast-like morphology (Motrescu and Rio, 2008). These observations support the idea that MMP-11 acts at different levels in the TME. First, at early stage when cancer cells develop or invade the normal stromal tissue, MMP-11 expression by CAAs may directly participates in the invasion process (Andarawewa et al., 2005). Second, in the constituted tumor where fibroblasts are the predominant TME cell-type, MMP-11 expression by CAFs is thought to help cancer cells survival (Andarawewa et al., 2003). However, the mechanisms of MMP-11 on tumor progression remains partially understood (Figure 1.15). To specifically study the function of MMP-11 released by CAAs, we generated a novel MMP-11 transgenic mouse model (aP2-mMMP11-IRES-GFP-polyA). This mouse model is based on the use of the fatty-acid-binding protein 4/adipocyte protein 2 (Fabp4/aP2) promoter, which is specifically expressed in adipose tissue (Graves et al., 1991; Lee et al., 2013), to direct MMP-11 expression. Then, we performed orthotopic injection of E0771 breast cancer cells into the mammary gland fat pad to study the nature of tumor growth.

In parallel to these studies, I contributed to the investigation of a potential new therapeutic agent for breast cancer.

Myo-Inositol trispyrophosphate (ITPP), was first reported in 2005 (Fylaktakidou et al., 2005), is a novel membrane-permeant allosteric effector of hemoglobin (Hb). It enhances the regulated oxygen release capacity of red blood cells, thus counteracting the effects of hypoxia in diseases such as cardiovascular diseases (Biolo et al., 2009). This chemical compound also inhibites human pancreatic tumor xenografts growth and has an anti-angiogenic effect in immunocompromised NOD.SCID mice. In addition, ITPP showed the eradication of early hepatoma tumors in rats (Aprahamian et al., 2011; Raykov et al., 2014), possibly via the suppression of hypoxia inducible factor-1α (HIF-1α) and down-regulation of hypoxia-inducible genes such as VEGF. Similar results were also obtained in glioma and colon cancer models (Sihn et al., 2007; Derbal-Wolfrom et al., 2013). In order to study the therapeutic effect of ITPP, we used the MMTV-PyMT mouse breast cancer progression model. Of note, Doxorubicin, which is a classic anthracycline and antitumor antibiotic that inhibits the activity of topoisomerase II and works in part by interfering with the DNA transcription (Pommier et al., 2010; Tacar et al., 2013), was used as a control.

To conclude, in my thesis, I have investigated: 1) the impact of MMP-11 on MMTV-PyMT mouse breast cancer progression; 2) the impact of MMP-11 overexpression restricted to adipocytes on mammary gland tumorigenesis; 3) the impact of ITPP on MMTV-PyMT mouse breast cancer progression.

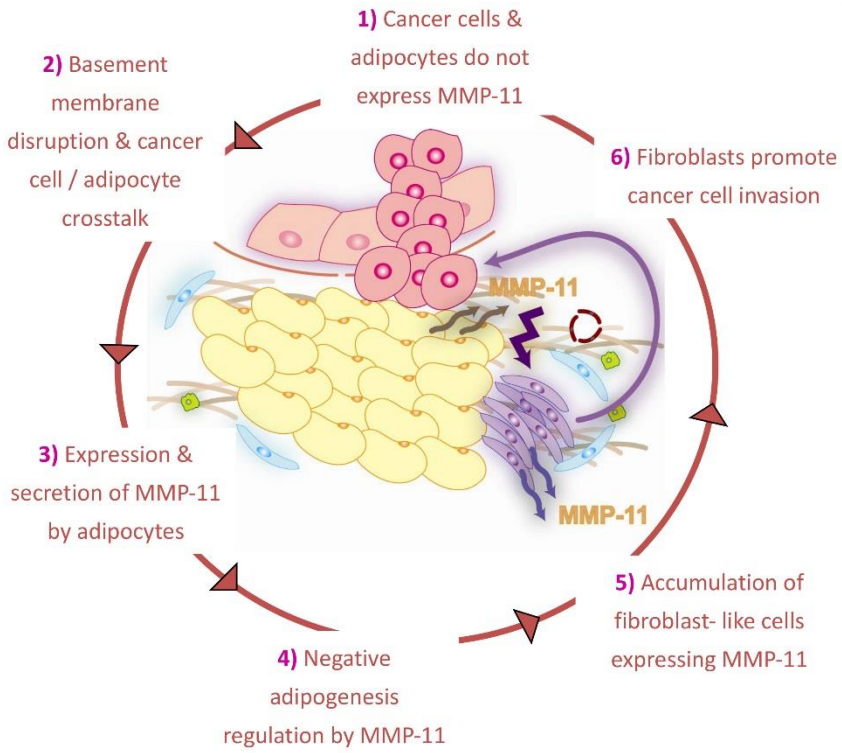

Figure 1.15 Schematic representation of the vicious breast tumor progression cycle. Adipocytes/pre-adipocytes and MMP-11 participate in a highly complex vicious cycle to support tumor progression, and this process is orchestrated by cancer cells. At the beginning, both the invasive cancer cells and the resting adipocytes/pre-adipocytes do not express MMP-11. When basement membrane was disrupted, cancer cell/adipocyte interaction induces the expression and secretion of MMP-11 by the adipocyte. MMP-11 negatively regulates adipogenesis, leading to adipocytes dedifferentiation and accumulation of MMP-11- expressing fibroblast-like cells. These MMP-11-expressing cells then favor invasive breast cancer cells progression and potentiate this vicious cycle. (Adapted from (Motrescu and Rio, 2008)).

CHAPTER 2 Results

Part I The impact of MMP-11 on MMTV-PyMT mouse breast cancer progression

Preclinical studies revealed that MMP-11 favored breast cancer progression, and its expression status correlated with patient outcome (Chenard et al., 1996). More recently, MMP-11 was shown to have a major role in controlling energy metabolism and protected mice from diabesity and promotes metabolic switch. MMP-11 transgenic mice also exhibit defective adaptive thermogenesis due to altered mitochondrial function (Dali-Youcef et al., 2016). We speculated that MMP-11 has a promoting effect on mouse mammary tumor progression by modulating tumor metabolism. To characterize this molecular mechanism of MMP-11 in cancer, we used a preclinical model of breast cancer progression and genetic manipulation of MMP-11 expression.

In this study, I crossed mice either overexpressing-(Gain of Function, GOF) or deficient-(Loss of Function, LOF) for MMP-11 with a genetic model of mammary tumors, the MMTV-PyMT strain, which recapitulate many processes found in human breast cancer progression, to uncover the mechanism by which MMP-11 favors tumor growth.

2.1.1 Identification of the GOF and LOF mice genotypes

The genetic status for the PyMT transgene and MMP-11 gene were identified by genotyping before randomization of the mice for the experiments. In the GOF model, I selected $PyMT^{Tg}$::$MMP11^{WT}$ and $PyMT^{Tg}$::$MMP11^{Tg}$ female mice (Figure 2.1 A), both lines were in the FVB/N background. In the LOF model, I selected $PyMT^{Tg}$::$MMP11^{WT}$ and $PyMT^{Tg}$::$MMP11^{KO}$ female mice (Figure 2.1 B), lines were in a different background, but all the mice were in a 129/SvJ mixed FVB/N background. Six to eight mice were randomly assigned to different groups in different experimental time points. Because of the different backgrounds, palpable tumors developed at 9-10 weeks old in GOF mice, and at 13-14 weeks old in LOF mice. According to our animal procedure, mice were sacrificed at different time point, GOF model was stopped at 14 weeks old, LOF model was stopped at 17 weeks old (Figure 2.1 C).

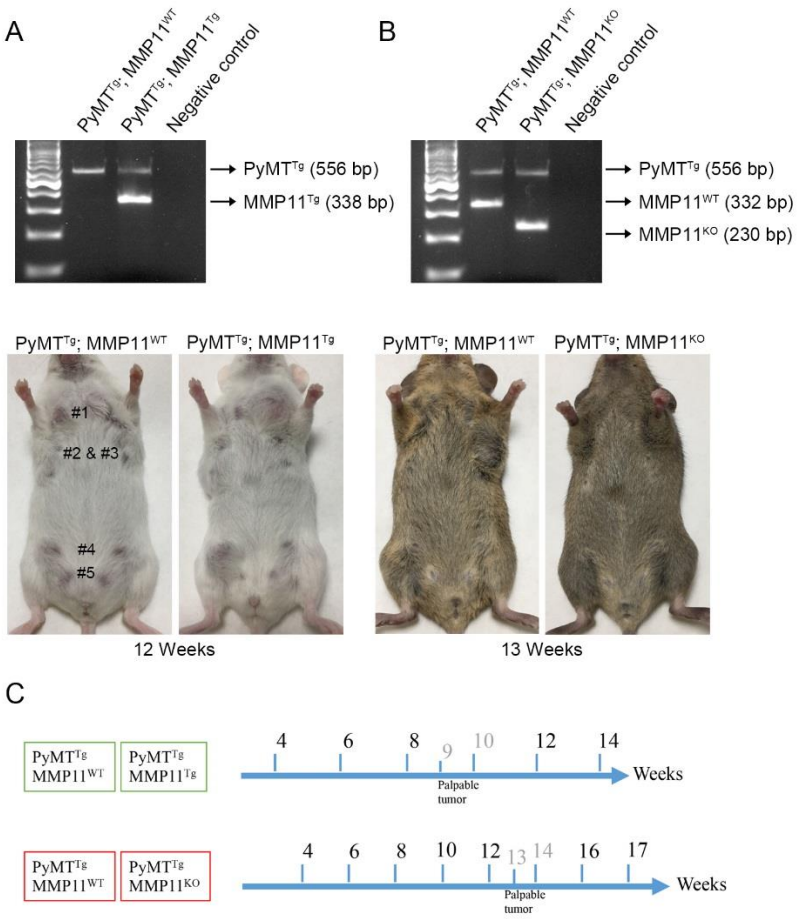

Figure 2.1 Identification of PyMT and MMP-11 genotypes. (A) Identification of PyMT and MMP-11 genes with genomic DNA by PCR in the GOF group. Representative mice harboring tumors and the mammary glands identification number are shown. (B) Identification of PyMT and MMP-11 genes with genomic DNA by PCR in the LOF group. Representative mice tumors are shown. (C) Schematic represents the workflow of GOF and LOF experimental models. 6-8 mice/group/time points.

2.1.2 MMP-11 decreases MMTV-PyMT mice body weight

Because it was shown that MMP-11 overexpression is associated with a lean phenotype, we measured body weight in the different cohorts. In the GOF model, MMP-11 decreases postnatal mice body weight from 3 to 9 weeks old. But there was no difference at 9-10 weeks old after palpable tumor occurred (Figure 2.2 A). In the LOF model, deficiency of MMP-11 increased postnatal mice body weight from 3 to 12 weeks old. But there was no difference after palpable tumor occurred at 13-14 weeks old (Figure 2.2 B).

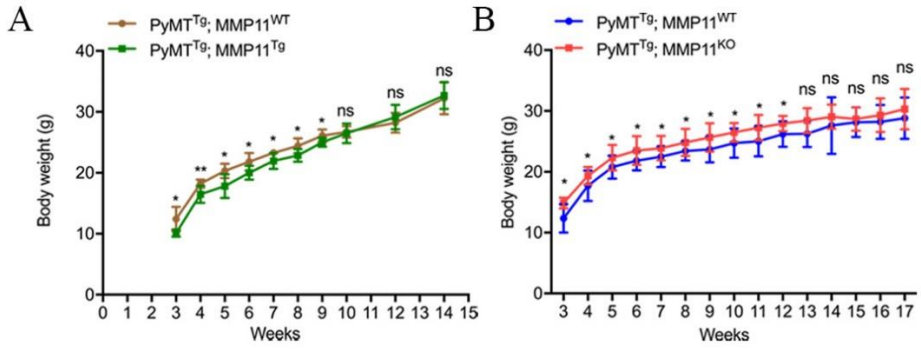

Figure 2.2 Analysis of mice body weight. (A) Overexpression of MMP-11 decreased mice body weight before 9 weeks old. (B) Knockout of MMP-11 increased mice body weight before 12 weeks old. 6-8 mice/group, data represent mean±SD, *P < 0.05, **P < 0.01 (unpaired t-test).

2.1.3 MMP-11 promotes mammary tumor growth in MMTV-PyMT mice

We next addressed tumor incidence and the kinetics of tumor development. In the GOF model, the percentage of tumor free mice was not significantly different in the presence of MMP-11 compared with control (Figure 2.3 A). In the absence of MMP-11 (LOF), the percentage of tumor free mice was significantly delayed (Figure 2.3 B). By using a caliper to measure volume in identified palpable tumors, overexpression of MMP-11 (GOF) increased tumor volume in #1, #2, #3 and #4 mammary glands at 10 weeks old, and #1 mammary gland at 14 weeks old; MMP-11 deficiency (LOF) decreased tumor volume in #2, #3 and #4 mammary gland at 14 weeks old, and #1, #2 mammary gland at 17 weeks old (Figure 2.3 B). We also studied the extend of mammary gland lesions in the #4 mammary gland by using whole mount carmine-red staining. This staining enables to identify hyperplasia and neoplastic lesions area both in GOF and LOF groups at different time point before the end of experiment (Figure 2.3 C and D). The area of hyperplasia and neoplastic lesions in #4 mammary gland were analyzed by ImageJ software. MMP-11 transgenic mice (GOF) developed more lesions at 6, 8, 10 and 12 weeks old, while MMP-11 deficient mice (LOF) developed less lesions at 10 and 14 weeks old compared with their wildtype littermates. Mice were sacrificed according to the defined terminal end points, whole mount staining of the #4 mammary gland tumor lesions in GOF mice at 14 weeks old, LOF mice at 17 weeks old (Figure 2.3 E), and normal mammary gland of wildtype mice as control are shown in Figure 2.3 F. These data demonstrated that MMP-11 promotes MMTV-PyMT transgenic mice tumor development and growth.

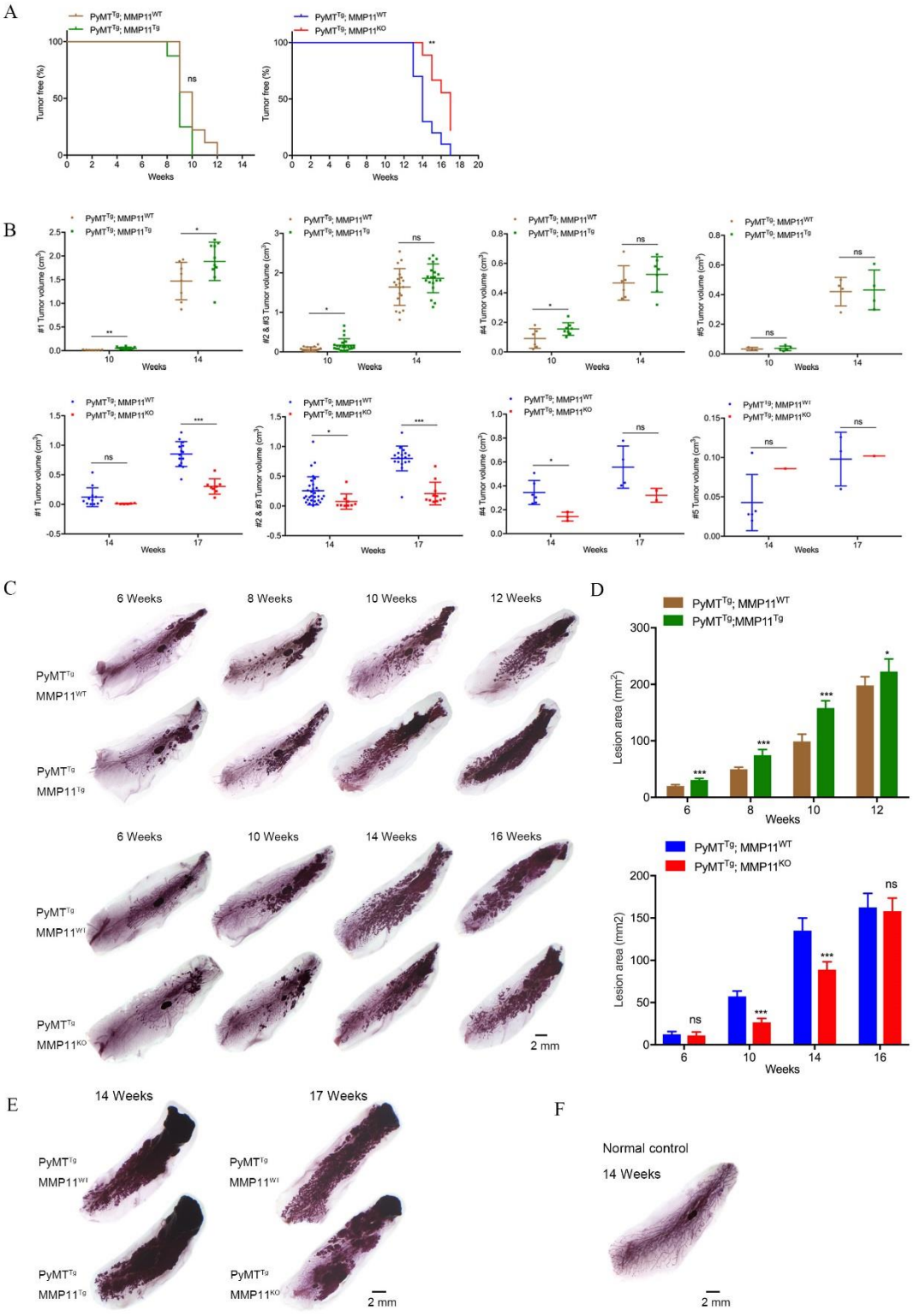

Figure 2.3 Analysis of mice tumor development in the GOF and LOF mice models. (A) No difference of percentage of tumor free mice between MMP-11 transgenic and wildtype group; Mice deficient of MMP-11 significantly decrease the percentage of tumor free mice. (B) Tumor volume was measured individually by caliper twice a week including all ten mammary glands, one dot corresponding to a palpable tumor. (C) #4 mammary glands whole mount carmine-red staining showed the developmental hyperplasia and neoplastic lesions at different time point. (D) Quantification of the lesion area of hyperplasia and neoplasm in B. (E) At the end of experiment, #4 mammary glands were shown. (F) Wildtype normal mammary gland served as controls. 6-8 mice/group, data represent mean±SD, *P < 0.05, **P < 0.01, ***P < 0.001 (unpaired t-test).

2.1.4 MMP-11 plays anti-necrotic and anti-apoptotic roles at early stage of mammary tumor development in MMTV-PyMT mice

In order to address the extent of tumor necrosis and apoptosis, serial sections were made from paraffin embedded tumor tissues formed in #4 mammary gland. The same size of tumor tissues from the same gland of wildtype control mice served as control. Tumor necrosis was analyzed by hematoxylin and eosin (HE) stain. The necrotic areas are characterized by a pink color because of cell death and cytolysis (Fischer et al., 2008). In the GOF model, mice overexpressing MMP-11 had decreased necrotic area at 8 weeks old, at 14 weeks old no significant differences were observed but overall at this end-point less necrosis was observed (Figure 2.4 A and B, indicated as "n"). Loss of MMP-11 increased the necrosis area at 14 and 17 weeks old (Figure 2.4 A and B, indicated as "n"). We next measured the extent of apoptosis by using an apoptotic assay (TUNEL assay). It revealed that the percentage of cell apoptosis in MMP-11 transgenic mice group (GOF) was less than in wildtype mice at 6 weeks old (Figure 2.4 C and D). In contrast, in LOF mice had an increased number of TUNEL-positive cells at 10 weeks old (Figure 2.4 C and D). However, there was no difference of the number of apoptotic cells between MMP-11 transgenic and wildtype mice at 10 weeks old (Figure 2.4 E and F).

Further investigation of apoptosis was made by western blot. Well-formed tumors from #1 mammary gland at early stage of 6 weeks of GOF and 10 weeks of LOF mice were isolated and protein were extracted, respectively. In parallel, tumors in MMP-11 wildtype control were also collected. The expression level of the anti-apoptotic protein bcl-2, from 6 weeks old GOF and 10 weeks old LOF mice tumor, increased and decreased compared with their MMP-11 wildtype controls, respectively (Figure 2.4 G and H).

These results revealed that the MMP-11 has anti-necrosis and anti-apoptotic roles in PyMT mice tumor early developmental stage.

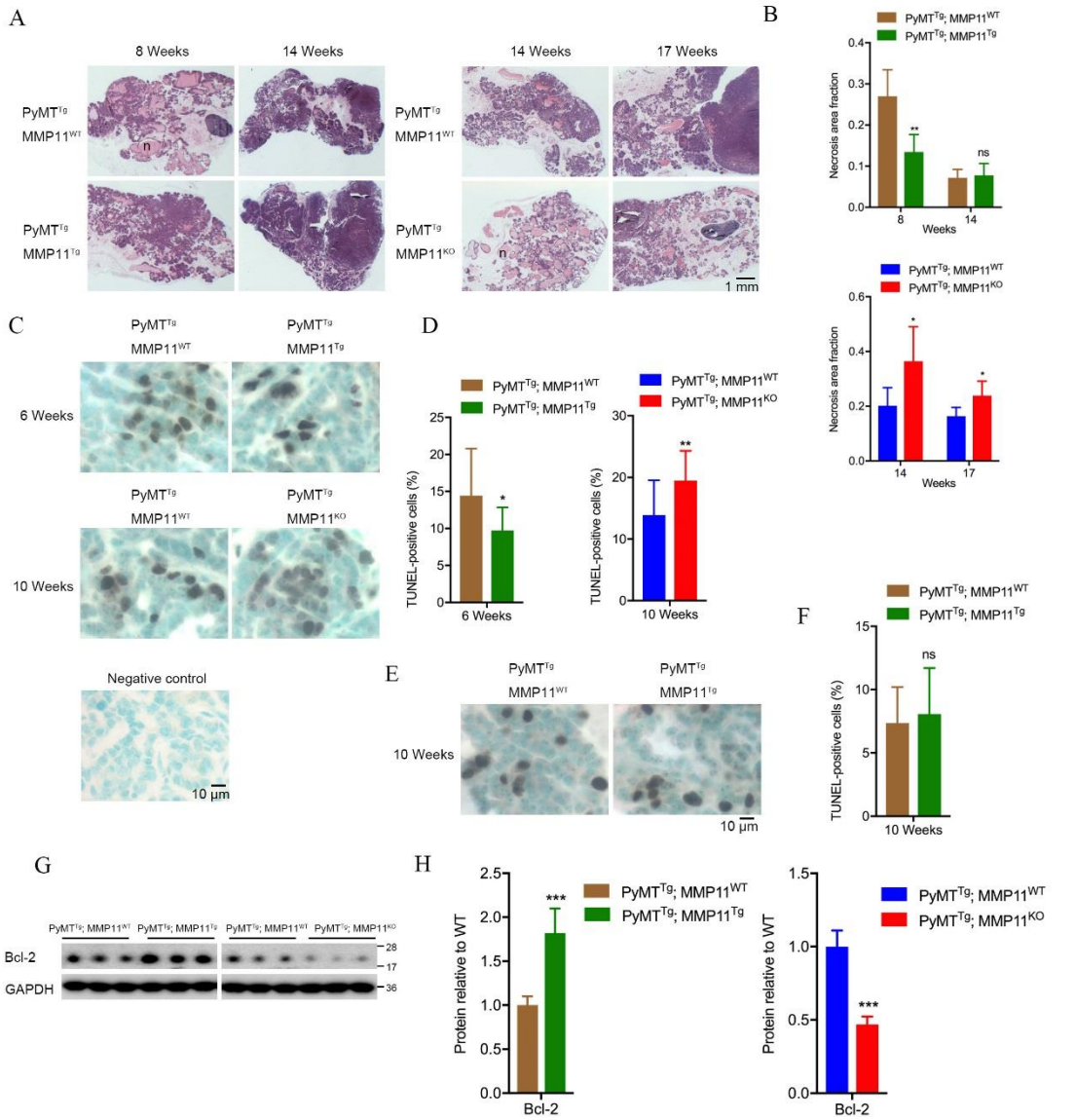

Figure 2.4 MMP-11 plays anti-necrotic and anti-apoptotic roles in tumor early stages. (A) HE staining showed overexpression of MMP-11 decreased tumor necrosis area, but deficiency of MMP-11 increased necrosis area compared with their control groups, respectively. (B) Quantification of tumor necrosis area fraction in A. (C) TUNEL assay revealed the positive staining apoptotic cells decreased in MMP-11 transgenic group, but increased in knockout group compared with their control groups, respectively. (D) Quantification of the percentage of TUNEL positive staining cells in C. (E) No difference of apoptotic cells in GOF model at 10 weeks old mice. (F) Quantification of the percentage of TUNEL positive staining cells in E. (G) Bcl-2 protein was detected by western blot in 6 weeks old GOF and 10 weeks old LOF mice models. GAPDH as loading control. (H) Quantification of bcl-2 protein relative level by normalized to wildtype control. Abbreviation: n, necrosis. 6-8 mice/group, data represent mean±SD, *P < 0.05, **P < 0.01, ***P < 0.001 (unpaired t-test).

2.1.5 MMP-11 plays a proliferative role at early stage of tumor development in MMTV-PyMT mice and induces the insulin-like growth factor-1 signalling pathway

To investigate the impact of MMP-11 on tumor proliferating cells, tissues sections corresponding to tumors grown in the #4 mammary gland were analyzed by

immunofluorescence using a specific antibody directed against the Ki-67, a protein encoded by the MKI67 gene and an accepted marker of cell proliferation (Scholzen and Gerdes, 2000). Positive cells were counted by ImageJ software. The proportion of Ki-67 positive staining cell increased significantly in $PyMT^{Tg}$:$MMP11^{Tg}$ in 6-week old mice as compared to $PyMT^{Tg}$:$MMP11^{WT}$ mice, whereas $PyMT^{Tg}$:$MMP11^{KO}$ mice displayed less Ki-67 positive stained cells at 10-week of age compared to their wildtype controls (Figure 2.5 A and B). However, at a later stage (8-week old mice) $PyMT^{Tg}$:$MMP11^{Tg}$ mice did not exhibit a significant difference in the percentage of proliferating cells as compared to $PyMT^{Tg}$:$MMP11^{WT}$ control mice (Figure 2.5 C and D). As a control of normal mammary gland immunofluorescence staining, here showed the alpha smooth muscle actin (α-SMA), which is a marker of stromal fibrogenic cells (Figure 2.5 E). These data showed that MMP-11 increases PyMT tumor cell proliferation at an early stage of tumor development.

Given that the IGF1 is well recognized to play an important role in neoplasia (Pollak, 2008), and that IGF1 bioavailability is increased upon MMP-11 overexpression (Dali-Youcef et al., 2016), we investigated whether the IGF1 signalling pathway is exacerbated in $PyMT^{Tg}$:$MMP11^{Tg}$ mice to support tumor growth. By analyzing #1 mammary tumor extracts at early stage of 6-week of GOF and 10-week of LOF mice, indeed, we observed a significant activation of this pathway as demonstrated by the significant increase in the phosphorylation of two important components of this cascade, namely protein kinase B (AKT) and FoxO1, in tumor protein extracts from $PyMT^{Tg}$:$MMP11^{Tg}$ mice as compared to control mice. Consistently, a decrease in the phosphorylation of AKT and FoxO1 was observed in $PyMT^{Tg}$:$MMP11^{KO}$ mice compared to controls (Figure 2.5 F and G).

The MMP11-mediated activation of the IGF1/AKT growth pathway was most likely due to the increase in IGF1 bioavailability as demonstrated by the decrease in the expression of IGFBP1 (Figure 2.5 F and G), the protein that controls the circulating levels of IGF1.

We conclude that MMP-11 overexpression promotes cell proliferation in $PyMT^{Tg}$:$MMP11^{Tg}$ mice and exacerbates the IGF1/AKT pathway, which is probably responsible for the mitogenic effect of IGF1 and the increase in cell proliferation.

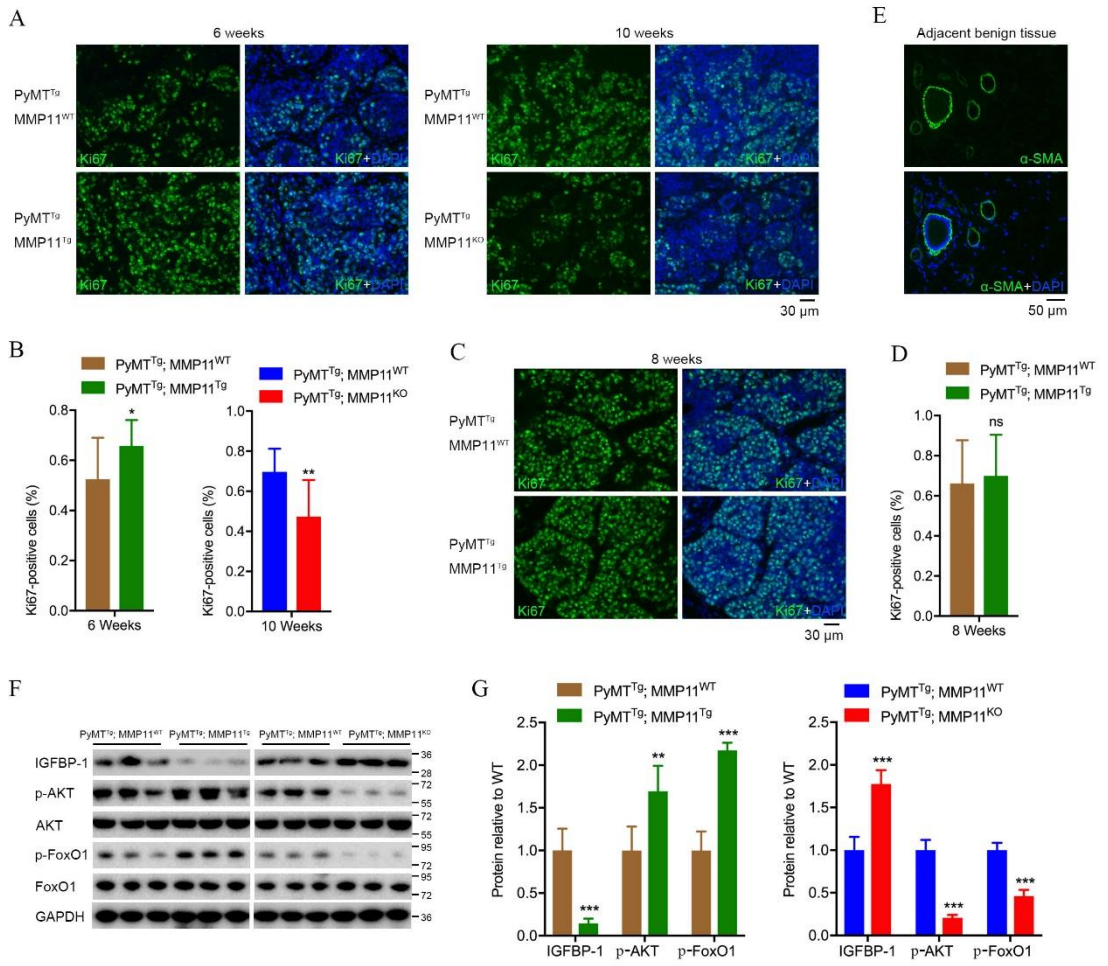

Figure 2.5 MMP-11 promotes tumor cell proliferation specially at early stage. (A) Immunofluorescence showed the Ki-67 positive cells increased in MMP-11 transgenic group at 6 weeks old, but knockout MMP-11 mice have less proliferating cells at 10 weeks old compared with their control mice, respectively. (B) Quantification of the percentage of Ki-67 positive cells in A. (C) No difference of Ki-67 staining cells in GOF model at 8 weeks old mice. (D) Quantification of the percentage of Ki-67 positive cells in C. (E) Normal mammary gland of α-SMA immunofluorescence staining. (F) Western blot analysis revealed the change of IGFBP-1/AKT/ FoxO1 signalling pathways in the GOF and LOF tumor mice groups. (G) Quantification of the ratios of phosphorylated proteins to total level compared to wildtype, respectively, normalized to GAPDH expression. 6-8 mice/group, data represent mean±SD, *P **<** 0.05, **P **<** 0.01, ***P **<** 0.001 (unpaired t-test).

2.1.6 MMP-11 increased lipid uptake and utilization and promotes metabolic switch

Cancer cells always exhibit a reprogrammed cell metabolism compare to normal cells resulting from specific energy demands. In the case of invasiveness, cancer cells also demand extra energy burden. We hypothesized that MMP-11 will stimulate lipid utilization and promote aerobic glycolysis, a process known as the Warburg effect, to support tumor growth. By analyzing #1 mammary tumor extracts at early stage of 6-week of GOF and 10-week of LOF mice, we observed a significant increase in the expression of the fatty acid transporter Cd36 and the oxidative genes peroxisome

proliferator activated receptor alpha (Pparα) and its target gene acyl coenzyme A oxidase (Aco), but also increased expression of acetyl-Coenzyme A carboxylase 1 and 2 (Acc 1 and Acc2), supporting an increased lipid uptake, utilization and turnover (Figure 2.6 A). Consistently, we observed the opposite expression profile in $PyMT^{Tg}$:$MMP11^{KO}$ mice as compared to their controls (Figure 2.6 A).

We then analyzed the expression of genes involved in lactate metabolism and observed an increase expression of genes involved in lactate production: lactate dehydrogenase A (Ldha), release: monocarboxylate transporter 4 (Mct4), uptake: monocarboxylate transporter 1 (Mct1) and metabolism: lactate dehydrogenase B (Ldhb) in $PyMT^{Tg}$:$MMP11^{Tg}$ mice as compared to controls (Figure 2.6 B). Interestingly, we found a significant reduction in the expression of Mct4 and Ldha in $PyMT^{Tg}$:$MMP11^{KO}$ mice suggesting a reduction in lactate production and release. No significant difference was observed in the expression of Mct1 and Ldhb (Figure 2.6 B). To determine whether the increase in aerobic glycolysis seen in $PyMT^{Tg}$:$MMP11^{Tg}$ mice was accompanied by a negative regulation of OXPHOS genes, we analyzed the expression of genes involved in the mitochondrial electron transport chain (ETC). Likewise, we observed in tumors from $PyMT^{Tg}$:$MMP11^{Tg}$ mice a significant decrease in the expression of Ndufb5, a gene that encodes a subunit of complex I of the mitochondrial respiratory chain which transfers electrons from NADH to ubiquinone; a decrease in Cox5b expression, a gene encoding the cytochrome c subunit 5b protein of complex IV of the ETC; and a diminished expression of Atp5b, a gene encoding ATP synthase subunit 5b of complex V, suggesting a decrease in mitochondrial respiration. Of note, we noted an increased expression of the mitochondrial encoded gene Cox2 (cytochrome c oxidase subunit 2, complex IV), suggesting an increase in mitochondria number (Figure 2.6 C). The results of MMP-11 deficiency mirrored those observed in MMP-11 overexpression (Figure 2.6 C).

In summary, we believe that MMP-11 overexpression confers an advantage for cancer cells to promote their growth through a metabolic reprogramming involving an increase of aerobic glycolysis, a decrease of mitochondrial respiration and an increase of lipid turnover.

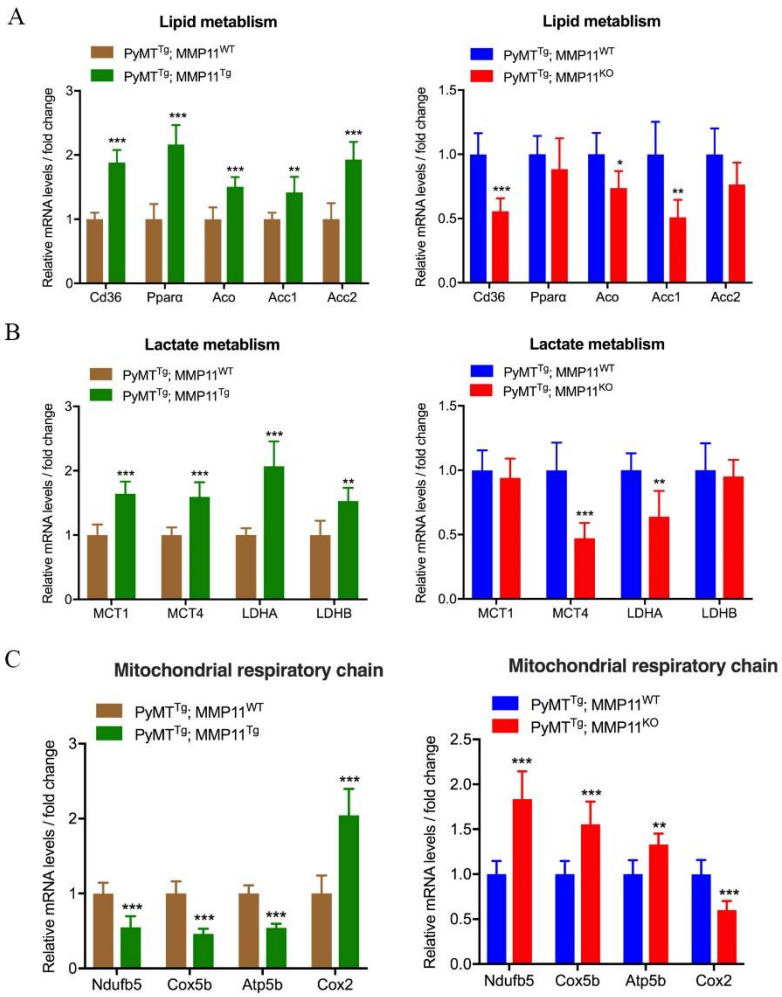

Figure 2.6 MMP-11 promotes tumor metabolic switch and lipid utilization. (A) RT-qPCR revealed the mRNA expression of genes involved in lipid metabolism in both GOF and LOF mice models tumor extract. (B) mRNA expression of genes involved in lactate metabolism in both GOF and LOF mice groups. (C) The level changes of genes implicated in mitochondrial respiratory chain in GOF and LOF mice groups. Data are presented as fold changes. 6-8 mice/group, data represent mean±SD, *P < 0.05, **P < 0.01, ***P < 0.001 (unpaired t-test).

2.1.7 MMP-11 increases endoplasmic reticulum stress response and alters mitochondrial unfolded protein response

Protein homeostasis or proteostasis is supported by a coordinated regulation of polypeptide production, folding, trafficking and degradation when unfolded or misfolded proteins accumulate within the cell. Endoplasmic reticulum (ER) ensures proper folding and processing of proteins that will be secreted and hence is a guarantor of proteostasis. In immune and metabolic cells, but also following the exposure of cells to a variety of stressors, proteostasis is disrupted and an ER unfolded protein response (UPR^{ER}) is initiated to restore protein homeostasis (Wang and Kaufman, 2016; Frakes and Dillin, 2017). In our study, we sought to analyze the impact of MMP-11 on ER stress and the UPR^{ER}. By analyzing #1 mammary tumor extracts and #4 mammary

tumor sections at early stage of 6-week of GOF and 10-week of LOF mice, interestingly, we found a significant increase in the phosphorylation of the α subunit of eukaryotic translation initiation factor 2 (eIF2α) in $PyMT^{Tg}$:$MMP11^{Tg}$ mice by immunofluorescence (Figure 2.7 A and B), which is a target of the protein kinase RNA (PKR)-like ER kinase (PERK) and an important sensor of ER stress (Frakes and Dillin, 2017). And also increased expression of genes of driving the UPR^{ER} program such as X-box binding protein (Xbp1), activating transcription factor 4 (Atf4) and activating transcription factor 6 (Atf6) in $PyMT^{Tg}$:$MMP11^{Tg}$ mice as compared to $PyMT^{Tg}$:$MMP11^{WT}$ controls (Figure 2.7 C). Reciprocal effects were also observed in $PyMT^{Tg}$:$MMP11^{KO}$ model compared to control animals (Figure 2.7 C).

Similar to the ER, the mitochondria is an organelle that possesses also a protein folding quality control that in response to stress will ensure, through mito-nuclear communication, proper folding of imported proteins from the cytosol, named the mitochondrial unfolded protein response or UPR^{mt} (Jovaisaite et al., 2014). In the context of our study, we observed clearly in tumors from $PyMT^{Tg}$:$MMP11^{Tg}$ mice an alteration of the CHOP/HSP60, HSP10/Clpp pathway of the UPR^{mt} as compared to $PyMT^{Tg}$:$MMP11^{WT}$ animals (Figure 2.7 D). Indeed, expression levels of the mitochondrial heat shock protein genes Hsp60 and Hsp10 were significantly decreased as well as those of the mitochondrial protease caseinolytic mitochondrial matrix peptidase proteolytic subunit (Clpp) and of the prohibitin Phb, a sensor of mitochondria stress and a promoter of longevity (Jovaisaite and Auwerx, 2015) (Figure 2.7 D). Since misfolded proteins are targeted for degradation by the ubiquitin-proteasome system (UPS), we sought to determine whether the abnormal UPR^{mt} was accompanied by a normal elimination of misfolded proteins. Interestingly, MMP-11 overexpression in the PyMT cancer model led to an abnormal proteasomal activity as shown by decreased expression of genes encoding the proteasomal subunits Psmb1 and Psmd1 as compared to control animals (Figure 2.7 E), suggesting an accumulation of misfolded proteins that could be responsible for the impaired mitochondrial function. Consistently, we observed the opposite phenomenon in $PyMT^{Tg}$:$MMP11^{KO}$ mice, as shown by an increased UPR^{mt} response with enhanced expression of Hsp60, Hsp10 and Clpp, and enhanced proteasomal activity with increased expression of Psmb1 and Psmd1 as compared to their $PyMT^{Tg}$:$MMP11^{WT}$ control animals (Figure 2.7 D and E).

Previous reports have already demonstrated that mitochondrial dysfunction induced by ETC perturbations and reactive oxygen species (ROS) generation inhibit proteasomal activity through proteasome disassembly in different organisms including mammalian cells (Livnat-Levanon et al., 2014; Segref et al., 2014). Since alterations in ETC leads to decreased ATP production (Smeitink et al., 2006) and that the UPS system relies on ATP for its function, we sought to determine whether MMP11-induced AMP-activated kinase (AMPK) activation is implicated in this process. Interestingly, we observed a significant increase in AMPK phosphorylation at threonine 172 residue in tumors from $PyMT^{Tg}$:$MMP11^{Tg}$ mice as compared to their controls. Consistently, $PyMT^{Tg}$:$MMP11^{KO}$ mice exhibited a significant decrease in AMPK activity compared to control animals (Figure 2.7 F and G).

Overall, MMP-11 exacerbates endoplasmic reticulum stress, alters the mitochondrial UPR and impairs proteasome activity that might be caused by increased oxidative stress, contributing thereby in energy depletion and activation of AMPK.

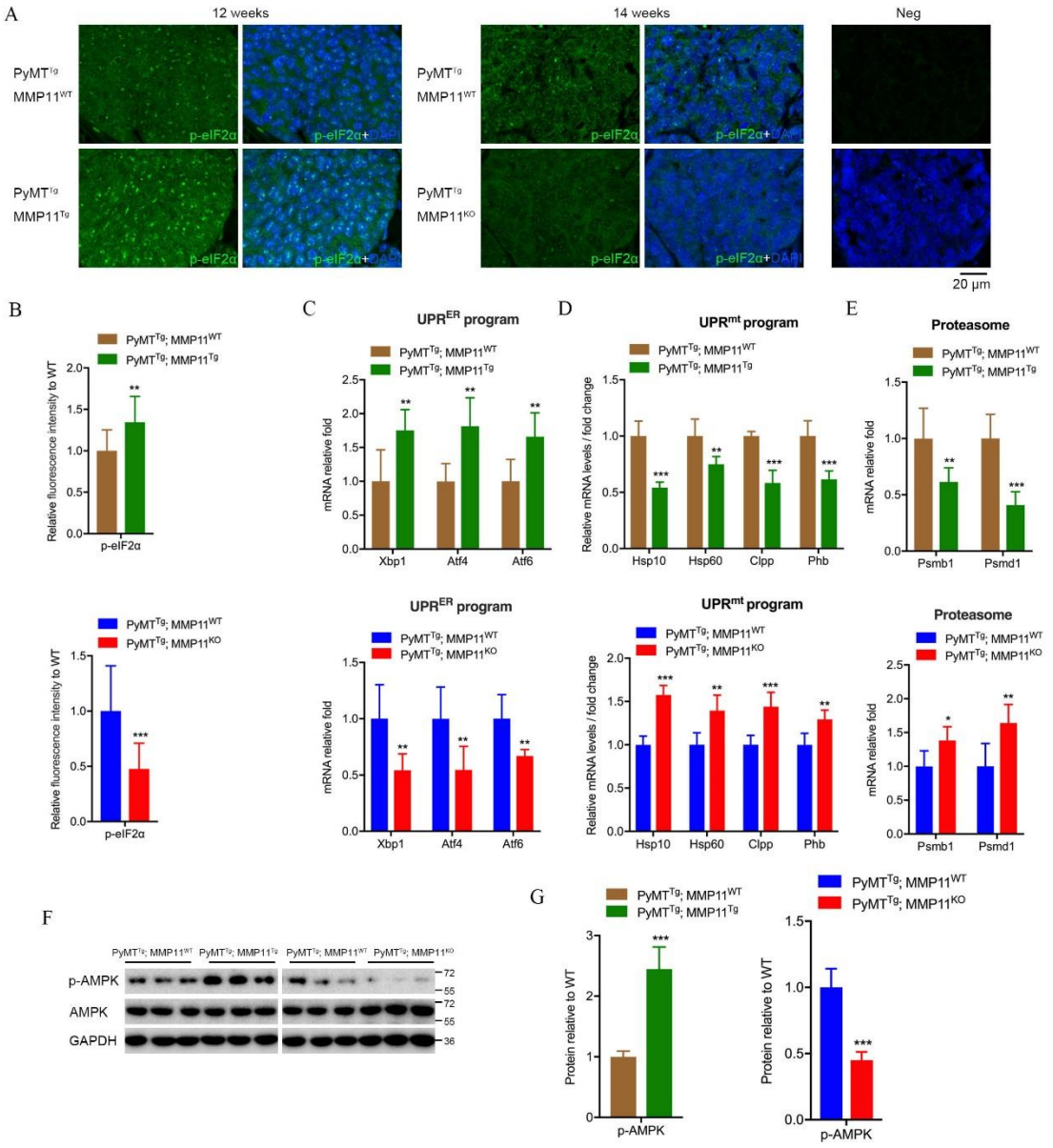

Figure 2.7 MMP-11 promotes tumor cellular stress responses. (A) Representative confocal images demonstrated the p-eIF2α staining in GOF and LOF mice tumor tissue slides. Negative staining without primary antibody. (B) Relative quantification of p-eIF2α fluorescence intensity in A. (C) RT-qPCR revealed the level changes of genes implicated in UPR^{ER} program in GOF and LOF mice models tumor extracts. (D) RT-qPCR revealed the level changes of genes implicated in UPR^{mt} program in GOF and LOF mice models. (E) RT-qPCR revealed the level changes of genes implicated in proteasome activity in GOF and LOF mice models. (F) Western blot analysis revealed the change of phosphorylated protein of AMPK in the GOF and LOF mice groups. (G) Quantification of the ratios of phosphorylated AMPK proteins to total levels compared to wildtype, respectively, normalized to GAPDH expression. Data are presented as fold changes. 6-8 mice/group, data represent mean±SD, *P < 0.05, **P < 0.01, ***P < 0.001 (unpaired t-test).

2.1.8 MMP-11 promotes MMTV-PyMT mice mammary tumor stroma fibrosis at limited time points

MMP-11 is expressed by CAAs in tumor periphery and is believed to favor adipocyte delipidation and transition to fibroblastic cells (Tan et al., 2011; Rio, 2013).

To study whether MMP-11 can facilitate tumor stroma fibrosis, the extent of tumor fibrosis was studied in the absence of MMP-11 and under conditions of MMP-11 overexpression. To this aim, mammary tumors taken from animals at 4, 6, 8, 12, 14 and 16 weeks of age were processed for immunochemistry. We used picro-sirius red (PSR) staining, which allows the histological visualization of collagen I and III fibers. The PSR staining can be observed using standard light microscopy or polarized light microscopy. Polarized light results in birefringence of the collagen fibers and allows the discrimination between type I (thick fibers, yellow-orange) and type III (thin fibers, green).

Because it is not possible with this method to separate and quantify type I and type III collagen in these PyMT tumor samples, I only showed here representative images to demonstrate the collagen formation in each group. In the tumors of GOF mice where MMP-11 is overexpressed, more collagens (bright filed, red), predominantly collagen I (polarized filed, yellow-orange) were observed at 4 and 6 weeks old compared with tumors at the same stages in control mice (Figure 2.8). At 8 and 12 weeks old no significant changes in collagen staining were observed. In the LOF model, MMP-11 knockout mice at 6, 8 and 14 weeks old showed no significant difference of collagen fibers structure compared with wildtype (bright and polarized filed). At 12 weeks old, MMP-11 knockout mice have less collagen formation compared with wildtype (bright and polarized filed), and knockout mice displayed more necrosis which stained homogeneous red color (Figure 2.8 A, indicated as “n”). However, in the adjacent normal tissue (4 weeks) and tumor center (8 weeks) of GOF model, there were no differences of collagen formation in transgenic and wildtype control mice examined by PSR (Figure 2.8 B). No difference was detected in the tumor center of 16 weeks LOF.

In conclusion, MMP-11 might modulate the number and composition of stromal collagen fibers in PyMT induced tumor at limited time points only. I speculate that in addition to MMP-11 many confounding factors may affect collagen formation and degradation in the tumor including necrosis. More methods are needed to demonstrate the tumor stroma fibrosis.

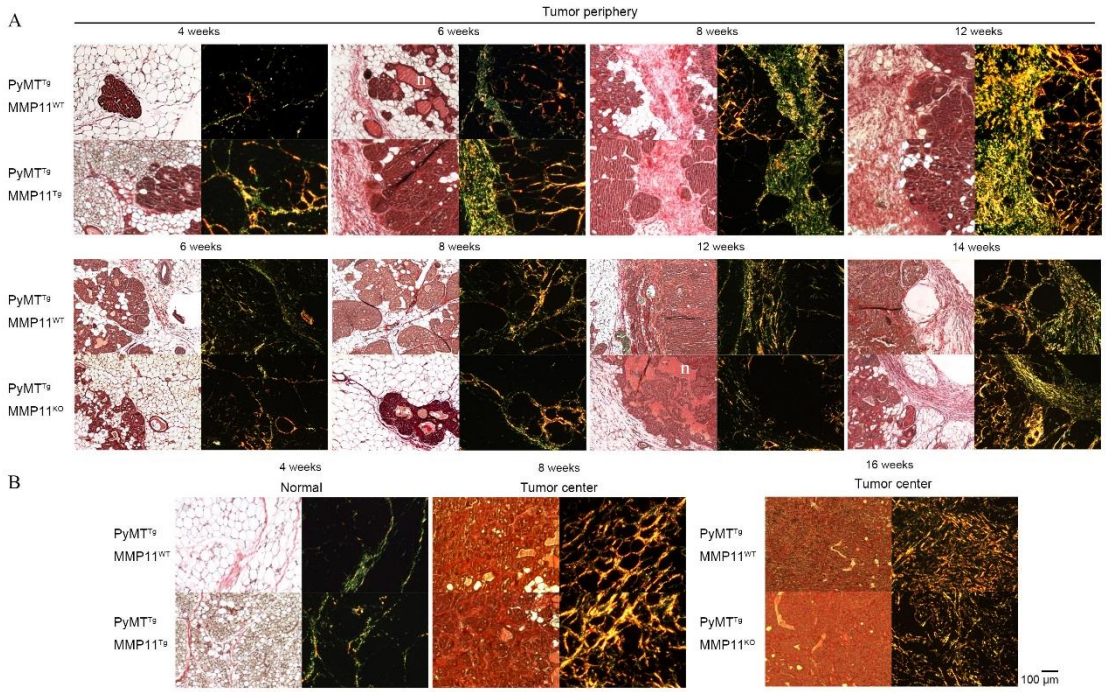

Figure 2.8 MMP-11 promotes mammary tumor stromal collagen formation at limited time points. (A) PSR staining of collagen in tumor periphery. Overexpression of MMP-11 have more red-stained collagens at 4 and 6 weeks old (bright filed), predominantly with type I collagen under polarized microscope (thick fibers, yellow-orange), except at 8 and 12 weeks old. Deficiency of MMP-11 displayed no significant difference of collagen fibers at the tumor front compare with control, except 12 weeks old knockout mice have less collagen and with some homogeneous red staining of necrosis area ("n"). (B) Staining of tumor adjacent normal mammary gland and tumor center of GOF and LOF models. There is no difference of collagen generation between two groups, respectively. Abbreviation: n, necrosis. 6-8 mice/group.

2.1.9 MMP-11 does not modulate mammary tumor angiogenesis and EMT in MMTV-PyMT mice

Angiogenesis and EMT could be considered as main tumor accelerating factors. To examine the extent of tumor angiogenesis in the presence of overexpressed MMP-11 and in the absence of MMP-11, expression of the angiogenesis marker CD31 was examined by immunofluorescent detection in the tumor of 6 weeks old and 10 weeks old mice. In addition, to examine the EMT extend, we studied the E-cadherin staining as a marker for epithelial cells in the same samples. Results showed that CD31 and E-cadherin staining were similar between MMP-11 experimental and control groups both in GOF and LOF models (Figure 2.9). In conclusion, the MMTV-PyMT mice tumor angiogenesis and EMT ability were not significantly affected by the expression of MMP-11.

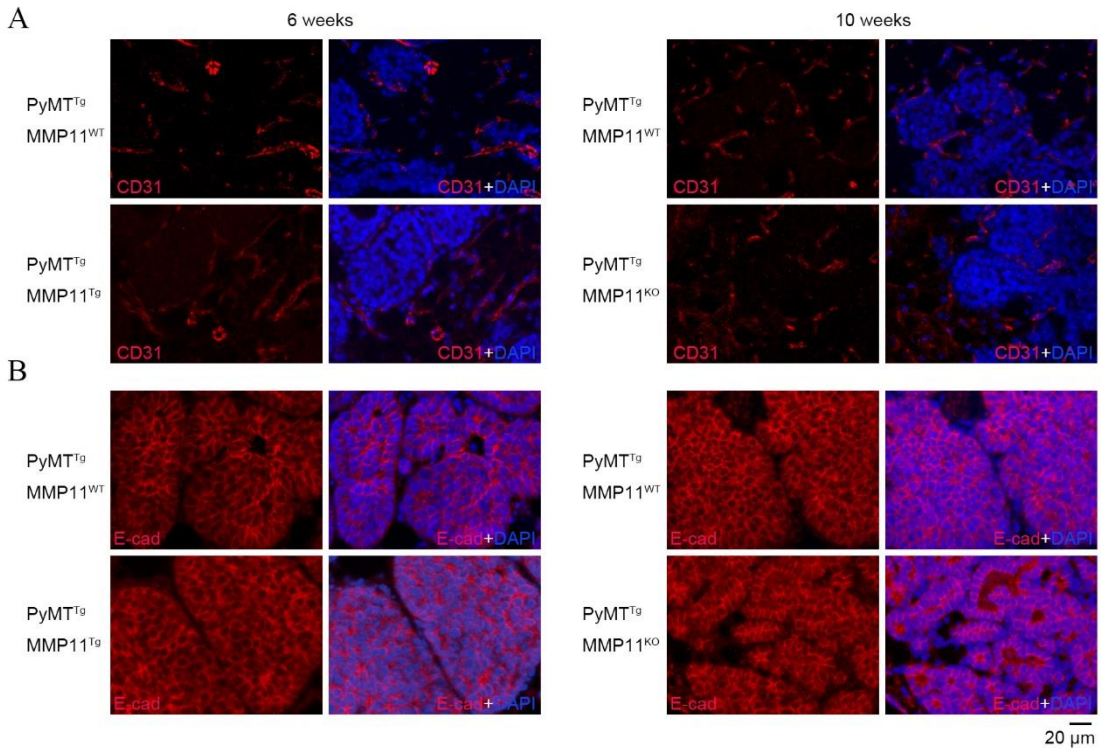

Figure 2.9 MMP-11 has no effects on mammary tumor angiogenesis and EMT. (A) Immunofluorescent staining by endothelial marker CD31 showed there is no difference between MMP-11 experimental and control groups both in 6 weeks old GOF and 10 weeks old LOF models. (B) Epthelial marker E-cadherin showed there is no difference between MMP-11 experimental and control groups both in 6 weeks old GOF and 10 weeks old LOF models. 6-8 mice/group.

2.1.10 MMP-11 reduces dissemination of mammary tumor to the lung in MMTV-PyMT mice

We investigated the function of MMP-11 on tumor cell metastasis to the lung in PyMT induced tumor mice. To this aim at the last time points of the study (14 weeks of GOF and 17 weeks of LOF), the left side lungs in the different mice groups were dissected for HE staining, and the visible metastatic foci were counted by ImageJ software. The staining revealed that 14 weeks old MMP-11 transgenic mice have less disseminated foci, but there is no significant difference in the size of metastatic lesions. However, LOF mice at 17 weeks old displayed smaller size of metastatic lesions compared with control lungs (Figure 2.10 A and B). Because we established in LOF model that tumor growth is much slower in MMP-11 deficient mice compared with wildtype control, I choose 13 weeks old wildtype control and 16 weeks old LOF that have the same average tumor volume of 0.2 cm^3 to look at the metastatic burden in the lung. Likewise, wildtype and transgenic mice were analyzed at 8 weeks old in GOF model before palpable tumor occurred. The middle lobes of the right side lung were

collected for analyzing the presence of PyMT gene expression. The PyMT mRNA is specifically expressed in mammary epithelial cells therefore its detection in other organs indicate metastasis spreading. By real-time RT-PCR quantification, overexpression of MMP-11 in the GOF model and deficiency of MMP-11 (LOF), reduced and increased PyMT mRNA relative levels in the lungs compared with control animals, respectively (Figure 2.10 C). Together these data showed that MMP-11 may play a preventing role in lung metastasis.

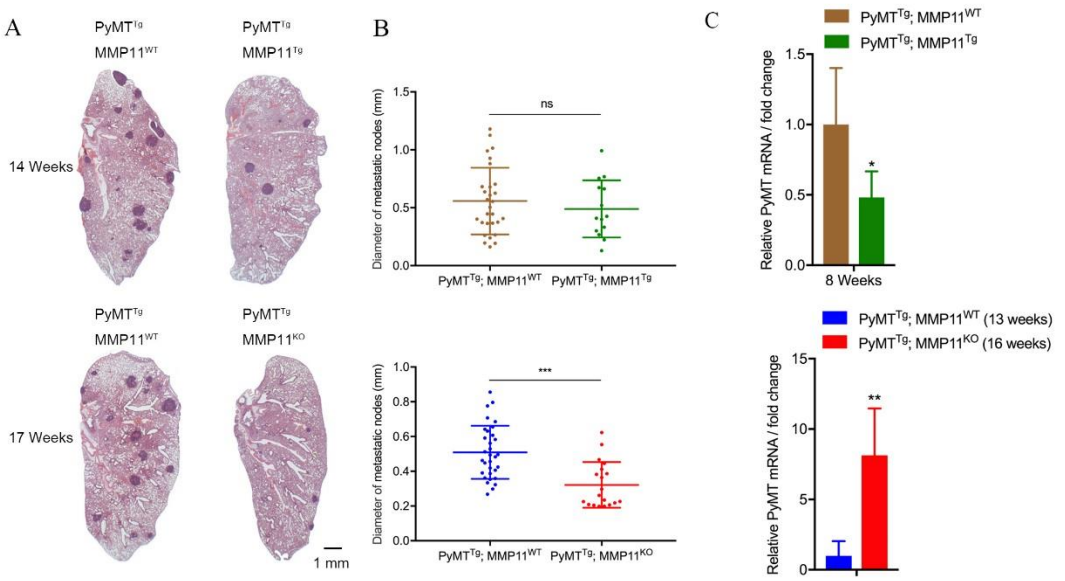

Figure 2.10 MMP-11 inhibits mammary tumor to lung dissemination. (A) HE stain of lung sections showed that either overexpression of MMP-11 or deficiency of MMP-11 decreased the number of metastasis foci, but the tumor diameter also decreased only in the LOF model. (B) RT-qPCR analyzed the PyMT gene in the lung which should present in the mammary gland epithelial cells. MMP-11 transgenic mice displayed lower mRNA level of PyMT gene in the GOF model at 8 weeks old. 16 weeks old MMP-11 knockout mice displayed higher mRNA level of PyMT gene compare with 13 weeks old wildtype control in the LOF model. 6-8 mice/group, data represent mean±SD, *P **<** 0.05, **P **<** 0.01, ***P **<** 0.001 (unpaired t-test).

In conclusion, overexpression of MMP-11 in MMTV-PyMT mice promoted tumor growth, decreased tumor cell apoptosis and enhanced proliferation at early stages of tumor development. MMP-11 also promoted mammary tumor cell lipid utilization and metabolic switch. Moreover, MMP-11 increased tumor cell ER stress and UPR^{mt} stress response. In contrast, overexpressed MMP-11 inhibited mammary tumor dissemination to the lung but did not limit metastatic tumor growth. Reciprocal results were observed in MMP-11 deficient animals. Overall, MMP-11 has promoting effects on mice mammary tumors, it should be considered as a potential target for cancer therapy in early breast cancer only.

Research article

Matrix metalloproteinase-11 promotes mouse mammary gland tumor progression

Bing Tan[1], Amélie Jaulin[1], Caroline Bund[4], Hassiba Outilaft[4], Marie-Pierrette Chenard[1,2], Fabien Alpy[1], A.E. Cicek[5], Izzie J. Namer[4], Catherine Tomasetto[1,✉] and Nassim Dali-Youcef[1,3,✉]

[1] Department of Functional Genomics and Cancer, Institut de Génétique et de Biologie Moléculaire et Cellulaire (IGBMC)/ CNRS UMR 7104/ INSERM U 964/ Université de Strasbourg, 1 rue Laurent Fries, 67404 Illkirch, France

[2] Département de pathologie, Hôpitaux Universitaires de Strasbourg, Hôpital de Hautepierre, 1 Avenue Molière, 67200 Strasbourg, France

[3] Laboratoire de Biochimie et Biologie Moléculaire, Pôle de Biologie, Hôpitaux Universitaires de Strasbourg, Nouvel Hôpital Civil, 1 place de l'hôpital, 67091 Strasbourg Cedex, France

[4] Service de Biophysique et Médecine Nucléaire, Hôpital de Hautepierre, Hôpitaux Universitaires de Strasbourg, Strasbourg, France/ ICube, Université de Strasbourg / CNRS, UMR 7357, Strasbourg, France

[5] Lane Center of Computational Biology, School of Computer Science, Carnegie Mellon University, Pittsburgh, USA/ Computer Engineering Department, Bilkent University, Ankara, Turkey

keywords: Warburg effect, breast cancer, UPR^{mt}, UPR^{ER}, metabolic flexibility

✉ Correspondence: Dr. C. Tomasetto (cat@igbmc.fr) or Dr. N. Dali-Youcef (dali@igbmc.fr), phone: +33 (0)3 88 65 34 23, +33 (0)3 88 65 32 01

Abstract

Breast cancer is the most common leading cause of death in women. Matrix metalloproteinase-11 (MMP11) a protein of the tumor microenvironment (TME), is secreted by modified adipocytes called “Cancer-Associated Adipocytes” (CAAs) at the tumor periphery (invasive front) and by "Cancer-Associated Fibroblasts" (CAFs) in the center of the tumor. Previous studies showed that elevated MMP11 expression is associated with a poorer outcome in breast cancer patients supporting the idea that MMP11 contributes to tumor progression but the mechanism of action remained unclear. We have previously shown that MMP-11 is a negative regulator of adipose tissue development and controls energy metabolism in vivo. These observations suggested that MMP-11 expression in the TME may directly participate in breast tumor progression by modulating the adipose tissue metabolism at the benefit of cancer cells. However, how MMP-11 acts in the TME notably at the interface of breast cancer cells and CAAs remains largely unknown. To study the role of MMP-11 on breast cancer progression, we developed a series of preclinical mouse mammary gland tumor models by genetic engineering. First, mice either deficient- (Loss of Function-LOF) or overexpressing- MMP-11 (Gain of Function-GOF) were crossed with a transgenic model of breast cancer induced by the polyoma middle T antigen (PyMT) driven by the murine mammary tumor virus promoter (MMTV) (MMTV-PyMT). Consistent results were obtained using GOF and LOF models, showing that MMP11 favored early tumor progression, by increasing proliferation and reducing apoptosis of cancer cells. Of interest, MMP-11 was associated with a metabolic switch in the tumor, an activation of the endoplasmic reticulum stress response, an alteration in the mitochondrial unfolded protein response and in proteasome activity. These data support the idea that MMP-11 contributes to an adaptive metabolic response, named metabolic flexibility, favoring cancer growth.

INTRODUCTION

Breast cancer is the most common leading cause of death in women (1). Besides cancer cells, the tumor microenvironment (TME) plays an important role in breast cancer progression (2). Of note, adipocytes are an emerging cellular component of the TME, they can have an impact on cancer cells by direct cell contact, but also have indirect impact by a paracrine action (3). Matrix metalloproteinase-11 (MMP-11), also called stromelysin-3, is a protein secreted by stromal cells present in invasive breast cancer. Its presence is associated with poor outcome of these patients (4-6). Studies showed more recently that high levels of MMP-11 have a negative function during adipogenesis in cultured adipoblasts and in mice (7). Actually, MMP-11 reduces adipoblast to adipocyte differentiation and favors adipocyte dedifferentiation into fibroblast-like cells. A recent study from the group showed that MMP-11 is a metabolic regulator acting at the level of the whole organism; increased MMP-11 expression is associated with a lean phenotype and a protection from diet-induced obesity; consistently loss of MMP-11 expression is associated with weight gain and metabolic syndrome (8). In the context of breast cancer progression, it is important to mention that MMP-11 expression marks distinct cell populations from the TME. In the tumor center, fibroblast cells are the prominent cellular components of the microenvironment. These cells called "Cancer-Associated Fibroblasts" (CAFs) express very high levels of MMP-11. In contrast, in the tumor periphery, adipocytes represent the principal cellular component of the microenvironment. Those are called “Cancer-Associated Adipocytes” (CAAs). Unlike remote breast adipocytes in which MMP-11 is barely expressed, CAAs located in the tumor invasive front express high level of MMP11, show lipid droplets leakage and tend to have an elongated fibroblast-like morphology (9). These observations support the idea that MMP-11 acts at different levels in the TME. First, at an early stage when cancer cells develop or invade the normal stromal tissue, MMP-11 expression by CAAs may directly participates in the invasion process (7). Second, in the constituted tumor where fibroblasts are the

predominant TME cell-type, MMP-11 expression by CAFs is thought to help cancer cells' survival (Andarawewa et al., 2003). However, the mechanisms mediating MMP-11-induced tumor progression remains partially understood. Notably the metabolic role of MMP-11 on tumor progression was not addressed. In this study we used a series of mouse preclinical models of MMP-11 gain-of-function and loss-of-function to examine the role of MMP11 on mammary tumor growth and metabolism. We crossed these mice with a genetic model of spontaneous mammary tumors: the MMTV-PyMT genetic strain (10,11). MMTV-PyMT females develop with high penetrance palpable mammary tumors which metastasize to the lung (12). In this study brought a novel insight into the metabolic role of MMP11 in tumor progression through induction of a metabolic switch from oxidative phosphorylation to aerobic glycolysis, increased lipid metabolism, increased endoplasmic reticulum (ER) stress and alteration in the mitochondrial unfolded protein response. All these changes contribute to a metabolic flexibility that cancer cells may have acquired to favor tumor growth.

RESULTS

MMP-11 decreases MMTV-PyMT mice body weight and increases mammary tumor incidence

We have recently shown that in a non-cancer model that MMP11-overexpressing mice were leaner than their control counterparts (8). We examined body weight in the double transgenic mice expressing MMP11 and PyMT. In the GOF breast cancer model $PyMT^{Tg}$:$MMP11^{Tg}$, MMP-11 decreases postnatal body weight of MMTV-PyMT mice from 3 to 9 weeks old but no difference was noticed after palpable tumor occurred at 9-10 weeks old (Figure 1A). In the LOF model ($PyMT^{Tg}$:$MMP11^{KO}$), MMP-11 inactivation was accompanied by increased postnatal mice body weight from 3 to 12 weeks old but no difference was observed after palpable tumor occurred at 13-14 weeks old (Figure 1A). Even though the tumor grew rapidly to a certain extent in $PyMT^{Tg}$:$MMP11^{Tg}$ mice, tumor incidence was not significantly different from $PyMT^{Tg}$:$MMP11^{WT}$control mice. However, tumor growth was delayed in $PyMT^{Tg}$:$MMP11^{KO}$ as compared to $PyMT^{Tg}$:$MMP11^{WT}$ controls (Figure 1B).
Our results showed that MMP11 affects body weight and tumor incidence in MMTV-PyMT mice at an early stage of tumor development.

MMP-11 promotes MMTV-PyMT mice mammary tumor growth

In order to assess the impact of MMP11 on tumor development, we measured palpable tumor size by a caliper in individual mammary glands of $PyMT^{Tg}$:$MMP11^{Tg}$ and $PyMT^{Tg}$:$MMP11^{KO}$ mice and compared it with their respective controls (supplementary figure 1). Mammary tumor latency for each of the ten murine mammary glands has generally been assumed to be stoichiometric. However, studies showed the different mammary glands have distinct tumor initiating properties (13). Overexpression of MMP-11 increased tumor volume in #1, #2, #3 and #4 mammary glands at 10 weeks old, and in #1 mammary gland at 14 weeks old (Figure 1C). Conversely, in $PyMT^{Tg}$:$MMP11^{KO}$ mice we observed a decreased tumor volume in #2, #3 and #4 mammary gland

at 14 weeks old, and in #1, #2 mammary gland at 17 weeks old (Figure1D). We then aimed to determine the nature of the tumor lesions and performed whole mount carmine-red staining in the #4 mammary gland and assessed the hyperplasia and neoplastic lesion area both in GOF and LOF mice at different time points. We choose this mammary gland because it can be easily dissected and the fat pad is well developed. Quantification of carmine red staining indicated that PyMT^{Tg}:MMP11^{Tg} mice developed increased lesion area at 6, 8, 10 and 12 weeks of age, whereas PyMT^{Tg}:MMP11^{KO} mice exhibited smaller lesions at 10 and 14 weeks of age as compared to their respective control littermates (Figure 1E). In both models, the tumor burden was similar at later stage close to the experimental end-point.

Our data demonstrated that MMP-11 accelerates MMTV-PyMT transgenic mice tumor development and growth at early stage.

MMP-11 reduces necrosis and apoptosis in early stage mammary gland tumor development in MMTV-PyMT mice

To determine the impact of MMP11 on tumor necrosis and apoptosis in MMTV-PyMT mice, we analyzed paraffin embedded #4 mammary gland tissue sections from PyMT^{Tg}:MMP11^{Tg} and PyMT^{Tg}:MMP11^{KO} mice and their control littermates by hematoxylin and eosin (HE) staining and Terminal deoxynucleotidyl transferase dUTP Nick End Labeling (TUNEL) assay, respectively. Cell death and cytolysis (necrosis) can be visualized by the light pink color while viable tumor cells are darker (purple color). PyMT^{Tg}:MMP11^{Tg} mice displayed decreased necrosis area at 8 weeks of age, but no significant difference in necrosis was observed at a later stage (14 weeks) as compared to PyMT^{Tg}:MMP11^{WT} mice. Consistently, PyMT^{Tg}:MMP11^{KO} mice exhibited an increase in necrosis area at 14 and 17 weeks of age as compared to controls (Figure 2A).

We then quantified the proportion of apoptotic cells in GOF and LOF mice as compared to their respective controls by TUNEL assay. We observed a significant reduction in the percentage of apoptotic cells in PyMT^{Tg}:MMP11^{Tg} mice as compared to PyMT^{Tg}:MMP11^{WT} control mice at 6 weeks of age but not at a later stage (10 weeks), whereas PyMT^{Tg}:MMP11^{KO} mice displayed a

significant increase in the proportion of TUNEL positive cells at 10 weeks of age (Figure 2B). Consistently, the expression level of the anti-apoptotic protein bcl-2 was significantly increased in PyMT^{Tg}:MMP11^{Tg} mice and decreased in PyMT^{Tg}:MMP11^{KO} mice as compared with their respective controls (Figure 2C). Our results demonstrate that at early stage of tumor development, MMP11 decreases cell death in mammary gland tumor and hence confers a survival advantage to tumors supporting thereby cancer growth.

MMP-11 promotes cell proliferation in MMTV-PyMT mice mammary tumor development at an early stage and induces the insulin-like growth factor-1 signalling pathway

To investigate the impact of MMP11 on tumor proliferating cells, tumor tissues sections were analyzed by immunofluorescence using a specific antibody directed against the Ki-67, a protein encoded by the *MKI67* gene and an accepted marker of cell proliferation (14). The proportion of Ki-67 positive cell increased significantly in PyMT^{Tg}:MMP11^{Tg} in 6-week old mice as compared to PyMT^{Tg}:MMP11^{WT} mice, whereas PyMT^{Tg}:MMP11^{KO} mice displayed less Ki-67 positive stained cells at 10 weeks of age compared to their wildtype controls (Figure 3A). However, at a later stage (8-week old mice) PyMT^{Tg}:MMP11^{Tg} mice did not exhibit a significant difference in the percentage of proliferating cells as compared to PyMT^{Tg}:MMP11^{WT} control mice (data not shown). These data showed that MMP-11 increases PyMT tumor cell proliferation at an early stage of tumor development.

Given that the IGF1 pathway is well recognized to play an important role in neoplasia (15), and that IGF1 bioavailability is increased upon MMP11 overexpression (8), we investigated whether the IGF1 signalling pathway is exacerbated in PyMT^{Tg}:MMP11^{Tg} mice. Indeed, we observed a significant activation of this pathway as demonstrated by the significant increase in the phosphorylation of two important components of this cascade, namely protein kinase B (AKT) and FoxO1, in tumor protein extracts from PyMT^{Tg}:MMP11^{Tg} mice as compared to control mice at 6 weeks of age (Figure 3B). Consistently, a decrease in the phosphorylation of AKT and FoxO1 was observed in PyMT^{Tg}:MMP11^{KO} mice compared to controls at 10 weeks of age (Figure 3B).

The MMP11-mediated activation of the IGF1/AKT growth pathway was most likely due to the increase in IGF1 bioavailability as demonstrated by the decrease in the expression of IGFBP1 in tumor samples (Figure 3B), the protein that controls the circulating levels of IGF1 (16).

Collectively these results showed that MMP11 overexpression promotes cell proliferation in PyMT^{Tg}:MMP11^{Tg} mice and exacerbates the IGF1/AKT pathway, supporting the notion that IGF1 mitogenic activity is responsible for the pro-proliferative function of MMP-11.

MMP-11 increased lipid uptake and utilization and promotes metabolic switch

Cancer cells always exhibit a reprogrammed cell metabolism compared to normal cells resulting from specific energy demands. We hypothesized that MMP-11 can favor lipid utilization and promote aerobic glycolysis, a process known as the Warburg effect, to support tumor growth (17,18). To address the metabolic role of MMP-11 in tumors, we measured the expression of key metabolic genes in tumor samples. Regarding lipid metabolism, in tumor samples from 6-week-aged PyMT^{Tg}:MMP11^{Tg} mice, we observed a significant increase in the expression of the fatty acid transporter *Cd36* and the oxidative genes peroxisome proliferator activated receptor alpha (*Pparα*) and its target gene acyl coenzyme A oxidase (*Aco*), but also increased expression of acetyl-Coenzyme A carboxylase 1 and 2 (*Acc 1* and *Acc2*), supporting an increased lipid uptake, utilization and turnover (Figure 4A) (19-21). Consistently, we observed the mirror expression profile in tumors from 10-week-aged PyMT^{Tg}:MMP11^{KO} mice as compared to their control littermates (Figure 4B).

In the same samples, we then analyzed the expression of genes involved in lactate metabolism and observed an increased expression of genes involved in lactate production: lactate dehydrogenase A (*Ldha*), release: monocarboxylate transporter 4 (*Mct4*), uptake: monocarboxylate transporter 1 (*Mct1*) and metabolism: lactate dehydrogenase B (*Ldhb*) in PyMT^{Tg}:MMP11^{Tg} mice as compared to controls (Figure 4C) (22,23). Interestingly, we found a significant reduction in the expression of *Mct4* and *Ldha* in PyMT^{Tg}:MMP11^{KO} mice suggesting a reduction in lactate production and release. No significant difference was observed in the expression of *Mct1* and *Ldhb* (Figure 4D). To

determine whether the increase in aerobic glycolysis seen in PyMT^{Tg}:MMP11^{Tg} mice was accompanied by a negative regulation of certain oxidative phosphorylation (OXPHOS) genes consistent with Warburg's concept, we analyzed the expression of genes involved in the mitochondrial electron transport chain (ETC). Likewise, we observed in tumors from PyMT^{Tg}:MMP11^{Tg} mice a significant decrease in the expression of *Ndufb5*, a gene that encodes a subunit of complex I of the mitochondrial respiratory chain which transfers electrons from NADH to ubiquinone; a decrease in *Cox5b* expression, a gene encoding the cytochrome c subunit 5b protein of complex IV of the ETC; and a diminished expression of *Atp5b,* a gene encoding ATP synthase subunit 5b of complex V. The alteration of these genes support a reduction in mitochondrial respiration in PyMT^{Tg}:MMP11^{Tg} derived tumors. Of note, we also observed an increased expression of the mitochondrial encoded gene Cox2 (cytochrome c oxidase subunit 2, complex IV), suggesting an increase in mitochondria number (Figure 4E). Expression profile of PyMT tumors arising in the absence of MMP-11 (LOF model) mirrored those observed in MMP-11-overexpression (Figure 4F).

Taken together these data suggest that MMP-11 overexpression confers an advantage for cancer cells to promote their growth through a metabolic reprogramming involving an increase in aerobic glycolysis, a decrease in mitochondrial respiration and an increase in lipid turnover.

MMP-11 increases endoplasmic reticulum stress response and alters mitochondrial unfolded protein response

Protein homeostasis or proteostasis is supported by a coordinated regulation of polypeptide production, folding, trafficking and degradation when unfolded or misfolded proteins accumulate within the cell. Endoplasmic reticulum (ER) ensures proper folding and processing of proteins that will be secreted and hence is a guarantor of proteostasis (24,25). In immune and metabolic cells, but also following the exposure of cells to a variety of stressors, proteostasis is disrupted and an ER unfolded protein response (UPR^{ER}) that is initiated to restore protein homeostasis (25,26). In our study, we sought to analyze the impact of MMP-11 on ER stress and the UPR^{ER} in tumor samples from 6-week-

aged PyMT^{Tg}:MMP11^{Tg} and 10-week-aged PyMT^{Tg}:MMP11^{KO} mice and their respective controls (Figure 5A and B). Interestingly, we found a significant increase in the phosphorylation of the α subunit of eukaryotic translation initiation factor 2 (eIF2α), a target of the protein kinase RNA (PKR)-like ER kinase (PERK) and an important sensor of ER stress (25), and in the expression of UPR^{ER} driver genes such as X-box binding protein (*Xbp1),* activating transcription factor 4 (*Atf4)* and activating transcription factor 6 (*Atf6)* in PyMT^{Tg}:MMP11^{Tg} mice as compared to PyMT^{Tg}:MMP11^{Tg} controls (Figure 5C and D).

Similar to the ER, the mitochondria is an organelle that possesses also a protein folding quality control, named the mitochondrial unfolded protein response or UPR^{mt} (27), that in response to stress will ensure, through mito-nuclear communication, proper folding of imported proteins from the cytosol. Indeed, when misfolded proteins accumulate in the mitochondria or in case of dysfunctional mitochondria, the UPR^{mt} is activated. Previous studies have shown that during transformation, the UPR^{mt} could play an important role to adapt to stress and maintain mitochondria integrity when oxidative stress increases (28). Interestingly, three main branches/axes of the UPR^{mt} have been discovered so far, the CHOP/HSP/ClpP arm, the ERα/NRF1/proteasome arm and the SIRT3/FoxO3a/SOD2 arm (28). In the context of our study, we observed in tumors from PyMT^{Tg}:MMP11^{Tg} mice an alteration of the CHOP/HSP60, HSP10/ClpP pathway of the UPR^{mt} as compared to PyMT^{Tg}:MMP11^{WT} animals. Indeed, expression levels of the mitochondrial heat shock protein genes *Hsp60*, and *Hsp10* were significantly decreased as well as those of the mitochondrial protease *caseinolytic mitochondrial matrix peptidase proteolytic subunit* (*ClpP*) and of the prohibitin *Phb*, a sensor of mitochondria stress and a promoter of longevity (29) (Figure 5E, left panel). Since misfolded proteins are targeted for degradation by the ubiquitin-proteasome system (UPS), we sought to determine whether the abnormal UPR^{mt} was accompanied by a normal elimination of misfolded proteins. Interestingly, MMP-11 overexpression in the PyMT cancer model led to an abnormal proteasomal activity as shown by decreased expression of genes encoding the proteasomal subunits *Psmb1* and *Psmd1* as compared to control animals (Figure 5E, left

panel), suggesting an accumulation of misfolded proteins that could be responsible for the impaired mitochondrial function. Consistently, we observed the opposite phenomenon in PyMT^{Tg}:MMP11^{KO} mice, as shown by an increased UPR^{mt} response with enhanced expression of *Hsp60*, *Hsp10* and *ClpP,* and enhanced proteasomal activity with increased expression of *Psmb1* and *Psmd1* as compared to their PyMT^{Tg}:MMP11^{WT} control animals (Figure 5E, right panel).

Previous reports have already demonstrated that mitochondrial dysfunction induced by electron transport chain (ETC) perturbations and reactive oxygen species (ROS) generation inhibit proteasomal activity through proteasome disassembly in different organisms including mammalian cells (30,31). Since alterations in ETC leads to decreased ATP production (32) and that the UPS system relies on ATP for its function, we sought to determine whether MMP11-induced AMP-activated kinase (AMPK) activation is implicated in this process. Interestingly, we observed a significant increase in AMPK phosphorylation at threonine 172 residue in tumors from PyMT^{Tg}:MMP11^{Tg} mice as compared to their controls at 6 weeks old. Consistently, PyMT^{Tg}:MMP11^{KO} mice exhibited a significant decrease in AMPK activity compared to control animals (Figure 5F). Overall, MMP-11 exacerbates endoplasmic reticulum stress, alters the mitochondrial UPR and impairs proteasome activity that might be caused by increased oxidative stress, contributing thereby in energy depletion and activation of AMPK.

DISCUSSION

We have recently reported a crucial function of MMP-11 in the regulation of whole body metabolism through activation of the IGF1/AKT/FoxO1 signaling cascade in a non-cancer context using gain- and loss-of-function genetic-engineered mice models (8). The present study brought new insights into the molecular mechanisms of MMP-11-mediated cancer progression in the spontaneous genetic MMTV-PyMT breast cancer mouse model. Indeed, we have shown that in PyMT tumors, MMP-11 exacerbated the IGF1/AKT signalling pathway through increased IGF1 availability by decreasing IGFBP1 protein levels, promoting tumor cell survival and significantly increasing cell proliferation in tumor samples from $PyMT^{Tg}$:$MMP11^{Tg}$ mice as compared to control $PyMT^{Tg}$:$MMP11^{WT}$ animals, resulting in accelerated cancer growth. Mechanistically, MMP-11 enhanced the notoriously known Warburg-like effect in tumors samples through a metabolic switch by decreasing oxidative phosphorylation and enhancing aerobic glycolysis most likely through the IGF1/AKT/FoxO1 cascade. Besides lactate utilization, MMP-11 enhanced also lipid turnover (e.g. synthesis, transport and metabolism) to serve as an additional nutrient source to fulfill tumor energetic needs and allowing new membrane formation and expansion. An interesting finding lies in the MMP-11-mediated increase in ER stress through the significant elevation in the expression of key components of the UPR^{ER}, namely *ATF4*, *ATF6* and *Xbp1* (25). The contribution of MMP-11-mediated increase in UPR^{ER} was strengthened by the increase phosphorylation of eIF2α, an upstream inducer of ATF4 and downstream effector of the ER stress-mediated kinase PERK (25). There is compelling evidence that UPR^{ER} is involved in tumorigenesis, more specifically in HER2-positive breast cancer (33), and hence constitutes an attractive target for anticancer treatment (34). Likewise, the hypoxic environment of the tumors has a dual supportive role in cancer. On one hand, it stimulates the IRE1 and PERK branches of the UPR^{ER} to enhance the insensitivity of cancer cells to apoptosis (35). On the other hand, hypoxic stress

in cancer stimulates the inositol requiring enzyme 1α (IRE1)/XBP1 arm of the UPR to blunt immune elimination of cancer cells, by decreasing the expression of major histocompatibility complex 1 (MHC1) molecules in antigen presenting dendritic cells, weakening thereby the function of $CD8^+$ lymphocytes to kill cancer cells (36). Another aspect of MMP-11 role in mediating cancer growth is the defective mitochondrial unfolded protein response (UPR^{mt}) observed in tumors from $PyMT^{Tg}$:$MMP11^{Tg}$ mice as demonstrated by the decreased expression of important proteins of the UPR^{mt} such as the chaperone proteins HSP10 and HSP60 or the mitochondrial protease Clpp, which role is to eliminate misfolded or unfolded proteins in the mitochondrial matrix. This axis of the UPR^{mt} is referred as the CHOP pathway (37). These results were surprising, in the sense that tumor aggressiveness is often associated with mitochondria fitness and adaptation to stress. One possibility is that other axes of the UPR^{mt} may be activated. We measured the transcripts of nuclear factor erythroid 2–like 1 (Nfe2l1 also known as NRF1) and SIRT3, the 2 other branches of the UPR^{mt} (28). We did not found any difference in the transcription level of NRF1 in $PyMT^{Tg}$:$MMP11^{Tg}$ and $PyMT^{Tg}$:$MMP11^{KO}$ as compared to their respective controls, however SIRT3 expression was significantly increased in $PyMT^{Tg}$:$MMP11^{Tg}$ mice as compared to controls (data not shown). Interestingly, the SIRT3 axis of UPR^{mt} was shown to induce the antioxidant proteins superoxide dismutase 2 (SOD2) and catalase, and the subsequent elimination of irreversibly damaged mitochondria through mitophagy (38). This study suggested that SIRT3 may be an essential mechanism for cancer cells to adapt to proteotoxic and mitochondrial stress. This pathway needs to be studied in greater depth in our two mouse models.

Another observation that we presented is the MMP-11-mediated decrease in the expression of the proteasome subunits *Psmb1* and *Psmd1* that may result in decreased proteasome activity. Mitochondrial dysfunction produced by impaired ETC and ROS generation was shown to inhibit proteasome activity because of ATP depletion (30,31), ATP being crucial for proteasome assembly. Moreover, we observed a significant increase in AMPK phosphorylation, a kinase induced upon nutrient deprivation. It is tempting to speculate that non-degraded stressed mitochondria may amplify the proteotoxic and mitochondrial

stress contributing further in ATP-depletion and increase in AMPK activation, a known activator of autophagy (39). Supporting this hypothesis, a recent report has shown that accumulation of ubiquitin-proteins was correlated with reduction in cellular bioenergetics and increase in AMPK activation and autophagy (40). After all, autophagy is the process by which the cell recycles the constituents of irreversibly damaged organelles to generate energy and recover precursors necessary for cell growth. This hypothesis and the occurrence of autophagy need to be verified in our model.

In conclusion, we have reported that in the MMTV-PyMT mouse model of breast cancer, MMP11 promotes cancer growth by increasing cell proliferation and reducing cell death. At the mechanistic level, MMP-11 modulates major metabolic pathways such as the switch from oxidative phosphorylation to aerobic glycolysis. In addition, MMP11 favors adaptative organelle processes following proteotoxic stress such as the UPR^{ER} and $UPR^{mt.}$. All these processes are at the benefit of cancer cells enabling them to cope with nutrient availability and, allowing them to survive in harsh conditions such as the presence of ROS.

Materials and methods

1 Generation of mice cohorts

This study was approved by the Ethical Committee. In the GOF model, MMTV-PyMT^{Tg} male mice (FVB/N-Tg(MMTV-PyVT)634Mul/J) were obtained from The Jackson Laboratory and crossed with K14-MMP11^{Tg} female mice (FVB/N background). The first mice generation were genotyped. In the LOF model, MMTV-PyMT^{Tg} male mice (FVB/N background) were crossed with MMP11-/- female mice (129/SvJ background). The first mice generation were genotyped. Then, PyMT^{Tg}; MMP11-/+ male mice crossed with PyMT^{WT}; MMP11-/+ female littermates. The last mice generation were genotyped. PyMT^{Tg}:MMP11^{WT} and PyMT^{Tg}:MMP11^{Tg} female mice, PyMT^{Tg}; MMP11^{WT} and PyMT^{Tg}; MMP11^{KO} female mice were randomly divided and used for experiments. Each group in different experimental time points contain at least 6-8 mice.

2 Mice genotyping

The genotyping of the PyMT transgene was done by standard PCR as recommended by the Jackson Laboratory. In brief, PCR reaction from mouse tail DNA was done as follows: 94ºC for 30 seconds, 64ºC for 1 minute, 72ºC for 1 minute, 35 cycles. Likewise, K14-MMP11 genotyping was done by standard PCR reaction using tail DNA: 94ºC for 1 minute, 60ºC for 20 seconds, 72ºC for 1 minute, 33 cycles; MMP11KO/WT gene PCR reaction: 94ºC for 15 seconds, 62ºC for 15 seconds, 72ºC for 1 minute, 33 cycles.

	Forward	Reverse
PyMT	GGAAGCAAGTACTTCACAAGGG	GGAAAGTCACTAGGAGCAGGG
MMP11^{Tg}	CGGTTTCCACCATCCGAGGA	GTGGAAACGCCAATAGTCTCC
MMP11^{KO}	GTGGAAACGCCAATAGTCTCC	GCCGCTTTTCTGGATTCATCG
MMP11^{WT}	GTGGAAACGCCAATAGTCTCC	TTCTAACATCCCTCTGGGCTC

3 Mice weight and tumor measurement

Mice weight was measured by electronic balance twice a week. Caliper was used to measure the tumor length, width and height twice a week. Tumor volume was calculated following the formula (4/3) x 3.14159 x (length/2) x (width/2) x (height/2).

4 Carmine-alum red staining

The #4 mammary glands were spread onto glass slides and fixed in carnoy solution (75% glacial acetic acid, 25% absolute EtOH) overnight. A sequential rehydratation in 2 steps (100%EtOH and 70% EtOH) of one hour each was followed by 30 minutes in distilled water. Then carmine-alum (Sigma, C1022, USA) stain was added overnight. Dehydratation was done in a stepwise incubation in 70% EtOH, 95% EtOH and 100% EtOH for 1 hour each step. The slides were fixed in Histosol overnight and mounted with Permount.

5 HE staining

Paraffin embedding #4 mammary gland tumor tissue slides were immersed into 100% histosol for 2 times, 5 minutes each. Followed by 100%, 90%, 80% ethanol and H2O for 5 minutes each. Stained for 3 minutes in Harris Hematoxylin. Washed in acid alcohol for 2 seconds and in running tap water for 3 minutes. Next they were stained for 30 seconds in 0.1% aqueous eosin Y. Rinsed in tap water for 30 seconds. Dehydrated in 80%, 90%, 100% ethanol for 5 minutes each. Fixed by two washes of 100% histosol, 5 minutes each and mounted with Permount.

6 TUNEL assay

For this assay, we used the TUNEL kit from Abcam (ab206386). Paraffin embedding tumor tissue slides were treated as recommended by the user guide booklet. Slides were mounted using histosol mounting media.

7 Immunofluorescent staining

Paraffin embedding #4 mammary gland tumor tissue slides were immersed into 100% histosol for 2 times, 5 minutes each. Follow by 100%, 90%, 80% ethanol and H2O for 5 minutes each. Tissue specimens were rinsed 1 time in PBS 1x. Antigen unmasking was done by incubation at 95ºC in Tris-EDTA buffer for 20 min. Permeabilization was done in PBS 1x containing 1% Triton X-100 for 1 hour. Blocking in BSA 5% for 1 hour. The primary antibody (Rabbit anti-Ki67, 1:500, Bethyl, IHC-00375; Rabbit anti-pEIF2α, 1:500, CST, #3597s; Rabbit anti-EIF2α, 1:500, CST, #9722s) was incubated in BSA 5% at 4ºC for overnight. The slides were rinsed 3 times in PBS 1x, 5 minutes each. Incubated with secondary antibodies in PBS 1x for 2 hours. Nuclei were stained with Hoechst dye diluted in PBS 1x for 10 minutes. Wash with PBS 1x for 2 times, 5 minutes each. Coverslip were mounted with Prolong Gold antifade. Images were taken

using a fluorescence microscope or an inverted laser confocal fluorescence microscopy

8 Western blot

Mice tumor tissues were taken from #1 mammary gland and protein extracts were obtained by tissue grinding in RIPA lysis buffer. After protein concentration were quantified by The BCA method. Protein extract were analyzed by SDS-PAGE gel and Nitrocellulose transfer. Membranes were incubated with primary antibodies (Rabbit anti-Bcl2, 1:500, Abcam, ab59348; Rabbit anti-IGFBP1, 1:1000, Abcam, ab181141; Rabbit anti-GAPDH, 1: 5000, Sigma, G9545; Rabbit anti-pAKT, 1:1000, CST, #4060; Rabbit anti-AKT, 1:1000, CST, #9272; Rabbit anti-pFoxO1, 1:1000, CST, #9461; Rabbit anti-FoxO1, 1:1000, CST, #2880; Rabbit anti-pAMPK, 1:1000, CST, #2535; Rabbit anti-AMPK, 1:1000, CST, #2532).

9 RT-qPCR

Mice tumor tissues were taken from #1 mammary gland, and lung tissues were taken from right side middle lobe, then homogenized in Trizol reagent (Sigma, T9424, USA). The reverse transcription step by done using Superscript II Reverse transcriptase kit (Sigma, 18090050, USA). The quantitative PCR step by using SYBR Green kit (Sigma, S4438, USA). Data were normalized to GAPDH or 36B4 expression.

	Forward	Reverse
PyMT	CGGCGGAGCGAGGAACTGAGGAGAG	TCAGAAGACTCGGCAGTCTTAGGCG
Cd36	GATGTGGAACCCATAACTGGATTCAC	GGTCCCAGTCTCATTTAGCCACAGTA
Pparα	AGGAAGCCGTTCTGTGACAT	TTGAAGGAGCTTTGGGAAGA
Aco	CCCAACTGTGACTTCCATT	GGCATGTAACCCGTAGCACT
Acc1	GACAGACTGATCGCAGAGAAAG	TGGAGAGCCCCACACACA
Acc2	CCCAGCCGAGTTTGTCACT	GGCGATGAGCACCTTCTCTA
Ndufb5	CTTCGAACTTCCTGCTCCTT	GGCCCTGAAAAGAACTACG
Sdha	GGAACACTCCAAAAACAGACCT	CCACCACTGGGTATTGAGTAGAA
Sdhc	GCTGCGTTCTTGCTGAGACA	ATCTCCTCCTTAGCTGTGGTT
Cox2	AATTAGCTCCTTAGTCCTCT	CTTGGTCGGTTTGATGTTAC
Cox5b	AAGTGCATCTGCTTGTCTCG	GTCTTCCTTGGTGCCTGAAG

Atp5b	GGTTCATCCTGCCAGAGACTA	AATCCCTCATCGAACTGGACG
Hsp10	CTGACAGGTTCAATCTCTCCAC	AGGTGGCATTATGCTTCCAG
Hsp60	ACAGTCCTTCGCCAGATGAGAC	TGGATTAGCCCCTTTGCTGA
Clpp	CACACCAAGCAGAGCCTACA	TCCAAGATGCCAAACTCTTG
Phb	TCGGGAAGGAGTTCACAGAG	CAGCCTTTTCCACCACAAAT
Phb2	CAAGGACTTCAGCCTCATCC	GCCACTTGCTTGGCTTCTAC
Mct1	GCATTTCCCAAATCCATCAC	CGGCTGCCGTATTTATTCAC
Mct4	GGTCAGCGTCTTTTTCAAGG	CCGTGGTGAGGTAGATCTGG
Ldha	AGACAAACTCAAGGGCGAGA	CAGCTTGCAGTGTGGACTGT
Ldhb	TAAGCACCGTGTGATTGGAA	AGACTCCTGCCACATTCACC
Xbp1	GGTCTGCTGAGTCCGCAGCAGG	AGGCTTGGTGTATACATGG
ATF4	CCTTCGACCAGTCGGGTTTG	CTGTCCCGGAAAAGGCATCC
ATF6	CTGTGCTGAGGAGACAGCAG	CTTGGGACTTTGAGCCTCTG
Psma1	TGCGTGCGTTTTTGATTTTAGAC	CCCTCAGGGCAGGATTCATC
Psmb1	CGTTGAAGGCATAAGGCGAAAA	TTCCACTGCTGCTTACCGAG
Psmd1	GTGATAAAACACTTTCGAGGCCA	TGAATGCAGTCGTGAATGACTT
GAPDH	ACTGGCATGGCCTTCCGTGTTC	TCTTGCTCAGTGTCCTTGCTGG
36b4	AGATTCGGGATATGCTGTTGG	AAAGCCTGGAAGAAGGAGGTC

10 Data analysis

The quantification of hyperplasia and neoplastic lesions area, tumor necrosis area, TUNEL staining cells, Ki-67 staining cells, p-eIF2α relative intensity and western blot were performed by Image J 1.51n. Statistical analysis was performed by Graphpad Prism 7.

Bibliography

1. Polyak K, Metzger Filho O. SnapShot: breast cancer. Cancer Cell. 2012;22:562–562.e1.
2. Hanahan D, Coussens LM. Accessories to the crime: functions of cells recruited to the tumor microenvironment. Cancer Cell. 2012;21:309–22.
3. Rio M-C, Dali-Youcef N, Tomasetto C. Local adipocyte cancer cell paracrine loop: can “sick fat” be more detrimental? Horm Mol Biol Clin Investig. 2015;21:43–56.
4. Basset P, Bellocq JP, Wolf C, Stoll I, Hutin P, Limacher JM, et al. A novel metalloproteinase gene specifically expressed in stromal cells of breast carcinomas. Nature. 1990;348:699–704.
5. Chenard MP, O’Siorain L, Shering S, Rouyer N, Lutz Y, Wolf C, et al. High levels of stromelysin-3 correlate with poor prognosis in patients with breast carcinoma. Int J Cancer. 1996;69:448–51.
6. Rouyer N, Wolf C, Chenard MP, Rio MC, Chambon P, Bellocq JP, et al. Stromelysin-3 gene expression in human cancer: an overview. Invasion Metastasis. 1994;14:269–75.
7. Andarawewa KL, Motrescu ER, Chenard M-P, Gansmuller A, Stoll I, Tomasetto C, et al. Stromelysin-3 is a potent negative regulator of adipogenesis participating to cancer cell-adipocyte interaction/crosstalk at the tumor invasive front. Cancer Res. 2005;65:10862–71.
8. Dali-Youcef N, Hnia K, Blaise S, Messaddeq N, Blanc S, Postic C, et al. Matrix metalloproteinase 11 protects from diabesity and promotes metabolic switch. Sci Rep. 2016;6:25140.
9. Motrescu ER, Rio M-C. Cancer cells, adipocytes and matrix metalloproteinase 11: a vicious tumor progression cycle. Biol Chem. 2008;389:1037–41.
10. Guy CT, Webster MA, Schaller M, Parsons TJ, Cardiff RD, Muller WJ. Expression of the neu protooncogene in the mammary epithelium of transgenic mice induces metastatic disease. Proc Natl Acad Sci U S A. 1992;89:10578–82.
11. Lin EY, Jones JG, Li P, Zhu L, Whitney KD, Muller WJ, et al.

Progression to malignancy in the polyoma middle T oncoprotein mouse breast cancer model provides a reliable model for human diseases. Am J Pathol. 2003;163:2113–26.

12. Fluck MM, Schaffhausen BS. Lessons in signaling and tumorigenesis from polyomavirus middle T antigen. Microbiol Mol Biol Rev MMBR. 2009;73:542–63, Table of Contents.

13. Davie SA, Maglione JE, Manner CK, Young D, Cardiff RD, MacLeod CL, et al. Effects of FVB/NJ and C57Bl/6J strain backgrounds on mammary tumor phenotype in inducible nitric oxide synthase deficient mice. Transgenic Res. 2007;16:193–201.

14. Scholzen T, Gerdes J. The Ki-67 protein: from the known and the unknown. J Cell Physiol. 2000;182:311–22.

15. Pollak M. Insulin and insulin-like growth factor signalling in neoplasia. Nat Rev Cancer. 2008;8:915–28.

16. Wheatcroft SB, Kearney MT. IGF-dependent and IGF-independent actions of IGF-binding protein-1 and -2: implications for metabolic homeostasis. Trends Endocrinol Metab. 2009;20:153–62.

17. Warburg O. On the origin of cancer cells. Science. 1956;123:309–14.

18. Lunt SY, Vander Heiden MG. Aerobic glycolysis: meeting the metabolic requirements of cell proliferation. Annu Rev Cell Dev Biol. 2011;27:441–64.

19. Glatz JFC, Luiken JJFP. From fat to FAT (CD36/SR-B2): Understanding the regulation of cellular fatty acid uptake. Biochimie. 2017;136:21–6.

20. Wakil SJ, Abu-Elheiga LA. Fatty acid metabolism: target for metabolic syndrome. J Lipid Res. 2009;50 Suppl:S138–43.

21. Keller H, Mahfoudi A, Dreyer C, Hihi AK, Medin J, Ozato K, et al. Peroxisome proliferator-activated receptors and lipid metabolism. Ann N Y Acad Sci. 1993;684:157–73.

22. Pinheiro C, Longatto-Filho A, Azevedo-Silva J, Casal M, Schmitt FC, Baltazar F. Role of monocarboxylate transporters in human cancers: state of the art. J Bioenerg Biomembr. 2012;44:127–39.

23. Kennedy KM, Dewhirst MW. Tumor metabolism of lactate: the influence and therapeutic potential for MCT and CD147 regulation. Future Oncol.

2009;6:127–48.

24. Powers ET, Morimoto RI, Dillin A, Kelly JW, Balch WE. Biological and Chemical Approaches to Diseases of Proteostasis Deficiency. Annu Rev Biochem. 2009;78:959–91.

25. Frakes AE, Dillin A. The UPRER: Sensor and Coordinator of Organismal Homeostasis. Mol Cell. 2017;66:761–71.

26. Wang M, Kaufman RJ. Protein misfolding in the endoplasmic reticulum as a conduit to human disease. Nature. 2016;529:326–35.

27. Jovaisaite V, Mouchiroud L, Auwerx J. The mitochondrial unfolded protein response, a conserved stress response pathway with implications in health and disease. J Exp Biol. 2014;217:137–43.

28. Kenny TC, Manfredi G, Germain D. The Mitochondrial Unfolded Protein Response as a Non-Oncogene Addiction to Support Adaptation to Stress during Transformation in Cancer and Beyond. Front Oncol [Internet]. 2017 [cited 2018 Mar 29];7. Available from: https://www-frontiersin-org.gate2.inist.fr/articles/10.3389/fonc.2017.00159/full

29. Jovaisaite V, Auwerx J. The mitochondrial unfolded protein response-synchronizing genomes. Curr Opin Cell Biol. 2015;33:74–81.

30. Livnat-Levanon N, Kevei É, Kleifeld O, Krutauz D, Segref A, Rinaldi T, et al. Reversible 26S proteasome disassembly upon mitochondrial stress. Cell Rep. 2014;7:1371–80.

31. Segref A, Kevei É, Pokrzywa W, Schmeisser K, Mansfeld J, Livnat-Levanon N, et al. Pathogenesis of human mitochondrial diseases is modulated by reduced activity of the ubiquitin/proteasome system. Cell Metab. 2014;19:642–52.

32. Smeitink JA, Zeviani M, Turnbull DM, Jacobs HT. Mitochondrial medicine: a metabolic perspective on the pathology of oxidative phosphorylation disorders. Cell Metab. 2006;3:9–13.

33. Kim JY, Heo S-H, Song IH, Park IA, Kim Y-A, Gong G, et al. Activation of the PERK-eIF2α Pathway Is Associated with Tumor-infiltrating Lymphocytes in HER2-Positive Breast Cancer. Anticancer Res. 2016;36:2705–11.

34. Shen K, Johnson DW, Vesey DA, McGuckin MA, Gobe GC. Role of the unfolded protein response in determining the fate of tumor cells and the promise

of multi-targeted therapies. Cell Stress Chaperones. 2018;23:317–34.

35. Fels DR, Koumenis C. The PERK/eIF2alpha/ATF4 module of the UPR in hypoxia resistance and tumor growth. Cancer Biol Ther. 2006;5:723–8.

36. Cubillos-Ruiz JR, Bettigole SE, Glimcher LH. Tumorigenic and Immunosuppressive Effects of Endoplasmic Reticulum Stress in Cancer. Cell. 2017;168:692–706.

37. Zhao Q, Wang J, Levichkin IV, Stasinopoulos S, Ryan MT, Hoogenraad NJ. A mitochondrial specific stress response in mammalian cells. EMBO J. 2002;21:4411–9.

38. Papa L, Germain D. SirT3 regulates the mitochondrial unfolded protein response. Mol Cell Biol. 2014;34:699–710.

39. Kim J, Kundu M, Viollet B, Guan K-L. AMPK and mTOR regulate autophagy through direct phosphorylation of Ulk1. Nat Cell Biol. 2011;13:132–41.

40. Jiang S, Park DW, Gao Y, Ravi S, Darley-Usmar V, Abraham E, et al. Participation of proteasome-ubiquitin protein degradation in autophagy and the activation of AMP-activated protein kinase. Cell Signal. 2015;27:1186–97.

Figures Legends

Figure 1. MMP-11 promotes MMTV-PyMT mice mammary tumor growth.

(A) Weight gain progression in the GOF (left) and LOF (right) mouse model. (B) Tumor free curves of GOF (left) and LOF (right) mouse models. The percentage of mice with at least one palpable tumor is indicated for the follow-up of GOF and LFO for 12 and 18 weeks, respectively. (C-D) The dot-plot graphs show the tumor volumes that were measured individually in all ten mammary glands. (E) Representative images of wholemount staining of mouse mammary glands at different ages (left), and quantification of the all the lesion areas. A number of 6-8 mice per group were studied, data represent mean±SD, *P < 0.05, **P < 0.01, ***P < 0.001 (unpaired t-test).

Figure 2. MMP-11 reduces necrosis and apoptosis at early stage mammary gland tumor development.

(A) Histological features of PyMT tumors. Comparative histological examination of carcinomas in the two models using hematoxylin-eosin staining at the time point indicated. Pink staining reflects necrotic lesions. Representative images are shown on the left and quantification of necrotic lesions are shown on the right. (B) In situ detection of apoptosis in mammary gland tumors by TUNEL analysis. Representative apoptotic staining by TUNEL assay on the left and on the right quantification of percentage of apoptotic cells at indicated time points (three fields/mice were quantified). (C) Apoptosis protein analysis. Bcl-2 protein was determined by western blot analysis, GAPDH was used as internal control. Representative western blot on the left and quantification on the right. The level of Bcl2 protein was set to one in control tumor samples. Please note that compared to their controls, the bcl-2 anti-apoptotic protein level was significantly increased in tumors samples from MMP-11 transgenic mice but decreased in MMP-11 knockout mice. Abbreviation: n, necrosis. Three microscopic fields at the indicated magnification for each mice were quantified, 6-8 mice/group, data represent mean±SEM, *P < 0.05, **P < 0.01, ***P < 0.001 (unpaired t-test).

Figure 3. MMP-11 promotes tumor cell proliferation at early stage and induces the IGF-1 signalling pathway.

(A) Tumor proliferation. Ki-67 immunofluorescence was performed to assess in vivo proliferation at the time point indicated; Ki-67 (green), Hoechst (blue). Representative images are shown on the top panel. Quantification of three microscopic fields at the indicated magnification for each mice were quantified. (B) Immunoblots for proteins involved in the IGF1 signalling pathway in the tumors of GOF and LOF mice compared to controls (left), right panel: quantification of the ratios of IGFBP1 (top), phosphorylated pAKT, and pFOXO1 proteins relative to AKT, and FOXO1, respectively (bottom), normalized to GAPDH expression (data are presented as fold change of $PyMT^{Tg}$:$MMP11^{Tg}$ and $PyMT^{Tg}$:$MMP11^{KO}$ tumor sample values to their respective controls). 6-8 mice/group, data represent mean±SEM, *P < 0.05, **P < 0.01, ***P < 0.001 (unpaired t-test).

Figure 4. MMP-11 increased lipid utilization and promotes metabolic switch.

(A-B) Expression profile of genes involved in lipid metabolism: Cd36, Pparα, Aco, Acc1 and Acc2 genes in PyMT tumor samples from 6-weeks old MMP-11 transgenic mice (A) and 10 weeks old MMP11- deficient mice (B) as compared to controls littermates. Expression profiles of genes involved in Lactate metabolism: Mct1, Mct4, Ldha and Ldhb genes(C-D) and in Mitochondrial respiratory chain Ndufb5, Cox2, Cox5b and Atp5b genes (E-F) in the same tumor. 6-8 mice/group, data represent mean±SEM, *P < 0.05, **P < 0.01, ***P < 0.001 (unpaired t-test).

Figure 5. MMP-11 increases ER stress response and alters UPR^{mt}.

(A-B) ER stress analysis using phosphorylation eIF2 alpha staining (green) and nuclei staining (blue) by immunofluorescence. Left panels representative images of p-eIF2α staining in tumors from GOF (A) and LOF (B) mice at the indicated time points. Right panels, quantification of overall green signals on three independent fields per mice. (C-D) RNA levels of the ER-stress genes

Xbp1, Atf4 and Atf6 in the tumor samples from GOF at 6-weeks old (C) and LOF at 10-week old (D) mice models, expressed as fold change with respect to the control tumor samples. (E) Fold change mRNA levels of the mitochondrial UPR genes: Hsp10, Hsp60, Clpp, Phb, Pmsa1, Pmsb1 and Pmsd1 in 6-week old MMP-11 transgenic mice (GOF) tumor sample and 10-weeks old MMP-11 knockout mice (LOF) as compared to controls tumor samples. (F) Immunoblot analysis of the AMPK signaling pathway. In the tumors of GOF at 6 weeks old and LOF mice at 10 weeks-old compared to controls (left), right panel: quantification of the ratio of AMPK phosphorylation at threonine 172 residue relative to total AMPK normalized to GAPDH protein levels. Quantification is presented as fold change to the respective controls. 6-8 mice/group, data represent mean±SEM, *P < 0.05, **P < 0.01, ***P < 0.001 (unpaired t-test).

Figure S1. Tumor growth in GOF and LOF mice models.

(A-B) Top panels, standard PCR genotyping of PyMT and MMP-11 genes with extracted genomic tail DNA by PCR in the GOF group (A) and LOF group (B). Bottom panels, representative mice harboring tumors and the mammary glands identification number are shown (C) Schematic workflow representation of GOF and LOF experimental models. 6-8 mice/group/time points.

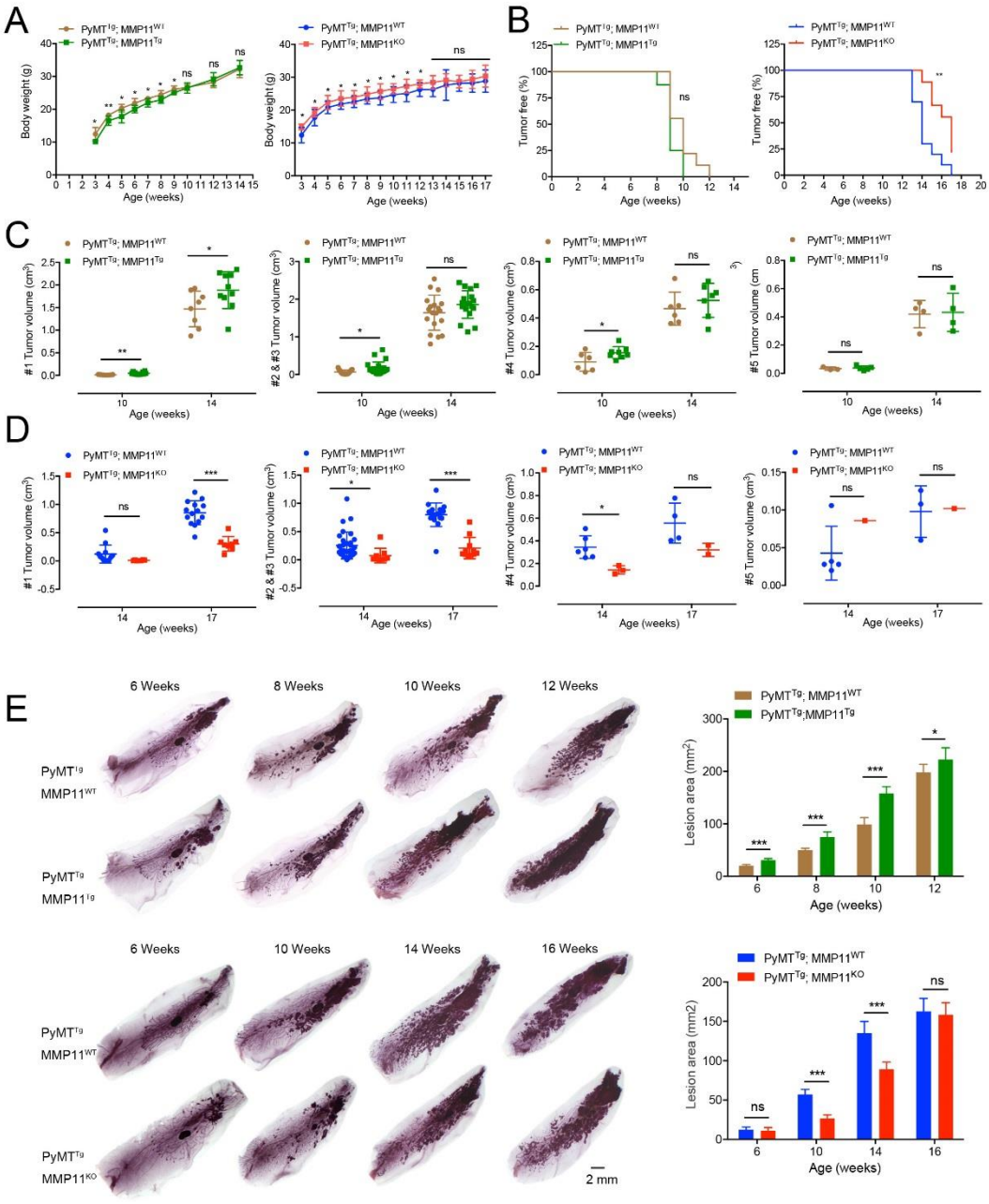

Tan et al., Figure 1

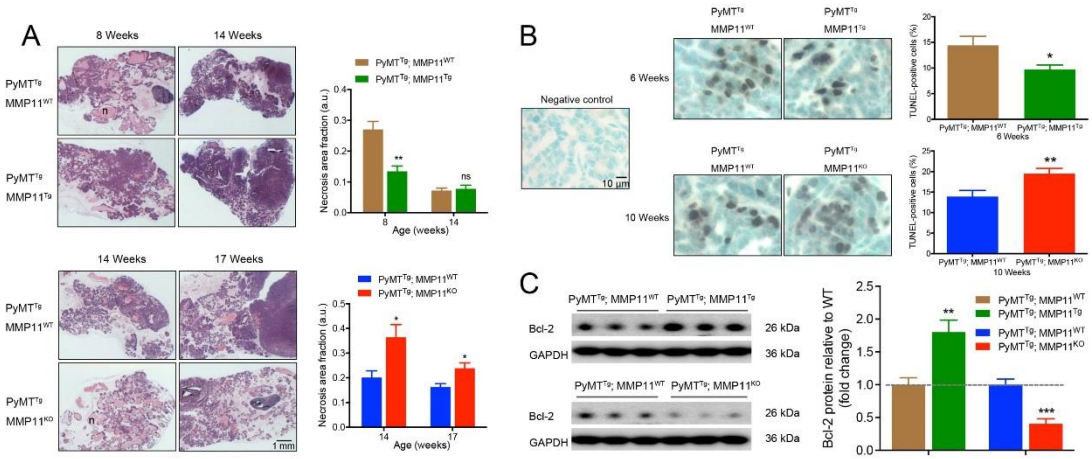

Tan et al., Figure 2

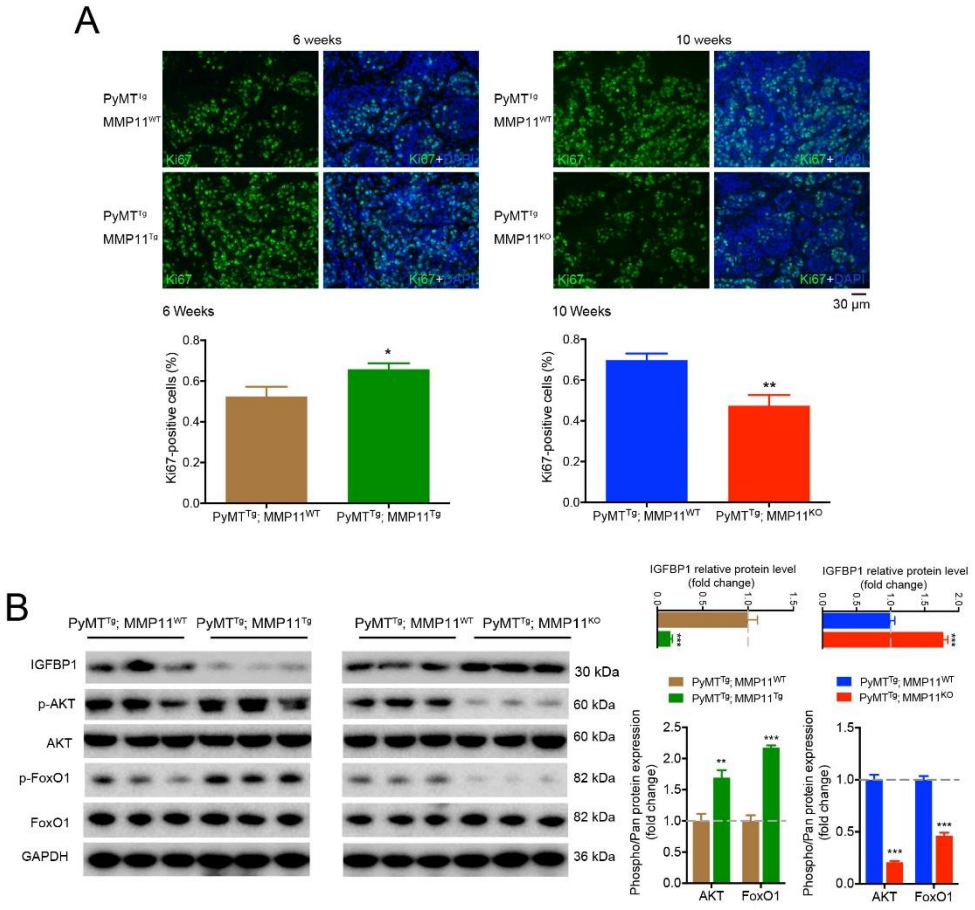

Tan et al., Figure 3

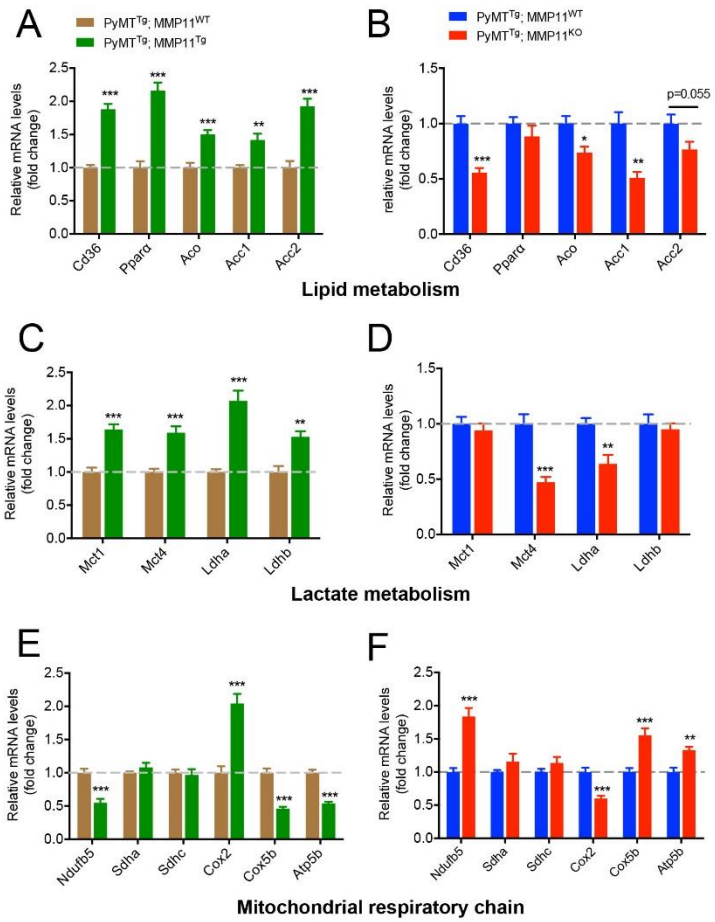

Tan et al., Figure 4

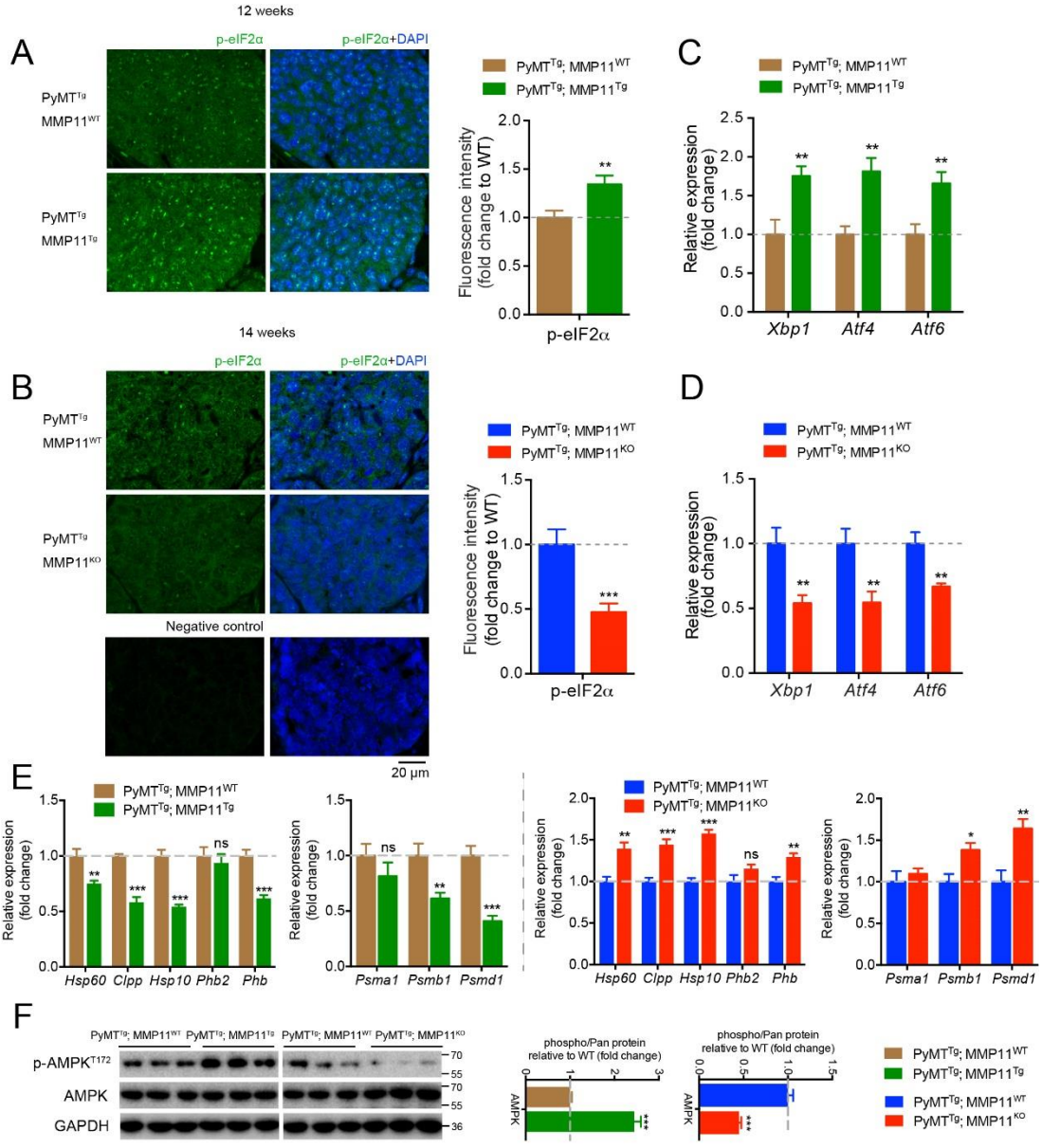

Tan et al., Figure 5

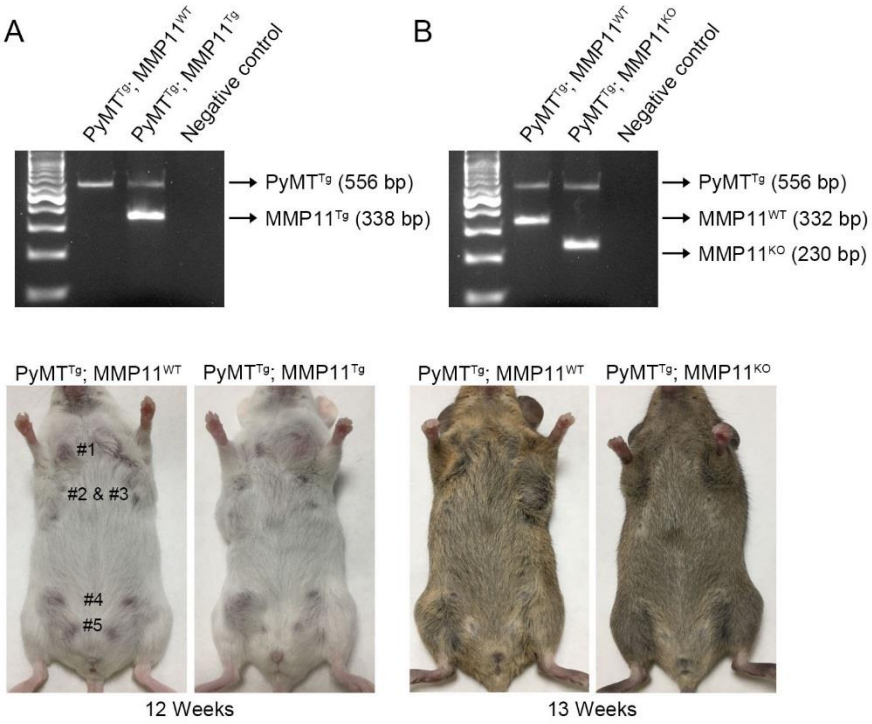

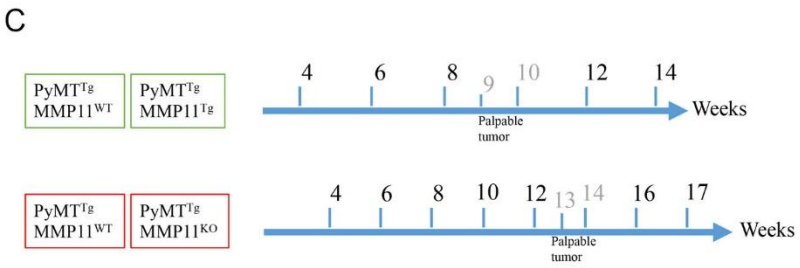

Tan et al., Figure S1

Part II The impact of MMP-11 overexpression restricted to adipocytes on mammary gland tumorigenesis

The loss of MMP-11 favors adipogenesis both in vitro and in vivo (Andarawewa et al., 2005; Motrescu et al., 2008). It has also been shown that MMP-11 is a negative regulator of adipogenesis, it is able to decrease mature adipocytes lipid deposition and promote dedifferentiation to preadipocytes (Andarawewa et al., 2005). The molecular mechanism of MMP-11 in cancer remains unclear but we speculate that malignant breast epithelial cells benefit from adjacent stromal CAAs delipidation and energy transfer and that MMP-11 amplifies this mechanism.

To address the effect of MMP-11 on mouse mammary tumor progression, I generated a new mouse model, where MMP-11 is specifically expressed in the adipose tissue. To this aim, I made a plasmid construct named aP2-mMMP11-IRES-GFP-polyA, where MMP-11 expression is driven by an adipose tissue specific promoter.

2.2.1 Generation of aP2-mMMP11-IRES-GFP-polyA construct

The designed construct contains the mouse aP2 gene promoter (Figure 2.11). The aP2 gene promoter drives the expression of the adipocyte protein 2 (aP2), also called fatty acid binding protein 4 (FABP4). This cytosolic protein involves in lipid trafficking and signalling in the mature adipocyte (Smathers and Petersen, 2011). This promoter/enhancer of approximately 5.4 kb is upstream from the aP2 gene transcriptional start site (Addgene plasmid #11424), and has been shown to be sufficient to direct gene expression in adipocytes (Ross et al., 1990). The mouse MMP-11 cDNA (GenBank accession NC_000076.6) sequence was cloned downstream to aP2 promoter and a rabbit beta-globlin intron/exon cassette. The rabbit beta-globin intron can improve MMP-11 gene expression. Moreover, in order to trace MMP-11 gene expression in mouse adipocytes, we added a fluorescent reporter gene, the green-fluorescent-protein (GFP) cassette, which is under the sequence of internal ribosome entry site (IRES). The IRES is an RNA element that allows translation initiation in a cap-independent manner during protein synthesis (Pelletier and Sonenberg, 1988). This technology allows for the protein expression of the two genes (MMP-11 and GFP) from one single mRNA. Following the GFP cassette I introduced a polyA-signal sequence, to produce and stabilize mature mRNA for translation.

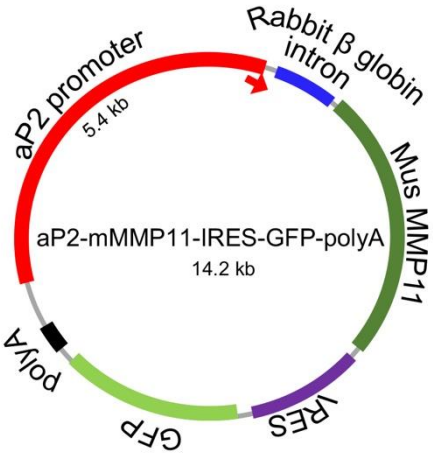

Figure 2.11 Different elements of aP2-mMMP11-IRES-GFP-polyA construct. aP2: adipocyte protein 2; Mus MMP-11: mouse MMP-11 sequence; IRES: internal ribosome entry site; GFP: green-fluorescent-protein.

2.2.1.1 Amplification of IRES-GFP sequence by PCR

In order to trace the expression of MMP-11, we employed a GFP cassette. pMX-PIE-PL construct (available in the laboratory) served as a template for the cloning of the IRES-GFP sequence. PCR forward primer beginning of the IRES sequence: 5'-GAGAGG/CGCGCCGCCCCCCCCCCTAACGTTACTGGCCGAAGC CGC-3' (slash indicate restriction enzyme site for Asc I); reverse primer at the end of the GFP sequence: 5'-AAGACCTGCAGGGGCCGG/CCGTCGACTTACTTGTACA GCTCGTCCATGCCGA-3' (slash indicate cut site for Fse I). To remove the primers, PCR reaction product was purified follow the protocol from the kit, Then, IRES-GFP sequence was verified by electrophoresis in 1% agarose gel (Figure 2.12). As expected, the IRES-GFP product has the right size.

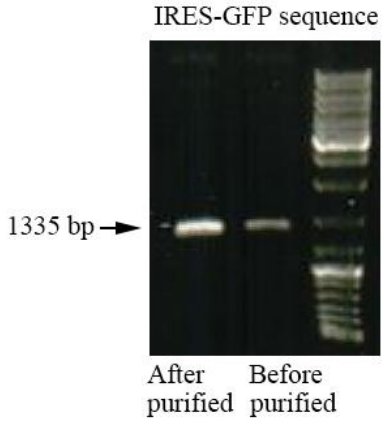

Figure 2.12 The IRES-GFP unit was generated from pMX-PIE-PL construct. After amplification by PCR reaction (Before purified) and purification by PCR clean up kit (After purified), The IRES-GFP sequence was verified in 1% agarose gel.

2.2.1.2 To obtain the same cutting ends of IRES-GFP and aP2-mMMP11-polyA

Both IRES-GFP sequence and aP2-mMMP11-polyA construct (available in the laboratory) were treated with restriction enzyme Asc I and Fse I to generate the same cutting ends (Figure 2.13 A). To remove the waste, these digestion products were purified follow the protocol from the kit. Then, IRES-GFP sequence (1308 bp) and aP2-mMMP11-polyA sequence (12.7 kb) were verified by electrophoresis in 1% agarose gel (Figure 2.13 B).

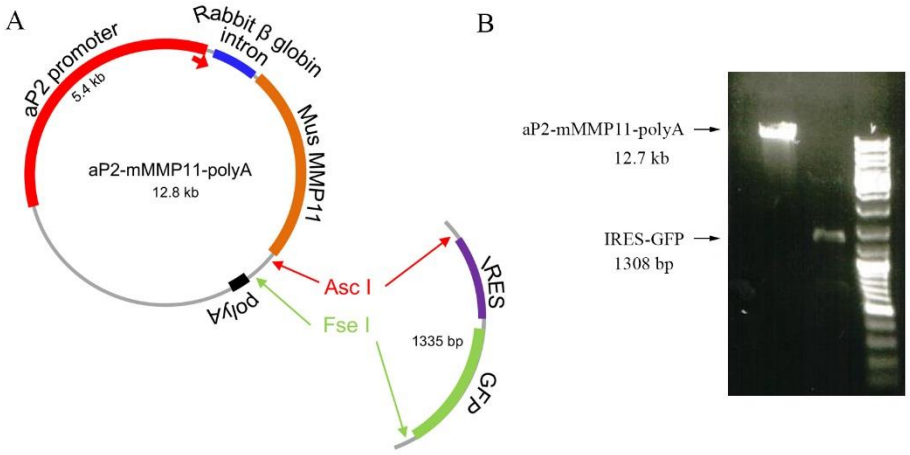

Figure 2.13 Same cutting ends were generated in IRES-GFP sequence and aP2-mMMP11-polyA construct. (A) The IRES-GFP sequence and aP2-mMMP11-polyA construct were cut with restriction enzyme Asc I and Fse I. (B) Electrophoresis in 1% agarose gel indicate the right size of both sequences.

2.2.1.3 Ligation of IRES-GFP and aP2-mMMP11-polyA

The ligation step was performed with T4 Ligase, aP2-mMMP11-IRES-GFP-polyA construct was generated. Because both IRES-GFP and aP2-mMMP11-polyA have Asc I and Fse I cutting ends, there were four possibilities during IRES-GFP inserted into the aP2-mMMP11-polyA vector: 1) IRES-GFP did not links with aP2-mMMP11-polyA vector; 2) IRES-GFP links with IRES-GFP via antisense strand; 3) aP2-mMMP11-polyA links with aP2-mMMP11-polyA via antisense strand; 4) IRES-GFP links with aP2-mMMP11-polyA vector (Figure 2.14 A), under this condition, mMMP-11 and GFP can be translated in proteins. This last form corresponds to the correct plasmid. Further to amplify the construct, I transferred plasmid into E. Coli-DH5α bacterial. Plasmid DNA was extracted from bacterial.

In order to confirm that the correct construct of aP2-mMMP11-IRES-GFP-polyA were obtained. The DNA was treated with restriction enzymes Asc I, Fse I and Sal I. aP2-mMMP11-IRES-GFP-polyA has the right size after enzymes treatment with the

control of aP2-mMMP11-polyA plasmid (Figure 2.14 B). #9 and #10 constructs were used for sequencing.

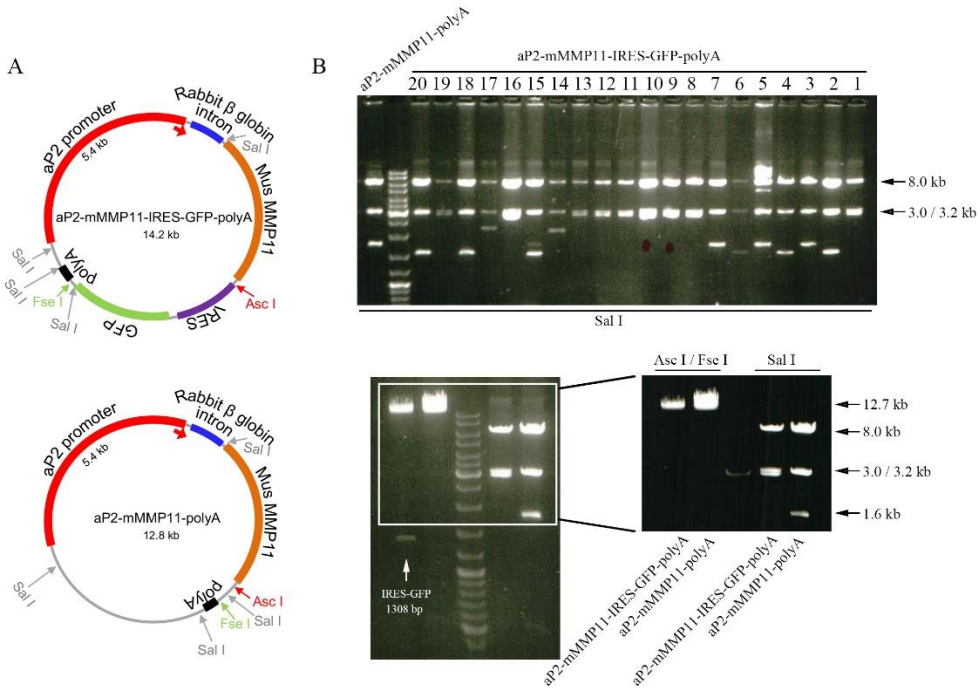

Figure 2.14 Confirmation of aP2-mMMP11-IRES-GFP-polyA construct. (A) The restriction enzyme sites of Asc I, Fse I and Sal I located in aP2-mMMP11-IRES-GFP-polyA and aP2-mMMP11-polyA constructs. (B) aP2-mMMP11-IRES-GFP-polyA construct was analyzed by Asc I, Fse I and Sal I, aP2-mMMP11-polyA served as control. Electrophoresis in 1% agarose gel.

2.2.1.4 Validation of aP2-mMMP11-IRES-GFP-polyA plasmid in vitro

In order to test if this construct expresses MMP-11 and GFP proteins in adipocytes in vitro, I transfected 3T3L1 preadipocyte cell line. A number of different constructs served as control (Figure 2.15). They had in common the presence of the mouse Fabp4/aP2 gene regulatory sequences. As shown in Figure 2.15 A, the different constructs were derived from the pBS-aP2-PolyA plasmid backbone. This plasmid is carrying the 5.4 kb aP2 promoter and the SV40 polyA signal (Addgene, pBS aP2 promoter (5.4kb) polyA, plasmid #11424). The mouse MMP-11 cDNA was cloned downstream of the promoter. Two coding sequences were introduced, coding for the wild-protein (mMMP11) and for a Flag-tagged protein (mMMP11-Flag). In all cases, a rabbit beta-globin intron/exon cassette was inserted between aP2 promoter and the mMMP11 cDNA coding sequences. Finally, a bi-cistronic construct was generated by introducing an IRES-GFP cassette downstream of the MMP-11 sequence, this plasmid was called aP2-mMMP11-IRES-GFP-polyA.

To know if the series aP2-mMMP11-polyA constructs were able to direct the overexpression of MMP-11 in adipocytes. All these vectors were transiently transfected into 3T3-L1 cells, which is a mouse pre-adipocyte cell line. Western blot was used to analyze protein expression after 3T3-L1 cells differentiation for two days. There was no MMP-11 protein expression in the absence of differentiation cocktail (data not shown). But all three constructs expressed MMP-11 under the condition of pre-adipocytes differentiation (Figure 2.15 B). Of note, MMP-11 and GFP proteins were expressed by aP2-mMMP11-IRES-GFP-polyA bicistronic construct. This result provided a good experimental foundation for generating transgenic mouse using the latter construct.

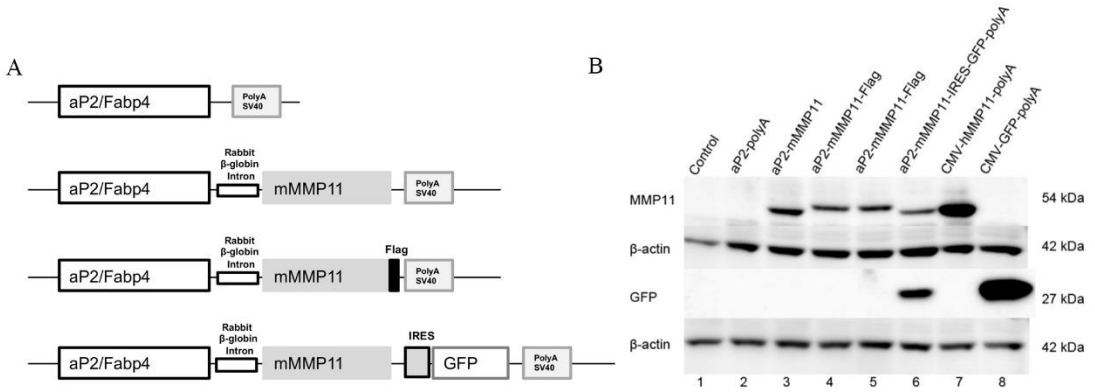

Figure 2.15 MMP-11 and GFP proteins were expressed by aP2-mMMP11-IRES-GFP-polyA construct. (A) The plasmid PBS-aP2-PolyA which has the specific promoter of the adipose cells 5.4 kb Fabp4/aP2 was used to generate a series of plasmids allowing tissue-specific expression of MMP-11. (B) These plasmids were transfected into 3T3-L1 pre-adipocytes, and the next day the pre-adipocytes were treated with differentiation medium for two days. 10 µg of protein extracts were analyzed with antibodies against MMP-11, actin, and GFP. MMP-11 is expressed by the various plasmids in particular by the bicistronic plasmid pBS-aP2-mMMP11-IRES-GFP-polyA (line 6) which expresses both MMP-11 and GFP. The constitutive vectors CMV-MMP11 and CMV-GFP are controls.

2.2.1.5 Linearization of aP2-mMMP11-IRES-GFP-polyA plasmid

There are two cleavage sites for restriction enzyme Xho I in the aP2-mMMP11-IRES-GFP-polyA vector (Figure 2.16 A), which can keep all components from aP2 promoter to the polyA end, without interupting MMP-11 and GFP sequences. So Xho I, was used to cleave and linearize aP2-mMMP11-IRES-GFP-polyA plasmid. Electrophoresis analysis showed that the enzyme cleavage was complete since only two bands were visualized (Figure 2.16 B). These results indicated that the linearization of aP2-mMMP11-IRES-GFP-polyA plasmid was good. We selected the band which contain the target sequence for purification. And the DNA of purified aP2-mMMP11-IRES-GFP-polyA was sent to the animal facility for generation of transgenic mice with adipocyte specific MMP-11 overexpression.

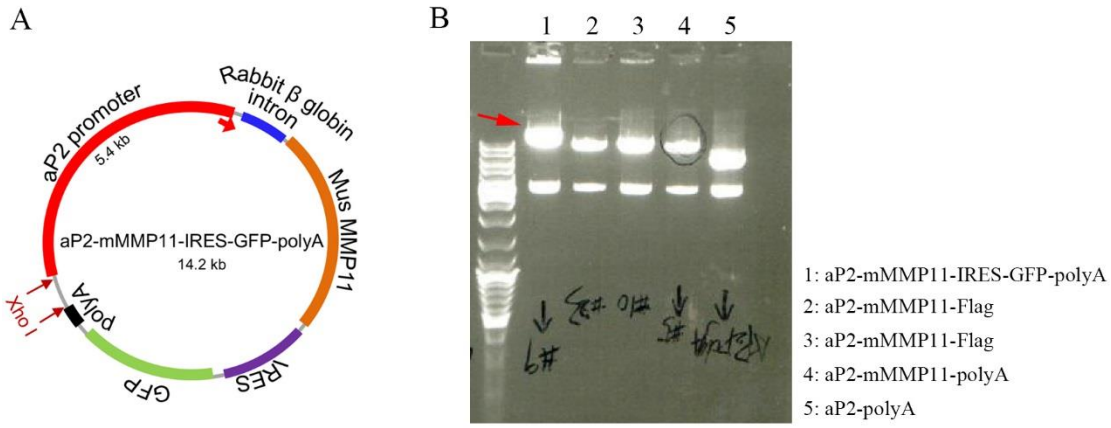

Figure 2.16 Linearization and purification of aP2-mMMP11-IRES-GFP-polyA construct. (A) Localization of the two cleavage sites for Xho I restriction enzyme in aP2-mMMP11-IRES-GFP-polyA vector. (B) Linearization of aP2-mMMP11-IRES-GFP-polyA by Xho I. Red arrowhead indicate the target DNA sequence of aP2-mMMP11-IRES-GFP-polyA without backbone for purification. Line 2, 3, 4 and 5 are linear controls.

2.2.2 Characterization of aP2-mMMP11-IRES-GFP-polyA transgenic mice lines

2.2.2.1 Verification of germline transmission of aP2-mMMP11-IRES-GFP-polyA transgenic mice lines

Founder mice (C57BL/6N background) were generated in the animal platform by microinjection. Here, three pairs of primers named a, b and c spanning the entire construct were used to detect insertion of the DNA construct in the genome (Figure 2.17 A). Primers were located in the beginning, in the middle and in the end of the construct, respectively. Out of 65 born mice, we got 4 positive founder mice (F0: #4, #14, #17 and #18) by tail DNA genotyping (Figure 2.17 B). Each founder mouse line was bread to test germ line transmission independently. The four founder mice were crossed with wildtype C57BL/6N mate. DNA genotyping showed that each line gave transgenic progeny in the F1 generation. The percentage of transgene transmission of F2 generation in mice #4, #14, #17 and #18 is 46.9%, 54.5%, 41.2% and 40.4%, respectively (Table 2.1). Transgene transmission is stable and Mendelian.

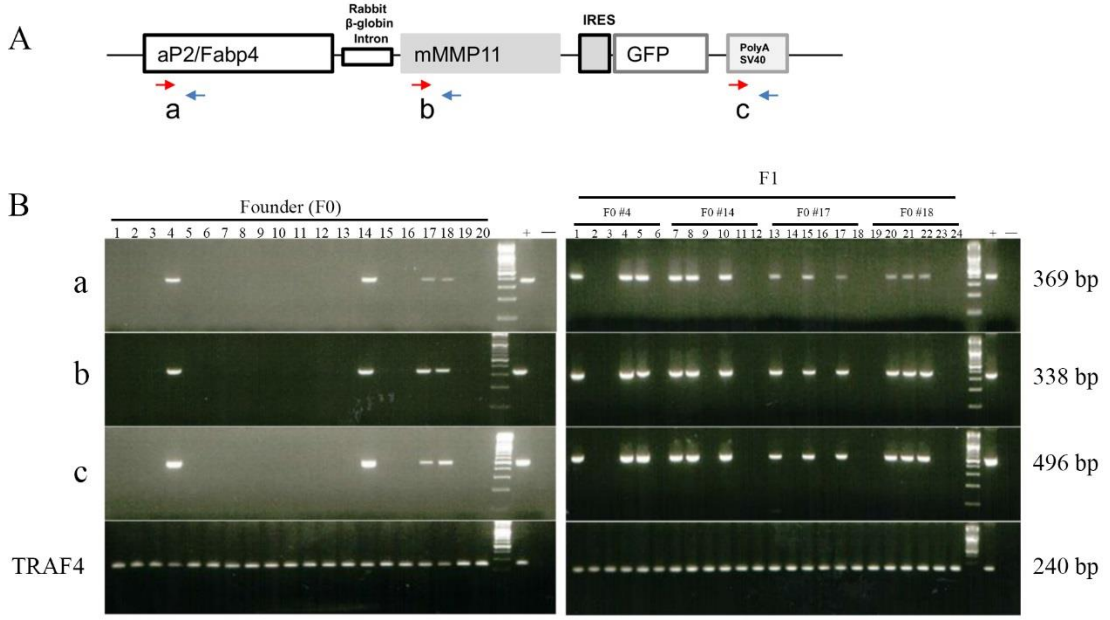

Figure 2.17 Germline transmission of transgene in each founder mouse. (A) Scheme illustrates the aP2-mMMP11-IRES-GFP-polyA construct and the position of three pairs of primers (a, b and c) for genotyping. (B) Founder mice tail DNA genotyping, three pairs of primers identified four positive mice: #4, #14, #17 and #18. F1 mice genotyping for the four positive lines verified the germline transmission. TRAF4 gene primer served as DNA control.

Founder mice	Female 4	Male 14	Male 17	Male 18
Number of F1	6	18	36	46
Positive F1	5	11	4	19
F1 positive rate	83.3%	61.1%	11.1%	41.3%
Number of F2	32	11	51	57
Positive F2	15	6	21	23
F2 positive rate	46.9%	54.5%	41.2%	40.4%

Table 2.1 The percentage of transgenic offspring in four founder mice lines.

2.2.2.2 Verification of MMP-11 and GFP expression of the aP2-mMMP11-IRES-GFP-polyA # 18 transgenic line

I examined the expression of MMP-11 and GFP within line # 18. These analyzes were carried out on several individuals of the F1, F2 and F3 generations. Transgene expression was investigated by RT semi-qPCR and qPCR on mRNA extracted from

brown adipose tissue (BAT), mammary gland white adipose tissue (mWAT), gonadal white adipose tissue (gWAT). The muscle was used as a control tissue. The location of bicistronic MMP-11 (b-MMP11) and GFP-specific primers were indicated (Figure 2.18 A). Consistently, the adipose tissue of Ad-MMP11^{Tg} # 18 mice express transgenic mRNA comprising the mMMP11 and GFP (Figure 2.18 B and C). The muscle is negative. Western blot analysis confirmed the expression of the transgene because the GFP protein was detected in the adipose tissue and only in transgenic mouse embryonic fibroblasts (MEFs) differentiated into adipocytes (Figure 2.18 D). Again, muscle was negative as non-differentiated MEFs. Similarly, mouse mammary gland adipose tissue whole mount immunofluorescence analysis detected GFP signal in transgenic mice (Figure 2.18 E). And GFP was also detected in transgenic BAT by immunohistochemistry (Figure 2.18 F).

Analysis of the Ad-MMP11^{Tg} # 18 line shows that it expresses the MMP-11 and GFP transgene specifically in adipose tissue. Since it is very difficult to detect mouse MMP-11 protein because it is unstable, we observed the adipose tissue phenotype of Ad-MMP11^{Tg} # 18 mice. It has been shown in the laboratory that constitutive and ectopic expression of MMP-11 alters adipose tissue by promoting decreased adipocyte size and reduced lipid accumulation (Dali-Youcef et al., 2016), a Mirror phenotype was shown in MMP-11 deficient mice (Andarawewa et al., 2005). I examined the adipose tissue morphology of Ad-MMP11^{Tg} # 18 (Figure 2.18 G). The morphology of the adipose tissues is also altered in this line, adipocytes in transgenic mice accumulate less lipids and show smaller size. These results confirm the tissue-specific expression of MMP-11 in line # 18.

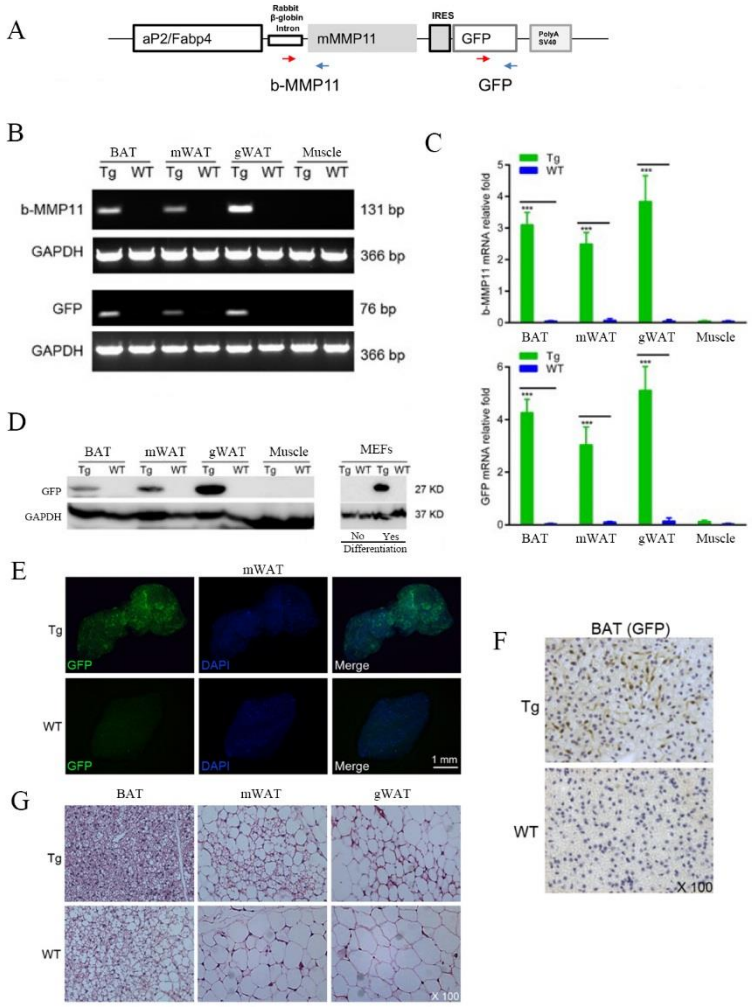

Figure 2.18 MMP-11 and GFP expression in #18 transgenic mouse line. (A) Scheme illustrates the location of qPCR primers in aP2-mMMP11-IRES-GFP-polyA construct. (B) Semi-quantitative PCR analysis showed the b-MMP11 and GFP mRNA expression was presented in the transgenic BAT, mWAT and gWAT, but absent in muscle. (C) qPCR analysis showed the mRNA relative fold of b-MMP11 and GFP. 5 mice/group, data represent mean±SD, ***P < 0.001(unpaired t-test). (D) Western blot detected the GFP protein from tissues of transgenic BAT, mWAT, gWAT and differentiated MEFs. But absence from transgenic muscle, wild type littermates and MEFs without differentiation. (E) Whole mount immunofluorescence detected the GFP signal in transgenic mWAT. (F) Brown signal of GFP was also presented in transgenic BAT by immunohistochemistry. (G) HE staining showed the size of adipocytes in transgenic BAT, mWAT and gWAT is smaller than wild type. Abbreviations: b-MMP11: bicistronic-MMP11. Tg: transgenic. WT: wild type. BAT: brown adipose tissue. mWAT: mammary gland white adipose tissue. gWAT: gonadal white adipose tissue. MEFs: mouse embryonic fibroblasts.

2.2.3 Adipocyte-specific MMP-11 promotes E0771 mouse breast tumor growth

In order to know whether adipocyte-derived MMP-11 promote mammary tumor growth in this new mouse model. Syngeneic E0771 mouse breast cancer cells were orthotopic injected into the #4 mammary gland fat pad of Ad-MMP11^{Tg} # 18 mice. It was found that tumor growth increased in transgenic mice compared with wildtype littermates (Figure 2.19). This is the first direct evidence of MMP-11 produced by adipocytes is involved in breast tumor growth.

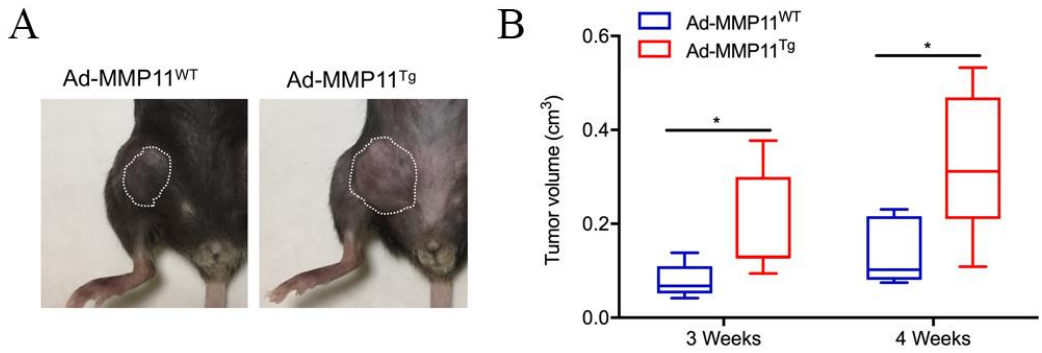

Figure 2.19 MMP-11 produced by adipocytes promotes E0771 mouse breast tumor growth**.** (A) 16 weeks old female mice from the same crosses (Tg and WT) were subjected to orthotopic injection of $2x10^5$/100ul E0771 cancer cells into #4 mammary gland fat pad under anesthesia condition. (B) The size of the tumor was measured by caliper twice a week for 4 weeks. The tumor growth in Ad-MMP11^{WT} control mice group were slower than the Ad-MMP11^{Tg}. 6 mice/group, data represent mean±SD, *P < 0.05 (unpaired t-test). The tumor volume was calculated by measuring the length and width, and according to the formula (4/3) x 3,14159 x (length/2) x $(width/2)^2$.

In conclusion, we obtained a novel mouse line that specifically expresses MMP-11 in the adipose tissue. Moreover, the above results confirm the direct involvement of MMP-11 produced by adipocytes in tumor growth. This relatively simple model will be favored for morphological and comparative analyzes of the tumor and the tumor microenvironment. In the next part of this study, we will build cohorts to conduct carcinogenesis experiments for morphological and molecular analysis.

Part III The impact of ITPP on MMTV-PyMT mouse breast cancer progression

Hypoxia is a major determinant of tumor growth and angiogenesis. Myo-Inositol trispyrophosphate (ITPP) is a recently identified membrane-permeant molecule that causes allosteric regulation of hemoglobin (Hb) oxygen binding affinity. Previous studies showed a potential therapeutic effect of ITPP on cancer development (Sihn et al., 2007; Aprahamian et al., 2011; Derbal-Wolfrom et al., 2013; Raykov et al., 2014). To date, the anti-cancer effect of ITPP was not tested on an integrated model of cancer development and progression. To directly test the potential of ITPP on breast cancer, I used a genetic mouse model of mammary gland tumor, the MMTV-PyMT model. Different treatments were used in order to study the potential of ITPP as a therapeutic agent alone and in combination with a known anti-cancer agent, doxorubicin, which is a DNA intercalating and powerful cytotoxic agent (Yang et al., 2014).

2.3.1 ITPP promotes mammary gland hyperplasia and tumor incidence

The therapeutic effect of ITPP on PyMT mammary gland tumor development was tested by starting treating 10 mice at 6 weeks old during 4 weeks. As control, a group of 10 mice were treated with doxorubicin alone. In order to keep high and stable concentrations of these drugs into the blood, ITPP was injected twice a week and doxorubicin once a week. Results in Figure 2.20 A and B showed that ITPP alone was associated with increased PyMT preneoplastic and tumor growth while doxorubicin alone limited hyperplasia and tumor growth. When combined, doxorubicin did not significantly counteract tumor promoting effect of ITPP. As shown in Figure 2.20 C, doxorubicin alone had a tendency to limit tumor burden while ITPP alone or in combination with doxorubicin did not delay tumor burden.

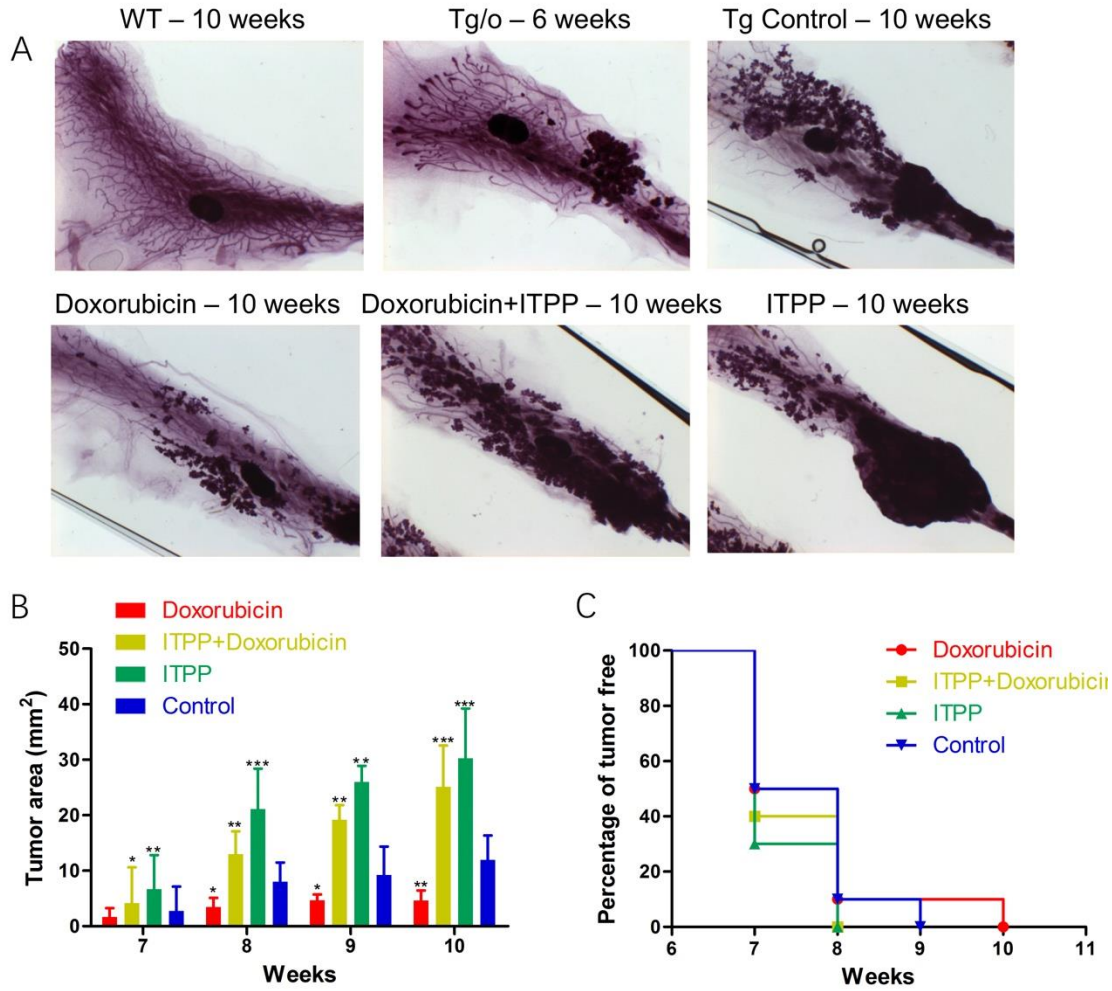

Figure 2.20 Morphological analysis of mammary glands hyperplasia and neoplasia. (A) By whole mount carmine-alum staining. Clockwise, mammary gland from a normal mouse at 10 weeks shows the presence of a dense network of ducts and small terminal end-buds. PyMT mammary gland at 6 weeks shows the presence of few hyperplastic lesions. At 10 weeks old hyperplastic lesions are scattered throughout the entire mammary gland. In doxorubicin treated mice at 10 weeks the presence of hyperplastic lesion is less dense, while in ITPP alone or ITPP plus doxorubicine treated mice hyperplastic lesions are present in the entire gland. (B) Tumor volume was measured twice a week from the first to fourth week of treatment. Doxorubicin attenuate tumor growth, while ITPP alone or in combination with doxorubicin favors tumor growth. (C) Tumor burden in the four groups of treated mice. 10 mice/group, data represent mean±SD, *P < 0.05, **P < 0.01, **P < 0.01 (pair t-test and one-way ANOVA).

2.3.2 ITPP did not promoted mammary tumor metastasis to lung

After treatment for 4 weeks, mice from these four groups were euthanized and right-middle lobes of lung were dissected out for examination of metastasis. No visible metastatic foci were found. Therefore, quantitation of lung metastasis was done by measuring the relative amounts of PyMT mRNA present in the lungs. RT-qPCR from the right-middle lobe lung showed that the lung metastasis was reduced by more than 50% in doxorubicin-treated mice compared with untreated, ITTP alone and ITPP plus doxorubicin-treated mice (Figure 2.21). Of note, ITPP alone or in combination with

doxorubicin did not have an adverse effect on metastasis to lung on MMTV-PyMT mouse model.

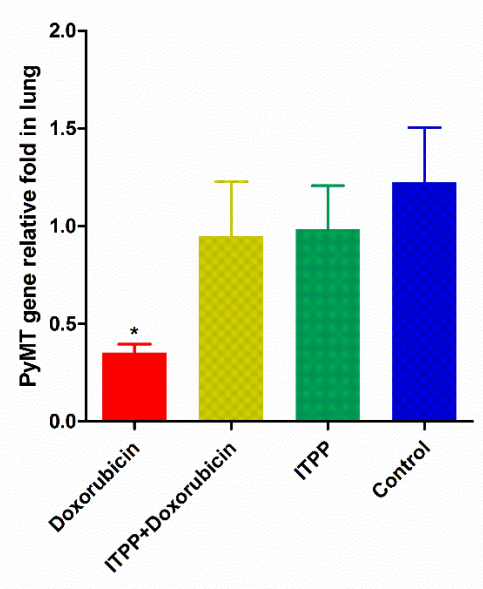

Figure 2.21 Quantitation of lung metastasis. Real-time RT-PCR was used to quantitate the relative amount of PyMT mRNA levels (normalized to GAPDH RNA level), which reflects the relative PyMT lung metastasis. 10 mice/group, data represent mean±SD, *P < 0.05 (pair t-test and one-way ANOVA).

In conclusion, ITPP have no therapeutic effect on breast cancer development in the MMTV-PyMT mouse model. Even though ITPP compound exert therapeutic effect on several tumor models as mentioned in the literatures (Aprahamian et al., 2011; Raykov et al., 2014), ITPP did not limit MMTV-PyMT mice breast tumor growth, on the opposite it was associated with increased tumor growth. Of note, ITPP did not increase metastasis to the lung indicating that despite its tumor growth promoting action it does not favor tumor progression. Morphological and molecular analyses are necessary to better characterize the changes mediated by ITPP on mammary tumor.

CHAPTER 3 Conclusions, Discussion and Perspectives

Part I

In this study, MMTV-PyMT mouse model was employed for crossing with MMP-11 transgenic mouse line and MMP-11 knockout mouse line. Mammary tumor occurs spontaneously in these two mouse lines with different time line. I further analyzed tumor growth and histology, lipid metabolism, cellular stress responses and lung metastasis.

3.1.1 MMP-11 promotes mammary tumor growth

In human breast cancer, MMP-11 is detected in the tumor center and periphery, but not in the adjacent normal tissue (Andarawewa et al., 2005; Tan et al., 2011). Overexpression of MMP-11 in MCF-7 cells has tumor promoting effect in xenografts in nude mice (Kasper et al., 2007). Consistent with these studies, by using MMP-11 transgenic mice overexpressing MMP-11 in the skin, we showed that the tumor development of PyMT mice was accelerated by the presence of MMP-11. PyMT::MMP11^{Tg} mice developed more pre-neoplastic lesions and tumor growth was increased at early stages. A mirror phenotype was observed when the course of PyMT tumor development was studied in the absence of MMP-11, indeed PyMT::MMP11^{KO} mice were delayed in tumor growth and less preneoplastic lesions were observed. Of interest, no difference in palpable tumor incidence was observed in PyMT::MMP11^{Tg} mice, it could be because tumor formation in the FVB/N pure background is very rapid. On the contrary, PyMT::MMP11^{KO} mice were in a mixed background and tumor development is slower, in that case tumor incidence was reduced in the absence of MMP-11.

As secreted in active form, MMP-11 circulates in the body fluid and has some systemic functions. Consistent with the notion that MMP-11 indeed has an adipocyte dedifferentiation function in vivo (Dali-Youcef et al., 2016), the body weight of MMP-11 transgenic mice is lower than control mice, and MMP-11 knockout mice has a higher body weight than control.

3.1.2 MMP-11 decreases tumor apoptosis but increases proliferation at early stages

In previous studies, MMP-11 was reported to increased tumorigenesis without affecting neoangiogenesis or cancer cell proliferation but by decreasing cancer cell death through apoptosis and necrosis (Boulay et al., 2001). Thus, during malignancy, the cellular function of MMP-11 was believed to favor cancer cell survival in the stromal environment. In this study, in PyMT driven breast tumors, we demonstrated that MMP-11 expression decreased necrosis and apoptotic cells in GOF model at early stage of tumor development. Reciprocally, loss of MMP-11 was associated with an increased necrosis and apoptosis compared with their control littermates. Consistently, whole protein analysis of tumor extracts showed the reciprocal change of expression level of the anti-apoptotic marker bcl-2.

However, by regulating IGF-1 signalling pathway, overexpression of MMP-11 enhances MCF-7 and MDA-MB-231 breast cancer cells proliferative capacity and increases tumor volumes both in vitro and in vivo (Kasper et al., 2007). Additionally, limiting MMP-11 expression using MMP-11 mRNA silencing methodology in the gastric cancer cells BGC823 showed significant decreased growth ability compared with mock transfectants and parental BGC823 cells. Furthermore, colony formation of MMP-11 deficient cells was dramatically inhibited in soft agar and the tumorigenicity was reduced in nude mice, respectively (Deng et al., 2005). These results provided new insights into the function of MMP-11 and suggested that MMP-11 may play an important role in the control of cell proliferation and tumor development. Indeed, the present study have shown that MMP-11 exacerbated the IGF1/AKT signalling pathway through increased IGF1 availability by decreasing IGFBP1 protein levels, promoted tumor cell survival and significantly increased cell proliferation in tumor samples from $PyMT^{Tg}$:$MMP11^{Tg}$ mice as compared to control $PyMT^{Tg}$:$MMP11^{WT}$ animals, resulting in cancer progression.

During cell cycle interphase, the Ki-67 antigen can be exclusively detected within the cell nucleus, whereas in mitosis most of the protein is relocated to the surface of the chromosomes (Cuylen et al., 2016). Ki-67 protein is present during all active phases of the cell cycle (G1, S, G2, and mitosis), but is absent in resting (quiescent) cells (G0) (Bruno and Darzynkiewicz, 1992). Proliferation was studied by measuring the ratio of Ki-67 positive tumor cells. Of interest in the GOF model increased proliferating cells were observed in early stage of tumor development at 6 weeks old, but no differences were observed at later stages. This is consistent with the notion that MMP-11

specifically acts at early stage of tumor development by favoring cross talk with the tumor microenvironment.

3.1.3 MMP-11 alters UPR^{mt} and promotes ER stress response and metabolic switch

We have recently reported a crucial function of MMP-11 in the regulation of whole body metabolism through activation of the IGF1/AKT/FoxO1 signaling cascade in a non-cancer context using gain- and loss-of-function genetic-engineered mice models (Dali-Youcef et al., 2016). The present study brought new insights into the molecular mechanisms of MMP11-mediated cancer progression in the MMTV-PyMT breast cancer mouse model. Mechanistically, MMP-11 enhanced the Warburg-like effect in tumors samples through a metabolic switch by decreasing oxidative phosphorylation and enhancing aerobic glycolysis most likely through the IGF1/AKT/FoxO1 cascade. Besides lactate utilization, MMP-11 enhanced also lipid turnover (e.g. synthesis, transport and metabolism) to serve as an additional nutrient source to fulfill tumor energetic needs allowing new membrane formation and expansion. An interesting finding lies in the MMP11-mediated increase in ER stress through the significant elevation in the expression of key components of the UPR^{ER}, namely ATF4, ATF6 and Xbp1 (Frakes and Dillin, 2017). The argument of MMP11-mediated increase in UPR^{ER} was strengthened by the increase in the MMP11-mediated phosphorylation of eIF2α, an upstream inducer of ATF4 and downstream effector of the ER stress-mediated kinase PERK (Frakes and Dillin, 2017). There is compelling evidence that UPR^{ER} is involved in tumorigenesis, more specifically in HER2-positive breast cancer (Kim et al., 2016a), and hence constitutes an attractive target for anticancer treatment (Shen et al., 2018). Likewise, the hypoxic environment of the tumors has a dual supportive role in cancer. On one hand, it stimulates the IRE1 and PERK branches of the UPR^{ER} to enhance the insensitivity of cancer cells to apoptosis (Fels and Koumenis, 2006). On the other hand, hypoxic stress in cancer stimulates the inositol requiring enzyme 1α (IRE1)/XBP1 arm of the UPR to blunt immune elimination of cancer cells, by decreasing the expression of major histocompatibility complex 1 (MHC1) molecules in antigen presenting dendritic cells, weakening thereby the function of $CD8^+$ lymhocytes to kill cancer cells (Cubillos-Ruiz et al., 2017). Another aspect of MMP-11 role in mediating cancer progression is the defective

mitochondrial unfolded protein response (UPR^{mt}) observed in tumors from $PyMT^{Tg}$:$MMP11^{Tg}$ mice as demonstrated by the decreased expression of important proteins of the UPR^{mt} such as the chaperone proteins HSP10 and HSP60 or the mitochondrial protease Clpp, which role is to eliminate misfolded or unfolded proteins in the mitochondrial matrix. This axis of the UPR^{mt} is referred as the CHOP pathway (Zhao et al., 2002). These results were surprising, in the sense that tumor aggressiveness is often associated with mitochondria fitness and adaptation to stress.

Another observation that we presented is that MMP11-mediated decrease in the expression of the proteasome subunits Psmb1 and Psmd1 and may result in decreased proteasome activity. Mitochondrial dysfunction produced by impaired ETC and ROS generation was shown to inhibit proteasome activity (Livnat-Levanon et al., 2014; Segref et al., 2014), because of ATP depletion being crucial for proteasome assembly. Moreover, we observed a significant increase in AMPK phosphorylation, a kinase induced upon nutrient deprivation. It is tempting to speculate that non-degraded stressed mitochondria may amplify the proteotoxic and mitochondrial stress contributing further in ATP-depletion and increase in AMPK activation, a known activator of autophagy (Kim et al., 2011). To give weight to this hypothesis, a recent report has shown that accumulation of ubiquitin-proteins was correlated with decreases in cellular bioenergetics and increase in AMPK activation and autophagy (Jiang et al., 2015). After all, autophagy is the process by which the cell recycles the constituents of irreversibly damaged organelles to generate energy and recover precursors necessary for cell growth. This hypothesis and the occurrence of autophagy need to be verified in our model.

In conclusion, we have reported that MMP-11 promotes cell proliferation and cancer progression in a model of breast cancer, the MMTV-PyMT mouse model and inhibits cell death by regulating important metabolic pathways such as the switch from oxidative phosphorylation to aerobic glycolysis, and adaptive organelle processes following proteotoxic stress such as the UPR^{ER} and UPR^{mt} in order to cope with nutrient availability within the cell all to the benefit of cancer cells, allowing them to survive in harsh conditions such as the presence of ROS.

3.1.4 MMP-11 reduces dissemination of mammary tumor to the lung

Previous study demonstrated that MMP-11 has a paradoxical role on tumor spreading. Using the MMTV-ras transgenic model our lab showed that the tumor incidence and burden was decreased in Ras^{Tg}:$MMP11^{KO}$ mouse model but more lung metastases were observed (Andarawewa et al., 2003), indicating that the cancer cells evolving in MMP11-deficient stroma have an increased potential to hematogenous dissemination. In addition, in another model, besides the reduction of the number of primary tumors, MMP-11 deficient mice have an unexpected increased number of colon-to-lung metastases (Brasse et al., 2010).

In our two experimental models, the progression of PyMT induced primary mammary tumor to lung metastasis was evaluated by HE staining and quantified by the size of metastatic lesions. In GOF model, even though there was no difference of the lesion size, the number of metastatic lesions were significantly decreased in MMP-11 transgenic mice. By quantitative analysis of PyMT gene mRNA level in the lung as an indicator of metastatic spreading in the lung, we observed that MMP-11 didn't promote mammary gland primary tumor to the lung metastasis at early metastatic stage of 8 weeks old. Wildtype mice have increased number and bigger size of metastatic lesions than MMP-11 knockout in the LOF model at 17 weeks old. In consideration of the tumor growth was significantly delayed in the knockout group than wildtype in LOF model, 13 weeks wildtype and 16 weeks old knockout mice which have the same tumor volume were utilized to evaluate the lung PyMT gene expression. Knockout mice lung has a higher level of PyMT mRNA than controls.

We conclude that MMP-11 mainly promotes primary tumor growth and invasion into the tumor microenvironment but probably does not promote tumor cell intravasation into blood vessels. The fact that the extent of tumor angiogenesis was not affected by MMP-11 might be a possible cause.

3.1.5 Perspectives

To further research the systemic metabolic changes of MMP-11 in our mice models, we will analysis the tumor tissues after injection of ^{13}C labeled D-glucose. Our lab also generated an adipocyte specific MMP-11 transgenic mouse model, named aP2-MMP11-IRES-GFP, this model will be employed for study the metabolic function of MMP-11.

Part II

In this study, I generated a new construct named aP2-MMP11-IRES-GFP, this construct was used to generate a new transgenic mouse line. Preliminary, in vivo experiment validated the role of MMP-11 produced by the adipose tissue in promoting tumorigenesis.

3.2.1 MMP-11 was expressed under the adipocyte specific aP2 promoter in 3T3-L1 cell line

During the last years, several researches uncovered the fact that adipocytes participate in cancer progression and metastasis (Dirat et al., 2011; Nieman et al., 2011; Tan et al., 2011; Carter and Church, 2012; Rio et al., 2015). Pioneer work on MMP-11 showed that it is involved in breast tumor development processes as a CAF and CAA component (Andarawewa et al., 2005; Motrescu and Rio, 2008).

To determine the specific function of MMP-11 which is produced by the adipose tissue during cancer development I used an in vivo strategy. The aim of this study was to model MMP-11 expression by CAAs in a controlled system. CAAs express many components favoring cancer progression (Rio et al., 2015), we reasoned that overexpressing MMP-11 in the adipose tissue could exacerbate the molecular changes driven by MMP-11 and may help to identifying them.

I generated a construct named aP2-MMP-11-IRES-GFP which has an adipocyte specific aP2 promoter. The aP2 protein also known as FABP4, facilitates the intracellular solubilization and trafficking of lipids (Thompson et al., 2009; Smathers and Petersen, 2011). It has been implicated as a good marker of adipose-specific genes representing the accumulation of lipids in mature adipocytes (Moseti et al., 2016). The 5.4 kb region upstream of the aP2 promoter drives the adipose-specific expression of transgenes in mouse models (Ross et al., 1990; Shin et al., 2009).

In addition to the MMP-11 open reading frame, we added a reporter cassette in the construct. It has been shown that it is very difficult to detect the mouse MMP-11 protein, possibly because the half-life is very short. Therefore, in order to trace the transgene expression, we introduced the open reading frame of the fluorescent protein GFP directly downstream of the MMP-11 cDNA sequence.

3.2.2 MMP-11 transgene was expressed in aP2-MMP11-IRES-GFP transgenic mouse model

Among 65 mice obtained after microinjection, only 4 positive founder mice were obtained. These founder mice were crossed with wildtype mice independently which share the same genetic background. Besides the germline transmission of MMP-11 transgene in all derived lines, only one line showed MMP-11 and GFP expression in the adipose tissue.

As reported before, MMP-11 knockout mice have a significantly higher body weight than wildtype littermates in either normal diet (Andarawewa et al., 2005) or high fat diet (Lijnen et al., 2002), but MMP-11 transgenic mice have lower body than control both 8 weeks old and 40 weeks old (Dali-Youcef et al., 2016). Here I didn't observe significant difference of the body weight in aP2-MMP-11 transgenic mice compared with their wildtype littermates (data not shown), I suppose that the expression level of MMP-11 protein in this model is not as high as in the MMP-11^{Tg} model used in the first part of my study. The size of adipocytes appeared smaller in aP2- MMP-11 transgenic mice tissues, confirming that MMP-11 limits mouse adipogenesis (Andarawewa et al., 2005; Motrescu et al., 2008; Tan et al., 2011; Dali-Youcef et al., 2016).

Therefore, we established a new transgenic mouse line named aP2-mMMP11-IRES-GFP-polyA, which directly express MMP-11 in mouse adipose tissue.

3.2.3 MMP-11 promoted E0771 tumor growth in vivo

The E0771 medullary breast adenocarcinoma cell line was originally isolated as a spontaneous tumor from C57BL/6 mouse (Sugiura and Stock, 1952) and adapted for anti-cancer drug testing (Sirotnak et al., 1984). To address the contribution of MMP-11 produced by adipocytes to tumor development, we used this syngeneic cell line in a first pilot experiment and observed accelerated tumor growth in the presence of MMP-11.

Adipocytes release various soluble factors, including cytokines, growth factors, adipokines, free fatty acids, etc., which support surrounding epithelial cancer cells survival and growth (Andarawewa et al., 2005; Dirat et al., 2011; Nieman et al., 2011; Tan et al., 2011; Carter and Church, 2012). For example, it has been shown that leptin appears to be able to control the proliferation of both normal and malignant breast epithelial cells (Hu et al., 2002). The adiponectin regulates mammary tumor development and angiogenesis, and vascular T-cadherin-adiponectin association may

contribute to the molecular cross-talk between tumor cells and the stromal compartment in breast cancer (Hebbard et al., 2008).

It is well known that IGF-I promotes mammary gland development and mammary gland fat tissue metabolic switch via IGF-I/IGF-IR signalling pathway (Richards et al., 2004; Dali-Youcef et al., 2016). However, the IGF-I signalling axis is further complicated by the presence of secreted, high-affinity IGF-binding protein-1 (IGFBP-1), the IGF-I/IGFBP-1 complex leads to IGF-I inactivation. Interestingly, it has been shown that MMP-11 can cleave IGFBP-1 and release bioavailable IGF-I (Mañes et al., 1997). The mechanisms by which MMP-11 exerts its function may involve the activation of IGF-I signalling and potentially AKT and/or other pathways. In addition, MMP-11 was shown to degrade Collagen VI, a specific collagen from the adipocytes basement membrane (Motrescu et al., 2008). Cleavage of Collagen VI by MMP-11 may facilitate adipocytes delipidation and dedifferentiation, thus promote cancer progression.

In consideration that MMP-11 is secreted as an active form, there may be four possible roles explaining MMP-11 action. First, MMP-11 might alter the adipocytes basement membrane by favoring Collagen VI degradation and accelerating dedifferentiation. Second, the delipidation of adipocyte may provide energy supply like free fatty acid for rapid tumor growth. Third, the adipocytes dedifferentiation in fibroblast-like cells can cause further tissue fibrosis and promote cancer cell migration and metastasis. Finally, MMP-11 might affect the expression/secretion of several soluble factors including which could be involve in signal transduction of adjacent malignant epithelial cells and sustain the cancer cell self-renewal ability. Clearly, further studies are needed to investigate the impact of MMP-11 on these pathways in mammary tumor development.

3.2.4 Perspectives

The aP2-MMP11-IRES-GFP transgenic mouse line provided us a novel model to investigate the function of CAAs derived-MMP-11 on mammary gland tumor progression. Next, it will be utilized for mammary gland duct in situ-injection of E0771 cancer cells which contain a luciferase reporter gene.

Part III

In this study, I tested the therapeutic action of ITPP on a genetic mouse model of breast cancer the MMTV-PyMT model. I observed that ITPP accelerated mammary gland carcinogenesis in PyMT mice.

3.3.1 ITPP had an adverse therapeutic effect on mammary gland tumor

ITPP is an allosteric effector of hemoglobin, which was first reported in 2005 (Fylaktakidou et al., 2005). It was shown to exert anti-tumor growth and anti-angiogenesis ability in several cancer types (Aprahamian et al., 2011; Raykov et al., 2014). To substantiate these findings, we chose the MMTV-PyMT model because mammary gland tumors arise with a high incidence in these mice. Moreover, PyMT mammary tumor recapitulates many processes found in human breast cancer with a poor prognosis (Guy et al., 1992; Lin et al., 2003). I observed that ITTP had an adverse therapeutic effect on mammary gland progression. Indeed, results showed ITPP treatment alone and in combination with doxorubicin was associated with an increase of pre- and neoplastic lesions and tumor growth.

However, in chick embryos of glioma model, ITPP exerts anti-angiogenic and growth reduction effect by 2 days' treatment (Sihn et al., 2007). Another study showed that ITPP treatment leads to HIF-1α suppression and decreased tumor volume of early hepatoma tumors in rats (Aprahamian et al., 2011). However, no therapeutic effect on tumor growth and no effect on the expression level of HIF-1α and VEGF were observed in a hepatocellular carcinoma Trim24-null genetic mouse model (Ignat et al., 2016). This drug also reduces colon cancer growth in a nude mice model by 8 weeks intraperitoneally injection (Derbal-Wolfrom et al., 2013). Furthermore, even in different rat and/or mouse models of pancreatic cancer, immunocompetent or immunodeficiency, ITPP have has an anti-cancer and anti-hypoxia function. In addition it enhances chemotherapy efficacy (Raykov et al., 2014).

In our study, ITPP (2g/kg twice a week for 4 weeks) were used to intraperitoneally injection of immunocompetent MMTV-PyMT mice with or without doxorubicin. Either the time of treatment, drug concentration or injection method was not the same as the studies mentioned before. We speculated that ITPP provide excessive amounts of oxygen for mammary tumor growth.

3.3.2 ITPP did not favor lung metastasis

Of interest, our data revealed that ITPP did not increase breast tumor metastasis to the lung, despite an adverse effect on the mammary hyperplasia and primary tumor incidence and growth. One possible mechanism is that ITPP decreased the HIF-1α and VEGF expression in cancer by providing overload of oxygen, which retarded tumor angiogenesis and tumor cells invasion into blood vessels and metastasis to the lung.

3.3.3 Perspectives

The mammary tumor angiogenesis and the expression level of HIF-1α and VEGF will be detected at the next step.

CHAPTER 4 Materials and Methods

Part I Techniques related to results part I

4.1.1 Generation of mice candidates

1) This study was approved by the Ethical Committee. In the GOF model, MMTV-PyMT^{Tg} male mice (FVB/N background) crossed with K14-MMP11^{Tg} female mice (FVB/N background). The first mice generation were genotyped. PyMT^{Tg}; MMP11^{WT} and PyMT^{Tg}; MMP11^{Tg} female mice were randomly divided and used for experiments. Each group in different experimental time points contain at least 6 mice.

2) In the LOF model, MMTV-PyMT^{Tg} male mice (FVB/N background) crossed with MMP11$^{-/-}$ female mice (129/SvJ background). The first mice generation were genotyped. Then, PyMT^{Tg}; MMP11$^{-/+}$ male mice crossed with PyMT^{WT}; MMP11$^{-/+}$ female littermates. The last mice generation were genotyped. PyMT^{Tg}; MMP11^{WT} and PyMT^{Tg}; MMP11^{KO} female mice were randomly divided and used for experiments. Each group in different experimental time points contain at least 6 mice.

4.1.2 Isolation of DNA from mouse tail biopsies

Solutions and regents

1) TNES (10 mM Tris-PH 7.5, 400 mM NaCl, 100 m MEDTA, 0.6% SDS).
2) 5 M NaCl.
3) Cold absolute ethanol.
4) 70% cold ethanol.
5) T10E1 (10 mM Tris-PH8.0, 1 mM EDTA).

Protocol

1) Obtain tail biopsies from 2-3 weeks old mice.
2) Add 600 ul of TNES and 20 ul proteinase K (20 mg/ ml).
3) Incubate overnight at 55ºC.
4) Let the tube cool down at RT, add 200 ul of 5 M NaCl, vortex.
5) Centrifuge 12000 rpm for 5 minutes.
6) Transfer supernatant to new tube and add 1 volume cold 100% ethanol.
7) Centrifuge 12000 rpm for 10 minutes. DNA pellet is formed in the bottom.
8) Rinse pellet with ~500 ul 70% ethanol, centrifuge 12000 rpm for 1min.

9) Remove ethanol and dry the pellet ~ 10 minutes.

10) Resuspend in 200 ul - 500 ul pre-warmed 55ºC of T10E1, vortex.

11) Put in 65ºC for 10min, vortex and short centrifuge.

12) Keep in 4ºC until use.

4.1.3 Mice genotyping

PCR reaction mix

1) 19 µl H_2O.
2) 2.5 µl buffer (100 mM Tris HCl, 500 mM KCl, 0.1% gelatin, 15 mM MgCl2).
3) 1.25 µl DMSO (dimethylsulfoxide).
4) 0.25 µl primer-A (1 µg/µl).
5) 0.25 µl primer-B (1 µg/µl).
6) 0.5 µl primer-C (1 µg/µl).
7) 0.5 µl Taq polymerase.
8) 1 µl genomic DNA.

PyMT gene PCR reaction: 94ºC for 30 seconds, 64ºC for 1 minute, 72ºC for 1 minute, 35 cycles; $MMP11^{Tg}$ gene PCR reaction: 94ºC for 1 minute, 60ºC for 20 seconds, 72ºC for 1 minute, 33 cycles; $MMP11^{KO/WT}$ gene PCR reaction: 94ºC for 15 seconds, 62ºC for 15 seconds, 72ºC for 1 minute, 33 cycles.

	Forward	Reverse
PyMT	GGAAGCAAGTACTTCACAAGGG	GGAAAGTCACTAGGAGCAGGG
$MMP11^{Tg}$	CGGTTTCCACCATCCGAGGA	GTGGAAACGCCAATAGTCTCC
$MMP11^{KO}$	GTGGAAACGCCAATAGTCTCC	GCCGCTTTTCTGGATTCATCG
$MMP11^{WT}$	GTGGAAACGCCAATAGTCTCC	TTCTAACATCCCTCTGGGCTC

Table 4.1 Primers used for mice genotyping.

4.1.4 Mice weight and tumor measurement

1) Mice weight was measured by electronic balance twice a week.

2) Caliper was used to measure the tumor length, width and height twice a week. Tumor volume was calculated following the formula (4/3) x 3.14159 x (length/2) x (width/2) x (height/2).

4.1.5 Carmine-alum red staining of whole mount mammary gland

1) The pair of # 4 (inguinal) mammary glands was dissected from each mouse. One side gland was analyzed by whole mount staining; the other side was fixed in 10% paraformaldehyde for 24 hours, dehydrated, embedded in paraffin, or quick frozen in Tissue-Tec OCT for cryostat sections.

2) The mammary glands were spread onto glass slides. RT for 10 minutes.

3) Fix tissue in carnoy solution (75% glacial acetic acid, 25% absolute EtOH). RT for overnight.

4) Put in 100%EtOH, 70% EtOH for 1 hour each step.

5) Put in distilled water for 30 minutes at RT.

6) Carmine-alum (Sigma, C1022, USA) stain overnight at RT.

7) Dehydrate in every gradient 70% EtOH, 95% EtOH and 100% EtOH for 1 hour each step.

8) Put in histosol overnight at RT.

9) Mount with Permount.

4.1.6 Picro-sirius red staining

Picro-sirius kit from American MasterTech (KTPSRPT). Paraffin embedding tumor tissue slides from #4 mammary gland were treated as follow:

1) 100% histosol for 3 times, 5 minutes each.

2) 100% ethanol for 2 times, 3 minutes each.

3) 95% ethanol for 3 minutes.

4) 80% ethanol for 3 minutes.

5) Tap water wash slides for 1 minute.

6) 1:1 fresh mix A and B Weigert's Hematoxylin solution, immerse slides for 20-30 minutes.

7) Tap water wash slides for 10 minutes.

8) Immerse slides into picro-sirius red solution for 1 hour at least.

9) 0.5% Acetic Acid for 5 seconds, 2 times each.

10) 100% ethanol for 5 seconds, 3 times each.

11) 100% histosol for 3 minutes.

12) Mounting with Permount.

4.1.7 HE staining

1) Paraffin embedding tumor tissue slides from #4 mammary gland were immersed into 100% histosol for 2 times, 5 minutes each.
2) Follow by 100%, 90%, 80% ethanol and H_2O for 5 minutes each.
3) Stain for 3 minutes in Harris Hematoxylin.
4) Decolorize in acid alcohol for 2 seconds.
5) Wash and blue the sections in running tap water for 3 minutes.
6) Stain for 30 seconds in 0.1% aqueous eosin Y.
7) Rinse in tap water for 30 seconds.
8) Dehydrate in 80%, 90%, 100% ethanol for 5 minutes each.
9) Clear in 2 times of 100% histosol, 5 minutes each.
10) Mounting with Permount.

4.1.8 In situ apoptosis detection (TUNEL assay)

TUNEL kit from Abcam (ab206386). Paraffin embedding tumor tissue slides from #4 mammary gland were treated as follow:

Rehydration

1) Immerse slides in xylene for 5 minutes at room temperature. Repeat.
2) Immerse slides in 100% ethanol for 5 minutes at room temperature. Repeat.
3) Immerse slides in 90% ethanol for 3 minutes at room temperature.
4) Immerse slides in 80% ethanol for 3 minutes at room temperature.
5) Immerse slides in 70% ethanol for 3 minutes at room temperature.
6) Rinse slides briefly with 1x TBS for 5 minutes.

Permeabilization

1) Dilute Proteinase K 1:100 in dH_2O.
2) Cover the specimen with 100ul of Proteinase K solution and incubate at room temperature for 20 minutes.
3) Rinse slides with 1x TBS for 5 minutes.

Quenching

1) Dilute 30% H_2O_2 1:10 in methanol.
2) Cover the specimen with 3% H_2O_2 incubate at room temperature for 5 minutes.
3) Rinse slides with 1x TBS for 5 minutes.

Equilibration

Cover the specimen with 100 ul TdT Equilibration Buffer. Incubate at room temperature for 30 minutes. Prepare the Labeling Reaction Mixture in last 5 minutes.

Labeling reaction

1) Prepare 1 ul TdT Enzyme to 39 ul TdT Labeling Reaction Mix for each sample.
2) Blot the TdT Equilibration Buffer from the specimen.
3) Immediately apply 40 ul of TdT Labling Reaction Mix onto each apecimen and cover with a coverslip.
4) Place slides in a humidified chamber and incubate at room temperature for 1.5 hours.

Termination of labeling reaction

1) Remove coverslip and Rinse slides with 1x TBS for 5 minutes.
2) Cover the entire specimen with 100 ul of stop buffer. Incubate at room temperature for 5 minutes.
3) Rinse slides with 1x TBS for 5 minutes.

Blocking

Cover the specimen with 100 ul of Blocking Buffer. Incubate at room temperature for 5 minutes.

Detection

1) Dilute the 25x Conjugate 1:25 in Blocking Buffer (mix 4 ul 25x Conjugate with 96 ul Blocking Buffer per specimen).
2) Blot the Blocking Buffer from the specimen and apply 100 ul of diluted 1x Conjugate to the specimen.
3) Place slides in a humidified chamber and incubate at room temperature for 30 minutes.
4) Rinse slides with 1x TBS for 5 minutes.

Development

1) Prepare working DAB solution by adding 4 ul DAB solution 1 to 116 ul DAB solution 2 (1:30 dilution).

2) Cover the entire specimen with 100 ul DAB solution and incubate at room temperature for 15 minutes.

Counterstain

1) Cover the specimen with 100 ul of Methyl Green Counterstain solution.
2) Incubate at room temperature for 3 minutes.
3) Draw off the counterstain and place in a Coplin jar slide hoder.
4) Dip slides 2-4 times into 100% ethanol.
5) Repeat using fresh 100% ethanol.
6) Dip slides 2-4 times into 100% histosol.
7) Mount a glass coverslip using mounting media over the specimen.

4.1.9 Immunofluorescent staining

1) Paraffin embedding tumor tissue slides from #4 mammary gland were immersed into 100% histosol for 2 times, 5 minutes each.
2) Follow by 100%, 90%, 80% ethanol and H_2O for 5 minutes each.
3) Rinse tissue specimens 1 time in PBS 1x.
4) Antigen unmasking in 95ºC Tris-EDTA buffer for 20 min.
4) Permeabilized in PBS 1x containing 1% Triton X-100 for 1 hour.
5) Block in BSA 5% for 1 hour.
6) Incubate primary antibody (Rabbit anti-Ki67, IHC-00375, 1:500, Bethyl; Rabbit anti-pEIF2α, #3597s, 1:500, CST; Rabbit anti-EIF2α, #9722s, 1:500, CST; Rabbit anti-Ecad, sc-7870, 1:500, Santa Cruz; Rabbit anti-CD31, ab-28364, 1:250, Abcam) in BSA 5% at 4ºC for overnight.
7) Rinse 3 times in PBS 1x, 5 minutes each.
8) Incubated with secondary antibodies in PBS 1x for 2 hours.
9) Stain nuclei with Hoechst dye diluted in PBS 1x for 10 minutes.
10) Wash with PBS 1x for 2 times, 5 minutes each.
11) Mount coverslip with Prolong Gold antifade.
12) Acquire images using fluorescence microscope or inverted laser confocal fluorescence microscopy

4.1.10 Mice tumor tissues protein extraction

Solutions and reagents

1) RIPA buffer

150 mM NaCl

1.0% NP-40 or 0.1% Triton X-100

0.5% sodium deoxycholate

0.1% SDS (sodium dodecyl sulphate)

50 mM Tris-HCl, pH 8.0

Protease inhibitor cocktail (Roche, 11873580001)

PhosSTOP (Roche, 04906837001).

2) Loading buffer

4% SDS

10% 2-mercaptoethanol

20% glycerol

0.004% bromophenol blue

0.125 M Tris-HCl

Protocol

1) Mince the tumor tissues which from #1 mammary gland in ice-cold RIPA buffer.

2) Centrifuge 10000 rpm/min for 10 minutes in a eppendorf tube at 4°C.

3) Gently remove the supernatant and place in a fresh tube on ice, discard the pellet.

4) Remove a small volume of lysate to perform protein quantification assay by BCA protein assay kit (Thermo, USA). Determine the protein concentration and volume for each cell lysate.

5) Add 6:1 volume of Loading buffer.

6) To reduce and denature samples, boil each cell lysate in sample buffer at 100°C for 5 min. Lysates can be stored at -80°C.

4.1.11 Western blot

Solutions and reagents

1) Running buffer

25 mM Tris base

190 mM glycine

0.1% SDS

2) Transfer buffer

25 mM Tris base

190 mM glycine

20% ethanol

3) Blocking buffer

3–5% milk in PBST 1x buffer.

4) Washing buffer

PBST 1x buffer

TBST 1x buffer

Loading and running the gel

1) Prepare the SDS-PAGE gel: the percentage required is dependent on the size of the protein of interest. Gradient gels can also be used.

2) Load equal amounts of protein into the wells of the gel, along with molecular weight marker. Load 20–30 ug of total protein from cell lysate or tissue homogenate.

3) Run the gel for 1–2 h at 100 V.

Transferring

Prepare the Gel-to-Membrane stack. The membrane can be nitrocellulose (0.45 μm pore size). Transfer for 1-2 h at 100V. Membrane will be checked using Red Ponceau staining before the blocking step.

Antibody Incubation

1) Block the membrane for 1 h at room temperature.

2) Incubate the membrane with primary antibodies (Rabbit anti-Bcl2, 1:500, Abcam, ab59348; Rabbit anti-IGFBP1, 1:1000, Abcam, ab181141; Rabbit anti-GAPDH, 1: 5000, Sigma, G9545; Rabbit anti-pAKT, 1:1000, CST, #4060; Rabbit anti-AKT, 1:1000, CST, #9272; Rabbit anti-pFoxO1, 1:1000, CST, #84192; Rabbit anti-FoxO1, 1:1000, CST, #2880; Rabbit anti-pAMPK, 1:1000, CST, #2535; Rabbit anti-AMPK, 1:1000, CST, #2532; Rabbit anti-pmTOR, 1:1000, CST, #2971; Rabbit anti-mTOR, 1:1000, CST, #2972) in 5% BSA overnight at 4°C.

3) Wash the membrane in PBST/ TBST 1x for 3 times, 5 min each.

4) Incubate the membrane with the horseradish peroxidase-conjugated secondary antibodies (1:10000) in PBST/ TBST 1x at room temperature for 2 h.

5) Wash the membrane in 3 times of PBST/ TBST 1x, 5 min each.

Signal development

1) Remove excess reagent and cover the membrane with ECL in transparent plastic wrap.

2) Acquire images using Imager-600 for chemiluminescence.

4.1.12 Total RNA extraction from mice tissues

Solutions and regents

1) Trizol reagent (Sigma, T9424, USA)
2) Chloroform
3) Isopropanol
4) 75% ethanol
5) RNase free H_2O

Protocol

1) Homogenize #1 mammary gland tumor or lung tissues from right side middle lobe in 1ml Trizol, with metal beads at 1000 times/min.
2) Incubation 5 minutes at room temperature. Pre-cold the centrifuge.
3) Add 200 ul chloroform.
4) Vortex 15 seconds.
5) Incubation 5 minutes at RT.
6) Centrifuge at 12000 rpm, 15 minutes at 4ºC.
7) Take aquous upper phase (V=600ul) to a new tube.
8) Add 500 ul isopropanol.
9) Incubation 10 minutes at RT.
10) Centrifuge at 12000 rpm, 10 minutes at 4ºC.
11) Checking the precipitation at the bottom of the tube, remove supernatant.
12) Add 1ml 75% ethanol, vortex (or keep at -80ºC).
13) Centrifuge at 7500 rpm, 5 minutes at 4ºC.
14) Remove supernatant, dry the pellet 10 minutes.

15) Add 50 ul RNase free H_2O, mix gently.

16) Incubation 10 minutes at 55ºC.

17) Aliquote and keep at -80ºC.

18) Check quality and quantity: Nanospect was used to measure RNA concentration and ratio of OD260/280(>1.7).

4.1.13 Reverse transcription

1) Add 0.5 ul Oligo-dT 200 ug/ml (Sigma, O4387, USA).

2) Add 1 ul 10 mM dNTP.

3) Add RNA 1ug (volume depends on RNA concentration).

4) Add H_2O up to 12 ul.

5) Warm 5 minutes at 65ºC, then 5ºC at 4ºC.

6) Add 4 ul First Strand Buffer 5X, 0.5 ul DTT 0.1 M, 0.5 ul Superscript II Reverse transcriptase (Sigma, 18090050, USA). 3 ul H_2O.

7) Incubation 50 minutes at 42ºC.

8) Inactivation the reaction at 72ºC for 15 minutes.

9) Keep cDNA in -80ºC.

4.1.14 Quantitative PCR

1) Mouse cDNA samples were diluted 1:10 for 50 ul total volume.

2) Mix 10 ul of 100 mM sense primer and 10 ul of 100 mM antisense primer into 80 ul H_2O.

3) Use the most highly expressed tissue sample cDNA to make standard curve, diluted as 1: 10, 1:20, 1:50, 1:100, 1:200, 1:500.

4) Add 8 ul SYBR GreenI mix (SYBR GreenI, H_2O and primer mix) and 2 ul cDNA by electronic pipettors.

5) Add 8 ul SYBR GreenI mix (SYBR GreenI, H_2O and primer mix) and 2 ul standard solution by electronic pipettors.

6) The qPCR step was conducted following the instructions on the SYBR Green kit (Sigma, S4438, USA). Data were normalized to GAPDH or 36b4 expression.

	Forward	Reverse
PyMT	CGGCGGAGCGAGGAACTGAGGAGAG	TCAGAAGACTCGGCAGTCTTAGGCG
Cd36	GATGTGGAACCCATAACTGGATTCAC	GGTCCCAGTCTCATTTAGCCACAGTA
Pparα	AGGAAGCCGTTCTGTGACAT	TTGAAGGAGCTTTGGGAAGA
Aco	CCCAACTGTGACTTCCATT	GGCATGTAACCCGTAGCACT
Acc1	GACAGACTGATCGCAGAGAAAG	TGGAGAGCCCCACACACA
Acc2	CCCAGCCGAGTTTGTCACT	GGCGATGAGCACCTTCTCTA
Ndufb5	CTTCGAACTTCCTGCTCCTT	GGCCCTGAAAAGAACTACG
Sdha	GGAACACTCCAAAAACAGACCT	CCACCACTGGGTATTGAGTAGAA
Sdhc	GCTGCGTTCTTGCTGAGACA	ATCTCCTCCTTAGCTGTGGTT
Cox2	AATTAGCTCCTTAGTCCTCT	CTTGGTCGGTTTGATGTTAC
Cox5b	AAGTGCATCTGCTTGTCTCG	GTCTTCCTTGGTGCCTGAAG
Atp5b	GGTTCATCCTGCCAGAGACTA	AATCCCTCATCGAACTGGACG
Hsp10	CTGACAGGTTCAATCTCTCCAC	AGGTGGCATTATGCTTCCAG
Hsp60	ACAGTCCTTCGCCAGATGAGAC	TGGATTAGCCCCTTTGCTGA
Clpp	CACACCAAGCAGAGCCTACA	TCCAAGATGCCAAACTCTTG
Phb	TCGGGAAGGAGTTCACAGAG	CAGCCTTTTCCACCACAAAT
Phb2	CAAGGACTTCAGCCTCATCC	GCCACTTGCTTGGCTTCTAC
Mct1	GCATTTCCCAAATCCATCAC	CGGCTGCCGTATTTATTCAC
Mct4	GGTCAGCGTCTTTTTCAAGG	CCGTGGTGAGGTAGATCTGG
Ldha	AGACAAACTCAAGGGCGAGA	CAGCTTGCAGTGTGGACTGT
Ldhb	TAAGCACCGTGTGATTGGAA	AGACTCCTGCCACATTCACC
Xbp1	GGTCTGCTGAGTCCGCAGCAGG	AGGCTTGGTGTATACATGG
ATF4	CCTTCGACCAGTCGGGTTTG	CTGTCCCGGAAAAGGCATCC
ATF6	CTGTGCTGAGGAGACAGCAG	CTTGGGACTTTGAGCCTCTG
Psma1	TGCGTGCGTTTTTGATTTTAGAC	CCCTCAGGGCAGGATTCATC
Psmb1	CGTTGAAGGCATAAGGCGAAAA	TTCCACTGCTGCTTACCGAG
Psmd1	GTGATAAAACACTTTCGAGGCCA	TGAATGCAGTCGTGAATGACTT
GAPDH	ACTGGCATGGCCTTCCGTGTTC	TCTTGCTCAGTGTCCTTGCTGG
36b4	AGATTCGGGATATGCTGTTGG	AAAGCCTGGAAGAAGGAGGTC

Table 4.2 Primers used for real-time quantitative-PCR.

4.1.15 Data analysis

The quantification of hyperplasia and neoplastic lesions area, tumor necrosis area, TUNEL staining cells, Ki-67 staining cells, pEIF2α relative intensity and western blot were performed by Image J 1.51n. Statistical analysis was performed by Graphpad Prism 7.

Part II Techniques related to results part II

4.2.1 Construction of aP2-mMMP11-IRES-GFP expression plasmid

1) The mouse MMP11 cDNA sequence comes from the pSG5-mMMP11 expression vector already available in the lab (Lefebvre O. unpublished).

2) The aP2-mMMP11-polyA construct was available in the laboratory. Briefly, the β globin intron-mMMP11 unit was amplified by PCR using specific primers: forward primer 5'-GAGAC GGCCG TGGATC GATCC GAGAA CTTCA GGGGA GT-3'; reverse primers 5'-GAGAC GGCCG ATAGG CCGGC CTATC CTGCA GGCTT AGGCG CGCCT CAGCG GAAAG TATTG GCAGG CTCAG CACA-3' and 5'-GAGAC GGCCG TTACT TGTCG TCATG CTCTT GTAGT CGCGG AAAGT ATTGG CAGGC TCAGC ACA-3' and digested using the restriction enzyme EagI and inserted into the unique NotI site of the pBS-aP2-polyA plasmid.

3) The IRES-GFP unit was obtained by PCR amplification from the pMX-PIE-PL plasmid (Rousseau A. unpublished) using the following primers: forward primer MCR851: (GAGAG GCGCG CCGCC CCCCC CCCTA ACGTT ACTGG CCGAAG CCGC) and reverse primer MCR852: (AAGAC CTGCA GGGGCC GGCCG TCGAC TTACTT GTACA GCTCG TCCAT GCCGA). PCR reaction program follow: 98.0℃ denature for 10 s; 60.0℃ annealing for 10 s; 72.0℃ extension for 30 s; and 26 cycles in total. Then PCR product was purified follow the protocol from the kit (NucleoSpin® Plasmid).

4) Both the amplified IRES-GFP unit and the aP2-mMMP11-polyA plasmid were cut by using the restricted enzymes AscI and FseI, and ligated by T4 ligase and 10*Lig mix in 4℃ overnight. The ligated construct was then confirmed by Asc I, Fse I and Sal I enzymes digestion. After transformation of E. Coli-DH5α bacterial, 2 positive clones were sequenced.

5) The plasmid aP2-mMMP11-IRES-GFP-polyA was linearized by digestion with the restriction enzyme Xho I. Then this plasmid was diluted at 100ng/ul and send to the ICS animal platform to make transgenic mouse. Briefly, this plasmid was microinjected into fertilized mice oocytes to be randomly integrated into the mouse genome. The animal platform provided founder mice tails for genotyping.

4.2.2 Mice genotyping

1) Isolation of mouse tail genomic DNA and preparation of PCR reaction mix is the same protocol as part I.

2) DNA primers used to genotype ap2-mMMP11-IRES-GFP-polyA mice were designed as follow: MMP-11 forward primer: 5′- CGGTTTCCACCATCCGAGGA-3′. MMP-11 reverse primer: 5′- GTGGAAACGCCAATAGTCTCC-3′. MMP-11gene PCR reaction: 94ºC for 1 minute, 60ºC for 20 seconds, 72ºC for 1 minute, 33 cycles.

3) PCR products were separated by electrophoresis in 3 % agarose gel.

4.2.3 3T3-L1 cell culture and differentiation

1) 3T3-L1 mouse cell line (ATCC, USA) was suspended in DMEM medium with 10% fetal calf serum and cultured in a humid incubator with 95% O2 and 5% CO2 at 37 °C.

2) When cells reached 80-90% confluency, performed different plasmid DNA transient transfection by using JetPEI.

3) Next day, change fresh medium containing 10 µg/ml insulin, 0.5 mol/l dexamethasone, and 0.5 mmol/l methylisobutylxanthine for maintain 2 days.

4) Medium was replaced every 2 days containing 10 µg/ml insulin only.

5) Cells were differentiated into adipocyte 10-12 days when lipid droplets appear.

4.2.4 Preparation of MEFs

1) Step 2-10 performed at the clean bench.

2) Sacrifice pregnant female (E12.5-E15.5). Spray with 70% ethanol and open the abdomen. Take out uteri into sterile cold 1x PBS.

3) Remove each embryo and place directly into a 6-well plate containing 3 ml PBS on ice.

4) Remove the heads and viscera from each embryo with forceps. Save a little piece of tissue for genotyping (300 ul yolk sac lysis buffer + 3 ul proteinase K 20mg/ml). Then transfer tissue to 6 cm plate containing 5 ml trypsin/ EDTA.

5) Mince embryos well using clean razor blades, transfer tissue and trypsin into 15 ml tube, vortex.

6) Put tube in 37ºC water bath for 5 minutes. Vortex and settle for ~1 minute.

7) Transfer supernatant to a new 15 ml tube.

8) Add 5ml fresh trypsin/ EDTA to resuspend again the pellet in step-6.

9) Put tube in 37ºC water bath for 5 minutes. Vortex again and settle for ~1 min. Transfer supernatant to the tube in step-7.

10) Spin 3 minutes at 1000 rpm.

11) Aspirate supernatant. Resuspend the pellet in 5 ml DMEM +15% FBS. Add into a new 10 cm dish, add 5 ml fresh DMEM + 15% FBS. Put in incubator.

4.2.5 Differentiation of MEFs

Same protocol as 4.2.3.

4.2.6 MEFs protein extraction

1) After lipid droplets appear in MEFs. Cells in 60 mm size plate were lysis in 300 ul IP-Flag buffer (50 mM Tris PH 7.5, 150 mM NaCl, 1 mM EDTA, 1% Triton X-100) on ice for 15 min, which containing protease inhibitor cocktail (Roche, Swissland).

2) Take out 20 ul protein sample to a new tube as cell total protein sample, add 20 ul protein loading blue. Sonication 1 s at 30% intensity. The left sample centrifuge 10000 rpm for 20 minutes at 4ºC.

3) Take supernatant to a new tube as cytoplasm protein. Take out 50 ul protein sample to a new tube as cell cytoplasm protein sample, add 20 ul protein loading blue.

4) Pallet was lysis in 300 ul RIPA buffer (formula as part II) on ice for 5 minutes as nucleus protein. Sonication 1 s at 30% intensity. Take out 50 ul protein sample to a new tube as cell nucleus protein sample, add 20 ul protein loading blue.

5) All samples stock in -20ºC until use.

4.2.7 Mice tissues and cultured-cell protein extraction

1) Mice tissues protein extraction is the same protocol as 4.1.10.

2) Cell lysis by IP-Flag buffer containing protease inhibitor cocktail.

4.2.8 Semi-quantitative PCR

1) Mice tissues (BAT, mWAT, gWAT and muscle) RNA extraction is the same protocol as 4.1.12.

2) Estimate concentration of RNA using Nanospect.

3) 1 ug of RNA used for reverse transcription following RT step, which is the same protocol as 4.1.13.

4) 1 ul of cDNA was used to PCR reaction.

cDNA primers sequence were designed as follow: b-MMP11 forward primer: 5′-GGATCCACTAGTTCTAGAGC-3′, b-MMP11 reverse primer: 5′-GGAATTCGCCCTATAGTGAG-3′. GFP forward primer: 5′-TACAACTACAACAGCCACAA-3′, GFP reverse primer: 5′-CGGATCTTGAAGTTCACCTT-3′.

5) PCR samples were loaded on a 3% agarose gel with ethidium bromide and checked on UV light.

4.2.9 Quantitative PCR

1) Same protocol as part 4.1.14.

2) b-MMP-11 forward primer: 5′-GGATCCACTAGTTCTAGAGC-3′; b-MMP-11 reverse primer: 5′-GGAATTCGCCCTATAGTGAG-3′. GFP forward primer: 5′-TACAACTACAACAGCCACAA-3′; GFP reverse primer: 5′-CGGATCTTGAAGTTCACCTT-3′. GAPDH forward primer: 5′-ACTGGCATGGCCTTCCGTGTTC-3′; GAPDH reverse primer: 5′-TCTTGCTCAGTGTCCTTGCTGG-3′.

4.2.10 Western blot

1) Same protocol as part 4.1.11.

2) Primary antibodies: Mouse anti-MMP11 (5ST-4A9, 1:5000, purified in the lab), rabbit anti-GFP (2A3, 1:5000, Merck), mouse anti-Actin (2D7, 1:5000, Euromedex).

4.2.11 HE staining

Same protocol as 4.1.7.

4.2.12 Whole mount mammary fat pad immunofluorescent staining

1) Mice fresh mammary gland fat tissues were fixed by 4% PFA for 2 hours in room temperature.

2) Then permeabilized in PBS 1x containing 1% Triton X-100 for 1 hour.

3) Block in BSA 5% for 1 hour.

4) Incubate primary antibody (Rabbit anti-GFP 2A3, 1:5000, Merck) in BSA 5% at 4ºC for overnight.

5) Rinse 3 times in PBS 1x, 5 minutes each.

6) Incubate with secondary antibody (ALEXA 488 anti-rabbit antibody) in PBS 1x for 2 hours.

7) Stain nuclei with Hoechst dye diluted in PBS 1x for 15 minutes.

8) Wash with PBS 1x for 2 times, 5 minutes each.

4.2.13 Immunohistochemistry

1) Paraffin embedding tissue slides were immersed into histosol: 2 changes, 5 minutes each.

2) 100% ethanol: 2 changes, 5 minutes each.

3) 95% ethanol: 2 changes, 5 minutes each.

4) Deionized water: 3 minutes.

5) PBS 1x: 5 minutes for 3 times.

6) Pre-warm the 0.01 M sodium citrate buffer for 3 minutes at 750 w in a plastic beaker in which one will put the slides.

7) Immerse the slides completely into the 0.01 M sodium citrate buffer and expose to microwave treatment for 5 minutes to retrieve antigens. Cool the slides after boil in the cold room for 30 minutes.

8) Wash sections in PBS 1x 5 minutes for 3 times.

9) Treat the sections with 3% H_2O_2 in PBS 1x for 30 minutes to inactivate endogenous peroxidase.

10) Rinse the sections in PBS 1x 5 minutes for 3 times.

11) Identify the position of the sections with Dakopen.

12) Incubate for 30 minutes with 5% NGS in PBS 1x.

13) Incubate with first antibody (Rabbit anti-GFP 2A3, 1:5000, Merck) overnight at 4ºC in humid chamber.

14) Rinse with PBS 1x 5 minutes for 3 times.

15) Incubate with the secondary antibody (biotinylated anti-rabbit) diluted at 1:400 in PBS 1x for 1 hour at room temperature in the humid chamber.

16) Rinse with PBS 1x 5 minutes for 3 times.

17) Incubate with Vectastain ABC reagent (prepared 30 min before use) for 30 minutes at room temperature.

18) Rinse with PBS 1x 5 minutes for 3 times.

19) Reveal the peroxidase activity by incubating the slides with the Peroxidase substrate solution (DAB) during 2-5 minutes, check under the microscope, stop in H_2O.

20) Rinse the slides with distillate water 10 minutes.

21) Mounting with Permount.

4.2.14 Orthotopic tumor model of E0771 cells

1) The experiment procedure was approved by the Ethical Committee. E0771 murine breast cancer cell line (C57BL/6) was suspended in RPMI 1640 medium supplemented with 10 mmol/L HEPES and 10% fetal calf serum and cultured in a humid incubator with 95% O2 and 5% CO2 at 37°C.

2) Cells were digested by Trypsin-EDTA (0.25%) and resuspended in PBS 1x. Cell concentration was measured and adjusted.

3) MMP-11 transgenic and wildtype control mice (C57BL/6N background, 6-8/per group) were anesthetized by isoflurane, $2x10^5$ cells/100 ul were subcutaneously injected into both sides of #4 mammary gland fat pad.

4) Tumor measurement was performed twice a week by caliper. Tumor volume was calculated following the formula (4/3) x 3.14159 x (length/2) x (width/2) x (height/2).

4.2.15 Data analysis

Statistical analysis was performed by Graphpad Prism 7.

Part III Techniques related to results part III

4.3.1 Animals treatment

1) The study proposal was obtained from the Ethical Committee. Forty female MMTV-PyMT (FVB/N-Tg) mice (6 weeks old) were randomly divided into 4 groups, every group contain 10 mice. First group was treated with chemotherapeutic doxorubicin at concentration of 2 mg/kg. Second group was treated with ITPP at concentration of 2 g/kg. Third group was treated with doxorubicin and ITPP. Fourth group was treated with the same volume of 0.9 % NaCl as control.

2) The treatment starts at 6 weeks old by intraperitoneal injection during 4 weeks. ITPP was injected on Monday and Friday, doxorubicin was injected on Wednesday, and 0.9 % NaCl was injected on Monday, Wednesday, and Friday.

4.3.2 Tumor area measurement

Palpable tumor volume was measured twice a week by using caliper. Tumor area was calculated following the formula 3.14*length*width/4.

4.3.3 Whole mount carmine-alum staining

Same protocol as 4.1.5.

4.3.4 Lung RNA extraction

Same protocol as 4.1.12. RNA extraction from the right middle lobes of lung.

4.3.5 RT-qPCR

Same protocol as 4.1.14. PyMT and GAPDH primers are the same as Table 4.2.

4.3.6 Data analysis

Statistical analysis was performed by Graphpad Prism 7.

CHAPTER 5 Talk and Poster Presentations

Talk:

MMP-11 favors MMTV-PyMT mouse mammary gland tumors. (Speaker: Bing Tan. IGBMC Internal Seminar, Auditorium. Sep 21, 2017).

International conferences and poster presentations:

1) *Poster Presentation*. Adipocyte-Derived Matrix Metalloproteinase-11 Favors Mouse Breast Cancer Progression. Bing Tan, Amélie Jaulin, Nassim Dali-Youcef, Catherine-Laure Tomasetto. (8th International Conference on Tumor Microenvironment. June 10-14, 2018, Lisbon, Portugal).

2) *Poster Presentation*. Adipocyte specific expressing MMP-11 transgenic mouse promote breast tumor growth. Bing Tan, Amélie Jaulin, Fabien Alpy, Nassim Dali-Youcef, Catherine-Laure Tomasetto. (3rd International Cancer Symposium. Sep 25-27, 2017, Lyon, France).

3) EuCC Meeting 2017 in Basel. (European Cancer Center. Basel, Freiburg, Strasbourg. May 12, 2017, Basel, Switzerland).

4) 40 ème anniversaire de la Société International de Sénologie, (May 9-11, 2016, Strasbourg, France).

CHAPTER 6 Résumé en Français

La métalloprotéase matricielle-11 facilite la progression des tumeurs de la glande mammaire murine

Résumé

Dans la plupart des pays industrialisés, le cancer du sein est la principale cause de décès chez les femmes. Le microenvironnement tumoral (TME) joue un rôle important dans la progression du cancer du sein. Le TME est un tissu complexe composé d'une matrice extracellulaire remaniée, de fibroblastes, de cellules inflammatoires et endothéliales. Récemment un nouveau composant cellulaire du TME a été identifié. Il est formé par des adipocytes modifiés situés en regard de cellules cancéreuses appelées "adipocytes associés au cancer" (CAA). Ces constituants ajoutent à la complexité du TME. La protéase matricielle Matrix Metalloproteinase-11 (MMP-11) est une protéine du TME, elle est sécrétée par les «fibroblastes associés au cancer» (CAF) au centre de la tumeur et par les CAA à la périphérie de la tumeur (le front d'invasion). Soutenant l'idée que la MMP-11 contribue à la progression tumorale, des études antérieures ont montré qu'une expression élevée était associée à une survie sans récidive plus courte des patientes atteintes d'un cancer du sein. Cependant, le mécanisme d'action spécifique de cette protéase est resté mal compris. Des études plus récentes ont montré que la MMP-11 est un régulateur négatif du développement du tissu adipeux et qu'elle module le métabolisme énergétique. Ces observations suggéraient que l'expression de MMP-11 dans le TME pourrait participer directement à la progression de la tumeur en modulant le métabolisme du tissu adipeux au profit des cellules cancéreuses. Cependant, la façon dont la MMP-11 agit, notamment à l'interface entre les cellules cancéreuses du sein et les CAAs, reste largement inconnue. Pour l'étudier, nous avons développé des modèles précliniques de cancer de la glande mammaire chez la souris par génie génétique. Tout d'abord, des souris déficientes (perte de fonction-LOF) ou surexprimant MMP-11 (Gain de Fonction-GOF) ont été croisées avec un modèle génétique de tumeurs mammaires (MMTV-PyMT). Des résultats cohérents ont été obtenus en utilisant les deux modèles. La MMP-11 favorise la progression tumorale précoce, en augmentant la prolifération et en réduisant l'apoptose des cellules cancéreuses. De plus, l'expression de la MMP-11 a été associée à un changement métabolique dans la tumeur, à une altération significative de l'Unfolded Protein Response mitochondriale (UPR^{mt}) et à une

activation du stress du réticulum endoplasmique (UPR^{ER}). Ces données confortent l'idée selon laquelle la MMP-11 contribue à une réponse métabolique adaptative favorisant la croissance du cancer. Deuxièmement, pour aborder directement la fonction de la MMP-11 produite par le tissu adipeux sur la progression du cancer, nous avons généré une lignée de souris transgénique (appelée aP2-MMP11-IRES-GFP) dans laquelle l'expression de MMP-11 est contrôlée par un promoteur spécifique du tissu adipeux. L'implantation directe de cellules cancéreuses syngéniques dans le coussinet mammaire de ces souris a montré que l'expression de la MMP-11 favorisait la croissance tumorale. Finalement, nos données soutiennent le concept selon lequel l'expression de MMP-11 par les adipocytes associés au cancer (CAA) contribuerait à une réponse métabolique adaptative favorisant la croissance du cancer. Ils renforcent aussi l'intérêt que représente la MMP-11 comme cible pour le traitement du cancer.

Introduction

Le cancer du sein est la principale cause de décès chez les femmes (Polyak and Metzger Filho, 2012). Outre les cellules cancéreuses, le microenvironnement tumoral (TME) joue un rôle important dans la progression du cancer du sein (Hanahan and Coussens, 2012). Les adipocytes sont une composante cellulaire émergente du TME, ils communiquent avec les cellules cancéreuses par contact direct mais également indirectement par la voie paracrine (Rio et al., 2015). La métalloprotéinase matricielle 11 (MMP-11), également appelée stromélysine-3, est une protéine sécrétée par les cellules stromales présentes dans les cancers invasifs. Sa présence est associée à un mauvais pronostic chez ces patients (Rouyer et al., 1994; Basset et al., 1997). Des études ont montré que des niveaux élevés de MMP-11 réduisaient l'adipogenèse in vitro et chez la souris (Andarawewa et al., 2005). En fait, MMP-11 empêche la différenciation des adipoblastes en adipocytes et favorise la dédifférenciation des adipocytes en cellules fibroblastiques. Une étude récente du groupe a montré que la MMP-11 est un régulateur métabolique agissant au niveau de l'organisme entier. La surexpression de la MMP-11 est associée à une maigreur constitutionnelle et à une protection contre l'obésité induite par un régime gras. En revanche, la perte d'expression de la MMP-11 est associée à un gain de poids et à un syndrome métabolique (Dali-Youcef et al., 2016). Dans le contexte du cancer du sein, il est important de mentionner que l'expression de la MMP-11 marque des populations cellulaires distinctes du TME.

Au centre de la tumeur, les cellules fibroblastiques sont les principales composantes cellulaires du TME. Ces cellules appelées «fibroblastes associés au cancer» (CAF) expriment des taux très élevés de MMP-11. En revanche, dans la périphérie de la tumeur, les adipocytes représentent la principale composante cellulaire du TME. Ceux-ci sont appelés "adipocytes associés au cancer" (CAA). Contrairement aux adipocytes mammaires situés à distance des cellules cancéreuses qui n'expriment pas la MMP-11, les CAAs situés à leur voisinage expriment des taux élevés de MMP-11, ont une réduction de la taille des gouttelettes lipidiques et ont tendance à adopter une morphologie allongée (Motrescu and Rio, 2008). Ces observations soutiennent l'idée que MMP-11 agit à différents niveaux dans le TME. D'abord au stade précoce où les cellules cancéreuses se développent au sein du stroma normal. L'expression de la MMP-11 par les CAAs participerait directement au processus d'invasion (Andarawewa et al., 2005). Puis, au niveau de la lésion tumorale établie où les fibroblastes sont le type de cellules du TME prédominant, l'expression de la MMP-11 par les CAF promeut la survie des cellules cancéreuses (Andarawewa et al., 2003). Cependant, comment la MMP-11 agit à l'échelle moléculaire n'est pas encore bien compris. Notamment le rôle de MMP-11 sur la progression tumorale n'a pas été abordé sous un angle métabolique. Dans cette étude, nous avons utilisé une série de modèles précliniques murins de gain-de-fonction et de perte de fonction pour examiner le rôle de la MMP-11 sur la croissance et le métabolisme des tumeurs mammaires. Nous avons croisé ces souris avec un modèle génétique de tumeurs mammaires spontanées : la souche génétique MMTV-PyMT (Guy et al., 1992; Lin et al., 2003). Les femelles MMTV-PyMT développent des tumeurs mammaires palpables qui se métastasent dans les poumons (Fluck and Schaffhausen, 2009). De plus, pour étudier spécifiquement la fonction de la MMP-11 libérée par les CAAs, nous avons généré un nouveau modèle de souris transgénique surexprimant la MMP-11 (aP2-mMMP11-IRES-GFP-polyA). Ce modèle de souris est basé sur l'utilisation du promoteur spécifique du tissu adipeux Fabp4 / aP2 (Graves et al., 1991). Ensuite, nous injecté des cellules de cancer du sein E0771 dans le coussinet adipeux de la glande mammaire, pour mesurer la croissance tumorale.

Résultats

MMP-11 favorise la progression des tumeurs mammaires

Deux modèles génétiques de MMP-11-GOF et de -LOF constitutifs avaient déjà été développés et étudiés dans le groupe (Dali-Youcef et al., 2016). Une lignée de souris transgénique (K14-MMP11^{Tg}) qui exprime MMP-11 dans les cellules épithéliales du corps entier constitue le modèle GOF et la lignée de souris knock-out pour la MMP-11 (MMP11^{KO}), le modèle LOF. J'ai croisé ces souris avec des souris transgéniques MMTV-PyMT, l'incidence des tumeurs et la croissance ont été examinées. En ce qui concerne l'incidence et la croissance des tumeurs, des résultats cohérents ont été obtenus, en présence d'une expression élevée de MMP-11, l'incidence des tumeurs n'a pas été significativement modifiée, mais le développement tumoral a été accéléré. Le nombre de lésions pré malignes et les volumes tumoraux sont augmentés chez les souris double transgénique PyMT^{Tg} :: MMP11^{Tg} par rapport aux souris PyMT^{Tg} transgéniques simples. La lignée K14-MMP11^{Tg} n'a pas développé de lésions tumorales. Un phénotype réciproque a été observé dans le modèle LOF, une incidence tumorale retardée, une réduction du nombre de lésions pré malignes et une réduction du volume tumoral pour les animaux PyMT^{Tg} :: MMP11^{KO} par rapport aux PyMT^{Tg}. Il est à noter que l'effet promoteur de la MMP-11 sur la croissance tumorale est limité au stade précoce, lorsque les nodules tumoraux ont atteint un volume supérieur à 0.5 cm^3, aucune différence significative de croissance n'a été observée. Pour mieux comprendre le mécanisme d'action de la MMP-11, la prolifération (coloration Ki67), la nécrose (HE) et l'apoptose (TUNEL et Bcl-2) ont été quantifiées. La surexpression de la MMP-11, se traduit par une diminution des zones de nécrose et une réduction du nombre de cellules en apoptose. En revanche dans les souris KO, la nécrose et l'apoptose sont accrues. A un stade plus avancé du développement tumoral, aucune différence significative dans le nombre de cellules apoptotiques n'a été observée. La prolifération des cellules tumorales a été augmentée et réduite respectivement en présence et en l'absence de MMP-11. L'angiogenèse n'a pas été modifiée. Au total, ces résultats montrent que la MMP-11 est associée à une prolifération et une survie accrue des cellules tumorales mammaires. Ils soulignent un rôle spécifique de la MMP-11 au début de la progression tumorale. Pour étudier les mécanismes moléculaires impliquant la MMP-11, la voie de signalisation IGF1 / AKT / FoxO1 a été étudiée. Des résultats antérieurs avaient identifié la protéine liant le IGFBP-1 comme substrat pour MMP-11 (Mañes et al.,

1997). Des études métaboliques ont montré que la MMP-11 active cet axe de signalisation en augmentant la capacité d'IGF1 d'activer son récepteur (Dali-Youcef et al., 2016). De manière cohérente, dans le contexte des tumeurs PyMT, l'expression de MMP-11 est associée à l'activation de cette voie de signalisation. De plus, nous avons observé un changement métabolique dans ces tumeurs. Dans les souris qui surexpriment la MMP-11, la glycolyse aérobie est augmentée ainsi que le renouvellement lipidique, ce qui suggère que MMP-11 promeut l'effet Warburg inverse et favorise l'utilisation des lipides comme source d'énergie et le lactate comme source d'énergie complémentaire. De manière étonnante, les souris MMP-11^{Tg} et MMP-11^{KO} ont des mitochondries morphologiquement altérées (Dali-Youcef et al., 2016). L'altération fonctionnelle des mitochondries est un phénomène courant dans les cellules cancéreuses. Cependant, dans cette étude, nous avons montré que les altérations mitochondriales trouvées dans les souris MMP-11^{Tg} n'entravaient pas la croissance tumorale. Afin de mieux caractériser les altérations mitochondriales associées à la surexpression et à la perte de MMP-11, nous avons étudié l'Unfolded protein response mitochondriale (UPR^{mt}). L'UPR^{mt} favorise la survie cellulaire et la régénération du réseau mitochondrial pour maintenir les fonctions cellulaires. De manière intéressante, nous avons observé respectivement une augmentation et une diminution de l'expression de certains gènes cibles de l'UPR^{mt} (la voie de signalisation CHOP→ATF5→ HSP60, HSP10, CLPP, LONG) dans les tumeurs MMP-11^{KO} et MMP-11^{Tg}. Il est intéressant de noter que des données sur des cellules de cancer du sein ERα positives ont montré que l'accumulation de protéines non repliées (misfolded) dans l'espace intermembrannaire mitochondrial (EIM) n'active pas l'axe CHOP de l'UPR^{mt}, mais active une voie UPR^{mt} distincte impliquant le facteur NRF1 et le protéasome (Papa and Germain, 2011). Des expériences en cours dans notre laboratoire permettront de trouver quelle voie UPR^{mt} est activée dans notre modèle de souris double transgénique PyMT^{Tg} :: MMP11^{Tg}. Aussi, nous avons observé, une augmentation et une diminution de l'expression des gènes du stress du reticulum endoplasmique (UPR^{ER}) respectivement dans les tumeurs de souris PyMT^{Tg} :: MMP11^{Tg} et PyMT^{Tg} :: MMP11^{KO} , un processus connu pour favoriser la croissance tumorale (Shen et al., 2018).

La MMP-11 produite par le tissu adipeux favorise la croissance de la tumeur mammaire

Pour montrer l'implication spécifique de la MMP-11 produite par les CAAs sur la progression tumorale, notamment son rôle modulateur du métabolisme tumoral. J'ai généré une nouvelle construction plasmidique dans laquelle un transcrit bi-cistronique portant les séquences codantes de MMP-11 et de la protéine fluorescente GFP est exprimé sous le contrôle du promoteur spécifique du tissu adipeux, le promoteur aP2 (Ross et al., 1990). Cette construction nommée aP2-MMP11-IRES-GFP a été utilisée pour générer une nouvelle lignée transgénique. Le gène aP2 (adipocyte protein 2), également appelé FABP4 (Fatty acid binding proein 4), est une protéine de transfert des acides gras principalement présente dans les adipocytes et les macrophages (Hertzel and Bernlohr, 2000). La construction a été testée in vitro durant la différenciation des adipoblastes et in vivo dans les organes des souris transgéniques. En mesurant l'expression de la GFP dans divers tissus de souris, nous avons trouvé que le transcrit MMP11-IRES-GFP était présent dans le tissu adipeux brun, le tissu adipeux blanc inguinal et mammaire mais absent du muscle. En écho aux études antérieures, le tissu adipeux est altéré chez les souris aP2-MMP11-IRES-GFP^{Tg}. Les adipocytes sont plus petits et les gouttelettes lipidiques plus nombreuses et plus petites. Nous n'avons pas eu le temps d'exploiter pleinement ce modèle, mais une expérience préliminaire a été faite en injectant des cellules tumorales mammaires syngéniques E0771 dans le coussinet adipeux mammaire de ces souris. Le volume des tumeurs est augmenté dans les MMP11-IRES-GFP^{Tg} par rapport au groupe témoin. Ce résultat confirme l'idée que la MMP-11 libérée par les CAAs favorise la croissance tumorale mammaire.

Conclusion

Ces études soutiennent le concept selon lequel, l'expression de la MMP-11, notamment par les CAAs, contribue à la croissance des tumeurs mammaires. MMP-11 agit à un stade précoce de la progression tumorale et module le métabolisme tumoral.

CHAPTER 7 Bibliography

Ahmad, A., Marshall, J.F., Basset, P., Anglard, P., and Hart, I.R. (1997). Modulation of human stromelysin 3 promoter activity and gene expression by human breast cancer cells. Int. J. Cancer *73*, 290–296.

Ahn, G.-O., and Brown, J.M. (2008). Matrix metalloproteinase-9 is required for tumor vasculogenesis but not for angiogenesis: role of bone marrow-derived myelomonocytic cells. Cancer Cell *13*, 193–205.

Ahokas, K., Lohi, J., Illman, S.A., Llano, E., Elomaa, O., Impola, U., Karjalainen-Lindsberg, M.-L., and Saarialho-Kere, U. (2003). Matrix metalloproteinase-21 is expressed epithelially during development and in cancer and is up-regulated by transforming growth factor-beta1 in keratinocytes. Lab. Investig. J. Tech. Methods Pathol. *83*, 1887–1899.

Aiken, A., and Khokha, R. (2010). Unraveling metalloproteinase function in skeletal biology and disease using genetically altered mice. Biochim. Biophys. Acta *1803*, 121–132.

Alaseem, A., Alhazzani, K., Dondapati, P., Alobid, S., Bishayee, A., and Rathinavelu, A. (2017). Matrix Metalloproteinases: A challenging paradigm of cancer management. Semin. Cancer Biol.

Alexander, C.M., Hansell, E.J., and Behrendtsen, O. (1996). Expression and function of matrix metalloproteinases and their inhibitors at the maternal-embryonic boundary during mouse embryo implantation. Development *122*, 1723–1736.

Allan, J.A., Docherty, A.J.P., Barker, P.J., Huskisson, N.S., Reynolds, J.J., and Murphy, G. (1995). Binding of gelatinases A and B to type-I collagen and other matrix components. Biochem. J. *309*, 299–306.

Amano, T., Kwak, O., Fu, L., Marshak, A., and Shi, Y.-B. (2005). The matrix metalloproteinase stromelysin-3 cleaves laminin receptor at two distinct sites between the transmembrane domain and laminin binding sequence within the extracellular domain. Cell Res. *15*, 150–159.

Andarawewa, K.L., Boulay, A., Masson, R., Mathelin, C., Stoll, I., Tomasetto, C., Chenard, M.-P., Gintz, M., Bellocq, J.-P., and Rio, M.-C. (2003). Dual stromelysin-3 function during natural mouse mammary tumor virus-ras tumor progression. Cancer Res. *63*, 5844–5849.

Andarawewa, K.L., Motrescu, E.R., Chenard, M.-P., Gansmuller, A., Stoll, I., Tomasetto, C., and Rio, M.-C. (2005). Stromelysin-3 is a potent negative regulator of adipogenesis participating to cancer cell-adipocyte interaction/crosstalk at the tumor invasive front. Cancer Res. *65*, 10862–10871.

Anderson, I.C., Sugarbaker, D.J., Ganju, R.K., Tsarwhas, D.G., Richards, W.G., Sunday, M., Kobzik, L., and Shipp, M.A. (1995). Stromelysin-3 is overexpressed by stromal elements in primary non-small cell lung cancers and regulated by retinoic acid in pulmonary fibroblasts. Cancer Res. *55*, 4120–4126.

Anglard, P., Melot, T., Guérin, E., Thomas, G., and Basset, P. (1995). Structure and promoter characterization of the human stromelysin-3 gene. J. Biol. Chem. *270*, 20337–20344.

Aprahamian, M., Bour, G., Akladios, C.Y., Fylaktakidou, K., Greferath, R., Soler, L., Marescaux, J., Egly, J.-M., Lehn, J.-M., and Nicolau, C. (2011). Myo-InositolTrisPyroPhosphate treatment leads to HIF-1α suppression and eradication of early hepatoma tumors in rats. Chembiochem Eur. J. Chem. Biol. *12*, 777–783.

Aras, A.B., Guven, M., Balak, N., Ayan, E., Uyar, S.B., and Elmaci, I. (2016). Evaluation of the Association Between Matrix Metalloproteinase 11 and Intervertebral Disc Disease. Turk. Neurosurg. *26*, 274–279.

Arcidiacono, B., Chiefari, E., Laria, A.E., Messineo, S., Bilotta, F.L., Britti, D., Foti, D.P., Foryst-Ludwig, A., Kintscher, U., and Brunetti, A. (2017). Expression of matrix metalloproteinase-11 is increased under conditions of insulin resistance. World J. Diabetes *8*, 422–428.

Ardi, V.C., Kupriyanova, T.A., Deryugina, E.I., and Quigley, J.P. (2007). Human neutrophils uniquely release TIMP-free MMP-9 to provide a potent catalytic stimulator of angiogenesis. Proc. Natl. Acad. Sci. U. S. A. *104*, 20262–20267.

Ardi, V.C., Van den Steen, P.E., Opdenakker, G., Schweighofer, B., Deryugina, E.I., and Quigley, J.P. (2009). Neutrophil MMP-9 proenzyme, unencumbered by TIMP-1, undergoes efficient activation in vivo and catalytically induces angiogenesis via a basic fibroblast growth factor (FGF-2)/FGFR-2 pathway. J. Biol. Chem. *284*, 25854–25866.

Arpino, V., Brock, M., and Gill, S.E. (2015). The role of TIMPs in regulation of extracellular matrix proteolysis. Matrix Biol. J. Int. Soc. Matrix Biol. *44–46*, 247–254.

Asano, T., Tada, M., Cheng, S., Takemoto, N., Kuramae, T., Abe, M., Takahashi, O., Miyamoto, M., Hamada, J.-I., Moriuchi, T., et al. (2008). Prognostic values of matrix metalloproteinase family expression in human colorectal carcinoma. J. Surg. Res. *146*, 32–42.

Atikuzzaman, M., Alvarez-Rodriguez, M., Vicente-Carrillo, A., Johnsson, M., Wright, D., and Rodriguez-Martinez, H. (2017). Conserved gene expression in sperm reservoirs between birds and mammals in response to mating. BMC Genomics *18*, 98.

Baciu, P.C., Suleiman, E.A., Deryugina, E.I., and Strongin, A.Y. (2003). Membrane type-1 matrix metalloproteinase (MT1-MMP) processing of pro-alphav integrin regulates cross-talk between alphavbeta3 and alpha2beta1 integrins in breast carcinoma cells. Exp. Cell Res. *291*, 167–175.

Baker, A.H., Zaltsman, A.B., George, S.J., and Newby, A.C. (1998). Divergent effects of tissue inhibitor of metalloproteinase-1, -2, or -3 overexpression on rat vascular smooth muscle cell invasion, proliferation, and death in vitro. TIMP-3 promotes apoptosis. J. Clin. Invest. *101*, 1478–1487.

Balaban, S., Shearer, R.F., Lee, L.S., van Geldermalsen, M., Schreuder, M., Shtein, H.C., Cairns, R., Thomas, K.C., Fazakerley, D.J., Grewal, T., et al. (2017). Adipocyte lipolysis links obesity to breast cancer growth: adipocyte-derived fatty acids drive breast cancer cell proliferation and migration. Cancer Metab. *5*.

Balbín, M., Fueyo, A., Tester, A.M., Pendás, A.M., Pitiot, A.S., Astudillo, A., Overall, C.M., Shapiro, S.D., and López-Otín, C. (2003). Loss of collagenase-2 confers increased skin tumor susceptibility to male mice. Nat. Genet. *35*, 252–257.

Ban, J.Y., Kim, S.K., Kang, S.W., Yoon, K.L., and Chung, J.-H. (2010). Association between polymorphisms of matrix metalloproteinase 11 (MMP-11) and Kawasaki disease in the Korean population. Life Sci. *86*, 756–759.

Barrasa, J.I., Olmo, N., Santiago-Gómez, A., Lecona, E., Anglard, P., Turnay, J., and Lizarbe, M.A. (2012). Histone deacetylase inhibitors upregulate MMP11 gene expression through Sp1/Smad complexes in human colon adenocarcinoma cells. Biochim. Biophys. Acta *1823*, 570–581.

Baserga, R. (2000). The contradictions of the insulin-like growth factor 1 receptor. Oncogene *19*, 5574–5581.

Basset, P., Bellocq, J.P., Wolf, C., Stoll, I., Hutin, P., Limacher, J.M., Podhajcer, O.L., Chenard, M.P., Rio, M.C., and Chambon, P. (1990). A novel metalloproteinase

gene specifically expressed in stromal cells of breast carcinomas. Nature *348*, 699–704.

Basset, P., Okada, A., Chenard, M.P., Kannan, R., Stoll, I., Anglard, P., Bellocq, J.P., and Rio, M.C. (1997). Matrix metalloproteinases as stromal effectors of human carcinoma progression: therapeutic implications. Matrix Biol. J. Int. Soc. Matrix Biol. *15*, 535–541.

Bauters, D., Van Hul, M., and Lijnen, H.R. (2014). Gelatinase B (MMP-9) gene silencing does not affect murine preadipocyte differentiation. Adipocyte *3*, 50–53.

Bauters, D., Scroyen, I., Van Hul, M., and Lijnen, H.R. (2015). Gelatinase A (MMP-2) promotes murine adipogenesis. Biochim. Biophys. Acta *1850*, 1449–1456.

Bauvois, B. (2012). New facets of matrix metalloproteinases MMP-2 and MMP-9 as cell surface transducers: outside-in signaling and relationship to tumor progression. Biochim. Biophys. Acta *1825*, 29–36.

Belardi, V., Gallagher, E.J., Novosyadlyy, R., and LeRoith, D. (2013). Insulin and IGFs in obesity-related breast cancer. J. Mammary Gland Biol. Neoplasia *18*, 277–289.

Benjamin, M.M., and Khalil, R.A. (2012). Matrix metalloproteinase inhibitors as investigative tools in the pathogenesis and management of vascular disease. EXS *103*, 209–279.

Bergers, G., Brekken, R., McMahon, G., Vu, T.H., Itoh, T., Tamaki, K., Tanzawa, K., Thorpe, P., Itohara, S., Werb, Z., et al. (2000). Matrix metalloproteinase-9 triggers the angiogenic switch during carcinogenesis. Nat. Cell Biol. *2*, 737–744.

Biolo, A., Greferath, R., Siwik, D.A., Qin, F., Valsky, E., Fylaktakidou, K.C., Pothukanuri, S., Duarte, C.D., Schwarz, R.P., Lehn, J.-M., et al. (2009). Enhanced exercise capacity in mice with severe heart failure treated with an allosteric effector of hemoglobin, myo-inositol trispyrophosphate. Proc. Natl. Acad. Sci. U. S. A. *106*, 1926–1929.

Blumenthal, M.N., Zhong, W., Miller, M., Wendt, C., Connett, J.E., and Pei, D. (2010). Serum metalloproteinase leukolysin (MMP-25/MT-6): a potential metabolic marker for atopy-associated inflammation. Clin. Exp. Allergy J. Br. Soc. Allergy Clin. Immunol. *40*, 859–866.

Bochet, L., Lehuede, C., Dauvillier, S., Wang, Y.Y., Dirat, B., Laurent, V., Dray, C., Guiet, R., Maridonneau-Parini, I., Le Gonidec, S., et al. (2013). Adipocyte-Derived

Fibroblasts Promote Tumor Progression and Contribute to the Desmoplastic Reaction in Breast Cancer. Cancer Res. *73*, 5657–5668.

Bode, W., Gomis-Rüth, F.X., and Stöckler, W. (1993). Astacins, serralysins, snake venom and matrix metalloproteinases exhibit identical zinc-binding environments (HEXXHXXGXXH and Met-turn) and topologies and should be grouped into a common family, the "metzincins." FEBS Lett. *331*, 134–140.

Boire, A., Covic, L., Agarwal, A., Jacques, S., Sherifi, S., and Kuliopulos, A. (2005). PAR1 is a matrix metalloprotease-1 receptor that promotes invasion and tumorigenesis of breast cancer cells. Cell *120*, 303–313.

Bonuccelli, G., Tsirigos, A., Whitaker-Menezes, D., Pavlides, S., Pestell, R.G., Chiavarina, B., Frank, P.G., Flomenberg, N., Howell, A., Martinez-Outschoorn, U.E., et al. (2010). Ketones and lactate "fuel" tumor growth and metastasis: Evidence that epithelial cancer cells use oxidative mitochondrial metabolism. Cell Cycle Georget. Tex *9*, 3506–3514.

Boulay, A., Masson, R., Chenard, M.P., El Fahime, M., Cassard, L., Bellocq, J.P., Sautès-Fridman, C., Basset, P., and Rio, M.C. (2001). High cancer cell death in syngeneic tumors developed in host mice deficient for the stromelysin-3 matrix metalloproteinase. Cancer Res. *61*, 2189–2193.

Bournet, B., Pointreau, A., Souque, A., Oumouhou, N., Muscari, F., Lepage, B., Senesse, P., Barthet, M., Lesavre, N., Hammel, P., et al. (2012). Gene expression signature of advanced pancreatic ductal adenocarcinoma using low density array on endoscopic ultrasound-guided fine needle aspiration samples. Pancreatol. Off. J. Int. Assoc. Pancreatol. IAP Al *12*, 27–34.

Brasse, D., Mathelin, C., Leroux, K., Chenard, M.-P., Blaise, S., Stoll, I., Tomasetto, C., and Rio, M.-C. (2010). Matrix metalloproteinase 11/stromelysin-3 exerts both activator and repressor functions during the hematogenous metastatic process in mice. Int. J. Cancer *127*, 1347–1355.

Brown, S.B., and Hankinson, S.E. (2015). Endogenous estrogens and the risk of breast, endometrial, and ovarian cancers. Steroids *99*, 8–10.

Bruno, S., and Darzynkiewicz, Z. (1992). Cell cycle dependent expression and stability of the nuclear protein detected by Ki-67 antibody in HL-60 cells. Cell Prolif. *25*, 31–40.

Bruyère, F., Melen-Lamalle, L., Blacher, S., Roland, G., Thiry, M., Moons, L., Frankenne, F., Carmeliet, P., Alitalo, K., Libert, C., et al. (2008). Modeling lymphangiogenesis in a three-dimensional culture system. Nat. Methods *5*, 431–437.

Buache, E., Thai, R., Wendling, C., Alpy, F., Page, A., Chenard, M.-P., Dive, V., Ruff, M., Dejaegere, A., Tomasetto, C., et al. (2014). Functional relationship between matrix metalloproteinase-11 and matrix metalloproteinase-14. Cancer Med. *3*, 1197–1210.

Buchsbaum, R.J., and Oh, S.Y. (2016). Breast Cancer-Associated Fibroblasts: Where We Are and Where We Need to Go. Cancers *8*.

Bullard, K.M., Lund, L., Mudgett, J.S., Mellin, T.N., Hunt, T.K., Murphy, B., Ronan, J., Werb, Z., and Banda, M.J. (1999). Impaired wound contraction in stromelysin-1-deficient mice. Ann. Surg. *230*, 260–265.

Bulun, S.E., Chen, D., Moy, I., Brooks, D.C., and Zhao, H. (2012). Aromatase, breast cancer and obesity: a complex interaction. Trends Endocrinol. Metab. TEM *23*, 83–89.

Burns, J.M., Summers, B.C., Wang, Y., Melikian, A., Berahovich, R., Miao, Z., Penfold, M.E.T., Sunshine, M.J., Littman, D.R., Kuo, C.J., et al. (2006). A novel chemokine receptor for SDF-1 and I-TAC involved in cell survival, cell adhesion, and tumor development. J. Exp. Med. *203*, 2201–2213.

Bussard, K.M., Mutkus, L., Stumpf, K., Gomez-Manzano, C., and Marini, F.C. (2016). Tumor-associated stromal cells as key contributors to the tumor microenvironment. Breast Cancer Res. BCR *18*, 84.

Butler, G.S., and Overall, C.M. (2013). Matrix metalloproteinase processing of signaling molecules to regulate inflammation. Periodontol. 2000 *63*, 123–148.

Cancer Genome Atlas Network (2015). Comprehensive genomic characterization of head and neck squamous cell carcinomas. Nature *517*, 576–582.

Capilla, E., and Navarro, I. (2015). Editorial: Control of Adipocyte Differentiation and Metabolism. Front. Endocrinol. *6*, 132.

Carneiro, P., Fernandes, M.S., Figueiredo, J., Caldeira, J., Carvalho, J., Pinheiro, H., Leite, M., Melo, S., Oliveira, P., Simões-Correia, J., et al. (2012). E-cadherin dysfunction in gastric cancer--cellular consequences, clinical applications and open questions. FEBS Lett. *586*, 2981–2989.

Carneiro, P., Figueiredo, J., Bordeira-Carriço, R., Fernandes, M.S., Carvalho, J., Oliveira, C., and Seruca, R. (2013). Therapeutic targets associated to E-cadherin dysfunction in gastric cancer. Expert Opin. Ther. Targets *17*, 1187–1201.

Carter, J.C., and Church, F.C. (2012). Mature breast adipocytes promote breast cancer cell motility. Exp. Mol. Pathol. *92*, 312–317.

Castro-Castro, A., Marchesin, V., Monteiro, P., Lodillinsky, C., Rossé, C., and Chavrier, P. (2016). Cellular and Molecular Mechanisms of MT1-MMP-Dependent Cancer Cell Invasion. Annu. Rev. Cell Dev. Biol. *32*, 555–576.

Caterina, J.J., Skobe, Z., Shi, J., Ding, Y., Simmer, J.P., Birkedal-Hansen, H., and Bartlett, J.D. (2002). Enamelysin (matrix metalloproteinase 20)-deficient mice display an amelogenesis imperfecta phenotype. J. Biol. Chem. *277*, 49598–49604.

Chakraborti, S., Mandal, M., Das, S., Mandal, A., and Chakraborti, T. (2003). Regulation of matrix metalloproteinases: an overview. Mol. Cell. Biochem. *253*, 269–285.

Chaudhary, A.K., Singh, M., Bharti, A.C., Asotra, K., Sundaram, S., and Mehrotra, R. (2010). Genetic polymorphisms of matrix metalloproteinases and their inhibitors in potentially malignant and malignant lesions of the head and neck. J. Biomed. Sci. *17*, 10.

Chen, P., Abacherli, L.E., Nadler, S.T., Wang, Y., Li, Q., and Parks, W.C. (2009). MMP7 shedding of syndecan-1 facilitates re-epithelialization by affecting alpha(2)beta(1) integrin activation. PloS One *4*, e6565.

Chen, Y.-K., Tung, C.-W., Lee, J.-Y., Hung, Y.-C., Lee, C.-H., Chou, S.-H., Lin, H.-S., Wu, M.-T., and Wu, I.-C. (2016). Plasma matrix metalloproteinase 1 improves the detection and survival prediction of esophageal squamous cell carcinoma. Sci. Rep. *6*, 30057.

Chenard, M.P., O'Siorain, L., Shering, S., Rouyer, N., Lutz, Y., Wolf, C., Basset, P., Bellocq, J.P., and Duffy, M.J. (1996). High levels of stromelysin-3 correlate with poor prognosis in patients with breast carcinoma. Int. J. Cancer *69*, 448–451.

Cheng, K., Xie, G., and Raufman, J.-P. (2007). Matrix metalloproteinase-7-catalyzed release of HB-EGF mediates deoxycholyltaurine-induced proliferation of a human colon cancer cell line. Biochem. Pharmacol. *73*, 1001–1012.

Chernov, A.V., and Strongin, A.Y. (2011). Epigenetic regulation of matrix metalloproteinases and their collagen substrates in cancer. Biomol. Concepts *2*, 135–147.

Chetty, C., Lakka, S.S., Bhoopathi, P., and Rao, J.S. (2010). MMP-2 alters VEGF expression via alphaVbeta3 integrin-mediated PI3K/AKT signaling in A549 lung cancer cells. Int. J. Cancer *127*, 1081–1095.

Chin, J.R., and Werb, Z. (1997). Matrix metalloproteinases regulate morphogenesis, migration and remodeling of epithelium, tongue skeletal muscle and cartilage in the mandibular arch. Development *124*, 1519–1530.

Christopoulos, P.F., Corthay, A., and Koutsilieris, M. (2018). Aiming for the Insulin-like Growth Factor-1 system in breast cancer therapeutics. Cancer Treat. Rev. *63*, 79–95.

Churg, A., Wang, R.D., Tai, H., Wang, X., Xie, C., Dai, J., Shapiro, S.D., and Wright, J.L. (2003). Macrophage metalloelastase mediates acute cigarette smoke-induced inflammation via tumor necrosis factor-alpha release. Am. J. Respir. Crit. Care Med. *167*, 1083–1089.

Cinti, S., Mitchell, G., Barbatelli, G., Murano, I., Ceresi, E., Faloia, E., Wang, S., Fortier, M., Greenberg, A.S., and Obin, M.S. (2005). Adipocyte death defines macrophage localization and function in adipose tissue of obese mice and humans. J. Lipid Res. *46*, 2347–2355.

Clancy, J.W., Sedgwick, A., Rosse, C., Muralidharan-Chari, V., Raposo, G., Method, M., Chavrier, P., and D'Souza-Schorey, C. (2015). Regulated delivery of molecular cargo to invasive tumour-derived microvesicles. Nat. Commun. *6*, 6919.

Clark, E., and Weaver, A. (2008). A new role for cortactin in invadopodia: Regulation of protease secretion. Eur. J. Cell Biol. *87*, 581–590.

Clark, I.M., Swingler, T.E., Sampieri, C.L., and Edwards, D.R. (2008). The regulation of matrix metalloproteinases and their inhibitors. Int. J. Biochem. Cell Biol. *40*, 1362–1378.

Codony-Servat, J., Albanell, J., Lopez-Talavera, J.C., Arribas, J., and Baselga, J. (1999). Cleavage of the HER2 ectodomain is a pervanadate-activable process that is inhibited by the tissue inhibitor of metalloproteases-1 in breast cancer cells. Cancer Res. *59*, 1196–1201.

Cole, S.E., Wiltshire, T., and Reeves, R.H. (1998). Physical mapping of the evolutionary boundary between human chromosomes 21 and 22 on mouse chromosome 10. Genomics *50*, 109–111.

Colnot, C., Thompson, Z., Miclau, T., Werb, Z., and Helms, J.A. (2003). Altered fracture repair in the absence of MMP9. Dev. Camb. Engl. *130*, 4123–4133.

Conant, K., St Hillaire, C., Nagase, H., Visse, R., Gary, D., Haughey, N., Anderson, C., Turchan, J., and Nath, A. (2004). Matrix metalloproteinase 1 interacts with neuronal integrins and stimulates dephosphorylation of Akt. J. Biol. Chem. *279*, 8056–8062.

Cornelius, L.A., Nehring, L.C., Harding, E., Bolanowski, M., Welgus, H.G., Kobayashi, D.K., Pierce, R.A., and Shapiro, S.D. (1998). Matrix metalloproteinases generate angiostatin: effects on neovascularization. J. Immunol. Baltim. Md 1950 *161*, 6845–6852.

Correia, A.L., Mori, H., Chen, E.I., Schmitt, F.C., and Bissell, M.J. (2013). The hemopexin domain of MMP3 is responsible for mammary epithelial invasion and morphogenesis through extracellular interaction with HSP90β. Genes Dev. *27*, 805–817.

Corry, D.B., Kiss, A., Song, L.-Z., Song, L., Xu, J., Lee, S.-H., Werb, Z., and Kheradmand, F. (2004). Overlapping and independent contributions of MMP2 and MMP9 to lung allergic inflammatory cell egression through decreased CC chemokines. FASEB J. Off. Publ. Fed. Am. Soc. Exp. Biol. *18*, 995–997.

Couldrey, C., Moitra, J., Vinson, C., Anver, M., Nagashima, K., and Green, J. (2002). Adipose tissue: A vital in vivo role in mammary gland development but not differentiation. Dev. Dyn. *223*, 459–468.

Coussens, L.M., and Werb, Z. (2001). Inflammatory cells and cancer: think different! J. Exp. Med. *193*, F23-26.

Cox, J.H., Dean, R.A., Roberts, C.R., and Overall, C.M. (2008). Matrix metalloproteinase processing of CXCL11/I-TAC results in loss of chemoattractant activity and altered glycosaminoglycan binding. J. Biol. Chem. *283*, 19389–19399.

Cubillos-Ruiz, J.R., Bettigole, S.E., and Glimcher, L.H. (2017). Tumorigenic and Immunosuppressive Effects of Endoplasmic Reticulum Stress in Cancer. Cell *168*, 692–706.

Curran, S., and Murray, G.I. (1999). Matrix metalloproteinases in tumour invasion and metastasis. J. Pathol. *189*, 300–308.

Cuylen, S., Blaukopf, C., Politi, A.Z., Müller-Reichert, T., Neumann, B., Poser, I., Ellenberg, J., Hyman, A.A., and Gerlich, D.W. (2016). Ki-67 acts as a biological surfactant to disperse mitotic chromosomes. Nature *535*, 308–312.

Dali-Youcef, N., Hnia, K., Blaise, S., Messaddeq, N., Blanc, S., Postic, C., Valet, P., Tomasetto, C., and Rio, M.-C. (2016). Matrix metalloproteinase 11 protects from diabesity and promotes metabolic switch. Sci. Rep. *6*, 25140.

Damjanovski, S., ATSUKOISHIZUYAOKA, and Shi YB (1999). Spatial and temporal regulation of collagenases-3, -4,and stromelysin -3 implicates distinct functions in apoptosis and tissue remodeling during frog metamorphosis. Cell Res. *9*, 91–105.

De Ieso, M.L., and Yool, A.J. (2018). Mechanisms of Aquaporin-Facilitated Cancer Invasion and Metastasis. Front. Chem. *6*, 135.

Deatrick, K.B., Luke, C.E., Elfline, M.A., Sood, V., Baldwin, J., Upchurch, G.R., Jaffer, F.A., Wakefield, T.W., and Henke, P.K. (2013). The effect of matrix metalloproteinase 2 and matrix metalloproteinase 2/9 deletion in experimental post-thrombotic vein wall remodeling. J. Vasc. Surg. *58*, 1375-1384.e2.

Delany, A.M., and Canalis, E. (1998). Dual regulation of stromelysin-3 by fibroblast growth factor-2 in murine osteoblasts. J. Biol. Chem. *273*, 16595–16600.

Deng, H., Guo, R.-F., Li, W.-M., Zhao, M., and Lu, Y.-Y. (2005). Matrix metalloproteinase 11 depletion inhibits cell proliferation in gastric cancer cells. Biochem. Biophys. Res. Commun. *326*, 274–281.

Deok-Hoon Kong, Mi Kim, Ji Jang, Hee-Jun Na, and Sukmook Lee (2017). A Review of Anti-Angiogenic Targets for Monoclonal Antibody Cancer Therapy. Int. J. Mol. Sci. *18*, 1786.

Derbal-Wolfrom, L., Pencreach, E., Saandi, T., Aprahamian, M., Martin, E., Greferath, R., Tufa, E., Choquet, P., Lehn, J.-M., Nicolau, C., et al. (2013). Increasing the oxygen load by treatment with myo-inositol trispyrophosphate reduces growth of colon cancer and modulates the intestine homeobox gene Cdx2. Oncogene *32*, 4313–4318.

Derosa, G., D'Angelo, A., Tinelli, C., Devangelio, E., Consoli, A., Miccoli, R., Penno, G., Del Prato, S., Paniga, S., and Cicero, A.F.G. (2007). Evaluation of

metalloproteinase 2 and 9 levels and their inhibitors in diabetic and healthy subjects. Diabetes Metab. *33*, 129–134.

Derynck, R., Akhurst, R.J., and Balmain, A. (2001). TGF-beta signaling in tumor suppression and cancer progression. Nat. Genet. *29*, 117–129.

Deryugina, E.I., and Quigley, J.P. (2015). Tumor angiogenesis: MMP-mediated induction of intravasation- and metastasis-sustaining neovasculature. Matrix Biol. J. Int. Soc. Matrix Biol. *44–46*, 94–112.

Dirat, B., Bochet, L., Dabek, M., Daviaud, D., Dauvillier, S., Majed, B., Wang, Y.Y., Meulle, A., Salles, B., Le Gonidec, S., et al. (2011). Cancer-associated adipocytes exhibit an activated phenotype and contribute to breast cancer invasion. Cancer Res. *71*, 2455–2465.

Du, H.-T., Du, L.-L., Tang, X.-L., Ge, H.-Y., and Liu, P. (2017). Blockade of MMP-2 and MMP-9 inhibits corneal lymphangiogenesis. Graefes Arch. Clin. Exp. Ophthalmol. Albrecht Von Graefes Arch. Klin. Exp. Ophthalmol. *255*, 1573–1579.

Du, R., Lu, K.V., Petritsch, C., Liu, P., Ganss, R., Passegué, E., Song, H., Vandenberg, S., Johnson, R.S., Werb, Z., et al. (2008). HIF1alpha induces the recruitment of bone marrow-derived vascular modulatory cells to regulate tumor angiogenesis and invasion. Cancer Cell *13*, 206–220.

Dufour, A., Sampson, N.S., Zucker, S., and Cao, J. (2008). Role of the hemopexin domain of matrix metalloproteinases in cell migration. J. Cell. Physiol. *217*, 643–651.

Dunsmore, S.E., Saarialho-Kere, U.K., Roby, J.D., Wilson, C.L., Matrisian, L.M., Welgus, H.G., and Parks, W.C. (1998). Matrilysin expression and function in airway epithelium. J. Clin. Invest. *102*, 1321–1331.

Dupé, V., Ghyselinck, N.B., Thomazy, V., Nagy, L., Davies, P.J., Chambon, P., and Mark, M. (1999). Essential roles of retinoic acid signaling in interdigital apoptosis and control of BMP-7 expression in mouse autopods. Dev. Biol. *208*, 30–43.

Egeblad, M., and Werb, Z. (2002). New functions for the matrix metalloproteinases in cancer progression. Nat. Rev. Cancer *2*, 161–174.

Eiro, N., Fernandez-Gomez, J., Sacristán, R., Fernandez-Garcia, B., Lobo, B., Gonzalez-Suarez, J., Quintas, A., Escaf, S., and Vizoso, F.J. (2017). Stromal factors involved in human prostate cancer development, progression and castration resistance. J. Cancer Res. Clin. Oncol. *143*, 351–359.

Eiro, N., González, L., Martínez-Ordoñez, A., Fernandez-Garcia, B., González, L.O., Cid, S., Dominguez, F., Perez-Fernandez, R., and Vizoso, F.J. (2018). Cancer-associated fibroblasts affect breast cancer cell gene expression, invasion and angiogenesis. Cell. Oncol. Dordr.

English, W.R., Puente, X.S., Freije, J.M., Knauper, V., Amour, A., Merryweather, A., Lopez-Otin, C., and Murphy, G. (2000). Membrane type 4 matrix metalloproteinase (MMP17) has tumor necrosis factor-alpha convertase activity but does not activate pro-MMP2. J. Biol. Chem. *275*, 14046–14055.

Farmer, S.R. (2006). Transcriptional control of adipocyte formation. Cell Metab. *4*, 263–273.

Fata, J.E., Leco, K.J., Moorehead, R.A., Martin, D.C., and Khokha, R. (1999). Timp-1 is important for epithelial proliferation and branching morphogenesis during mouse mammary development. Dev. Biol. *211*, 238–254.

Federici, M., Hribal, M.L., Menghini, R., Kanno, H., Marchetti, V., Porzio, O., Sunnarborg, S.W., Rizza, S., Serino, M., Cunsolo, V., et al. (2005). Timp3 deficiency in insulin receptor-haploinsufficient mice promotes diabetes and vascular inflammation via increased TNF-alpha. J. Clin. Invest. *115*, 3494–3505.

Feinberg, T.Y., Rowe, R.G., Saunders, T.L., and Weiss, S.J. (2016). Functional roles of MMP14 and MMP15 in early postnatal mammary gland development. Dev. Camb. Engl. *143*, 3956–3968.

Fels, D.R., and Koumenis, C. (2006). The PERK/eIF2alpha/ATF4 module of the UPR in hypoxia resistance and tumor growth. Cancer Biol. Ther. *5*, 723–728.

Ferreras, M., Felbor, U., Lenhard, T., Olsen, B.R., and Delaissé, J. (2000). Generation and degradation of human endostatin proteins by various proteinases. FEBS Lett. *486*, 247–251.

Fink, K., and Boratyński, J. (2012). [The role of metalloproteinases in modification of extracellular matrix in invasive tumor growth, metastasis and angiogenesis]. Postepy Hig. Med. Doswiadczalnej Online *66*, 609–628.

Fiorentino, M., Fu, L., and Shi, Y.-B. (2009). Mutational analysis of the cleavage of the cancer-associated laminin receptor by stromelysin-3 reveals the contribution of flanking sequences to site recognition and cleavage efficiency. Int. J. Mol. Med. *23*, 389–397.

Fischer, A.H., Jacobson, K.A., Rose, J., and Zeller, R. (2008). Hematoxylin and eosin staining of tissue and cell sections. CSH Protoc. *2008*, pdb.prot4986.
Fluck, M.M., and Schaffhausen, B.S. (2009). Lessons in signaling and tumorigenesis from polyomavirus middle T antigen. Microbiol. Mol. Biol. Rev. MMBR *73*, 542–563, Table of Contents.
Frakes, A.E., and Dillin, A. (2017). The UPRER: Sensor and Coordinator of Organismal Homeostasis. Mol. Cell *66*, 761–771.
Fujita, Y., Shiomi, T., Yanagimoto, S., Matsumoto, H., Toyama, Y., and Okada, Y. (2006). Tetraspanin CD151 is expressed in osteoarthritic cartilage and is involved in pericellular activation of pro-matrix metalloproteinase 7 in osteoarthritic chondrocytes. Arthritis Rheum. *54*, 3233–3243.
Fylaktakidou, K.C., Lehn, J.-M., Greferath, R., and Nicolau, C. (2005). Inositol tripyrophosphate: a new membrane permeant allosteric effector of haemoglobin. Bioorg. Med. Chem. Lett. *15*, 1605–1608.
Galis, Z.S., Johnson, C., Godin, D., Magid, R., Shipley, J.M., Senior, R.M., and Ivan, E. (2002). Targeted disruption of the matrix metalloproteinase-9 gene impairs smooth muscle cell migration and geometrical arterial remodeling. Circ. Res. *91*, 852–859.
Gall, A.L., Ruff, M., Kannan, R., Cuniasse, P., Yiotakis, A., Dive, V., Rio, M.C., Basset, P., and Moras, D. (2001). Crystal structure of the stromelysin-3 (MMP-11) catalytic domain complexed with a phosphinic inhibitor mimicking the transition-state. J. Mol. Biol. *307*, 577–586.
Gallagher, E.J., and LeRoith, D. (2011). Minireview: IGF, Insulin, and Cancer. Endocrinology *152*, 2546–2551.
Galliera, E., Tacchini, L., and Corsi Romanelli, M.M. (2015). Matrix metalloproteinases as biomarkers of disease: updates and new insights. Clin. Chem. Lab. Med. *53*, 349–355.
Garg, P., Rojas, M., Ravi, A., Bockbrader, K., Epstein, S., Vijay-Kumar, M., Gewirtz, A.T., Merlin, D., and Sitaraman, S.V. (2006). Selective ablation of matrix metalloproteinase-2 exacerbates experimental colitis: contrasting role of gelatinases in the pathogenesis of colitis. J. Immunol. Baltim. Md 1950 *177*, 4103–4112.
Gialeli, C., Kletsas, D., Mavroudis, D., Kalofonos, H.P., Tzanakakis, G.N., and Karamanos, N.K. (2009). Targeting epidermal growth factor receptor in solid tumors:

critical evaluation of the biological importance of therapeutic monoclonal antibodies. Curr. Med. Chem. *16*, 3797–3804.
Giannandrea, M., and Parks, W.C. (2014). Diverse functions of matrix metalloproteinases during fibrosis. Dis. Model. Mech. *7*, 193–203.
Golubkov, V.S., Chekanov, A.V., Shiryaev, S.A., Aleshin, A.E., Ratnikov, B.I., Gawlik, K., Radichev, I., Motamedchaboki, K., Smith, J.W., and Strongin, A.Y. (2007). Proteolysis of the membrane type-1 matrix metalloproteinase prodomain: implications for a two-step proteolytic processing and activation. J. Biol. Chem. *282*, 36283–36291.
Gomes, A.M., Bhat, R., Correia, A.L., Mott, J.D., Ilan, N., Vlodavsky, I., Pavão, M.S.G., and Bissell, M. (2015). Mammary Branching Morphogenesis Requires Reciprocal Signaling by Heparanase and MMP-14. J. Cell. Biochem. *116*, 1668–1679.
Gómez-Macías, G.S., Garza-Rodríguez, M.L., Garza-Guajardo, R., Monsiváis-Ovalle, D., Ancer-Rodríguez, J., Barrera-Saldaña, H.A., and Barboza-Quintana, O. (2018). Overexpression of the matrix metalloproteinase 11 gene is a potential biomarker for type 1 endometrial cancer. Oncol. Lett. *16*, 1073–1078.
Gomis-Rüth, F.X. (2003). Structural aspects of the metzincin clan of metalloendopeptidases. Mol. Biotechnol. *24*, 157–202.
Grabowska, M.M., and Day, M.L. (2012). Soluble E-cadherin: more than a symptom of disease. Front. Biosci. Landmark Ed. *17*, 1948–1964.
Graves, R.A., Tontonoz, P., Ross, S.R., and Spiegelman, B.M. (1991). Identification of a potent adipocyte-specific enhancer: involvement of an NF-1-like factor. Genes Dev. *5*, 428–437.
Green, K.A., and Lund, L.R. (2005). ECM degrading proteases and tissue remodelling in the mammary gland. BioEssays News Rev. Mol. Cell. Dev. Biol. *27*, 894–903.
Gucciardo, E., Mobashir, M., and Lehti, K. (2016). Proactive for invasion: Reuse of matrix metalloproteinase for structural memory. J. Cell Biol. *213*, 11–13.
Guérin, E., Ludwig, M.G., Basset, P., and Anglard, P. (1997). Stromelysin-3 induction and interstitial collagenase repression by retinoic acid. Therapeutical implication of receptor-selective retinoids dissociating transactivation and AP-1-mediated transrepression. J. Biol. Chem. *272*, 11088–11095.

Gui, Y., Pan, Q., Chen, X., Xu, S., Luo, X., and Chen, L. (2017). The association between obesity related adipokines and risk of breast cancer: a meta-analysis. Oncotarget *8*, 75389–75399.

Gupta, A., Zhou, C.Q., and Chellaiah, M.A. (2013). Osteopontin and MMP9: Associations with VEGF Expression/Secretion and Angiogenesis in PC3 Prostate Cancer Cells. Cancers *5*, 617–638.

Gutiérrez-Fernández, A., Inada, M., Balbín, M., Fueyo, A., Pitiot, A.S., Astudillo, A., Hirose, K., Hirata, M., Shapiro, S.D., Noël, A., et al. (2007). Increased inflammation delays wound healing in mice deficient in collagenase-2 (MMP-8). FASEB J. Off. Publ. Fed. Am. Soc. Exp. Biol. *21*, 2580–2591.

Gutiérrez-Fernández, A., Fueyo, A., Folgueras, A.R., Garabaya, C., Pennington, C.J., Pilgrim, S., Edwards, D.R., Holliday, D.L., Jones, J.L., Span, P.N., et al. (2008). Matrix metalloproteinase-8 functions as a metastasis suppressor through modulation of tumor cell adhesion and invasion. Cancer Res. *68*, 2755–2763.

Gutschalk, C.M., Yanamandra, A.K., Linde, N., Meides, A., Depner, S., and Mueller, M.M. (2013). GM-CSF enhances tumor invasion by elevated MMP-2, -9, and -26 expression. Cancer Med. *2*, 117–129.

Guy, C.T., Cardiff, R.D., and Muller, W.J. (1992a). Induction of mammary tumors by expression of polyomavirus middle T oncogene: a transgenic mouse model for metastatic disease. Mol. Cell. Biol. *12*, 954–961.

Guy, C.T., Webster, M.A., Schaller, M., Parsons, T.J., Cardiff, R.D., and Muller, W.J. (1992b). Expression of the neu protooncogene in the mammary epithelium of transgenic mice induces metastatic disease. Proc. Natl. Acad. Sci. U. S. A. *89*, 10578–10582.

Hakulinen, J., Sankkila, L., Sugiyama, N., Lehti, K., and Keski-Oja, J. (2008). Secretion of active membrane type 1 matrix metalloproteinase (MMP-14) into extracellular space in microvesicular exosomes. J. Cell. Biochem. *105*, 1211–1218.

Han, K.-Y., Chang, J.-H., Lee, H., and Azar, D.T. (2016). Proangiogenic Interactions of Vascular Endothelial MMP14 With VEGF Receptor 1 in VEGFA-Mediated Corneal Angiogenesis. Invest. Ophthalmol. Vis. Sci. *57*, 3313–3322.

Hanahan, D., and Coussens, L.M. (2012). Accessories to the crime: functions of cells recruited to the tumor microenvironment. Cancer Cell *21*, 309–322.

Hannemann, J., Velds, A., Halfwerk, J.B.G., Kreike, B., Peterse, J.L., and van de Vijver, M.J. (2006). Classification of ductal carcinoma in situ by gene expression profiling. Breast Cancer Res. BCR *8*, R61.

Hannocks, M.-J., Zhang, X., Gerwien, H., Chashchina, A., Burmeister, M., Korpos, E., Song, J., and Sorokin, L. (2017). The gelatinases, MMP-2 and MMP-9, as fine tuners of neuroinflammatory processes. Matrix Biol. J. Int. Soc. Matrix Biol.

Haro, H., Crawford, H.C., Fingleton, B., Shinomiya, K., Spengler, D.M., and Matrisian, L.M. (2000). Matrix metalloproteinase-7-dependent release of tumor necrosis factor-alpha in a model of herniated disc resorption. J. Clin. Invest. *105*, 143–150.

Hartenstein, B., Dittrich, B.T., Stickens, D., Heyer, B., Vu, T.H., Teurich, S., Schorpp-Kistner, M., Werb, Z., and Angel, P. (2006). Epidermal development and wound healing in matrix metalloproteinase 13-deficient mice. J. Invest. Dermatol. *126*, 486–496.

Hassan, M., Watari, H., AbuAlmaaty, A., Ohba, Y., and Sakuragi, N. (2014). Apoptosis and molecular targeting therapy in cancer. BioMed Res. Int. *2014*, 150845.

Hautamaki, R.D., Kobayashi, D.K., Senior, R.M., and Shapiro, S.D. (1997). Requirement for macrophage elastase for cigarette smoke-induced emphysema in mice. Science *277*, 2002–2004.

Hebbard, L.W., Garlatti, M., Young, L.J.T., Cardiff, R.D., Oshima, R.G., and Ranscht, B. (2008). T-cadherin supports angiogenesis and adiponectin association with the vasculature in a mouse mammary tumor model. Cancer Res. *68*, 1407–1416.

Hefetz-Sela, S., and Scherer, P.E. (2013). Adipocytes: Impact on tumor growth and potential sites for therapeutic intervention. Pharmacol. Ther. *138*, 197–210.

Heldin, C.-H., Landström, M., and Moustakas, A. (2009). Mechanism of TGF-beta signaling to growth arrest, apoptosis, and epithelial-mesenchymal transition. Curr. Opin. Cell Biol. *21*, 166–176.

Heljasvaara, R., Nyberg, P., Luostarinen, J., Parikka, M., Heikkilä, P., Rehn, M., Sorsa, T., Salo, T., and Pihlajaniemi, T. (2005). Generation of biologically active endostatin fragments from human collagen XVIII by distinct matrix metalloproteases. Exp. Cell Res. *307*, 292–304.

Henckels, E., and Prywes, R. (2013). Fra-1 regulation of Matrix Metallopeptidase-1 (MMP-1) in metastatic variants of MDA-MB-231 breast cancer cells. F1000Research *2*, 229.

Hennighausen, L., and Robinson, G.W. (2001). Signaling pathways in mammary gland development. Dev. Cell *1*, 467–475.

Hens, J.R., and Wysolmerski, J.J. (2005). Key stages of mammary gland development: molecular mechanisms involved in the formation of the embryonic mammary gland. Breast Cancer Res. BCR *7*, 220–224.

Herschkowitz, J.I., Simin, K., Weigman, V.J., Mikaelian, I., Usary, J., Hu, Z., Rasmussen, K.E., Jones, L.P., Assefnia, S., Chandrasekharan, S., et al. (2007). Identification of conserved gene expression features between murine mammary carcinoma models and human breast tumors. Genome Biol. *8*, R76.

Hertzel, A.V., and Bernlohr, D.A. (2000). The mammalian fatty acid-binding protein multigene family: molecular and genetic insights into function. Trends Endocrinol. Metab. TEM *11*, 175–180.

van Hinsbergh, V.W.M., and Koolwijk, P. (2008). Endothelial sprouting and angiogenesis: matrix metalloproteinases in the lead. Cardiovasc. Res. *78*, 203–212.

Hojilla, C.V., Kim, I., Kassiri, Z., Fata, J.E., Fang, H., and Khokha, R. (2007). Metalloproteinase axes increase beta-catenin signaling in primary mouse mammary epithelial cells lacking TIMP3. J. Cell Sci. *120*, 1050–1060.

Holmbeck, K., Bianco, P., Caterina, J., Yamada, S., Kromer, M., Kuznetsov, S.A., Mankani, M., Robey, P.G., Poole, A.R., Pidoux, I., et al. (1999). MT1-MMP-deficient mice develop dwarfism, osteopenia, arthritis, and connective tissue disease due to inadequate collagen turnover. Cell *99*, 81–92.

Holtz, B., Cuniasse, P., Boulay, A., Kannan, R., Mucha, A., Beau, F., Basset, P., and Dive, V. (1999). Role of the S1’ subsite glutamine 215 in activity and specificity of stromelysin-3 by site-directed mutagenesis. Biochemistry (Mosc.) *38*, 12174–12179.

Houghton, A.M., Grisolano, J.L., Baumann, M.L., Kobayashi, D.K., Hautamaki, R.D., Nehring, L.C., Cornelius, L.A., and Shapiro, S.D. (2006a). Macrophage elastase (matrix metalloproteinase-12) suppresses growth of lung metastases. Cancer Res. *66*, 6149–6155.

Houghton, A.M., Quintero, P.A., Perkins, D.L., Kobayashi, D.K., Kelley, D.G., Marconcini, L.A., Mecham, R.P., Senior, R.M., and Shapiro, S.D. (2006b). Elastin

fragments drive disease progression in a murine model of emphysema. J. Clin. Invest. *116*, 753–759.

Hsin, C.-H., Chen, M.-K., Tang, C.-H., Lin, H.-P., Chou, M.-Y., Lin, C.-W., and Yang, S.-F. (2014). High Level of Plasma Matrix Metalloproteinase-11 Is Associated with Clinicopathological Characteristics in Patients with Oral Squamous Cell Carcinoma. PLoS ONE *9*, e113129.

Hu, X., Juneja, S.C., Maihle, N.J., and Cleary, M.P. (2002). Leptin--a growth factor in normal and malignant breast cells and for normal mammary gland development. J. Natl. Cancer Inst. *94*, 1704–1711.

Hua, H., Li, M., Luo, T., Yin, Y., and Jiang, Y. (2011). Matrix metalloproteinases in tumorigenesis: an evolving paradigm. Cell. Mol. Life Sci. CMLS *68*, 3853–3868.

Ignat, M., Akladios, C.Y., Lindner, V., Khetchoumian, K., Teletin, M., Muttter, D., Aprahamian, P.M., and Marescaux, J. (2016). Development of a methodology for in vivo follow-up of hepatocellular carcinoma in hepatocyte specific Trim24-null mice treated with myo-inositol trispyrophosphate. J. Exp. Clin. Cancer Res. *35*.

Ilan, N., Mohsenin, A., Cheung, L., and Madri, J.A. (2001). PECAM-1 shedding during apoptosis generates a membrane-anchored truncated molecule with unique signaling characteristics. FASEB J. Off. Publ. Fed. Am. Soc. Exp. Biol. *15*, 362–372.

Illman, S.A., Lehti, K., Keski-Oja, J., and Lohi, J. (2006). Epilysin (MMP-28) induces TGF-beta mediated epithelial to mesenchymal transition in lung carcinoma cells. J. Cell Sci. *119*, 3856–3865.

Illman, S.A., Lohi, J., and Keski-Oja, J. (2008). Epilysin (MMP-28)--structure, expression and potential functions. Exp. Dermatol. *17*, 897–907.

Inman, J.L., Robertson, C., Mott, J.D., and Bissell, M.J. (2015). Mammary gland development: cell fate specification, stem cells and the microenvironment. Dev. Camb. Engl. *142*, 1028–1042.

Ishizuya-Oka, A., Ueda, S., and Shi, Y.-B. (1996). Transient expression of stromelysin-3 mRNA in the amphibian small intestine during metamorphosis. Cell Tissue Res. *283*, 325–329.

Ishizuya-Oka, A., Li, Q., Amano, T., Damjanovski, S., Ueda, S., and Shi, Y.B. (2000). Requirement for matrix metalloproteinase stromelysin-3 in cell migration and apoptosis during tissue remodeling in Xenopus laevis. J. Cell Biol. *150*, 1177–1188.

Işlekel, H., Oktay, G., Terzi, C., Canda, A.E., Füzün, M., and Küpelioğlu, A. (2007). Matrix metalloproteinase-9,-3 and tissue inhibitor of matrix metalloproteinase-1 in colorectal cancer: relationship to clinicopathological variables. Cell Biochem. Funct. *25*, 433–441.

Itoh, Y., and Seiki, M. (2006). MT1-MMP: a potent modifier of pericellular microenvironment. J. Cell. Physiol. *206*, 1–8.

Itoh, Y., Takamura, A., Ito, N., Maru, Y., Sato, H., Suenaga, N., Aoki, T., and Seiki, M. (2001). Homophilic complex formation of MT1-MMP facilitates proMMP-2 activation on the cell surface and promotes tumor cell invasion. EMBO J. *20*, 4782–4793.

Itoh, Y., Ito, N., Nagase, H., Evans, R.D., Bird, S.A., and Seiki, M. (2006). Cell surface collagenolysis requires homodimerization of the membrane-bound collagenase MT1-MMP. Mol. Biol. Cell *17*, 5390–5399.

Itoh, Y., Ito, N., Nagase, H., and Seiki, M. (2008). The second dimer interface of MT1-MMP, the transmembrane domain, is essential for ProMMP-2 activation on the cell surface. J. Biol. Chem. *283*, 13053–13062.

Iyengar, P., Combs, T.P., Shah, S.J., Gouon-Evans, V., Pollard, J.W., Albanese, C., Flanagan, L., Tenniswood, M.P., Guha, C., Lisanti, M.P., et al. (2003). Adipocyte-secreted factors synergistically promote mammary tumorigenesis through induction of anti-apoptotic transcriptional programs and proto-oncogene stabilization. Oncogene *22*, 6408–6423.

Iyengar, P., Espina, V., Williams, T.W., Lin, Y., Berry, D., Jelicks, L.A., Lee, H., Temple, K., Graves, R., Pollard, J., et al. (2005). Adipocyte-derived collagen VI affects early mammary tumor progression in vivo, demonstrating a critical interaction in the tumor/stroma microenvironment. J. Clin. Invest. *115*, 1163–1176.

Jacob, A., and Prekeris, R. (2015). The regulation of MMP targeting to invadopodia during cancer metastasis. Front. Cell Dev. Biol. *3*, 4.

Jacob, A., Jing, J., Lee, J., Schedin, P., Gilbert, S.M., Peden, A.A., Junutula, J.R., and Prekeris, R. (2013). Rab40b regulates trafficking of MMP2 and MMP9 during invadopodia formation and invasion of breast cancer cells. J. Cell Sci. *126*, 4647–4658.

Jiang, S., Park, D.W., Gao, Y., Ravi, S., Darley-Usmar, V., Abraham, E., and Zmijewski, J.W. (2015). Participation of proteasome-ubiquitin protein degradation in

autophagy and the activation of AMP-activated protein kinase. Cell. Signal. *27*, 1186–1197.

Jovaisaite, V., and Auwerx, J. (2015). The mitochondrial unfolded protein response—synchronizing genomes. Curr. Opin. Cell Biol. *33*, 74–81.

Jovaisaite, V., Mouchiroud, L., and Auwerx, J. (2014). The mitochondrial unfolded protein response, a conserved stress response pathway with implications in health and disease. J. Exp. Biol. *217*, 137–143.

Kalluri, R., and Weinberg, R.A. (2009). The basics of epithelial-mesenchymal transition. J. Clin. Invest. *119*, 1420–1428.

Kannan, R., Ruff, M., Kochins, J.G., Manly, S.P., Stoll, I., El Fahime, M., Noël, A., Foidart, J.M., Rio, M.C., Dive, V., et al. (1999). Purification of active matrix metalloproteinase catalytic domains and its use for screening of specific stromelysin-3 inhibitors. Protein Expr. Purif. *16*, 76–83.

Kariagina, A., Aupperlee, M.D., and Haslam, S.Z. (2007). Progesterone receptor isoforms and proliferation in the rat mammary gland during development. Endocrinology *148*, 2723–2736.

Kasper, G., Reule, M., Tschirschmann, M., Dankert, N., Stout-Weider, K., Lauster, R., Schrock, E., Mennerich, D., Duda, G.N., and Lehmann, K.E. (2007). Stromelysin-3 over-expression enhances tumourigenesis in MCF-7 and MDA-MB-231 breast cancer cell lines: involvement of the IGF-1 signalling pathway. BMC Cancer *7*, 12.

Kassim, S.Y., Gharib, S.A., Mecham, B.H., Birkland, T.P., Parks, W.C., and McGuire, J.K. (2007). Individual matrix metalloproteinases control distinct transcriptional responses in airway epithelial cells infected with Pseudomonas aeruginosa. Infect. Immun. *75*, 5640–5650.

Kataoka, H., Uchino, H., Iwamura, T., Seiki, M., Nabeshima, K., and Koono, M. (1999). Enhanced tumor growth and invasiveness in vivo by a carboxyl-terminal fragment of alpha1-proteinase inhibitor generated by matrix metalloproteinases: a possible modulatory role in natural killer cytotoxicity. Am. J. Pathol. *154*, 457–468.

Kelley, L.C., Lohmer, L.L., Hagedorn, E.J., and Sherwood, D.R. (2014). Traversing the basement membrane in vivo: a diversity of strategies. J. Cell Biol. *204*, 291–302.

Kessenbrock, K., Plaks, V., and Werb, Z. (2010). Matrix metalloproteinases: regulators of the tumor microenvironment. Cell *141*, 52–67.

Kessenbrock, K., Dijkgraaf, G.J.P., Lawson, D.A., Littlepage, L.E., Shahi, P., Pieper, U., and Werb, Z. (2013). A role for matrix metalloproteinases in regulating mammary stem cell function via the Wnt signaling pathway. Cell Stem Cell *13*, 300–313.
Kessenbrock, K., Wang, C.-Y., and Werb, Z. (2015). Matrix metalloproteinases in stem cell regulation and cancer. Matrix Biol. J. Int. Soc. Matrix Biol. *44–46*, 184–190.
Khamis, Z.I., Iczkowski, K.A., Man, Y.-G., Bou-Dargham, M.J., and Sang, Q.-X.A. (2016). Evidence for a Proapoptotic Role of Matrix Metalloproteinase-26 in Human Prostate Cancer Cells and Tissues. J. Cancer *7*, 80–87.
Khokha, R., and Werb, Z. (2011). Mammary gland reprogramming: metalloproteinases couple form with function. Cold Spring Harb. Perspect. Biol. *3*.
Kim, J., Kundu, M., Viollet, B., and Guan, K.-L. (2011). AMPK and mTOR regulate autophagy through direct phosphorylation of Ulk1. Nat. Cell Biol. *13*, 132–141.
Kim, J.Y., Heo, S.-H., Song, I.H., Park, I.A., Kim, Y.-A., Gong, G., and Lee, H.J. (2016a). Activation of the PERK-eIF2α Pathway Is Associated with Tumor-infiltrating Lymphocytes in HER2-Positive Breast Cancer. Anticancer Res. *36*, 2705–2711.
Kim, S., Ahn, S.H., Lee, J.-S., Song, J.-E., Cho, S.-H., Jung, S., Kim, S.-K., Kim, S.-H., Lee, K.-P., Kwon, K.-S., et al. (2016b). Differential Matrix Metalloprotease (MMP) Expression Profiles Found in Aged Gingiva. PloS One *11*, e0158777.
Kirkin, V., Cahuzac, N., Guardiola-Serrano, F., Huault, S., Lückerath, K., Friedmann, E., Novac, N., Wels, W.S., Martoglio, B., Hueber, A.-O., et al. (2007). The Fas ligand intracellular domain is released by ADAM10 and SPPL2a cleavage in T-cells. Cell Death Differ. *14*, 1678–1687.
Köhrmann, A., Kammerer, U., Kapp, M., Dietl, J., and Anacker, J. (2009). Expression of matrix metalloproteinases (MMPs) in primary human breast cancer and breast cancer cell lines: New findings and review of the literature. BMC Cancer *9*, 188.
Kolb, C., Mauch, S., Peter, H.H., Krawinkel, U., and Sedlacek, R. (1997). The matrix metalloproteinase RASI-1 is expressed in synovial blood vessels of a rheumatoid arthritis patient. Immunol. Lett. *57*, 83–88.
Komori, K., Nonaka, T., Okada, A., Kinoh, H., Hayashita-Kinoh, H., Yoshida, N., Yana, I., and Seiki, M. (2004). Absence of mechanical allodynia and Abeta-fiber sprouting after sciatic nerve injury in mice lacking membrane-type 5 matrix metalloproteinase. FEBS Lett. *557*, 125–128.

Koolwijk, P., Sidenius, N., Peters, E., Sier, C.F., Hanemaaijer, R., Blasi, F., and van Hinsbergh, V.W. (2001). Proteolysis of the urokinase-type plasminogen activator receptor by metalloproteinase-12: implication for angiogenesis in fibrin matrices. Blood *97*, 3123–3131.

Koop, S., Khokha, R., Schmidt, E.E., MacDonald, I.C., Morris, V.L., Chambers, A.F., and Groom, A.C. (1994). Overexpression of metalloproteinase inhibitor in B16F10 cells does not affect extravasation but reduces tumor growth. Cancer Res. *54*, 4791–4797.

Koshikawa, N., Giannelli, G., Cirulli, V., Miyazaki, K., and Quaranta, V. (2000). Role of cell surface metalloprotease MT1-MMP in epithelial cell migration over laminin-5. J. Cell Biol. *148*, 615–624.

Kou, Y.-B., Zhang, S.-Y., Zhao, B.-L., Ding, R., Liu, H., and Li, S. (2013). Knockdown of MMP11 inhibits proliferation and invasion of gastric cancer cells. Int. J. Immunopathol. Pharmacol. *26*, 361–370.

Krishnaswamy, V.R., Mintz, D., and Sagi, I. (2017). Matrix metalloproteinases: The sculptors of chronic cutaneous wounds. Biochim. Biophys. Acta *1864*, 2220–2227.

Kudo, T., Takino, T., Miyamori, H., Thompson, E.W., and Sato, H. (2007). Substrate choice of membrane-type 1 matrix metalloproteinase is dictated by tissue inhibitor of metalloproteinase-2 levels. Cancer Sci. *98*, 563–568.

Kumar, S., Tinson, A., Mulligan, B.P., and Ojha, S. (2016). Gelatin Binding Proteins in Reproductive Physiology. Indian J. Microbiol. *56*, 383–393.

Kwan, J.A., Schulze, C.J., Wang, W., Leon, H., Sariahmetoglu, M., Sung, M., Sawicka, J., Sims, D.E., Sawicki, G., and Schulz, R. (2004). Matrix metalloproteinase-2 (MMP-2) is present in the nucleus of cardiac myocytes and is capable of cleaving poly (ADP-ribose) polymerase (PARP) in vitro. FASEB J. Off. Publ. Fed. Am. Soc. Exp. Biol. *18*, 690–692.

Lagoutte, E., Villeneuve, C., Lafanechère, L., Wells, C.M., Jones, G.E., Chavrier, P., and Rossé, C. (2016). LIMK Regulates Tumor-Cell Invasion and Matrix Degradation Through Tyrosine Phosphorylation of MT1-MMP. Sci. Rep. *6*, 24925.

Landskroner-Eiger, S., Qian, B., Muise, E.S., Nawrocki, A.R., Berger, J.P., Fine, E.J., Koba, W., Deng, Y., Pollard, J.W., and Scherer, P.E. (2009). Proangiogenic contribution of adiponectin toward mammary tumor growth in vivo. Clin. Cancer Res. Off. J. Am. Assoc. Cancer Res. *15*, 3265–3276.

Landskroner-Eiger, S., Park, J., Israel, D., Pollard, J.W., and Scherer, P.E. (2010). Morphogenesis of the developing mammary gland: stage-dependent impact of adipocytes. Dev. Biol. *344*, 968–978.

Langenskiöld, M., Holmdahl, L., Falk, P., and Ivarsson, M.-L. (2005). Increased plasma MMP-2 protein expression in lymph node-positive patients with colorectal cancer. Int. J. Colorectal Dis. *20*, 245–252.

Lauer, J.L., Bhowmick, M., Tokmina-Roszyk, D., Lin, Y., Van Doren, S.R., and Fields, G.B. (2014). The role of collagen charge clusters in the modulation of matrix metalloproteinase activity. J. Biol. Chem. *289*, 1981–1992.

Lee, B.-K., Kim, M.-J., Jang, H.-S., Lee, H.-R., Ahn, K.-M., Lee, J.-H., Choung, P.-H., and Kim, M.-J. (2008). A high concentration of MMP-2/gelatinase A and MMP-9/gelatinase B reduce NK cell-mediated cytotoxicity against an oral squamous cell carcinoma cell line. Vivo Athens Greece *22*, 593–597.

Lee, K.Y., Russell, S.J., Ussar, S., Boucher, J., Vernochet, C., Mori, M.A., Smyth, G., Rourk, M., Cederquist, C., Rosen, E.D., et al. (2013). Lessons on conditional gene targeting in mouse adipose tissue. Diabetes *62*, 864–874.

Lee, M.-H., Atkinson, S., and Murphy, G. (2007). Identification of the extracellular matrix (ECM) binding motifs of tissue inhibitor of metalloproteinases (TIMP)-3 and effective transfer to TIMP-1. J. Biol. Chem. *282*, 6887–6898.

Lee, P.P., Hwang, J.J., Murphy, G., and Ip, M.M. (2000). Functional significance of MMP-9 in tumor necrosis factor-induced proliferation and branching morphogenesis of mammary epithelial cells. Endocrinology *141*, 3764–3773.

Lee, S., Jilani, S.M., Nikolova, G.V., Carpizo, D., and Iruela-Arispe, M.L. (2005). Processing of VEGF-A by matrix metalloproteinases regulates bioavailability and vascular patterning in tumors. J. Cell Biol. *169*, 681–691.

Lefebvre, O., Régnier, C., Chenard, M.P., Wendling, C., Chambon, P., Basset, P., and Rio, M.C. (1995). Developmental expression of mouse stromelysin-3 mRNA. Dev. Camb. Engl. *121*, 947–955.

Levi, E., Fridman, R., Miao, H.Q., Ma, Y.S., Yayon, A., and Vlodavsky, I. (1996). Matrix metalloproteinase 2 releases active soluble ectodomain of fibroblast growth factor receptor 1. Proc. Natl. Acad. Sci. U. S. A. *93*, 7069–7074.

Levy, A., Zucman, J., Delattre, O., Mattei, M.G., Rio, M.C., and Basset, P. (1992). Assignment of the human stromelysin 3 (STMY3) gene to the q11.2 region of chromosome 22. Genomics *13*, 881–883.

Li, L., and Li, H. (2013). Role of microRNA-mediated MMP regulation in the treatment and diagnosis of malignant tumors. Cancer Biol. Ther. *14*, 796–805.

Li, J., Liang, V.C., Sedgwick, T., Wong, J., and Shi, Y.B. (1998). Unique organization and involvement of GAGA factors in transcriptional regulation of the Xenopus stromelysin-3 gene. Nucleic Acids Res. *26*, 3018–3025.

Li, W., Li, S., Deng, L., Yang, S., Li, M., Long, S., Chen, S., Lin, F., and Xiao, L. (2015). Decreased MT1-MMP in gastric cancer suppressed cell migration and invasion via regulating MMPs and EMT. Tumour Biol. J. Int. Soc. Oncodevelopmental Biol. Med. *36*, 6883–6889.

Li, W.-M., Wei, Y.-C., Huang, C.-N., Ke, H.-L., Li, C.-C., Yeh, H.-C., Chang, L.-L., Huang, C.-H., Li, C.-F., and Wu, W.-J. (2016). Matrix metalloproteinase-11 as a marker of metastasis and predictor of poor survival in urothelial carcinomas. J. Surg. Oncol. *113*, 700–707.

Lijnen, H.R., Van Hoef, B., Vanlinthout, I., Verstreken, M., Rio, M.C., and Collen, D. (1999). Accelerated neointima formation after vascular injury in mice with stromelysin-3 (MMP-11) gene inactivation. Arterioscler. Thromb. Vasc. Biol. *19*, 2863–2870.

Lijnen, H.R., Van, H.B., Frederix, L., Rio, M.C., and Collen, D. (2002). Adipocyte hypertrophy in stromelysin-3 deficient mice with nutritionally induced obesity. Thromb. Haemost. *87*, 530–535.

Limb, G.A., Matter, K., Murphy, G., Cambrey, A.D., Bishop, P.N., Morris, G.E., and Khaw, P.T. (2005). Matrix metalloproteinase-1 associates with intracellular organelles and confers resistance to lamin A/C degradation during apoptosis. Am. J. Pathol. *166*, 1555–1563.

Lin, C.-W., Yang, S.-F., Chuang, C.-Y., Lin, H.-P., and Hsin, C.-H. (2015). Association of matrix metalloproteinase-11 polymorphisms with susceptibility and clinicopathologic characteristics for oral squamous cell carcinoma. Head Neck *37*, 1425–1431.

Lin, E.Y., Jones, J.G., Li, P., Zhu, L., Whitney, K.D., Muller, W.J., and Pollard, J.W. (2003). Progression to malignancy in the polyoma middle T oncoprotein mouse breast

cancer model provides a reliable model for human diseases. Am. J. Pathol. *163*, 2113–2126.

Lin, Y., Ukaji, T., Koide, N., and Umezawa, K. (2018). Inhibition of Late and Early Phases of Cancer Metastasis by the NF-κB Inhibitor DHMEQ Derived from Microbial Bioactive Metabolite Epoxyquinomicin: A Review. Int. J. Mol. Sci. *19*.

Liotta, L.A. (2016). Adhere, Degrade, and Move: The Three-Step Model of Invasion. Cancer Res. *76*, 3115–3117.

Littlepage, L.E., Sternlicht, M.D., Rougier, N., Phillips, J., Gallo, E., Yu, Y., Williams, K., Brenot, A., Gordon, J.I., and Werb, Z. (2010). Matrix metalloproteinases contribute distinct roles in neuroendocrine prostate carcinogenesis, metastasis, and angiogenesis progression. Cancer Res. *70*, 2224–2234.

Liu, J., and Khalil, R.A. (2017). Matrix Metalloproteinase Inhibitors as Investigational and Therapeutic Tools in Unrestrained Tissue Remodeling and Pathological Disorders. Prog. Mol. Biol. Transl. Sci. *148*, 355–420.

Liu, Z., Shipley, J.M., Vu, T.H., Zhou, X., Diaz, L.A., Werb, Z., and Senior, R.M. (1998). Gelatinase B-deficient mice are resistant to experimental bullous pemphigoid. J. Exp. Med. *188*, 475–482.

Livnat-Levanon, N., Kevei, É., Kleifeld, O., Krutauz, D., Segref, A., Rinaldi, T., Erpapazoglou, Z., Cohen, M., Reis, N., Hoppe, T., et al. (2014). Reversible 26S proteasome disassembly upon mitochondrial stress. Cell Rep. *7*, 1371–1380.

Loechel, F., Fox, J.W., Murphy, G., Albrechtsen, R., and Wewer, U.M. (2000). ADAM 12-S cleaves IGFBP-3 and IGFBP-5 and is inhibited by TIMP-3. Biochem. Biophys. Res. Commun. *278*, 511–515.

Löffek, S., Schilling, O., and Franzke, C.-W. (2011). Series "matrix metalloproteinases in lung health and disease": Biological role of matrix metalloproteinases: a critical balance. Eur. Respir. J. *38*, 191–208.

Lu, X., Wang, Q., Hu, G., Van Poznak, C., Fleisher, M., Reiss, M., Massagué, J., and Kang, Y. (2009). ADAMTS1 and MMP1 proteolytically engage EGF-like ligands in an osteolytic signaling cascade for bone metastasis. Genes Dev. *23*, 1882–1894.

Ludwig, M.G., Basset, P., and Anglard, P. (2000). Multiple regulatory elements in the murine stromelysin-3 promoter. Evidence for direct control by CCAAT/enhancer-binding protein beta and thyroid and retinoid receptors. J. Biol. Chem. *275*, 39981–39990.

Lumeng, C.N., Bodzin, J.L., and Saltiel, A.R. (2007). Obesity induces a phenotypic switch in adipose tissue macrophage polarization. J. Clin. Invest. *117*, 175–184.
Luo, J. (2005). The role of matrix metalloproteinases in the morphogenesis of the cerebellar cortex. Cerebellum Lond. Engl. *4*, 239–245.
Luo, D., Guérin, E., Ludwig, M.G., Stoll, I., Basset, P., and Anglard, P. (1999). Transcriptional induction of stromelysin-3 in mesodermal cells is mediated by an upstream CCAAT/enhancer-binding protein element associated with a DNase I-hypersensitive site. J. Biol. Chem. *274*, 37177–37185.
Luo, D., Mari, B., Stoll, I., and Anglard, P. (2002). Alternative splicing and promoter usage generates an intracellular stromelysin 3 isoform directly translated as an active matrix metalloproteinase. J. Biol. Chem. *277*, 25527–25536.
Luo, J.-L., Maeda, S., Hsu, L.-C., Yagita, H., and Karin, M. (2004). Inhibition of NF-kappaB in cancer cells converts inflammation- induced tumor growth mediated by TNFalpha to TRAIL-mediated tumor regression. Cancer Cell *6*, 297–305.
Lynch, C.C., Hikosaka, A., Acuff, H.B., Martin, M.D., Kawai, N., Singh, R.K., Vargo-Gogola, T.C., Begtrup, J.L., Peterson, T.E., Fingleton, B., et al. (2005). MMP-7 promotes prostate cancer-induced osteolysis via the solubilization of RANKL. Cancer Cell *7*, 485–496.
Ma, X., Lee, P., Chisholm, D.J., and James, D.E. (2015a). Control of adipocyte differentiation in different fat depots; implications for pathophysiology or therapy. Front. Endocrinol. *6*, 1.
Ma, Y., Chiao, Y.A., Clark, R., Flynn, E.R., Yabluchanskiy, A., Ghasemi, O., Zouein, F., Lindsey, M.L., and Jin, Y.-F. (2015b). Deriving a cardiac ageing signature to reveal MMP-9-dependent inflammatory signalling in senescence. Cardiovasc. Res. *106*, 421–431.
Macciò, A., and Madeddu, C. (2011). Obesity, inflammation, and postmenopausal breast cancer: therapeutic implications. ScientificWorldJournal *11*, 2020–2036.
Macias, H., and Hinck, L. (2012). Mammary gland development. Wiley Interdiscip. Rev. Dev. Biol. *1*, 533–557.
Malaquin, N., Vercamer, C., Bouali, F., Martien, S., Deruy, E., Wernert, N., Chwastyniak, M., Pinet, F., Abbadie, C., and Pourtier, A. (2013). Senescent fibroblasts enhance early skin carcinogenic events via a paracrine MMP-PAR-1 axis. PloS One *8*, e63607.

Mañes, S., Mira, E., Barbacid, M.M., Ciprés, A., Fernández-Resa, P., Buesa, J.M., Mérida, I., Aracil, M., Márquez, G., and Martínez-A, C. (1997a). Identification of insulin-like growth factor-binding protein-1 as a potential physiological substrate for human stromelysin-3. J. Biol. Chem. *272*, 25706–25712.

Mañes, S., Mira, E., Barbacid, M.M., Ciprés, A., Fernández-Resa, P., Buesa, J.M., Mérida, I., Aracil, M., Márquez, G., and Martínez-A, C. (1997b). Identification of insulin-like growth factor-binding protein-1 as a potential physiological substrate for human stromelysin-3. J. Biol. Chem. *272*, 25706–25712.

Manicone, A.M., and McGuire, J.K. (2008). Matrix metalloproteinases as modulators of inflammation. Semin. Cell Dev. Biol. *19*, 34–41.

Manicone, A.M., Gharib, S.A., Gong, K.-Q., Eddy, W.E., Long, M.E., Frevert, C.W., Altemeier, W.A., Parks, W.C., and Houghton, A.M. (2017). Matrix Metalloproteinase-28 Is a Key Contributor to Emphysema Pathogenesis. Am. J. Pathol. *187*, 1288–1300.

Maquoi, E., Polette, M., Nawrocki, B., Bischof, P., Noël, A., Pintiaux, A., Santavicca, M., Schaaps, J.P., Pijnenborg, R., and Birembaut, P. (1997). Expression of Stromelysin-3 in the human placenta and placental bed. Placenta *18*, 277–285.

Maquoi, E., Assent, D., Detilleux, J., Pequeux, C., Foidart, J.-M., and Noël, A. (2012). MT1-MMP protects breast carcinoma cells against type I collagen-induced apoptosis. Oncogene *31*, 480–493.

del Mar Barbacid, M., Fernández-Resa, P., Buesa, J.M., Márquez, G., Aracil, M., Quesadaand, A.R., and Mira, E. (1998). Expression and purification of human stromelysin 1 and 3 from baculovirus-infected insect cells. Protein Expr. Purif. *13*, 243–250.

Marchenko, G.N., Marchenko, N.D., and Strongin, A.Y. (2003). The structure and regulation of the human and mouse matrix metalloproteinase-21 gene and protein. Biochem. J. *372*, 503–515.

Marchenko, N.D., Marchenko, G.N., Weinreb, R.N., Lindsey, J.D., Kyshtoobayeva, A., Crawford, H.C., and Strongin, A.Y. (2004). Beta-catenin regulates the gene of MMP-26, a novel metalloproteinase expressed both in carcinomas and normal epithelial cells. Int. J. Biochem. Cell Biol. *36*, 942–956.

Maretzky, T., Reiss, K., Ludwig, A., Buchholz, J., Scholz, F., Proksch, E., de Strooper, B., Hartmann, D., and Saftig, P. (2005). ADAM10 mediates E-cadherin

shedding and regulates epithelial cell-cell adhesion, migration, and beta-catenin translocation. Proc. Natl. Acad. Sci. U. S. A. *102*, 9182–9187.

Mari, B.P., Anderson, I.C., Mari, S.E., Ning, Y., Lutz, Y., Kobzik, L., and Shipp, M.A. (1998). Stromelysin-3 is induced in tumor/stroma cocultures and inactivated via a tumor-specific and basic fibroblast growth factor-dependent mechanism. J. Biol. Chem. *273*, 618–626.

von Marschall, Z., Riecken, E.O., and Rosewicz, S. (1998). Stromelysin 3 is overexpressed in human pancreatic carcinoma and regulated by retinoic acid in pancreatic carcinoma cell lines. Gut *43*, 692–698.

Martins, D., and Schmitt, F. (2018). Microenvironment in breast tumorigenesis: Friend or foe? Histol. Histopathol. 18021.

Masson, O., Prébois, C., Derocq, D., Meulle, A., Dray, C., Daviaud, D., Quilliot, D., Valet, P., Muller, C., and Liaudet-Coopman, E. (2011). Cathepsin-D, a key protease in breast cancer, is up-regulated in obese mouse and human adipose tissue, and controls adipogenesis. PloS One *6*, e16452.

Masson, R., Lefebvre, O., Noël, A., Fahime, M.E., Chenard, M.P., Wendling, C., Kebers, F., LeMeur, M., Dierich, A., Foidart, J.M., et al. (1998). In vivo evidence that the stromelysin-3 metalloproteinase contributes in a paracrine manner to epithelial cell malignancy. J. Cell Biol. *140*, 1535–1541.

Masson, V., de la Ballina, L.R., Munaut, C., Wielockx, B., Jost, M., Maillard, C., Blacher, S., Bajou, K., Itoh, T., Itohara, S., et al. (2005). Contribution of host MMP-2 and MMP-9 to promote tumor vascularization and invasion of malignant keratinocytes. FASEB J. Off. Publ. Fed. Am. Soc. Exp. Biol. *19*, 234–236.

McQuibban, G.A. (2000). Inflammation Dampened by Gelatinase A Cleavage of Monocyte Chemoattractant Protein-3. Science *289*, 1202–1206.

McQuibban, G.A., Butler, G.S., Gong, J.H., Bendall, L., Power, C., Clark-Lewis, I., and Overall, C.M. (2001). Matrix metalloproteinase activity inactivates the CXC chemokine stromal cell-derived factor-1. J. Biol. Chem. *276*, 43503–43508.

McQuibban, G.A., Gong, J.-H., Wong, J.P., Wallace, J.L., Clark-Lewis, I., and Overall, C.M. (2002). Matrix metalloproteinase processing of monocyte chemoattractant proteins generates CC chemokine receptor antagonists with anti-inflammatory properties in vivo. Blood *100*, 1160–1167.

Meissburger, B., Ukropec, J., Roeder, E., Beaton, N., Geiger, M., Teupser, D., Civan, B., Langhans, W., Nawroth, P.P., Gasperikova, D., et al. (2011a). Adipogenesis and insulin sensitivity in obesity are regulated by retinoid-related orphan receptor gamma. EMBO Mol. Med. *3*, 637–651.

Meissburger, B., Stachorski, L., Röder, E., Rudofsky, G., and Wolfrum, C. (2011b). Tissue inhibitor of matrix metalloproteinase 1 (TIMP1) controls adipogenesis in obesity in mice and in humans. Diabetologia *54*, 1468–1479.

Menendez, J.A., and Lupu, R. (2007). Fatty acid synthase and the lipogenic phenotype in cancer pathogenesis. Nat. Rev. Cancer *7*, 763–777.

Meng, L., Zhou, J., Sasano, H., Suzuki, T., Zeitoun, K.M., and Bulun, S.E. (2001). Tumor necrosis factor alpha and interleukin 11 secreted by malignant breast epithelial cells inhibit adipocyte differentiation by selectively down-regulating CCAAT/enhancer binding protein alpha and peroxisome proliferator-activated receptor gamma: mechanism of desmoplastic reaction. Cancer Res. *61*, 2250–2255.

Migneco, G., Whitaker-Menezes, D., Chiavarina, B., Castello-Cros, R., Pavlides, S., Pestell, R.G., Fatatis, A., Flomenberg, N., Tsirigos, A., Howell, A., et al. (2010). Glycolytic cancer associated fibroblasts promote breast cancer tumor growth, without a measurable increase in angiogenesis: evidence for stromal-epithelial metabolic coupling. Cell Cycle Georget. Tex *9*, 2412–2422.

Mikhailova, M., Xu, X., Robichaud, T.K., Pal, S., Fields, G.B., and Steffensen, B. (2012). Identification of collagen binding domain residues that govern catalytic activities of matrix metalloproteinase-2 (MMP-2). Matrix Biol. J. Int. Soc. Matrix Biol. *31*, 380–388.

Miksztowicz, V., Morales, C., Zago, V., Friedman, S., Schreier, L., and Berg, G. (2014). Effect of insulin-resistance on circulating and adipose tissue MMP-2 and MMP-9 activity in rats fed a sucrose-rich diet. Nutr. Metab. Cardiovasc. Dis. NMCD *24*, 294–300.

Min, K.-W., Kim, D.-H., Do, S.-I., Pyo, J.-S., Kim, K., Chae, S.W., Sohn, J.H., Oh, Y.-H., Kim, H.J., Choi, S.H., et al. (2013). Diagnostic and prognostic relevance of MMP-11 expression in the stromal fibroblast-like cells adjacent to invasive ductal carcinoma of the breast. Ann. Surg. Oncol. *20 Suppl 3*, S433-442.

Mitsiades, N., Yu, W.H., Poulaki, V., Tsokos, M., and Stamenkovic, I. (2001). Matrix metalloproteinase-7-mediated cleavage of Fas ligand protects tumor cells from chemotherapeutic drug cytotoxicity. Cancer Res. *61*, 577–581.

Moghaddam, A., Heller, R., Daniel, V., Swing, T., Akbar, M., Gerner, H.-J., and Biglari, B. (2017). Exploratory study to suggest the possibility of MMP-8 and MMP-9 serum levels as early markers for remission after traumatic spinal cord injury. Spinal Cord *55*, 8–15.

Mohan, M.J., Seaton, T., Mitchell, J., Howe, A., Blackburn, K., Burkhart, W., Moyer, M., Patel, I., Waitt, G.M., Becherer, J.D., et al. (2002). The tumor necrosis factor-alpha converting enzyme (TACE): a unique metalloproteinase with highly defined substrate selectivity. Biochemistry (Mosc.) *41*, 9462–9469.

Monti, D., Troiano, L., Tropea, F., Grassilli, E., Cossarizza, A., Barozzi, D., Pelloni, M.C., Tamassia, M.G., Bellomo, G., and Franceschi, C. (1992). Apoptosis--programmed cell death: a role in the aging process? Am. J. Clin. Nutr. *55*, 1208S-1214S.

Moore-Smith, L.D., Isayeva, T., Lee, J.H., Frost, A., and Ponnazhagan, S. (2017). Silencing of TGF-β1 in tumor cells impacts MMP-9 in tumor microenvironment. Sci. Rep. *7*, 8678.

Morris, P.G., Hudis, C.A., Giri, D., Morrow, M., Falcone, D.J., Zhou, X.K., Du, B., Brogi, E., Crawford, C.B., Kopelovich, L., et al. (2011). Inflammation and increased aromatase expression occur in the breast tissue of obese women with breast cancer. Cancer Prev. Res. Phila. Pa *4*, 1021–1029.

Moseti, D., Regassa, A., and Kim, W.-K. (2016). Molecular Regulation of Adipogenesis and Potential Anti-Adipogenic Bioactive Molecules. Int. J. Mol. Sci. *17*.

Mosig, R.A., and Martignetti, J.A. (2013). Loss of MMP-2 in murine osteoblasts upregulates osteopontin and bone sialoprotein expression in a circuit regulating bone homeostasis. Dis. Model. Mech. *6*, 397–403.

Mosig, R.A., Dowling, O., DiFeo, A., Ramirez, M.C.M., Parker, I.C., Abe, E., Diouri, J., Aqeel, A.A., Wylie, J.D., Oblander, S.A., et al. (2007). Loss of MMP-2 disrupts skeletal and craniofacial development and results in decreased bone mineralization, joint erosion and defects in osteoblast and osteoclast growth. Hum. Mol. Genet. *16*, 1113–1123.

Mote, P.A., Arnett-Mansfield, R.L., Gava, N., deFazio, A., Mulac-Jericevic, B., Conneely, O.M., and Clarke, C.L. (2006). Overlapping and distinct expression of progesterone receptors A and B in mouse uterus and mammary gland during the estrous cycle. Endocrinology *147*, 5503–5512.

Motrescu, E.R., and Rio, M.-C. (2008). Cancer cells, adipocytes and matrix metalloproteinase 11: a vicious tumor progression cycle. Biol. Chem. *389*, 1037–1041.

Motrescu, E.R., Blaise, S., Etique, N., Messaddeq, N., Chenard, M.-P., Stoll, I., Tomasetto, C., and Rio, M.-C. (2008). Matrix metalloproteinase-11/stromelysin-3 exhibits collagenolytic function against collagen VI under normal and malignant conditions. Oncogene *27*, 6347–6355.

Mu, D., Cambier, S., Fjellbirkeland, L., Baron, J.L., Munger, J.S., Kawakatsu, H., Sheppard, D., Broaddus, V.C., and Nishimura, S.L. (2002). The integrin alpha(v)beta8 mediates epithelial homeostasis through MT1-MMP-dependent activation of TGF-beta1. J. Cell Biol. *157*, 493–507.

Mucha, A., Cuniasse, P., Kannan, R., Beau, F., Yiotakis, A., Basset, P., and Dive, V. (1998). Membrane Type-1 Matrix Metalloprotease and Stromelysin-3 Cleave More Efficiently Synthetic Substrates Containing Unusual Amino Acids in Their P_1' Positions. J. Biol. Chem. *273*, 2763–2768.

Mudgett, J.S., Hutchinson, N.I., Chartrain, N.A., Forsyth, A.J., McDonnell, J., Singer, I.I., Bayne, E.K., Flanagan, J., Kawka, D., Shen, C.F., et al. (1998). Susceptibility of stromelysin 1-deficient mice to collagen-induced arthritis and cartilage destruction. Arthritis Rheum. *41*, 110–121.

Müller, A., Homey, B., Soto, H., Ge, N., Catron, D., Buchanan, M.E., McClanahan, T., Murphy, E., Yuan, W., Wagner, S.N., et al. (2001). Involvement of chemokine receptors in breast cancer metastasis. Nature *410*, 50–56.

Murphy, G. (2008). The ADAMs: signalling scissors in the tumour microenvironment. Nat. Rev. Cancer *8*, 929–941.

Murphy, G. (2011). Tissue inhibitors of metalloproteinases. Genome Biol. *12*, 233.

Murphy, G., and Nagase, H. (2008). Progress in matrix metalloproteinase research. Mol. Aspects Med. *29*, 290–308.

Murphy, G., Segain, J.P., O'Shea, M., Cockett, M., Ioannou, C., Lefebvre, O., Chambon, P., and Basset, P. (1993). The 28-kDa N-terminal domain of mouse

stromelysin-3 has the general properties of a weak metalloproteinase. J. Biol. Chem. *268*, 15435–15441.

Murphy, G.J., Murphy, G., and Reynolds, J.J. (1991). The origin of matrix metalloproteinases and their familial relationships. FEBS Lett. *289*, 4–7.

Musumeci, G., Castrogiovanni, P., Szychlinska, M.A., Aiello, F.C., Vecchio, G.M., Salvatorelli, L., Magro, G., and Imbesi, R. (2015). Mammary gland: From embryogenesis to adult life. Acta Histochem. *117*, 379–385.

Nagase, H. (1998). Cell surface activation of progelatinase A (proMMP-2) and cell migration. Cell Res. *8*, 179–186.

Nagase, H., and Visse, R. (2009). Matrix Metalloproteinases: An Overview. In Drug Design of Zinc-Enzyme Inhibitors, C.T. Supuran, and J.-Y. Winum, eds. (Hoboken, NJ, USA: John Wiley & Sons, Inc.), pp. 487–517.

Nagase, H., Suzuki, K., Morodomi, T., Enghild, J.J., and Salvesen, G. (1992). Activation mechanisms of the precursors of matrix metalloproteinases 1, 2 and 3. Matrix Stuttg. Ger. Suppl. *1*, 237–244.

Nakahara, H., Howard, L., Thompson, E.W., Sato, H., Seiki, M., Yeh, Y., and Chen, W.T. (1997). Transmembrane/cytoplasmic domain-mediated membrane type 1-matrix metalloprotease docking to invadopodia is required for cell invasion. Proc. Natl. Acad. Sci. U. S. A. *94*, 7959–7964.

Nakamura, E.S., Koizumi, K., Kobayashi, M., and Saiki, I. (2004). Inhibition of lymphangiogenesis-related properties of murine lymphatic endothelial cells and lymph node metastasis of lung cancer by the matrix metalloproteinase inhibitor MMI270. Cancer Sci. *95*, 25–31.

Nakamura, M., Miyamoto, S., Maeda, H., Ishii, G., Hasebe, T., Chiba, T., Asaka, M., and Ochiai, A. (2005). Matrix metalloproteinase-7 degrades all insulin-like growth factor binding proteins and facilitates insulin-like growth factor bioavailability. Biochem. Biophys. Res. Commun. *333*, 1011–1016.

Narimiya, T., Wada, S., Kanzaki, H., Ishikawa, M., Tsuge, A., Yamaguchi, Y., and Nakamura, Y. (2017). Orthodontic tensile strain induces angiogenesis via type IV collagen degradation by matrix metalloproteinase-12. J. Periodontal Res. *52*, 842–852.

Nath, D., Williamson, N.J., Jarvis, R., and Murphy, G. (2001). Shedding of c-Met is regulated by crosstalk between a G-protein coupled receptor and the EGF receptor

and is mediated by a TIMP-3 sensitive metalloproteinase. J. Cell Sci. *114*, 1213–1220.

Naylor, M.J., and Ormandy, C.J. (2002). Mouse strain-specific patterns of mammary epithelial ductal side branching are elicited by stromal factors. Dev. Dyn. *225*, 100–105.

Nicotra, G., Castino, R., Follo, C., Peracchio, C., Valente, G., and Isidoro, C. (2010). The dilemma: does tissue expression of cathepsin D reflect tumor malignancy? The question: does the assay truly mirror cathepsin D mis-function in the tumor? Cancer Biomark. Sect. Dis. Markers *7*, 47–64.

Nieman, K.M., Kenny, H.A., Penicka, C.V., Ladanyi, A., Buell-Gutbrod, R., Zillhardt, M.R., Romero, I.L., Carey, M.S., Mills, G.B., Hotamisligil, G.S., et al. (2011). Adipocytes promote ovarian cancer metastasis and provide energy for rapid tumor growth. Nat. Med. *17*, 1498–1503.

Noël, A., Santavicca, M., Stoll, I., L'Hoir, C., Staub, A., Murphy, G., Rio, M.-C., and Basset, P. (1995). Identification of Structural Determinants Controlling Human and Mouse Stromelysin-3 Proteolytic Activities. J. Biol. Chem. *270*, 22866–22872.

Nozawa, H., Chiu, C., and Hanahan, D. (2006). Infiltrating neutrophils mediate the initial angiogenic switch in a mouse model of multistage carcinogenesis. Proc. Natl. Acad. Sci. U. S. A. *103*, 12493–12498.

Nuti, E., Cuffaro, D., Bernardini, E., Camodeca, C., Panelli, L., Chaves, S., Ciccone, L., Tepshi, L., Vera, L., Orlandini, E., et al. (2018). Development of Thioaryl-Based Matrix Metalloproteinase-12 Inhibitors with Alternative Zinc-Binding Groups: Synthesis, Potentiometric, NMR, and Crystallographic Studies. J. Med. Chem. *61*, 4421–4435.

Oblander, S.A., Zhou, Z., Gálvez, B.G., Starcher, B., Shannon, J.M., Durbeej, M., Arroyo, A.G., Tryggvason, K., and Apte, S.S. (2005). Distinctive functions of membrane type 1 matrix-metalloprotease (MT1-MMP or MMP-14) in lung and submandibular gland development are independent of its role in pro-MMP-2 activation. Dev. Biol. *277*, 255–269.

Oh, J., Takahashi, R., Adachi, E., Kondo, S., Kuratomi, S., Noma, A., Alexander, D.B., Motoda, H., Okada, A., Seiki, M., et al. (2004). Mutations in two matrix metalloproteinase genes, MMP-2 and MT1-MMP, are synthetic lethal in mice. Oncogene *23*, 5041–5048.

Ohuchi, E., Imai, K., Fujii, Y., Sato, H., Seiki, M., and Okada, Y. (1997). Membrane type 1 matrix metalloproteinase digests interstitial collagens and other extracellular matrix macromolecules. J. Biol. Chem. *272*, 2446–2451.

Opdenakker, G., Van den Steen, P.E., and Van Damme, J. (2001). Gelatinase B: a tuner and amplifier of immune functions. Trends Immunol. *22*, 571–579.

Paiva, K.B.S., and Granjeiro, J.M. (2014). Bone tissue remodeling and development: focus on matrix metalloproteinase functions. Arch. Biochem. Biophys. *561*, 74–87.

Paiva, K.B.S., and Granjeiro, J.M. (2017). Matrix Metalloproteinases in Bone Resorption, Remodeling, and Repair. Prog. Mol. Biol. Transl. Sci. *148*, 203–303.

Palavalli, L.H., Prickett, T.D., Wunderlich, J.R., Wei, X., Burrell, A.S., Porter-Gill, P., Davis, S., Wang, C., Cronin, J.C., Agrawal, N.S., et al. (2009). Analysis of the matrix metalloproteinase family reveals that MMP8 is often mutated in melanoma. Nat. Genet. *41*, 518–520.

Pang, L., Wang, D.-W., Zhang, N., Xu, D.-H., and Meng, X.-W. (2016). Elevated serum levels of MMP-11 correlate with poor prognosis in colon cancer patients. Cancer Biomark. Sect. Dis. Markers *16*, 599–607.

Papa, L., and Germain, D. (2011). Estrogen receptor mediates a distinct mitochondrial unfolded protein response. J. Cell Sci. *124*, 1396–1402.

Park, H.I., Ni, J., Gerkema, F.E., Liu, D., Belozerov, V.E., and Sang, Q.X. (2000). Identification and characterization of human endometase (Matrix metalloproteinase-26) from endometrial tumor. J. Biol. Chem. *275*, 20540–20544.

Park, J., Euhus, D.M., and Scherer, P.E. (2011). Paracrine and endocrine effects of adipose tissue on cancer development and progression. Endocr. Rev. *32*, 550–570.

Parks, W.C., Wilson, C.L., and López-Boado, Y.S. (2004). Matrix metalloproteinases as modulators of inflammation and innate immunity. Nat. Rev. Immunol. *4*, 617–629.

Patterson, M.L., Atkinson, S.J., Knäuper, V., and Murphy, G. (2001). Specific collagenolysis by gelatinase A, MMP-2, is determined by the hemopexin domain and not the fibronectin-like domain. FEBS Lett. *503*, 158–162.

Patterton, D., Hayes, W.P., and Shi, Y.B. (1995). Transcriptional activation of the matrix metalloproteinase gene stromelysin-3 coincides with thyroid hormone-induced cell death during frog metamorphosis. Dev. Biol. *167*, 252–262.

Pavlides, S., Whitaker-Menezes, D., Castello-Cros, R., Flomenberg, N., Witkiewicz, A.K., Frank, P.G., Casimiro, M.C., Wang, C., Fortina, P., Addya, S., et al. (2009).

The reverse Warburg effect: aerobic glycolysis in cancer associated fibroblasts and the tumor stroma. Cell Cycle Georget. Tex *8*, 3984–4001.
Pavlovich, A.L., Manivannan, S., and Nelson, C.M. (2010). Adipose stroma induces branching morphogenesis of engineered epithelial tubules. Tissue Eng. Part A *16*, 3719–3726.
Pedersen, M.E., Vuong, T.T., Rønning, S.B., and Kolset, S.O. (2015). Matrix metalloproteinases in fish biology and matrix turnover. Matrix Biol. J. Int. Soc. Matrix Biol. *44–46*, 86–93.
Pei, D., and Weiss, S.J. (1995). Furin-dependent intracellular activation of the human stromelysin-3 zymogen. Nature *375*, 244–247.
Pei, D., Majmudar, G., and Weiss, S.J. (1994). Hydrolytic inactivation of a breast carcinoma cell-derived serpin by human stromelysin-3. J. Biol. Chem. *269*, 25849–25855.
Pei, D., Kang, T., and Qi, H. (2000). Cysteine array matrix metalloproteinase (CA-MMP)/MMP-23 is a type II transmembrane matrix metalloproteinase regulated by a single cleavage for both secretion and activation. J. Biol. Chem. *275*, 33988–33997.
Peinado, H., Zhang, H., Matei, I.R., Costa-Silva, B., Hoshino, A., Rodrigues, G., Psaila, B., Kaplan, R.N., Bromberg, J.F., Kang, Y., et al. (2017). Pre-metastatic niches: organ-specific homes for metastases. Nat. Rev. Cancer *17*, 302–317.
Pelletier, J., and Sonenberg, N. (1988). Internal initiation of translation of eukaryotic mRNA directed by a sequence derived from poliovirus RNA. Nature *334*, 320–325.
Pendás, A.M., Folgueras, A.R., Llano, E., Caterina, J., Frerard, F., Rodríguez, F., Astudillo, A., Noël, A., Birkedal-Hansen, H., and López-Otín, C. (2004). Diet-induced obesity and reduced skin cancer susceptibility in matrix metalloproteinase 19-deficient mice. Mol. Cell. Biol. *24*, 5304–5313.
Peschon, J.J., Slack, J.L., Reddy, P., Stocking, K.L., Sunnarborg, S.W., Lee, D.C., Russell, W.E., Castner, B.J., Johnson, R.S., Fitzner, J.N., et al. (1998). An essential role for ectodomain shedding in mammalian development. Science *282*, 1281–1284.
Pilcher, B.K., Dumin, J.A., Sudbeck, B.D., Krane, S.M., Welgus, H.G., and Parks, W.C. (1997). The activity of collagenase-1 is required for keratinocyte migration on a type I collagen matrix. J. Cell Biol. *137*, 1445–1457.

Pilka, R., Kudela, M., Eriksson, P., and Casslén, B. (2005). [MMP-26 mRNA and estrogen receptor alpha co-expression in normal and pathological endometrium]. Ceska Gynekol. *70*, 56–62.

Poincloux, R., Lizarraga, F., and Chavrier, P. (2009). Matrix invasion by tumour cells: a focus on MT1-MMP trafficking to invadopodia. J. Cell Sci. *122*, 3015–3024.

Pollak, M. (2008). Insulin and insulin-like growth factor signalling in neoplasia. Nat. Rev. Cancer *8*, 915–928.

Polyak, K., and Metzger Filho, O. (2012). SnapShot: breast cancer. Cancer Cell *22*, 562-562.e1.

Polyak, K., and Weinberg, R.A. (2009). Transitions between epithelial and mesenchymal states: acquisition of malignant and stem cell traits. Nat. Rev. Cancer *9*, 265–273.

Pommier, Y., Leo, E., Zhang, H., and Marchand, C. (2010). DNA topoisomerases and their poisoning by anticancer and antibacterial drugs. Chem. Biol. *17*, 421–433.

Powell, W.C., Fingleton, B., Wilson, C.L., Boothby, M., and Matrisian, L.M. (1999). The metalloproteinase matrilysin proteolytically generates active soluble Fas ligand and potentiates epithelial cell apoptosis. Curr. Biol. CB *9*, 1441–1447.

Quail, D.F., and Joyce, J.A. (2013). Microenvironmental regulation of tumor progression and metastasis. Nat. Med. *19*, 1423–1437.

Ra, H.-J., and Parks, W.C. (2007). Control of matrix metalloproteinase catalytic activity. Matrix Biol. J. Int. Soc. Matrix Biol. *26*, 587–596.

Rabot, A., Sinowatz, F., Berisha, B., Meyer, H.H.D., and Schams, D. (2007). Expression and localization of extracellular matrix-degrading proteinases and their inhibitors in the bovine mammary gland during development, function, and involution. J. Dairy Sci. *90*, 740–748.

Radisky, D.C., Levy, D.D., Littlepage, L.E., Liu, H., Nelson, C.M., Fata, J.E., Leake, D., Godden, E.L., Albertson, D.G., Nieto, M.A., et al. (2005). Rac1b and reactive oxygen species mediate MMP-3-induced EMT and genomic instability. Nature *436*, 123–127.

Raykov, Z., Grekova, S.P., Bour, G., Lehn, J.M., Giese, N.A., Nicolau, C., and Aprahamian, M. (2014). Myo-inositol trispyrophosphate-mediated hypoxia reversion controls pancreatic cancer in rodents and enhances gemcitabine efficacy. Int. J. Cancer *134*, 2572–2582.

Redondo-Muñoz, J., Ugarte-Berzal, E., Terol, M.J., Van den Steen, P.E., Hernández del Cerro, M., Roderfeld, M., Roeb, E., Opdenakker, G., García-Marco, J.A., and García-Pardo, A. (2010). Matrix metalloproteinase-9 promotes chronic lymphocytic leukemia b cell survival through its hemopexin domain. Cancer Cell *17*, 160–172.

Rehman, A.A., Ahsan, H., and Khan, F.H. (2013). α-2-Macroglobulin: a physiological guardian. J. Cell. Physiol. *228*, 1665–1675.

Ren, F., Tang, R., Zhang, X., Madushi, W.M., Luo, D., Dang, Y., Li, Z., Wei, K., and Chen, G. (2015). Overexpression of MMP Family Members Functions as Prognostic Biomarker for Breast Cancer Patients: A Systematic Review and Meta-Analysis. PloS One *10*, e0135544.

Richards, R.G., Klotz, D.M., Walker, M.P., and Diaugustine, R.P. (2004). Mammary gland branching morphogenesis is diminished in mice with a deficiency of insulin-like growth factor-I (IGF-I), but not in mice with a liver-specific deletion of IGF-I. Endocrinology *145*, 3106–3110.

Rikimaru, A., Komori, K., Sakamoto, T., Ichise, H., Yoshida, N., Yana, I., and Seiki, M. (2007). Establishment of an MT4-MMP-deficient mouse strain representing an efficient tracking system for MT4-MMP/MMP-17 expression in vivo using beta-galactosidase. Genes Cells Devoted Mol. Cell. Mech. *12*, 1091–1100.

Rio, M.-C. (2002). Stromelysin-3, a Particular Member of the Matrix Metalloproteinase Family. In Proteases and Their Inhibitors in Cancer Metastasis, J.-M. Foidart, and R.J. Muschel, eds. (Dordrecht: Kluwer Academic Publishers), pp. 81–107.

Rio, M.-C. (2011). The Role of Cancer-Associated Adipocytes (CAA) in the Dynamic Interaction Between the Tumor and the Host. In Tumor-Associated Fibroblasts and Their Matrix, M.M. Mueller, and N.E. Fusenig, eds. (Dordrecht: Springer Netherlands), pp. 111–123.

Rio, M.-C. (2013). Matrix Metalloproteinase-11/Stromelysin 3. In Handbook of Proteolytic Enzymes, (Elsevier), pp. 779–786.

Rio, M.C., Lefebvre, O., Santavicca, M., Noël, A., Chenard, M.P., Anglard, P., Byrne, J.A., Okada, A., Régnier, C.H., Masson, R., et al. (1996). Stromelysin-3 in the biology of the normal and neoplastic mammary gland. J. Mammary Gland Biol. Neoplasia *1*, 231–240.

Rio, M.-C., Dali-Youcef, N., and Tomasetto, C. (2015). Local adipocyte cancer cell paracrine loop: can “sick fat” be more detrimental? Horm. Mol. Biol. Clin. Investig. *21*, 43–56.

Roach, H.I., Yamada, N., Cheung, K.S.C., Tilley, S., Clarke, N.M.P., Oreffo, R.O.C., Kokubun, S., and Bronner, F. (2005). Association between the abnormal expression of matrix-degrading enzymes by human osteoarthritic chondrocytes and demethylation of specific CpG sites in the promoter regions. Arthritis Rheum. *52*, 3110–3124.

Robichaud, N., del Rincon, S.V., Huor, B., Alain, T., Petruccelli, L.A., Hearnden, J., Goncalves, C., Grotegut, S., Spruck, C.H., Furic, L., et al. (2015). Phosphorylation of eIF4E promotes EMT and metastasis via translational control of SNAIL and MMP-3. Oncogene *34*, 2032–2042.

Robichaud, T.K., Steffensen, B., and Fields, G.B. (2011). Exosite Interactions Impact Matrix Metalloproteinase Collagen Specificities. J. Biol. Chem. *286*, 37535–37542.

Rockstroh, D., Löffler, D., Kiess, W., Landgraf, K., and Körner, A. (2016). Regulation of human adipogenesis by miR125b-5p. Adipocyte *5*, 283–297.

Rodriguez-Viciana, P., Collins, C., and Fried, M. (2006). Polyoma and SV40 proteins differentially regulate PP2A to activate distinct cellular signaling pathways involved in growth control. Proc. Natl. Acad. Sci. U. S. A. *103*, 19290–19295.

Rojiani, M.V., Ghoshal-Gupta, S., Kutiyanawalla, A., Mathur, S., and Rojiani, A.M. (2015). TIMP-1 overexpression in lung carcinoma enhances tumor kinetics and angiogenesis in brain metastasis. J. Neuropathol. Exp. Neurol. *74*, 293–304.

Roscilli, G., Cappelletti, M., De Vitis, C., Ciliberto, G., Di Napoli, A., Ruco, L., Mancini, R., and Aurisicchio, L. (2014). Circulating MMP11 and specific antibody immune response in breast and prostate cancer patients. J. Transl. Med. *12*, 54.

Ross, S.R., Graves, R.A., Greenstein, A., Platt, K.A., Shyu, H.L., Mellovitz, B., and Spiegelman, B.M. (1990). A fat-specific enhancer is the primary determinant of gene expression for adipocyte P2 in vivo. Proc. Natl. Acad. Sci. U. S. A. *87*, 9590–9594.

Rosse, C., Lodillinsky, C., Fuhrmann, L., Nourieh, M., Monteiro, P., Irondelle, M., Lagoutte, E., Vacher, S., Waharte, F., Paul-Gilloteaux, P., et al. (2014). Control of MT1-MMP transport by atypical PKC during breast-cancer progression. Proc. Natl. Acad. Sci. *111*, E1872–E1879.

Rossi, M.L., Rehman, A.A., and Gondi, C.S. (2014). Therapeutic options for the management of pancreatic cancer. World J. Gastroenterol. *20*, 11142–11159.
Rouyer, N., Wolf, C., Chenard, M.P., Rio, M.C., Chambon, P., Bellocq, J.P., and Basset, P. (1994). Stromelysin-3 gene expression in human cancer: an overview. Invasion Metastasis *14*, 269–275.
Rozanov, D.V., Sikora, S., Godzik, A., Postnova, T.I., Golubkov, V., Savinov, A., Tomlinson, S., and Strongin, A.Y. (2004). Non-proteolytic, receptor/ligand interactions associate cellular membrane type-1 matrix metalloproteinase with the complement component C1q. J. Biol. Chem. *279*, 50321–50328.
Ryu, O.H., Fincham, A.G., Hu, C.C., Zhang, C., Qian, Q., Bartlett, J.D., and Simmer, J.P. (1999). Characterization of recombinant pig enamelysin activity and cleavage of recombinant pig and mouse amelogenins. J. Dent. Res. *78*, 743–750.
Sahin, U., Weskamp, G., Kelly, K., Zhou, H.-M., Higashiyama, S., Peschon, J., Hartmann, D., Saftig, P., and Blobel, C.P. (2004). Distinct roles for ADAM10 and ADAM17 in ectodomain shedding of six EGFR ligands. J. Cell Biol. *164*, 769–779.
Sakakura, T. (1987). Mammary embryogenesis. Mammary Gland *37*, 66.
Sakamoto, T., and Seiki, M. (2009). Cytoplasmic tail of MT1-MMP regulates macrophage motility independently from its protease activity. Genes Cells Devoted Mol. Cell. Mech. *14*, 617–626.
Sambiasi, D., Summa, S.D., Digennaro, M., Pilato, B., Paradiso, A., and Tommasi, S. (2017). Adipokines in hereditary breast cancer patients and healthy relatives. Oncotarget *8*, 101255–101261.
Sand, J.M., Larsen, L., Hogaboam, C., Martinez, F., Han, M., Røssel Larsen, M., Nawrocki, A., Zheng, Q., Karsdal, M.A., and Leeming, D.J. (2013). MMP mediated degradation of type IV collagen alpha 1 and alpha 3 chains reflects basement membrane remodeling in experimental and clinical fibrosis--validation of two novel biomarker assays. PloS One *8*, e84934.
Santavicca, M., Noel, A., Angliker, H., Stoll, I., Segain, J.P., Anglard, P., Chretien, M., Seidah, N., and Basset, P. (1996). Characterization of structural determinants and molecular mechanisms involved in pro-stromelysin-3 activation by 4-aminophenylmercuric acetate and furin-type convertases. Biochem. J. *315 (Pt 3)*, 953–958.

Santibanez, J.F., Obradović, H., Kukolj, T., and Krstić, J. (2018). Transforming growth factor-β, matrix metalloproteinases, and urokinase-type plasminogen activator interaction in the cancer epithelial to mesenchymal transition. Dev. Dyn. Off. Publ. Am. Assoc. Anat. *247*, 382–395.

Sarvaiya, P.J., Guo, D., Ulasov, I., Gabikian, P., and Lesniak, M.S. (2013). Chemokines in tumor progression and metastasis. Oncotarget *4*, 2171–2185.

Sazeides, C., and Le, A. (2018). Metabolic Relationship between Cancer-Associated Fibroblasts and Cancer Cells. Adv. Exp. Med. Biol. *1063*, 149–165.

Schlage, P., and auf dem Keller, U. (2015). Proteomic approaches to uncover MMP function. Matrix Biol. J. Int. Soc. Matrix Biol. *44–46*, 232–238.

Scholzen, T., and Gerdes, J. (2000). The Ki-67 protein: from the known and the unknown. J. Cell. Physiol. *182*, 311–322.

Schönbeck, U., Mach, F., Sukhova, G.K., Atkinson, E., Levesque, E., Herman, M., Graber, P., Basset, P., and Libby, P. (1999). Expression of stromelysin-3 in atherosclerotic lesions: regulation via CD40-CD40 ligand signaling in vitro and in vivo. J. Exp. Med. *189*, 843–853.

Schröpfer, A., Kammerer, U., Kapp, M., Dietl, J., Feix, S., and Anacker, J. (2010). Expression pattern of matrix metalloproteinases in human gynecological cancer cell lines. BMC Cancer *10*, 553.

Segref, A., Kevei, É., Pokrzywa, W., Schmeisser, K., Mansfeld, J., Livnat-Levanon, N., Ensenauer, R., Glickman, M.H., Ristow, M., and Hoppe, T. (2014). Pathogenesis of human mitochondrial diseases is modulated by reduced activity of the ubiquitin/proteasome system. Cell Metab. *19*, 642–652.

Seiki, M. (2003). Membrane-type 1 matrix metalloproteinase: a key enzyme for tumor invasion. Cancer Lett. *194*, 1–11.

Seo, G.Y., Ho, M.T., Bui, N.T., Kim, Y.M., Koh, D., Lim, Y., Hyun, C., and Cho, M. (2015). Novel naphthochalcone derivative accelerate dermal wound healing through induction of epithelial-mesenchymal transition of keratinocyte. J. Biomed. Sci. *22*, 47.

Seubert, B., Grünwald, B., Kobuch, J., Cui, H., Schelter, F., Schaten, S., Siveke, J.T., Lim, N.H., Nagase, H., Simonavicius, N., et al. (2015). Tissue inhibitor of metalloproteinases (TIMP)-1 creates a premetastatic niche in the liver through SDF-1/CXCR4-dependent neutrophil recruitment in mice. Hepatol. Baltim. Md *61*, 238–248.

Shao, L., Zhang, B., Wang, L., Wu, L., Kan, Q., and Fan, K. (2017). MMP-9-cleaved osteopontin isoform mediates tumor immune escape by inducing expansion of myeloid-derived suppressor cells. Biochem. Biophys. Res. Commun. *493*, 1478–1484.

Shen, K., Johnson, D.W., Vesey, D.A., McGuckin, M.A., and Gobe, G.C. (2018). Role of the unfolded protein response in determining the fate of tumor cells and the promise of multi-targeted therapies. Cell Stress Chaperones *23*, 317–334.

Shen, Q., Lee, E.S., Pitts, R.L., Wu, M.H., and Yuan, S.Y. (2010). Tissue inhibitor of metalloproteinase-2 regulates matrix metalloproteinase-2-mediated endothelial barrier dysfunction and breast cancer cell transmigration through lung microvascular endothelial cells. Mol. Cancer Res. MCR *8*, 939–951.

Sheu, B.C., Hsu, S.M., Ho, H.N., Lien, H.C., Huang, S.C., and Lin, R.H. (2001). A novel role of metalloproteinase in cancer-mediated immunosuppression. Cancer Res. *61*, 237–242.

Shi, J., Son, M.-Y., Yamada, S., Szabova, L., Kahan, S., Chrysovergis, K., Wolf, L., Surmak, A., and Holmbeck, K. (2008). Membrane-type MMPs enable extracellular matrix permissiveness and mesenchymal cell proliferation during embryogenesis. Dev. Biol. *313*, 196–209.

Shi, Y.-B., Fu, L., Hasebe, T., and Ishizuya-Oka, A. (2007). Regulation of extracellular matrix remodeling and cell fate determination by matrix metalloproteinase stromelysin-3 during thyroid hormone-dependent post-embryonic development. Pharmacol. Ther. *116*, 391–400.

Shih, C.-L.M., and Ajuwon, K.M. (2015). Inhibition of MMP-13 prevents diet-induced obesity in mice and suppresses adipogenesis in 3T3-L1 preadipocytes. Mol. Biol. Rep. *42*, 1225–1232.

Shin, J., Li, B., Davis, M.E., Suh, Y., and Lee, K. (2009). Comparative analysis of fatty acid-binding protein 4 promoters: conservation of peroxisome proliferator-activated receptor binding sites. J. Anim. Sci. *87*, 3923–3934.

Shipley, J.M., Wesselschmidt, R.L., Kobayashi, D.K., Ley, T.J., and Shapiro, S.D. (1996). Metalloelastase is required for macrophage-mediated proteolysis and matrix invasion in mice. Proc. Natl. Acad. Sci. U. S. A. *93*, 3942–3946.

Shoshani, O., and Zipori, D. (2011). Mammalian cell dedifferentiation as a possible outcome of stress. Stem Cell Rev. *7*, 488–493.

Sihn, G., Walter, T., Klein, J.-C., Queguiner, I., Iwao, H., Nicolau, C., Lehn, J.-M., Corvol, P., and Gasc, J.-M. (2007). Anti-angiogenic properties of myo-inositol trispyrophosphate in ovo and growth reduction of implanted glioma. FEBS Lett. *581*, 962–966.

Simian, M., Bissell, M.J., Barcellos-Hoff, M.H., and Shyamala, G. (2009). Estrogen and progesterone receptors have distinct roles in the establishment of the hyperplastic phenotype in PR-A transgenic mice. Breast Cancer Res. BCR *11*, R72.

Singer, C.F., Marbaix, E., Lemoine, P., Courtoy, P.J., and Eeckhout, Y. (1999). Local cytokines induce differential expression of matrix metalloproteinases but not their tissue inhibitors in human endometrial fibroblasts. Eur. J. Biochem. *259*, 40–45.

Sirotnak, F.M., DeGraw, J.I., Schmid, F.A., Goutas, L.J., and Moccio, D.M. (1984). New folate analogs of the 10-deaza-aminopterin series. Further evidence for markedly increased antitumor efficacy compared with methotrexate in ascitic and solid murine tumor models. Cancer Chemother. Pharmacol. *12*, 26–30.

Si-Tayeb, K., Monvoisin, A., Mazzocco, C., Lepreux, S., Decossas, M., Cubel, G., Taras, D., Blanc, J.-F., Robinson, D.R., and Rosenbaum, J. (2006). Matrix metalloproteinase 3 is present in the cell nucleus and is involved in apoptosis. Am. J. Pathol. *169*, 1390–1401.

Skoglund, J., Emterling, A., Arbman, G., Anglard, P., and Sun, X.-F. (2004). Clinicopathological significance of stromelysin-3 expression in colorectal cancer. Oncology *67*, 67–72.

Slattery, M.L., Sweeney, C., Wolff, R., Herrick, J., Baumgartner, K., Giuliano, A., and Byers, T. (2007). Genetic variation in IGF1, IGFBP3, IRS1, IRS2 and risk of breast cancer in women living in Southwestern United States. Breast Cancer Res. Treat. *104*, 197–209.

Smathers, R.L., and Petersen, D.R. (2011). The human fatty acid-binding protein family: evolutionary divergences and functions. Hum. Genomics *5*, 170–191.

Smeitink, J.A., Zeviani, M., Turnbull, D.M., and Jacobs, H.T. (2006). Mitochondrial medicine: a metabolic perspective on the pathology of oxidative phosphorylation disorders. Cell Metab. *3*, 9–13.

Sohail, A., Sun, Q., Zhao, H., Bernardo, M.M., Cho, J.-A., and Fridman, R. (2008). MT4-(MMP17) and MT6-MMP (MMP25), A unique set of membrane-anchored

matrix metalloproteinases: properties and expression in cancer. Cancer Metastasis Rev. *27*, 289–302.

Son, H.-J., and Moon, A. (2010). Epithelial-mesenchymal Transition and Cell Invasion. Toxicol. Res. *26*, 245–252.

Soria-Valles, C., Gutiérrez-Fernández, A., Guiu, M., Mari, B., Fueyo, A., Gomis, R.R., and López-Otín, C. (2014). The anti-metastatic activity of collagenase-2 in breast cancer cells is mediated by a signaling pathway involving decorin and miR-21. Oncogene *33*, 3054–3063.

Sounni, N.E., Dehne, K., van Kempen, L., Egeblad, M., Affara, N.I., Cuevas, I., Wiesen, J., Junankar, S., Korets, L., Lee, J., et al. (2010). Stromal regulation of vessel stability by MMP14 and TGFbeta. Dis. Model. Mech. *3*, 317–332.

Soysal, S.D., Tzankov, A., and Muenst, S.E. (2015). Role of the Tumor Microenvironment in Breast Cancer. Pathobiol. J. Immunopathol. Mol. Cell. Biol. *82*, 142–152.

Stawski, L., Haines, P., Fine, A., Rudnicka, L., and Trojanowska, M. (2014). MMP-12 deficiency attenuates angiotensin II-induced vascular injury, M2 macrophage accumulation, and skin and heart fibrosis. PloS One *9*, e109763.

Steinhusen, U., Weiske, J., Badock, V., Tauber, R., Bommert, K., and Huber, O. (2001). Cleavage and shedding of E-cadherin after induction of apoptosis. J. Biol. Chem. *276*, 4972–4980.

Sternlicht, M.D., and Werb, Z. (2001). How matrix metalloproteinases regulate cell behavior. Annu. Rev. Cell Dev. Biol. *17*, 463–516.

Stetler-Stevenson, W.G. (1999). Matrix metalloproteinases in angiogenesis: a moving target for therapeutic intervention. J. Clin. Invest. *103*, 1237–1241.

Stickens, D., Behonick, D.J., Ortega, N., Heyer, B., Hartenstein, B., Yu, Y., Fosang, A.J., Schorpp-Kistner, M., Angel, P., and Werb, Z. (2004). Altered endochondral bone development in matrix metalloproteinase 13-deficient mice. Dev. Camb. Engl. *131*, 5883–5895.

Stracke, J.O., Hutton, M., Stewart, M., Pendás, A.M., Smith, B., López-Otin, C., Murphy, G., and Knäuper, V. (2000). Biochemical characterization of the catalytic domain of human matrix metalloproteinase 19. Evidence for a role as a potent basement membrane degrading enzyme. J. Biol. Chem. *275*, 14809–14816.

Stricker, T.P., Dumin, J.A., Dickeson, S.K., Chung, L., Nagase, H., Parks, W.C., and Santoro, S.A. (2001). Structural analysis of the alpha(2) integrin I domain/procollagenase-1 (matrix metalloproteinase-1) interaction. J. Biol. Chem. *276*, 29375–29381.

Struyf, S., Proost, P., Vandercappellen, J., Dempe, S., Noyens, B., Nelissen, S., Gouwy, M., Locati, M., Opdenakker, G., Dinsart, C., et al. (2009). Synergistic up-regulation of MCP-2/CCL8 activity is counteracted by chemokine cleavage, limiting its inflammatory and anti-tumoral effects. Eur. J. Immunol. *39*, 843–857.

Subbaramaiah, K., Howe, L.R., Bhardwaj, P., Du, B., Gravaghi, C., Yantiss, R.K., Zhou, X.K., Blaho, V.A., Hla, T., Yang, P., et al. (2011). Obesity is associated with inflammation and elevated aromatase expression in the mouse mammary gland. Cancer Prev. Res. Phila. Pa *4*, 329–346.

Sugiura, K., and Stock, C.C. (1952). Studies in a tumor spectrum. II. The effect of 2,4,6-triethylenimino-s-triazine on the growth of a variety of mouse and rat tumors. Cancer *5*, 979–991.

Sun, S., Bay-Jensen, A.-C., Karsdal, M.A., Siebuhr, A.S., Zheng, Q., Maksymowych, W.P., Christiansen, T.G., and Henriksen, K. (2014). The active form of MMP-3 is a marker of synovial inflammation and cartilage turnover in inflammatory joint diseases. BMC Musculoskelet. Disord. *15*, 93.

Sundel, R.P. (2015). Kawasaki disease. Rheum. Dis. Clin. North Am. *41*, 63–73, viii.

Suzuki, K., Enghild, J.J., Morodomi, T., Salvesen, G., and Nagase, H. (1990). Mechanisms of activation of tissue procollagenase by matrix metalloproteinase 3 (stromelysin). Biochemistry (Mosc.) *29*, 10261–10270.

Suzuki, M., Raab, G., Moses, M.A., Fernandez, C.A., and Klagsbrun, M. (1997). Matrix metalloproteinase-3 releases active heparin-binding EGF-like growth factor by cleavage at a specific juxtamembrane site. J. Biol. Chem. *272*, 31730–31737.

Tacar, O., Sriamornsak, P., and Dass, C.R. (2013). Doxorubicin: an update on anticancer molecular action, toxicity and novel drug delivery systems. J. Pharm. Pharmacol. *65*, 157–170.

Takeuchi, T., Adachi, Y., Nagayama, T., and Furihata, M. (2011). Matrix metalloproteinase-11 overexpressed in lobular carcinoma cells of the breast promotes anoikis resistance. Virchows Arch. Int. J. Pathol. *459*, 291–297.

Takimoto, K., Kawashima, N., Suzuki, N., Koizumi, Y., Yamamoto, M., Nakashima, M., and Suda, H. (2014). Down-regulation of inflammatory mediator synthesis and infiltration of inflammatory cells by MMP-3 in experimentally induced rat pulpitis. J. Endod. *40*, 1404–1409.

Tan, J., Buache, E., Chenard, M.-P., Dali-Youcef, N., and Rio, M.-C. (2011). Adipocyte is a non-trivial, dynamic partner of breast cancer cells. Int. J. Dev. Biol. *55*, 851–859.

Tan, J., Buache, E., Alpy, F., Daguenet, E., Tomasetto, C.-L., Ren, G.-S., and Rio, M.-C. (2014a). Stromal matrix metalloproteinase-11 is involved in the mammary gland postnatal development. Oncogene *33*, 4050–4059.

Tan, J., Buache, E., Alpy, F., Daguenet, E., Tomasetto, C.-L., Ren, G.-S., and Rio, M.-C. (2014b). Stromal matrix metalloproteinase-11 is involved in the mammary gland postnatal development. Oncogene *33*, 4050–4059.

Tang, S., Gao, L., Bi, Q., Xu, G., Wang, S., Zhao, G., Chen, Z., Zheng, X., Pan, Y., Zhao, L., et al. (2013). SDR9C7 promotes lymph node metastases in patients with esophageal squamous cell carcinoma. PloS One *8*, e52184.

Tauro, B.J., Mathias, R.A., Greening, D.W., Gopal, S.K., Ji, H., Kapp, E.A., Coleman, B.M., Hill, A.F., Kusebauch, U., Hallows, J.L., et al. (2013). Oncogenic H-ras reprograms Madin-Darby canine kidney (MDCK) cell-derived exosomal proteins following epithelial-mesenchymal transition. Mol. Cell. Proteomics MCP *12*, 2148–2159.

Thompson, B.R., Mazurkiewicz-Muñoz, A.M., Suttles, J., Carter-Su, C., and Bernlohr, D.A. (2009). Interaction of adipocyte fatty acid-binding protein (AFABP) and JAK2: AFABP/aP2 as a regulator of JAK2 signaling. J. Biol. Chem. *284*, 13473–13480.

Timmermans-Sprang, E.P.M., Gracanin, A., and Mol, J.A. (2017). Molecular Signaling of Progesterone, Growth Hormone, Wnt, and HER in Mammary Glands of Dogs, Rodents, and Humans: New Treatment Target Identification. Front. Vet. Sci. *4*, 53.

Torre, C., Wang, S.J., Xia, W., and Bourguignon, L.Y.W. (2010). Reduction of hyaluronan-CD44-mediated growth, migration, and cisplatin resistance in head and neck cancer due to inhibition of Rho kinase and PI-3 kinase signaling. Arch. Otolaryngol. Head Neck Surg. *136*, 493–501.

Trivedi, A., Zhang, H., Ekeledo, A., Lee, S., Werb, Z., Plant, G.W., and Noble-Haeusslein, L.J. (2016). Deficiency in matrix metalloproteinase-2 results in long-term vascular instability and regression in the injured mouse spinal cord. Exp. Neurol. *284*, 50–62.

Trujillo, M.E., and Scherer, P.E. (2006). Adipose tissue-derived factors: impact on health and disease. Endocr. Rev. *27*, 762–778.

Turunen, S.P., Tatti-Bugaeva, O., and Lehti, K. (2017). Membrane-type matrix metalloproteases as diverse effectors of cancer progression. Biochim. Biophys. Acta *1864*, 1974–1988.

Ugarte-Berzal, E., Bailón, E., Amigo-Jiménez, I., Albar, J.P., García-Marco, J.A., and García-Pardo, A. (2014). A novel CD44-binding peptide from the pro-matrix metalloproteinase-9 hemopexin domain impairs adhesion and migration of chronic lymphocytic leukemia (CLL) cells. J. Biol. Chem. *289*, 15340–15349.

Ulici, V., Hoenselaar, K.D., Agoston, H., McErlain, D.D., Umoh, J., Chakrabarti, S., Holdsworth, D.W., and Beier, F. (2009). The role of Akt1 in terminal stages of endochondral bone formation: angiogenesis and ossification. Bone *45*, 1133–1145.

Uría, J.A., and López-Otín, C. (2000). Matrilysin-2, a new matrix metalloproteinase expressed in human tumors and showing the minimal domain organization required for secretion, latency, and activity. Cancer Res. *60*, 4745–4751.

Urriola-Muñoz, P., Li, X., Maretzky, T., McIlwain, D.R., Mak, T.W., Reyes, J.G., Blobel, C.P., and Moreno, R.D. (2018). The xenoestrogens biphenol-A and nonylphenol differentially regulate metalloprotease-mediated shedding of EGFR ligands. J. Cell. Physiol. *233*, 2247–2256.

Valdivia, A., Peralta, R., Matute-González, M., García Cebada, J.M., Casasola, I., Jiménez-Medrano, C., Aguado-Pérez, R., Villegas, V., González-Bonilla, C., Manuel-Apolinar, L., et al. (2011). Co-expression of metalloproteinases 11 and 12 in cervical scrapes cells from cervical precursor lesions. Int. J. Clin. Exp. Pathol. *4*, 674–682.

Vandooren, J., Van den Steen, P.E., and Opdenakker, G. (2013). Biochemistry and molecular biology of gelatinase B or matrix metalloproteinase-9 (MMP-9): the next decade. Crit. Rev. Biochem. Mol. Biol. *48*, 222–272.

Vargová, V., Pytliak, M., and Mechírová, V. (2012). Matrix metalloproteinases. EXS *103*, 1–33.

Vashishta, A., Ohri, S.S., and Vetvicka, V. (2009). Pleiotropic effects of cathepsin D. Endocr. Metab. Immune Disord. Drug Targets *9*, 385–391.

Vaysse, C., Lømo, J., Garred, Ø., Fjeldheim, F., Lofteroed, T., Schlichting, E., McTiernan, A., Frydenberg, H., Husøy, A., Lundgren, S., et al. (2017). Inflammation of mammary adipose tissue occurs in overweight and obese patients exhibiting early-stage breast cancer. Npj Breast Cancer *3*.

Vecchi, M., Rudolph-Owen, L.A., Brown, C.L., Dempsey, P.J., and Carpenter, G. (1998). Tyrosine phosphorylation and proteolysis. Pervanadate-induced, metalloprotease-dependent cleavage of the ErbB-4 receptor and amphiregulin. J. Biol. Chem. *273*, 20589–20595.

Veltmaat, J.M., Mailleux, A.A., Thiery, J.P., and Bellusci, S. (2003). Mouse embryonic mammogenesis as a model for the molecular regulation of pattern formation. Differ. Res. Biol. Divers. *71*, 1–17.

Vincenti, M.P., and Brinckerhoff, C.E. (2002). Transcriptional regulation of collagenase (MMP-1, MMP-13) genes in arthritis: integration of complex signaling pathways for the recruitment of gene-specific transcription factors. Arthritis Res. *4*, 157–164.

Vincenti, M.P., and Brinckerhoff, C.E. (2007). Signal transduction and cell-type specific regulation of matrix metalloproteinase gene expression: can MMPs be good for you? J. Cell. Physiol. *213*, 355–364.

Visse, R., and Nagase, H. (2003). Matrix metalloproteinases and tissue inhibitors of metalloproteinases: structure, function, and biochemistry. Circ. Res. *92*, 827–839.

Vona-Davis, L., and Rose, D.P. (2007). Adipokines as endocrine, paracrine, and autocrine factors in breast cancer risk and progression. Endocr. Relat. Cancer *14*, 189–206.

Vu, T.H., Shipley, J.M., Bergers, G., Berger, J.E., Helms, J.A., Hanahan, D., Shapiro, S.D., Senior, R.M., and Werb, Z. (1998). MMP-9/gelatinase B is a key regulator of growth plate angiogenesis and apoptosis of hypertrophic chondrocytes. Cell *93*, 411–422.

Waldhauer, I., Goehlsdorf, D., Gieseke, F., Weinschenk, T., Wittenbrink, M., Ludwig, A., Stevanovic, S., Rammensee, H.-G., and Steinle, A. (2008). Tumor-associated MICA is shed by ADAM proteases. Cancer Res. *68*, 6368–6376.

Wang, M., and Kaufman, R.J. (2016). Protein misfolding in the endoplasmic reticulum as a conduit to human disease. Nature *529*, 326–335.

Wang, C., Ma, H.-X., Jin, M.-S., Zou, Y.-B., Teng, Y.-L., Tian, Z., Wang, H.-Y., Wang, Y.-P., and Duan, X.-M. (2014). Association of matrix metalloproteinase (MMP)-2 and -9 expression with extra-gastrointestinal stromal tumor metastasis. Asian Pac. J. Cancer Prev. APJCP *15*, 4187–4192.

Wang, M., Qin, X., Mudgett, J.S., Ferguson, T.A., Senior, R.M., and Welgus, H.G. (1999). Matrix metalloproteinase deficiencies affect contact hypersensitivity: stromelysin-1 deficiency prevents the response and gelatinase B deficiency prolongs the response. Proc. Natl. Acad. Sci. U. S. A. *96*, 6885–6889.

Wang, T., Fahrmann, J.F., Lee, H., Li, Y.-J., Tripathi, S.C., Yue, C., Zhang, C., Lifshitz, V., Song, J., Yuan, Y., et al. (2018). JAK/STAT3-Regulated Fatty Acid β-Oxidation Is Critical for Breast Cancer Stem Cell Self-Renewal and Chemoresistance. Cell Metab. *27*, 136-150.e5.

Wang, W., Pan, H., Murray, K., Jefferson, B.S., and Li, Y. (2009). Matrix metalloproteinase-1 promotes muscle cell migration and differentiation. Am. J. Pathol. *174*, 541–549.

Wang, X., Hu, Y., Cui, J., Zhou, Y., and Chen, L. (2017a). Coordinated targeting of MMP-2/MMP-9 by miR-296-3p/FOXCUT exerts tumor-suppressing effects in choroidal malignant melanoma. Mol. Cell. Biochem.

Wang, Y.Y., Attané, C., Milhas, D., Dirat, B., Dauvillier, S., Guerard, A., Gilhodes, J., Lazar, I., Alet, N., Laurent, V., et al. (2017b). Mammary adipocytes stimulate breast cancer invasion through metabolic remodeling of tumor cells. JCI Insight *2*.

Watson, C.J., and Khaled, W.T. (2008). Mammary development in the embryo and adult: a journey of morphogenesis and commitment. Development *135*, 995–1003.

Weathington, N.M., van Houwelingen, A.H., Noerager, B.D., Jackson, P.L., Kraneveld, A.D., Galin, F.S., Folkerts, G., Nijkamp, F.P., and Blalock, J.E. (2006). A novel peptide CXCR ligand derived from extracellular matrix degradation during airway inflammation. Nat. Med. *12*, 317–323.

Wells, J.M., Gaggar, A., and Blalock, J.E. (2015). MMP generated matrikines. Matrix Biol. J. Int. Soc. Matrix Biol. *44–46*, 122–129.

Whitaker-Menezes, D., Martinez-Outschoorn, U.E., Lin, Z., Ertel, A., Flomenberg, N., Witkiewicz, A.K., Birbe, R.C., Howell, A., Pavlides, S., Gandara, R., et al.

(2011). Evidence for a stromal-epithelial “lactate shuttle” in human tumors: MCT4 is a marker of oxidative stress in cancer-associated fibroblasts. Cell Cycle Georget. Tex *10*, 1772–1783.

White, D.E., Kurpios, N.A., Zuo, D., Hassell, J.A., Blaess, S., Mueller, U., and Muller, W.J. (2004). Targeted disruption of beta1-integrin in a transgenic mouse model of human breast cancer reveals an essential role in mammary tumor induction. Cancer Cell *6*, 159–170.

Wilson, C.L., Ouellette, A.J., Satchell, D.P., Ayabe, T., López-Boado, Y.S., Stratman, J.L., Hultgren, S.J., Matrisian, L.M., and Parks, W.C. (1999). Regulation of intestinal alpha-defensin activation by the metalloproteinase matrilysin in innate host defense. Science *286*, 113–117.

Winer, A., Adams, S., and Mignatti, P. (2018). Matrix Metalloproteinase Inhibitors in Cancer Therapy: Turning Past Failures Into Future Successes. Mol. Cancer Ther. *17*, 1147–1155.

Wiseman, B.S., Sternlicht, M.D., Lund, L.R., Alexander, C.M., Mott, J., Bissell, M.J., Soloway, P., Itohara, S., and Werb, Z. (2003). Site-specific inductive and inhibitory activities of MMP-2 and MMP-3 orchestrate mammary gland branching morphogenesis. J. Cell Biol. *162*, 1123–1133.

Wolf, C., Rouyer, N., Lutz, Y., Adida, C., Loriot, M., Bellocq, J.P., Chambon, P., and Basset, P. (1993). Stromelysin 3 belongs to a subgroup of proteinases expressed in breast carcinoma fibroblastic cells and possibly implicated in tumor progression. Proc. Natl. Acad. Sci. U. S. A. *90*, 1843–1847.

Wolf, K., Wu, Y.I., Liu, Y., Geiger, J., Tam, E., Overall, C., Stack, M.S., and Friedl, P. (2007). Multi-step pericellular proteolysis controls the transition from individual to collective cancer cell invasion. Nat. Cell Biol. *9*, 893–904.

Won, H.S., Kim, Y.A., Lee, J.S., Jeon, E.K., An, H.J., Sun, D.S., Ko, Y.H., and Kim, J.S. (2013). Soluble interleukin-6 receptor is a prognostic marker for relapse-free survival in estrogen receptor-positive breast cancer. Cancer Invest. *31*, 516–521.

Wong, H.L.X., Jin, G., Cao, R., Zhang, S., Cao, Y., and Zhou, Z. (2016). MT1-MMP sheds LYVE-1 on lymphatic endothelial cells and suppresses VEGF-C production to inhibit lymphangiogenesis. Nat. Commun. *7*, 10824.

Wu, D., Li, M., Wang, L., Zhou, Y., Zhou, J., Pan, H., and Qu, P. (2014). microRNA‐145 inhibits cell proliferation, migration and invasion by targeting matrix metallopeptidase-11 in renal cell carcinoma. Mol. Med. Rep. *10*, 393–398.

Wu, E., Mari, B.P., Wang, F., Anderson, I.C., Sunday, M.E., and Shipp, M.A. (2001). Stromelysin-3 suppresses tumor cell apoptosis in a murine model. J. Cell. Biochem. *82*, 549–555.

Xiao, Z., Chen, C., Meng, T., Zhang, W., and Zhou, Q. (2016). Resveratrol attenuates renal injury and fibrosis by inhibiting transforming growth factor-β pathway on matrix metalloproteinase 7. Exp. Biol. Med. *241*, 140–146.

Yadav, L., Puri, N., Rastogi, V., Satpute, P., Ahmad, R., and Kaur, G. (2014). Matrix metalloproteinases and cancer - roles in threat and therapy. Asian Pac. J. Cancer Prev. APJCP *15*, 1085–1091.

Yamamoto, K., Miyazaki, K., and Higashi, S. (2014). Pericellular proteolysis by matrix metalloproteinase-7 is differentially modulated by cholesterol sulfate, sulfatide, and cardiolipin. FEBS J. *281*, 3346–3356.

Yan, C., and Boyd, D.D. (2007). Regulation of matrix metalloproteinase gene expression. J. Cell. Physiol. *211*, 19–26.

Yan, D., Dai, H., and Liu, J.-W. (2011). Serum levels of MMP-11 correlate with clinical outcome in Chinese patients with advanced gastric adenocarcinoma. BMC Cancer *11*, 151.

Yana, I., and Weiss, S.J. (2000). Regulation of Membrane Type-1 Matrix Metalloproteinase Activation by Proprotein Convertases. Mol. Biol. Cell *11*, 2387–2401.

Yang, F., Teves, S.S., Kemp, C.J., and Henikoff, S. (2014a). Doxorubicin, DNA torsion, and chromatin dynamics. Biochim. Biophys. Acta BBA - Rev. Cancer *1845*, 84–89.

Yang, F.Q., Liu, M., Yang, F.P., Zhang, X.L., Yang, B., Guo, C.C., Huang, J.H., Che, J.P., Yan, Y., and Zheng, J.H. (2014b). Matrix metallopeptidase 2 (MMP2) mediates MHC class I polypeptide-related sequence A (MICA) shedding in renal cell carcinoma. Actas Urol. Esp. *38*, 172–178.

Yang, H.-L., Korivi, M., Lin, M.-W., Chen, S.-C., Chou, C.-W., and Hseu, Y.-C. (2015). Anti-angiogenic properties of coenzyme Q0 through downregulation of

MMP-9/NF-κB and upregulation of HO-1 signaling in TNF-α-activated human endothelial cells. Biochem. Pharmacol. *98*, 144–156.

Yang, J., Kasberg, W.C., Celo, A., Liang, Z., Quispe, K., and Stack, M.S. (2017). Post-translational modification of the membrane type 1 matrix metalloproteinase (MT1-MMP) cytoplasmic tail impacts ovarian cancer multicellular aggregate dynamics. J. Biol. Chem. *292*, 13111–13121.

Yonemori, M., Seki, N., Yoshino, H., Matsushita, R., Miyamoto, K., Nakagawa, M., and Enokida, H. (2016). Dual tumor-suppressors miR-139-5p and miR-139-3p targeting matrix metalloprotease 11 in bladder cancer. Cancer Sci. *107*, 1233–1242.

Yu, Q., and Stamenkovic, I. (2000). Cell surface-localized matrix metalloproteinase-9 proteolytically activates TGF-beta and promotes tumor invasion and angiogenesis. Genes Dev. *14*, 163–176.

Yu, W.-H., Woessner, J.F., McNeish, J.D., and Stamenkovic, I. (2002). CD44 anchors the assembly of matrilysin/MMP-7 with heparin-binding epidermal growth factor precursor and ErbB4 and regulates female reproductive organ remodeling. Genes Dev. *16*, 307–323.

Yu, Y., Xiao, C.-H., Tan, L.-D., Wang, Q.-S., Li, X.-Q., and Feng, Y.-M. (2014). Cancer-associated fibroblasts induce epithelial-mesenchymal transition of breast cancer cells through paracrine TGF-β signalling. Br. J. Cancer *110*, 724–732.

Zarrabi, K., Dufour, A., Li, J., Kuscu, C., Pulkoski-Gross, A., Zhi, J., Hu, Y., Sampson, N.S., Zucker, S., and Cao, J. (2011). Inhibition of matrix metalloproteinase 14 (MMP-14)-mediated cancer cell migration. J. Biol. Chem. *286*, 33167–33177.

Zhang, X., Huang, S., Guo, J., Zhou, L., You, L., Zhang, T., and Zhao, Y. (2016). Insights into the distinct roles of MMP-11 in tumor biology and future therapeutics (Review). Int. J. Oncol. *48*, 1783–1793.

Zhao, Q., Wang, J., Levichkin, I.V., Stasinopoulos, S., Ryan, M.T., and Hoogenraad, N.J. (2002). A mitochondrial specific stress response in mammalian cells. EMBO J. *21*, 4411–4419.

Zhao, Y.-G., Xiao, A.-Z., Newcomer, R.G., Park, H.I., Kang, T., Chung, L.W.K., Swanson, M.G., Zhau, H.E., Kurhanewicz, J., and Sang, Q.-X.A. (2003). Activation of pro-gelatinase B by endometase/matrilysin-2 promotes invasion of human prostate cancer cells. J. Biol. Chem. *278*, 15056–15064.

Zhao, Z.-S., Chu, Y.-Q., Ye, Z.-Y., Wang, Y.-Y., and Tao, H.-Q. (2010). Overexpression of matrix metalloproteinase 11 in human gastric carcinoma and its clinicopathologic significance. Hum. Pathol. *41*, 686–696.

Zhou, D., Tian, Y., Sun, L., Zhou, L., Xiao, L., Tan, R.J., Tian, J., Fu, H., Hou, F.F., and Liu, Y. (2017). Matrix Metalloproteinase-7 Is a Urinary Biomarker and Pathogenic Mediator of Kidney Fibrosis. J. Am. Soc. Nephrol. *28*, 598–611.

Zuo, J.-H., Zhu, W., Li, M.-Y., Li, X.-H., Yi, H., Zeng, G.-Q., Wan, X.-X., He, Q.-Y., Li, J.-H., Qu, J.-Q., et al. (2011). Activation of EGFR promotes squamous carcinoma SCC10A cell migration and invasion via inducing EMT-like phenotype change and MMP-9-mediated degradation of E-cadherin. J. Cell. Biochem. *112*, 2508–2517.